THE UNIVERSITY OF
SYDNEY

PERTURBATION OF CELLULAR AND VASCULAR FUNCTION BY HYPERGLYCAEMIA AND HYPERLIPIDAEMIA AND THEIR ROLE IN CARDIOVASCULAR DISEASE

CHRISTINE ELIZABETH HYUN JIN KIM

A thesis submitted in the fulfilment of the requirements for the degree of

Doctor of Philosophy

THE UNIVERSITY OF SYDNEY

Discipline of Medicine

The University of Sydney

Australia

2013

“To raise new questions, new possibilities, to regard old problems from a new angle, requires creative imagination and marks real advance in science.”

Albert Einstein (1879-1955)

“Faith is taking the first step even when you don’t see the whole staircase.”

Martin Luther King. Jr (1929-1968)

“The best thing about the future is that it comes one day at a time.”

Abraham Lincoln (1809-1865)

DECLARATION

The work presented in this thesis is the original work conducted by the author at the Heart Research Institute, Sydney, unless otherwise stated.

The work presented was conducted under the supervision of my principle supervisor Prof. Michael Jonathon Davies and my associate supervisor Dr. David Marc van Reyk.

No content of this thesis has been submitted previously as part of a higher degree, however results have been presented at scientific meetings and submitted for publication as informed.

Christine Elizabeth Hyun Jin Kim

BHlthSc, MSc.

TABLE OF CONTENTS

ACKNOWLEDGEMENT

I would firstly like to thank on behalf of my late father (who recently passed away on August 8th, 2010) to everyone who has provided great and persistent love, support and care during the most challenging days of his daughter's life. I would also like to personally express my gratitude to all those that have gone out of their way in giving me their support. It has been a great honour to be a member of the Heart Research Institute, it has certainly been some of the best days of my life which I will never to forget and always cherish.

This research was carried out in the Free Radical Group, the Heart Research Institute (HRI). Salary support was from University Postgraduate Award (UPA) Scholarship, Faculty of Medicine, University of Sydney and further support grant from HRI. The animals for the carnosine project were financially supported by Eli Lilly and the animal housing and plasma analysis were carried out by Dr David van Reyk (University of Technology, Sydney) and Dr Bronwyn Brown. The animal plasma and heart samples for the TEMPOL project were kindly supplied by Prof. Jim Mitchell (Radiation Biology Branch, Center for Cancer Research, National Cancer Institute, Bethesda, MS, USA).

This PhD was not possible without the two greatest supervisors (in the world); Prof. Michael Davies and Dr David van Reyk. I still feel that there is so much more to learn under your wing.

Prof. Michael Davies, thank you for giving me the opportunity to take up this position despite the situation I was in and for the unexpected situations that came through. You are simply the best supervisor and boss anyone could ever have beyond what I have prayed for. To me you were an angel during my PhD, always leading me in the right direction in the gentlest and most profound ways.

Dr David van Reyk, thank you for leading me into this great research environment. Your continued support, protection, drive and interest definitely challenged and stimulated my heart, brain and soul. You are in fact the best lecturer I have ever met since my undergraduate years and it has been a great privilege to have worked alongside such a brilliant mind.

Assoc./Prof. Clare Hawkins as a postgraduate student coordinator for your kind support, advice and guidance during my study.

Dr Lucinda McRobb for your histology expertise and guidance in the dissection of the heart sections for the carnosine project.

Dr Christina Bursill and her group for their expertise and assistance in the immunohistochemical materials and procedures for the animal studies.

Mr Pat Pisansarakit for generously elutriating all the monocytes presented in this thesis and beyond.

Dr Bronwyn Brown, Dr Philip Morgan and Dr Dave Pattison (Free Radical and Inflammation Group) for their scientific expertise, advice in laboratory procedures, understanding of my project and providing ease during my stressful times.

Dr Naomi Stanley for your warm welcome, instructions on basic tissue culture work and general trouble shooting in the laboratory.

Dr Aldwin Suryo for refining my laboratory skills, in particularly with Western blots.

Polina, Tracey, Shudi, Fahd, George, Luke, Dom, Rosie, Dr Kate Hadfield, Dr Tessa Barnett, Dr Christine Chuang, Dr Jair Kwan for their friendship, assistance and encouragement in the highs and lows of the PhD life.

I would also like to thank all past and present academic and technical staff who has made the Heart Research Institute a pleasant place to work.

I would also like to thank all the support and prayers from my church; New Life Community Church and Saesoon Presbyterian Church (Mother Church), ministered by Pastor Joshua Choi and Pastor Kyu Hyun Lee.

I would love to thank my friends and family for all their love, support, prayers and confidence in where God has placed me in. Especially to my family who never lost faith in me; my father Kwang Il Kim, my mother Jin Hwa (Lee) Kim, my sister Gloria Yae-Jin Kim and the newest member of our to-be family Shuai Zheng. I love you all too much!

Lastly I would love to give all thanks, praise and glory to God, the creator of the Heavens, Earth and me.

ABSTRACT

Cardiovascular disease, diabetes mellitus and obesity are the leading causes of death, disability and reduced quality of life globally. Hyperglycaemia and hyperlipidaemia are the two major causational risk factors for the metabolic and vascular complications of Type 1 and 2 diabetes, accumulation of excess body weight and atherosclerosis. The research reported in this thesis investigates some of the molecular mechanisms linking diabetes with atherosclerosis, as well examining potential anti-glycative and antioxidant compounds, which may improve cardiovascular related diseases induced by hyperglycaemia and hyperlipidaemia.

People with diabetes have an elevated risk of atherosclerosis. The accumulation of lipid within macrophage cells in the artery wall is believed to arise via the uptake and subsequent processing of modified low-density lipoproteins (LDL) via the endolysosomal system. Chapter 3 explores the effects of prolonged exposure to elevated glucose upon macrophage lysosomal function to determine whether this contributes to modulated LDL and protein catabolism. Exposure to elevated glucose, but not mannitol (to control for osmotic effects), was found to result in a concentration-dependent decrease in the activity, and to a lesser extent protein levels, of four lysosomal cathepsins. Lysosomal acid lipase (LAL) activity, the major hydrolase for cholesteryl esters, was also significantly reduced. Arysulfatase activity, lysosomal associated marker protein-1 (LAMP-1) levels (commonly used markers of lysosomal numbers) and lysosomal dye accumulation were also decreased at the highest glucose concentrations, though to a lesser extent.

Chapter 4 extended this work by monitoring the effects of high glucose upon lysosomes during the maturation of human monocytes to monocyte-derived macrophages (HMDM) under normal 5.5 mM and high 20 mM glucose conditions. High glucose concentrations were shown to have an inhibitory effect on lysosomal function in monocytes within two days of culturing and the magnitude of the glucose-induced changes increased as the cells matured into macrophages. Thus high glucose modulated the activity of the lysosomal cathepsin B, L and LAL enzymes, their proteins levels and also lysosomal numbers during monocyte maturation with these effects becoming more pronounced over time except in the case of LAL. This

inhibition of lysosomal function may lead to cellular cholesterol accumulation and contribute to the generation of macrophage foam cells and atherosclerotic plaque development in people with diabetes.

Carnosine has been shown previously to modulate triglyceride and glycation levels in both cell and whole animal systems. In Chapter 5 investigations were undertaken to determine whether prolonged supplementation with carnosine inhibits atherosclerosis in hyperglycaemic and hyperlipidaemic mice. To assess the possible anti-atherogenic properties of carnosine, streptozotocin-induced diabetic apo $E^{-/-}$ mice were maintained for twenty weeks, post-induction of diabetes. Half of the animals received carnosine (2 g/L) in their drinking water. Diabetes was confirmed by significant increases in blood glucose and glycated haemoglobin, plasma triglyceride and total cholesterol levels, brachiocephalic artery and aortic sinus plaque area; and a significantly lower body mass. Supplementation with carnosine was shown to increase plasma carnosine levels. Although this did not result in smaller plaque areas in the diabetic mice, carnosine supplementation significantly reduced triglyceride levels and the area of plaque occupied by extracellular lipid, and increased the number of macrophages, α-actin-positive for smooth muscle cells and plaque collagen content. These findings indicate that in a well-established model of diabetes-associated atherosclerosis, prolonged carnosine supplementation has a significant impact on markers of atherosclerotic plaque stability. Carnosine supplementation may therefore be of benefit in lowering triglyceride levels and suppressing plaque instability in diabetes-associated atherosclerosis at least in this animal model.

The nitroxide compound TEMPOL has been shown to prevent obesity-induced changes in adipokine secretion in both cell and whole animal systems. Chapter 6 investigated whether TEMPOL supplementation inhibits inflammation and atherosclerosis in mice that were fed a high fat diet. Adult male C57BL/6 and apo $E^{-/-}$ mice were fed for 7 weeks either on a standard chow diet or a high-fat diet. Half the mice were supplemented with 10 mg/g TEMPOL in their food. High fat feeding resulted in a substantial increase in body mass and hyperlipidaemia. Dietary TEMPOL resulted in a marked reduction in weight gain and plasma lipid levels. In the hyperlipidaemic and obese mice, a significant elevation in plasma lipid levels and the inflammatory markers IL-6, MCP-1, MPO, SAA were observed, along with an

increase in leptin and decrease in adiponectin. TEMPOL supplementation reversed these effects. No significant differences were detected in plaque area. These data indicate that in a well-established model of obesity-associated hyperlipidaemia, TEMPOL had a significant impact on weight gain, hyperlipidaemia and inflammation. TEMPOL supplementation may therefore be of potential value in suppressing obesity and metabolic disorders. However whether TEMPOL inhibits atherosclerosis requires further investigation.

Chapter 7 extended these *in vivo* studies by examining the impact of TEMPOL supplementation upon macrophage lysosomal function and the potential anti-inflammatory and anti-glycaemic properties of TEMPOL on cytokine expression in hyperglycaemic macrophages. TEMPOL did not affect the inhibition of lysosomal cathepsin B, L and LAL activities observed between the different concentrations of glucose. Levels of MCP-1, IL-6, MIF, CRP, TNF-α and MIP-1α were increased with LPS stimulation, and a dose dependent increase in TNF-α and MIP-1α expression was only seen with increasing concentrations of glucose. TEMPOL supplementation inhibited this elevation of TNF-α and MIP-1α induced by high glucose. These findings indicate that TEMPOL had a significant suppressive impact upon the pro-inflammatory cytokines TNF-α and MIP-1α in human macrophages that were matured in high glucose conditions. These data support the hypothesis that TEMPOL supplementation may be of therapeutic benefit in alleviating inflammation and oxidative stress induced by hyperglycaemia.

Overall, the data presented in this thesis are consistent with the hypothesis that the chronic elevated blood glucose levels detected in people with diabetes may have a detrimental impact upon macrophage lysosomal function, and that this may promote atherosclerosis. Long term exposure of human and murine macrophage cells to elevated glucose levels resulted in a depression of lysosomal proteolytic and lipase activities, their proteins levels and also lysosomal numbers in both maturing monocytes and macrophages. These functional changes may affect the capacity of macrophages to catabolise modified (lipo)proteins and enhance lipid accumulation in people with diabetes. Lysosomal damage may therefore contribute to the increased incidence, and rate of development of atherosclerosis in people with diabetes. The endogenous agent carnosine was examined in a murine model of diabetes-induced

atherosclerosis. The effect of carnosine supplementation was shown to have anti-hyperlipidaemic effects and properties that may enhance plaque stability which may be of therapeutic value in the treatment of diabetes-accelerated atherosclerosis. The nitroxide TEMPOL was investigated in two well-established obesity murine models by a high fat feeding. The intervention of TEMPOL was shown to effectively block weight gain in mice and relieve the associated hyperlipidaemia induced by a high fat diet. Further mechanistic studies showed that TEMPOL was able to reduce systemic inflammation and reverse the changed adipokine profile of obesity. TEMPOL was also shown to have an impact upon inflammation induced by high glucose in human macrophages. TEMPOL therefore appears to be a promising novel therapeutic target for chronic metabolic disorders such as diabetes, obesity, cardiovascular diseases.

LIST OF ABBREVIATIONS

α-SM-actin	alpha-smooth muscle-actin
4-HE	4-hydroxy-2-nonenal
4-MU	4-methylumbelliferone
4-MUO	4-methylumbelliferyl oleate
Ang II	angiotensin II
Apo	apolipoprotein
Apo A	apolipoprotein A
Apo B	apolipoprotein B
Apo C	apolipoprotein C
Apo E	apolipoprotein E
Apo $E^{-/-}$	apolipoprotein E knockout
ACAT	acetyl-coenzyme A cholesterol-acetyl transferase
ACE	angiotension-converting enzyme
AGE	advanced glycation end products
AGT	angiotension
AHA	American Heart Association
AP	alkaline phosphatase
ANOVA	analysis of variance
AR	aldose reductase
AZA	azaserine
ADP	adensine diphosphate
ATP	adenosine triphosphate
Brig 35	polyoxyethylene-23-lauryl ether
BIA	bioelectrical impedance analysis
BCA	Bicinchoninic assay
BHA	butylated hydroxyanisole
BMI	body mass index

BSA	bovine serum albumin
BVI	body volume index
conc.	concentration
CCL	chemokine (C-C motif) ligand
CD 36	Cluster of differentiation 36
CEL	carboxyethyllysine
CHAOS	Coronary artery disease, Hypertension, Atherosclerosis, Obesity and Stroke
CML	carboxylmethyl lysine
CN	carnosine
CRP	C-reative protein
CSF-1	colony stimulating factor-1
CTL	control
CVD	cardiovascular disease
DAG	diacylglycerol
DHAP	dihydroxy acetone phosphate
db/db	A model for diabetic dyslipidaemia induced by a point mutation in the Lepr gene which causes Type 2 diabetes, dyslipidaemia and obesity.
DIAB	diabetes
DM	diabetes mellitus
DMEM	Dulbecco's modified Eagle's medium
DMSO	dimethyl sulfoxide
DNA	deoxyribonucleic acid
DOLD	3-deoxyglucosone lysine dimer
DPX	di-N-butyl phthalate in xylene
DTT	dithiothreitol
eNOS	endothelial nitric oxide synthase
E64	N-[*N*-(L-3-trans-carboxyirane-2-carbonyl)-L-leucul]-agmatine
EC	endothelial cell
ECL	enhanced chemiluminescence
ECM	extracellular matrix

EDTA	ethylendiaminetetraacetic acid
EEA1	early endosome antigen 1
EGIR	European Group of Insulin Resistance
ELISA	enzyme-linked immunosorbent assay
FCS	fetal calf serum
FDA	Food and Drug Administration
Fruc-6-P	fructose-6-phosphate
g	gram
G1cNac	N-acetylglucosamine
GAPDH	glyceraldehyde-3-phosphate dehydrogenase
GFAT	glutamine: fructose-6-phosphate amidotransferase
GFR	glomerular filtration rate
GOLD	glyoxal-lysine dimer
GSH	glutathione
hr	hour
H&E	Haematoxylin and Eosin
HbA1c	glycated haemoglobin
HCl	hydrochloric acid
HDL	high-density lipoprotein
HDL-C	high-density liporprotein
HFD	high fat diet
HMDM	human monocyte-derived macrophages
HMG-CoA	3-hydroxy-3-methylglutaryl-coenzyme A
HOSCN	hypothiocyanous acid
HPLC	high-performance liquid chromatography
HRP	horseradish peroxidase
HBSS	Hank’s balanced salt solution
HS	human serum
iNOS	inducible nitric oxide synthase
IgG	Immunoglobulin G

ICAM-1	intracellular adhesion molecule-1
IDF	International Diabetes Federation
IDL	intermediate-density lipoprotein
IFN	interferon
IL	interleukin
JNK	c-jun-N-terminal kinase
kDa	kiloDalton
kcal	kilocalorie
L	litre
LAL	lysosomal acid lipase
LAMP-1	lysosomal associated marker protein-1
LCAT	lecithin cholesterol acyltransferase
LDH	lactate dehydrogenase
LDL	low-density lipoprotein
LDL-C	low-density lipoprotein-cholesterol
LDL-R	low-density lipoprotein receptor
Lepr	leptin receptor
LOX-1	lectin-type oxidised LDL receptor 1
LPS	lipopolysaccharide
LZR	lean Zucker rats
mg	milligram
min	minute
mL	millilitre
mM	mmoles/L
mRNA	messenger ribonucleic acid
M	macrophage
MCP-1	monocyte / macrophage chemotactic protein-1
MDA	malondialdehyde
MGO	methylgloxal
MIF	macrophage migration inhibitory factor

MIP	macrophage inflammatory protein
MOLD	methylgloxal-lysine dimer
MPO	myeloperoxidase
MTT	3-(4,5-dimethylthiazol-2-yl)-2,5-diphenltetrazolium bromide
ng	nanogram
NaCl	Sodium chloride
NAD	nicotinamide adenine
NADP	nicotinamide adenine dinucleotide
NCEH	neutral cholesterol-ester hydrolase
NADPH	nicotinamide adenine dinucleotide phosphate
NECP	National Cholesterol Education Program
NHNES	National Health and Nutrition Examination Survey
NO	nitric oxide
ob/ob	A mutant mouse that is unable to produce leptin, its food intake is uncontrolled and therefore eats excessively which causes obesity and Type 2 diabetes.
oxLDL	oxidized low-density lipoprotein
OGT	O- N-acetylglucosamine (G1cNAc)
OZR	obese Zucker rats
pg	picogram
PAGE	polyacrylamide gel electrophoresis
PAI-1	plasminogen activator inhibitor-1
PKD	protein kinase D
PARP	poly (ADP-ribose) polymerase
PBS	phosphate-buffered saline
PEG	polyethylene glycol
PERK	protein kinase RNA-like endoplasmic reticulum kinase
PKC	protein kinase C
PPAR-γ	peroxisome proliferator activated receptor-γ activation
rpm	revolution per minute
RAAS	renin-angiotensin aldosterone system

RAGE	receptor for advanced glycation end products
RBC	red blood cell
RNA	ribonucleic acid
ROI	reactive oxygen intermediates
ROS	reactive oxygen species
RPMI	Roswell Park Memorial Institute
RT-PCR	reverse transcription- polymerase chain reaction
s	second
Sp1	specificity protein-1
SAA	serum amyloid A
SDS	sodium dodecyl sulfate
SEM	standard error of mean
SHR	spontaneous hypertensive rats
SHHR	spontaneously hypertensive heart-failure rats
SMC	smooth muscle cell
SR-A1	steroid receptor RNA activator-1
SR-B1	scavenger receptor class B member 1
SREBP	sterol regulatory element-binding protein
STZ	streptozotocin
T1D	Type 1 diabetes
T2D	Type 2 diabetes
TEMPOL	4-hydroxyl-2,2,6,6-tetramethylpiperidine-N-oyl
TBS	Tris-buffered saline
TBST	Tris-buffered saline and Tween 20
TC	total cholesterol
TG	triglyceride
TGF	transforming growth factor
TNF-α	tumour necrosis factor- alpha
TZD	thiazolidinedones
UDP	uridine diphosphate

UPR	unfolding protein response
UPS	ubiquitin-proteasome system
UV	ultraviolet
v	version
v/v	volume per volume
VAT	visceral adipose tissue
VLDL	very low-density lipoprotein
VSMC	vascular smooth muscle cells
w/v	weight per volume
WBC	white blood cell
WC	waist circumference
WHO	World Health Organisation
WKY	Wistar-Kyoto (rats)
ZDF	Zucker Diabetic Fatty (rat)
ZSF	strain of ZDF crossed with SHHR

LIST OF FIGURES

LIST OF TABLES

PUBLICATIONS ARISING FROM THIS THESIS

Research Papers

1) Christine H. J. Kim, Fatemeh Moheimani, Aldwin Suryo Rahmanto, David M. van Reyk, Michael J. Davies. (2010) Inhibition of lysosomal function in macrophages incubated with elevated glucose concentrations: a potential contributory factor in diabetes-associated atherosclerosis. *Atherosclerosis*, 223 (1): 144-151.

2) Christine H. J. Kim, Bronwyn E. Brown, Fraser R. Torpy, Christina A. Bursill, Lucinda S. McRobb, Alison K. Heather, Michael J. Davies, David M. van Reyk. "Supplementation with carnosine decreases plasma triglycerides and modulates atherosclerotic plaque development in diabetic apo $E^{-/-}$ mice." Manuscript submitted to *Atherosclerosis* (23rd April 2013).

3) Christine H. J. Kim, David M. van Reyk, Michael J. Davies. "Development of lysosomal dysfunction during the maturation of human monocytes to macrophages in the presence of elevated glucose concentrations" Manuscript under preparation for *Atherosclerosis*.

4) Christine H. J. Kim, James Mitchell, David M. van Reyk, Michael J. Davies. "TEMPOL prevents obesity, decreases plasma hyperlipidaemia and inflammatory cytokines, and modulates atherosclerotic plaque composition in obese C57BL/6 and apo $E^{-/-}$ mice." Manuscript under preparation for *Atherosclerosis, Thrombosis, and Vascular Biology (ATVB).*

Conference Presentation (presenting author underlined)

1) Christine H. J. Kim, Bronwyn, E. Brown, Christina, A., Bursill, Fraser R. Torpy, Lucinda S. McRobb, Alison K. Heather, Michael J. Davies, David M. van Reyk. *"Supplementation with carnosine decreases plasma triglycerides and modulates atherosclerotic plaque composition in diabetic mice."* World Diabetes Congress 2013, Dec 2 - 6 2013, Melbourne, Victoria (poster).

2) Christine H. J. Kim, David M. van Reyk, Michael J. Davies. *"Lysosomal disruption in monocyte development to macrophages: a potential contributory factor in diabetes-associated atherosclerosis."* World Diabetes Congress 2013, Dec2 - 6 2013, Melbourne, Victoria (poster).

3) Christine H. J. Kim, David M. van Reyk, Michael J. Davies. *"TEMPOL prevents obesity, decreases plasma hyperlipidaemia and inflammatory cytokines, and modulates atherosclerotic plaque composition in obese mice."* World Diabetes Congress 2013, Dec2 - 6 2013, Melbourne, Victoria (poster).

4) Christine H. J. Kim, David M. van Reyk, Michael J. Davies. *"Inhibition of lysosomal function in macrophages incubated with elevated glucose concentrations: a potential contributory factor in diabetes-associated atherosclerosis."* 80th European Atherosclerosis Society Congress on May 25 – 28th May 2012, Milan, Italy (poster).

5) Christine H. J. Kim, David M. van Reyk, Michael J. Davies. *"Lysosomal disruption during maturation of human monocytes to macrophages in presence of elevated glucose: potential mechanistic insights into diabetes-associated atherosclerosis."* 80th European Atherosclerosis Society Congress on May 25 – 28th May 2012, Milan, Italy (poster).

6) Christine H. J. Kim, David M. van Reyk, Michael J. Davies. *"Perturbation of lysosomal function in macrophages exposed to elevated glucose concentrations: potential role in diabetes-associated atherosclerosis."* XVI International Symposium on Atherosclerosis hosted by The Australian Atherosclerosis Society (AAS) and The International Atherosclerosis Society, 25 – 29th March 2012, Sydney, NSW (oral).

7) Christine H. J. Kim, Fatemeh Moheimani, Aldwin Suryo Rahmanto, David M. van Reyk, Michael J. Davies. "*Perturbation of lysosomal function in macrophages exposed to elevated glucose concentrations: potential role in diabetes-associated atherosclerosis."*Australian Diabetes Society (ADS) and Australian Diabetes Education Association (ADEA) Annual Scientific Meeting 2011, Perth, WA (poster).

8) Christine H. J. Kim, David M. van Reyk, Michael J. Davies. "*Perturbation of lysosomal function in macrophages exposed to elevated glucose concentrations: potential role in diabetes-associated atherosclerosis."*Australian Diabetes Society (ADS) and Australian Diabetes Education Association (ADEA) Annual Scientific Meeting 2010, Sydney, NSW (poster).

9) David M. van Reyk, Bronwyn, E. Brown, Christine H. J. Kim, Fraser R. Torpy, Lucinda S. McRobb, Alison K. Heather, Michael J. Davies. *"Prolonged supplementation with carnosine decreases plasma triglycerides, but does not modulate diabetes status or atherosclerotic plaque development in streptozotocin-induced diabetic apo E $^{-/-}$ mice."*ADS and ADEA Annual Scientific Meeting 2010, Sydney, NSW (poster).

10) Christine H. J. Kim, David M. van Reyk, Michael J. Davies. *"Perturbation of lysosomal function in macrophages exposed to elevated glucose concentrations: potential role in diabetes-associated atherosclerosis."*Australian Society for Medical Research meeting 2010, Sydney, NSW (poster).

11) Bronwyn, E. Brown, Christine H. J. Kim, Michael J. Davies, David M. van Reyk. *"Prolonged supplementation with carnosine decreases plasma triglycerides, but does not modulate diabetes status or atherosclerotic plaque development in streptozotocin-induced diabetic apo E$^{-/-}$ mice."* 7th Congress of the Asian Pacific Society of Atherosclerosis and Vascular Diseases and the 2010 Annual Scientific Meeting of the Australian Atherosclerosis Society in Cairns, QLD (poster).

CHAPTER 1:

INTRODUCTION

1.1 Metabolic syndrome

The metabolic syndrome embodies a cluster of metabolic and haemodynamic disorders the prevalence of which are associated with lifestyle and other risk factors [1]. Factors characteristic of the metabolic syndrome include varying degrees of insulin resistance and glucose intolerance, central abdominal visceral obesity, abnormal lipid levels in the blood (elevated triglycerides, total cholesterol, and low density lipoprotein (LDL) cholesterol; and low high density lipoprotein (HDL) cholesterol), raised blood pressure, and prothrombotic and proinflammatory states [2,3,4]. The diagnostic criteria of metabolic syndrome, as determined by several major health authorities are shown in Table 1.1.

The metabolic syndrome is becoming a major global health crisis as it affects all ages, from children to adults and all racial / ethnic groups [2,5]. The prevalence has been reported to be as high as 50% in the United States and 34% in Australia. It is predicted to continue increasing in developed countries with continuing global modernisation [2,6,7,8,9]. The rising prevalence of obesity is a major contributor to the incidence of metabolic syndrome worldwide [2]. A direct association between high body mass index (BMI) and disease is observed for both genders across all racial or ethnic groups [2]. The prevalence of metabolic syndrome is the highest in obese children and adolescents, and the severity of this syndrome worsens as BMI increases, leading to obesity-related morbidity and premature deaths [2,5].

Several studies have indicated that the metabolic syndrome is a strong predictor of cardiovascular morbidity and mortality, diabetes and all-cause mortality in a number of populations worldwide [3,10,11,12,13]. Thus, the metabolic syndrome is referred to as the inducing factor for a “new cardiovascular epidemic,” as it triples the risk of a heart attack and doubles the risk of early mortality [14]. Furthermore those affected by the metabolic syndrome have a fivefold greater possibility of developing Type 2 diabetes [2].

1.1.1 Diagnostic criteria of the metabolic syndrome

The constellation of metabolic disorders which is now defined as the metabolic syndrome was first observed by the anatomist Morgagni in 1765, where he identified the close correlation between abdominal obesity and the occurrence of hypertension, atherosclerosis, dyslipidaemia, sleep apnea and hyperuricaemia. This syndrome became well established in the 20th century [15] when Kylin proposed that hypertension, atherosclerosis, dyslipidaemia and gout tended to appear together [16]. Subsequently, central obesity was noted as a key feature, by Vogue, in predisposing patients to diabetes, atherosclerosis, gout and uric calculi [17]. The definition of the metabolic syndrome was further refined by Reaven, as referring to a combination of hypertension, abdominal obesity, insulin resistance and hyperlipidaemia [18,19,20]. In 1988, Reaven established the clinical importance of this syndrome by proposing a conceptual framework connecting these independent biological events into a single pathophysiological paradigm [21].

The diagnostic criteria of the metabolic syndrome have yet to be standardised worldwide. The metabolic syndrome has also been known under different names including metabolic syndrome X, syndrome X, insulin resistance syndrome, cardiometabolic syndrome and Reaven's syndrome. In Australia it has been termed CHAOS, which stands for Coronary artery disease, Hypertension, Atherosclerosis, Obesity, and Stroke, to explicitly delineate the manifestations and complications that are associated with the elevated risk of cardiovascular disease, obesity and Type 2 diabetes [22,23,24].

Diagnostic criteria for the metabolic syndrome have been proposed by the World Health Organisation (WHO), the International Diabetes Federation (IDF), the United States National Cholesterol Education Program Adult Treatment Panel III (NECP) and the European Group for the Study of Insulin Resistance (EGIR) [2,14,16,25,26,27]. These criteria are given in Table 1.1.

	WHO	IDF	EGIR	NCEP ATP III
Criterion	Diabetes or impaired glucose tolerance or insulin resistance plus 2 or more of the following:	Central obesity Waist circumference Plus any 2 of the following:	Insulin resistance or hyperinsulinaemia (only non-diabetic subjects) plus two or more of the following:	Three or more of the following:
Blood Pressure or controlled by Medication	≥ 140/90 mmHg	≥130/85 mmHg	≥ 140/90 mmHg	≥130/85 mmHg
Triglyceride (TG) level	≥ 1.695 mmol/L	≥ 1.7 mmol/L	≥ 2.0 mmol/L	≥1.695 mmol/L
HDL-C level	≤ 0.9 mmol/L (M) ≤ 1.0 mmol/L (F)	1.03 mmol/L (M) ≤1.29 mmol/L (F)	≤1.0 mg/dL	≤40 mg/dL (M) ≤ 50 mg/dL (F)
Waist circumference	≥ 0.90 (M) ≥ 0.85 (F) (Waist: Hip Ratio)	Ethnicity Specific	≥ 94 cm (M) ≥ 80 cm (F)	≥ 102 cm (M) ≥ 88 cm (F)
Other features	Obesity: BMI ≥ 30 kg/m^2 Microalbuminuria: Urinary albumin excretion ratio > 20 μg/min or albumin: creatinine ratio >30 mg/g	Fasting plasma glucose ≥ 5.6 mmol/L or previously diagnosed Type 2 Diabetes	Fasting plasma glucose ≥ 6.1 mmol/L	Fasting plasma glucose ≥ 6.1 mmol/L (1100 mg/dL)

Table 1.1: Current diagnostic criteria for the Metabolic Syndrome

1.2 Cardiovascular disease

Cardiovascular disease (CVD) is a general term reflecting the dysfunction of the heart and the blood vessels (specifically the arteries and veins) subsequently affecting the circulation of the body system and as such affecting the supply of oxygen and nutrients to, and removal of waste from, the cells and tissues of the body [28]. Common cardiovascular conditions include rheumatic heart disease, peripheral arterial disease, hypertensive heart disease, heart failure, ischemic heart disease, cerebrovascular disease, inflammatory heart disease, congenital heart disease, deep vein thrombosis and pulmonary embolism [28].

CVD is the number one cause of death in developed countries [29] and worldwide total mortality approaches 17.5 million a year, representing a third of all global deaths [28]. One in every three adult men and women suffer from some form of CVD. It affects all age and ethnic groups and its prevalence is increasing as nations develop commercially and industrially, resulting in changes in diet and lifestyle that greatly increase CVD risk [29]. The increase in associated morbidities and the number of people dying prematurely is a substantial economic burden to developed and developing nations. For instance it is predicted that between 2006 and 2015 that the cost of China will be $558 billion from heart disease, stroke and diabetes [28].

CVD remains the leading cause of death in Australia and continues to be a heavy burden on the Australian population in terms of illness and disability and affects the health system economically. In 2004 - 2005, the total health care expenditure for cardiovascular diseases in Australia was approximately $6 billion, representing 11% of the total health care expenditure and was higher than for any other disease sector [30,31]. Health expenditure for CVD is estimated to rise to $16.2 billion in 2032-2033 [32]. In 2009, CVD was the cause of approximately 46 100 deaths, representing almost a third (32.8%) of all total deaths in Australia [31]. The onset of cardiovascular disease increases with age, with 13% aged between 35 and 44, 23% between the ages of 45 and 54, and 63% aged 75 years or over having been as reported as having a cardiovascular condition [33].

1.3 Atherosclerosis

Atherosclerosis is a chronic inflammatory disease characterised by the thickening and loss of elasticity in the walls of large and medium arteries leading to narrowing and constriction of the blood vessels that can give rise to severe complications such as myocardial infarction, stroke and limb amputation [34]. The accumulation of fat (cholesterol, cholesteryl esters and triglycerides derived from apolipoprotein B-100 containing lipid-protein particles) combined with vascular inflammation give rise to lesions in the vessel intima known as plaques.

Atheroma ('lump of gruel' in Greek) is characterised by three main compartments: the nodular build up of a soft flaky yellow substance consisting of large plaques rich in lipid-laden macrophages; cholesterol crystals; and calcification in chronic and advanced lesions. 'Sclerosis' refers to the hardening of the arteries due to fibrotic changes in the connective tissues of the walls. This chronic disease ultimately produces two critical problems. Firstly, lesion rupture, thrombus formation and the potential for thrombo-emboli to form that become lodged in smaller vessels leading to ischaemic damage. Though the clot can heal and contract, stenosis remains which results in narrowing of the artery causing reduced downstream blood supply to the tissues and organs. The second problem that may arise is that after a long and excessive period of inflammation the vessel wall is weakened and results in an aneurysm with an increased risk of vessel rupture and life-threatening haemorrhage [35].

1.3.1 Cholesterol and lipoproteins

The majority of cholesterol in the plasma is transported in protein-lipid particles, known as lipoproteins, including: very-low density lipoprotein (VLDL), low-density lipoprotein (LDL) and high-density lipoprotein (HDL). These lipoproteins are heterogeneous in size, density, composition and atherogenicity [36]. High levels of LDL, VLDL and remnant, intermediate-density lipoproteins (IDL), can promote atherosclerosis and thus high blood levels are major risk factors for coronary heart disease [37].

LDL (approx. 2.5 MDa) is a spherical-shaped particle that is the major carrier of cholesterol to cells [38]. The LDL particle is much smaller in size (180-250 Å in diameter) than when originally secreted as VLDL (600 to 800 Å in diameter). LDL

consists of around 22% protein, with a single molecule of apoB-100, 22% phospholipids, 8% cholesterol, 42% cholesteryl esters and 6% triglycerides (w/w) [38].

There are three LDL subclasses, L3-L1 (L1 as the smallest and L3 densest), and the differences between these subclasses are due to differences in lipid composition, density, size, chemical composition and apoB-100 structural changes [39]. Small and dense LDL particles have been associated with the development of coronary heart disease [39]. Different mechanisms have been proposed for the pro-atherogenic effects of LDL on the vasculature including; higher entrance and retention into the subendothelial space, greater affinity for binding to proteoglycans, and higher susceptibility to oxidation. Other risk factors associated with vascular disease are hypertriglyceridaemia, low HDL cholesterol, obesity, hyperglycaemia and insulin resistance [36].

The density of HDL is between 1.063 and 1.210 g/mL, the molecular masses are in the range of 1.7 and 4.0×10^5 g/mL and the protein content is between 45 and 55% [40]. HDL are heterogenous particles that are distinguished by their apolipoprotein composition including: only apo A-I (LP-A-I), both apo A-I and apo A-II (LP-A-I: A-II), both apo A-I and apo A-IV (LP-A-I: A-IV), and both apo A-I and apo E (LP-A-I: E) [41]. The major protein components (~ 90%) are apo A-I and apo A-II, with apo A-I three times more abundant than apo A-II based on mass. The remaining proteins (10%) include apo C-I, apo C-II, apo C-III and apo D [41].

HDL can be subdivided in to classes H5-H1 (with H5, H4 and H3 as the larger particles) as assessed by nuclear magnetic resonance [39]. HDL can also be divided into two major classes reported to possess different roles in protecting against atherosclerosis [42]. Apo A-I containing HDL particles (H5, H4 and H3 corresponding to HDL_2, 1.063 < density < 1.125 g/mL) are negatively correlated with coronary artery disease. H2 and H1, that correspond to HDL_3 (1.125 < density < 1.21 g/mL), are positively related with coronary artery disease [40]. HDL particles containing apoA-1 appear to prevent or decrease atherogenesis [42,43].

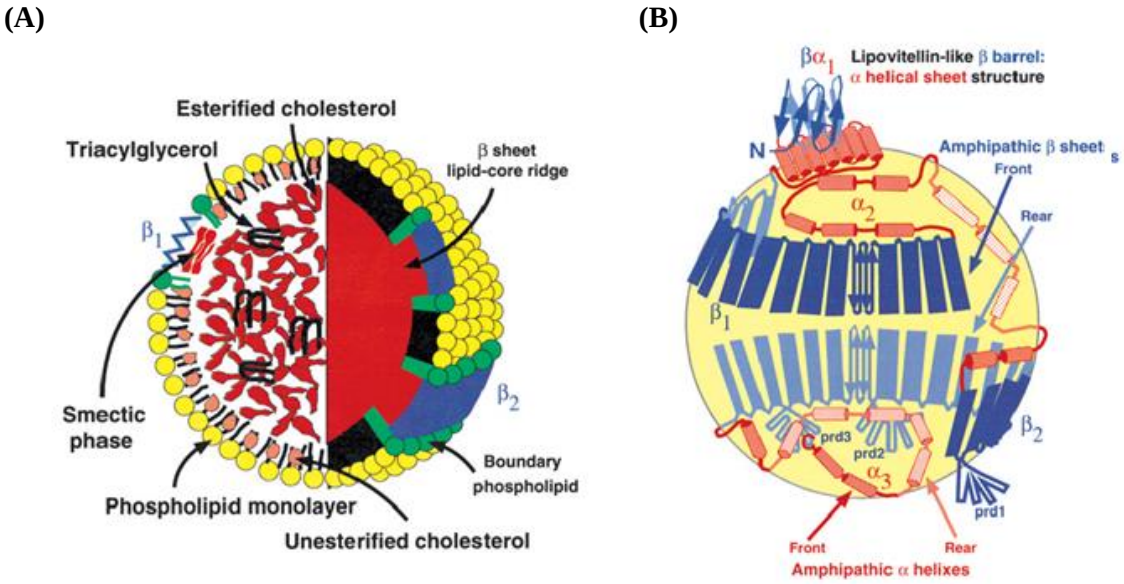

Figure 1.1: Schematic diagram of the structure of LDL and apoB-100 on the surface of LDL particle.
Spherical LDL (Panel A) and the proposed organisation of apoB-100 (Panel B) on the surface of LDL particle [41].

1.4 Pathogenesis of atherosclerosis

Atheroma and atherosclerosis can be referred to as benign and malignant conditions, respectively. Atheroma denotes a benign wound healing in response to injury and fibrous change which can be resolved. Atherosclerosis denotes a malignant transformation and multifactorial progression of chronic inflammation, fibroproliferation and angiogenesis [44]. It involves a succession of responses which results in systemic damage to the endothelium and the arterial intima instigated by the retention of modified low-density lipoproteins, haemodynamic factors and reductive-oxidative stress [44].

Atherosclerotic lesions develop and progress driven by an inflammatory response characterised by the release of numerous cytokines, increased proliferation of smooth muscle cells and their migration in to the intima, changes in connective tissue extracellular matrix and the accumulation of neutral lipid deposits principally in macrophages in the initial stages, but subsequently as large extracellular deposits [45].

Though the mechanism behind atherogenesis is not fully known, some hypotheses that are widely accepted are the ‘response to injury’ hypothesis, the ‘response to retention’ hypothesis and the ‘oxidation’ hypothesis. These are outlined below. Other hypotheses include: that platelets or fibrin are deposited on the intima in the initial stages of atherogenesis, and that the macroscopic gelatinous appearance may be an intimal thickening which may lead to the primary formation of atherosclerotic lesions [45,46].

The 'response to injury’ hypothesis, proposed by Russell Ross in 1973 focused on the notion that injury induced to the endothelial cells lining the artery walls caused endothelial dysfunction and disrupted the wall of the artery. This manifests in abnormal cellular interactions which are detailed below, chronic inflammation and plaque formation in the initial developmental stages of atherogenesis [47].

The ‘response to retention’ hypothesis postulates that the sub-endothelial retention and successive accumulation of lipids by the extracellular matrix is main trigger for the initiation of atherogenesis [48]. This theory was later expanded in 1994 to incorporate the oxidation hypothesis which proposes that oxidatively-modified low-density lipoproteins (ox-LDL) in the arterial wall generates a response that may be proinflammatory in terms of endothelial dysfunction as well as chemotactic, leading eventually to progression of atherosclerotic lesion formation [49].

Common to all these hypotheses is the key event of endothelial damage or dysfunction and the subsequent triggering of downstream pro-inflammatory events. Damage to the endothelium leads to monocyte and platelet adhesion thought to be mediated, at least in part, by redox signalling pathways. These monocytes migrate into the subendothelial space and differentiate into pro-inflammatory macrophages which may contribute to the modifications to LDL as well as promoting foam cell and thus fatty streak formation.

1.4.1 Stages of plaque formation

The atherosclerotic plaque is identified by arterial intimal thickening and is characterised by increased populations of smooth muscle cells, macrophages and lymphocytes, cholesterol deposits and solid layers of connective tissue matrix (as shown in Figure 1.2).

In the developmental stages of atherosclerosis, the earliest discernible lesion of atherosclerosis is the fatty streak appearing as a yellow raised area in the lumen of the artery arising from the accumulation of lipid-laden "foam cells" in the intimal layer of the artery [45]. These occur in medium and large-sized arteries and present as a fatty intramural thickening of the subintima that intrudes into the arterial lumen. This process may also affect the vascular network and the aetiology and clinical impact of atherosclerosis may differ from one vascular bed to another. The fatty streak comprises of three main segments. The first is the cellular segment predominately consisting of smooth muscle cells and macrophages. The second is the connective tissue matrix and extracellular lipid. The third segment is the intracellular lipid which accrues within macrophages and transforms them into foam cells [45].

The inflammatory process is further exacerbated by the death of foam cells and is the stimulus for vascular smooth muscle cells (VSMC) migration into the intima. The affected sites are weakened and softened which result in the thickening of the intima by oedematous pads and an increase in extracellular matrix molecules and VSMC collagen. The continued uptake of accumulated LDL molecules by macrophages engenders the additional release of inflammatory cytokines and growth factors propagating a succession of inflammation, lipid deposition and lesion expansion, generating the "atheroma" which is the prelude to atherosclerotic plaque formation [48].

Advanced plaques can be segregated into two types; fibro-lipid and fibrous plaques. The fibrous plaques cause tension within the subendothelial wall and result in a compensatory extension of the muscular wall, as well as developing a fibrous cap concealing the atheromatous core. Necrosis due to tissue damage tends to occur in the atheromatous core generating more tissue debris, and accumulation of proteoglycans, collagen, and lipid laden cells [48]. In the advanced stages of coronary atherosclerosis, a great reduction in lumen diameter is observed due to increased thickening of the wall, loss of elasticity and hardening due to calcification [48]. Plaque rupture resulting in progressive or sudden occlusion of the lumen, as well as the formation of thrombo-embolis, may lead to acute cardiovascular events and complications such as myocardial infarction, stroke and unstable angina.

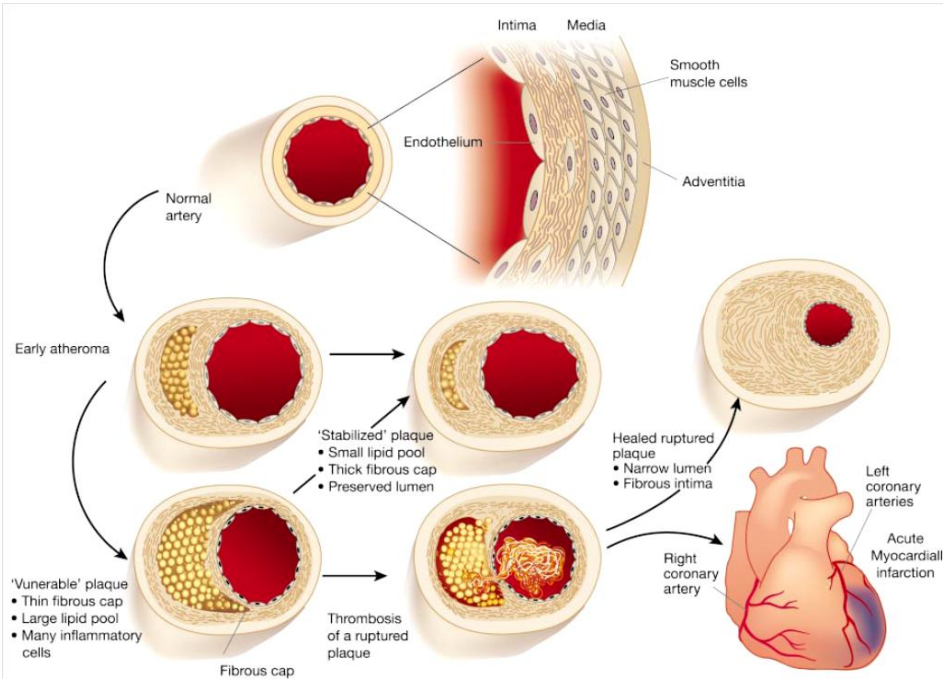

Figure 1.2: Schematic diagram of atherosclerotic plaque formation.
Adapted from reference [50].

1.4.2 Classification of atherosclerosis

There have been many attempts to establish and unify the developmental stages of atherosclerotic lesions. There are slight differences and variations in definitions between systems, and the practical classification of human atherosclerotic lesions is still in the process of development [51]. The American Heart Association Committee on Vascular Lesions of the Council on Arteriosclerosis, has recommended dividing the progression of atherosclerotic lesions, with numbers corresponding to the chronological series of events as shown in Figure 1.3 [51]. The lesions are divided into three main forms; Early (Type I-II), Intermediate (III) and Advanced (IV-VIII) [46,51,52].

Early lesions Type I and Type II represent small lipid deposits in the arterial intima, with Type II lesions often referred to as fatty streaks. Type I is known as the initial lesion consisting of macrophages, scattered foam cells and lipid deposits in the intima [52]. Type II lesions have thicker intracellular matrix mainly comprised of intimal macrophage foam cells in layers, and smooth muscle cells which also contain intracellular lipid droplets, with a lack of extracellular lipid. Type III lesions are known as the intermediate or transitional lesions between fatty streaks and more advanced

lesions. Type III lesions are also known as the preatheroma stage where some extracellular pools of lipid are observed which become confluent and pronounced in Type IV lesions [52].

The Type IV lesion is the first atheroma stage that may result in reportable symptoms, where the intimal structure and the arterial wall are deformed and disorganised. The earliest advanced lesion are characterised by the disruption of the well-defined intimal structure as the dense core of the lesion, consisting of accumulated extracellular lipid, forces the intima to protrude into the lumen of the artery. Macrophages, foam cells, lymphocytes become densely concentrated in the lesion leading to generation of a proteoglycan-rich layer within the intima. Smooth muscle cell migration and proliferation into the lesion may result in the lesion becoming fibrous, as these cells lay down extracellular matrix [46].

When the lipid core from Type IV becomes fibrous, this constitutes the transition to a Type V lesion, defined as fibroatheromas. In Type VI lesions, the arteries are considerably more narrowed than Type VI lesions, and may develop fissures, hematoma and thrombus. In Type VII, calcified regions are seen within the fibrotic lipid core. [46]. The last lesion in this classification is Type VIII. The lumen of the artery is narrowed to a great degree obstructing the blood flow. These lesions are prone to unstable surface defects causing rupture leading to serious complications such as haemorrhage, thrombosis, unstable angina, myocardial infarction, stroke, and sudden death [46,51].

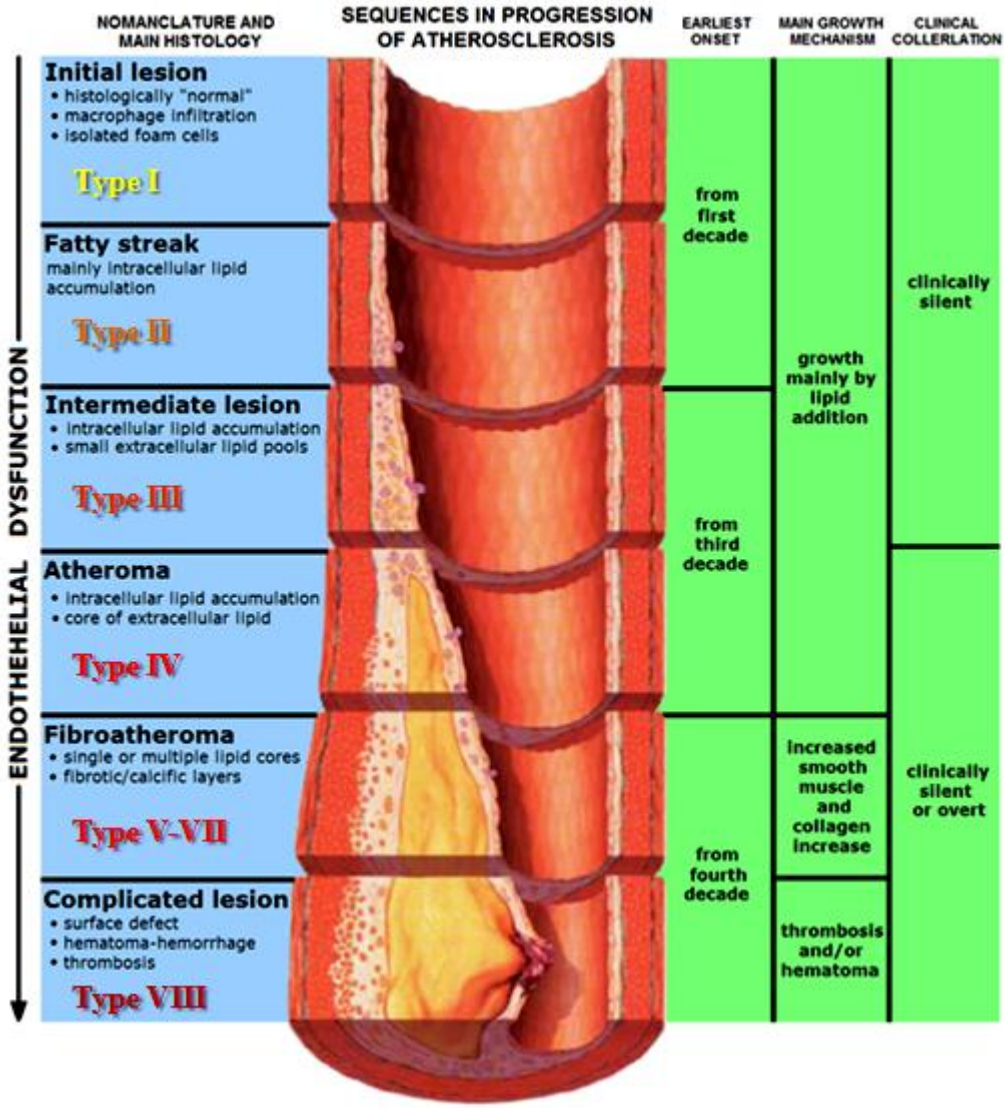

Figure 1.3: Pathological classification of atherosclerotic lesions
Thick and thin arrows represent the relative progression with which lesions develop at specific sites, or they show the relative incidence and magnitude of a pathway segment. Image modified from [53].

1.4.3 Current hypolipidaemic-agents for cardiovascular diseases

Statins are the most effective and widely used treatment for cardiovascular diseases accompanied with hypercholesterolaemia. Many forms of statins are available such as atorvastatin (Lipitor and Torvast), fluvastatin (Lesol), lovastatin (Mevacor, Altocor, Altoprev), pitavastin (Livalo, Pitava), pravastin (Pravachol, Selektin, Lipostat), rosuvastatin (Crestor) and simvastatin (Ezetimibe, Zocor, Lipex). Statins reduce cholesterol levels by inhibiting the enzyme HMG-CoA reductase, which restricts cholesterol synthesis and increases cellular LDL uptake. Statins have also shown to be

effective against atherosclerosis via enhancing endothelial function, sustaining inflammatory responses, preserving plaque stability and preventing thrombus formation. A major side effect is the increased risk of developing diabetes, with greater dosages leading to a more pronounced manifestation.

Fibrates (bezafibrate, cipofibrate, clofibrate, gemfibrozil and fenofibrate) are a class of amphipathic carboxylic acids commonly administered to treat various hyperlipidaemic disorders, predominantly hypercholesterolaemia. They have also been shown to be effective in metabolic syndrome by counteracting dyslipidaemia, lowering LDL and triglyceride levels, increasing HDL, improve insulin sensitivity, and reducing the incidence of Type 2 diabetes (T2D) and hypertension. Fibrates activate peroxisome proliferator-activated receptors-α (PPAR), influencing carbohydrate and fat metabolism and adipose tissue differentiation. They are structurally closely related to the thiazolidinediones (TZDs) which specifically activate PPAR-γ.

1.5 Diabetes mellitus

Diabetes mellitus (DM) embodies a range of metabolic disorders characterised by hyperglycaemia occurring from defects and deficiency in the secretion and / or action, of the hormone insulin. This results in either an absolute deficiency in insulin or a failure of the target organs to respond to increased insulin secretion (“insulin resistance”).

The word diabetes mellitus arises from two Greek words. The first part, *diabainein* meaning “siphon” or “passing through” refers to the characteristic polyuria (increase in the urinary frequency and volume) of this syndrome. The second part *mellitus* relates to honey referring to the high glucose levels in the urine. In addition to polyuria, other characteristic symptoms are a compensatory polydipsia (increased thirst) and polyphagia (increased hunger). Chronic hyperglycaemia in people with diabetes mellitus affects the function of many organs; in particular long-term damage to the eyes (causing potential blindness), kidneys, nerves, heart and blood vessels [54]. People with diabetes are at an elevated risk for cardiovascular, peripheral vascular and cerebrovascular disease [24].

1.5.1 Classification and prevalence of diabetes

According to the World Health Organisation, 171 million people across the globe had diabetes in the year 2000 which accounts for 2.5% of the world population. It is estimated that by 2030 this number will almost double, to affect 366 million people corresponding to 4.4% of the world population [55]. In 2012, it was reported that approximately 4.8 million people died from diabetes, more than 371 million people were living with diabetes worldwide with approximately 50% of these people left undiagnosed [56,57]. The economic cost of diabetes in 2013 has been estimated at approximately 471 billion US dollars [56].

The increase in incidence of diabetes in developing countries follows the trend of increasing urbanisation and the accompanying adoption of Western style diets and more sedentary lifestyles [57]. Indigenous populations have a higher prevalence than their corresponding non-indigenous populations in countries like Australia. The incidence of diabetes is four fold higher amongst indigenous Australians than non-indigenous populations [33].

There are three major types of diabetes: Type I, Type II and gestational diabetes [33]. Type I diabetes (T1DM), previously known as insulin-dependent diabetes, is an autoimmune disease where the immune system destroys the insulin-producing beta cells in the pancreas resulting in a failure to produce and secrete insulin. As a result, replacement insulin via injection is constantly required. T1DM accounts for 5 - 10% of total cases globally, and 10 - 15% in the Australian population, and may appear at any age but is commonly seen before 40 [33]. This type of diabetes may be activated by environmental factors such as viruses, diet or chemicals in people who are genetically susceptible [33,58].

Type II diabetes (T2DM), previously termed as non-insulin dependent diabetes ranges from insulin resistance to an absolute insulin deficiency. It is the most common form of diabetes affecting 90 - 95% of people with diabetes worldwide and 85 - 90% [33] in Australia. This type of diabetes has also been previously termed as late-onset diabetes, however nowadays the occurrence of T2DM has become relatively common in young people [33]. Familial and genetic factors as well as lifestyle factors such as excess weight, inactivity, high blood pressure and poor diet are major risk factors for its occurrence and progression [33]. Thus modification of diet and pattern of physical activity are the principal components of the treatment of T2DM [33]. Pharmaceuticals

are commonly used to treat people with T2DM. The initial stage of T2DM is characterised by hyperinsulinaemia. However, the disease may progress to a stage where there is an absolute insulin deficiency, and where insulin injections may be needed.

For some women, gestational diabetes mellitus occurs during pregnancy and these women are prone to develop type 2 diabetes. It occurs in 1 - 14% of pregnancies depending on the population investigated, and in Australia 5.5 - 8.8% of pregnant women develop gestational diabetes [33]. Risk factors for gestational diabetes may include a family history of diabetes, increased maternal age, obesity and being a member of a socio-economic or ethnic group with an increased likelihood of developing T2DM. Complications from gestational diabetes include babies which are large for their gestational age making vaginal delivery more difficult, hypertension, pre-term birth, uterine bleeding, foetal distress, pre-eclampsia, neonatal hypoglycaemia, respiratory distress and jaundice [33]. The carbohydrate intolerance usually stabilises after giving birth, however the mother has a greater risk of developing T2DM later in life, and the baby is more prone to develop obesity and impaired glucose tolerance later in life [58].

Other causes of diabetes, which are uncommon, include genetic mutations which lead to defects in beta cell function, insulin processing or actions; exocrine pancreatic defects; infections; drugs impairing insulin secretion and some toxins that damage pancreatic beta cells [33].

1.5.2 Pathophysiology and complications of hyperglycaemia leading to micro- and macrovascular disease

Hyperglycaemia is a hallmark of DM and drives an array of changes in the cells of the vasculature, which may be linked to the development and progression of microvascular complications in the retina, renal glomeruli and peripheral nerves. Thus chronic complications may lead to retinopathy and loss of vision, nephropathy leading to renal failure, peripheral neuropathy problems such as ulcers and amputations, as well as autonomic neuropathy causing gastrointestinal, genitourinary, and cardiovascular problems. As well as these microvascular complications, the risk of macrovascular disease, including atherosclerosis in the heart, arms and leg, is higher for people with diabetes [58,59].

1.5.3 Current pharmaceutical agents for diabetes

Anti-diabetic medications and anti-hyperglycaemic agents aim to treat diabetes mellitus by lowering blood glucose levels. Insulin injections used to treat the insulin deficiency of T1D. Oral hypoglycaemic agents such as insulin sensitisers are used to alleviate T2D in people that have insulin resistance. The main types of insulin sensitisers are biguanides (e.g. metformin, phenformin and buformin), the thiazolidinedones (TZD) (e.g. rosiglitazone, pioglitazone and troglitazone) and the sulfonylureas (tolbutamide, acetohexamide, tolazamide and chlorpropamide). Biguanides decrease hepatic glucose output and increase uptake of glucose by peripheral skeletal muscles [60]. TZD bind to PPARγ, a transcription factor mediating the transcription of genes regulating glucose and fat metabolism [61]. Sulfonylureas work by activating the endogenous release of insulin by pancreatic beta cells by inhibiting the potassium ATP channel [61]. Although the action of these compounds is fast, the main side effect is hypoglycaemia accompanied with weight gain and higher risk of death compared to biguanides and TZDs [62]. There are many reported side effects of these drugs including undesirable body weight gain, gastrointestinal discomfort, oedema, anaemia, cardio- and hepatotoxicity and as a result some medications like phenformin, buformin, rosiglitazone and troglitazone have been suspended or withdrawn from use [62]. Metformin is the most commonly prescribed anti-diabetic medication with this reducing the levels of LDL and triglycerides without effects on weight gain or blood pressure [63]. However there are contraindications for these species including renal disease or heart failure due to the risk of lactic acidosis, gastrointestinal disorders, and vitamin B12 deficiency [63,64].

1.6 Obesity: definition

Obesity is characterised by abnormal or excessive fat accumulation in adipose tissue and other organs leading to reduced life expectancy and detrimental health problems [65]. Obesity is related to multiple morbidities, including elevated risk of diabetes, cardiovascular disease, sleep apnoea, and cancer. The body fat level for healthy female is typically 20 - 27% of the total body mass, with the corresponding value healthy males being 15 - 22%. An overweight person generally has 10 - 20% more body mass than normal, with this comprised mostly of fat. Obesity is defined as

greater than 20% more than the normal body mass and morbid obesity is defined as greater than 40% above the ideal weight for one's age and height.

The body mass index (BMI) is a simple index that has been widely accepted by health organisations and health professionals to identify overweight and obese adults. It has been widely used in epidemiological investigations due to its simplicity and is advocated as a screening criterion in the initial clinical assessment of obesity [66]. The BMI is calculated by mass in kilograms divided by the square of the height in metres.

A BMI value less than 18.5 is underweight and is associated with greater health risks with lower BMI readings. A higher BMI than 25 is overweight and increases the risk of health impairment and in particularly greater than 30 is classified obese and is associated with greater health risks with excess fat-related disorders [67]. The severity of obesity is graded into classes I to III, as presented in Table 1.2.

Category	BMI (kg/m2)	Health Risk
Very severely underweight	< 15.0	Extremely high risk
Severely underweight	15.0 – 16.0	High risk
Underweight	16.0 – 18.5	Moderate risk
Normal (healthy weight)	18.5 – 24.9	Most healthy weight
Overweight	25 – 29.9	Moderate risk
Obese Class I (Moderately obese)	30 – 34.9	High risk
Obese Class II (Severely obese)	35 – 39.9	Very high risk
Obese Class III (Morbidly obese)	≥ 40	Extremely high risk

Table 1.2: Health risk according to body mass index (BMI)

1.6.1 Prevalence and causes of obesity

Obesity has become one of the core threats to global health and its prevalence has doubled since 1980 [68]. This occurred in almost every continent is parallel with industrial and economic development that has occurred across the globe (Figure 1.4). In countries like Australia and the United States, the majority of adults now considered to be overweight [67,69], and more than 10% of the world's adult population is obese. Being overweight and obesity now kills more people than undernourishment for the majority of populations [68]. The treatment of obesity continues to set a huge economic burden on the health care system [5].

Childhood obesity is becoming a serious medical and social concern worldwide [70,71]. In 2011, about 40 million children aged five years and under were overweight with more than 30 million children that live in developing countries, along with 10 million children in developed countries judged to be overweight [68]. Type 2 diabetes and cardiovascular diseases once thought to only appear in adults are now observed in obese children [68,70,71,72].

Obesity is the fifth leading risk factor for global deaths, and causes at least 2.8 million deaths in adults annually. Of these, 44% are also burdened with diabetes, 23% with ischemic heart disease and approximately 7% and 41% of cancers are attributed to being overweight or obese respectively [68]. The largest growth in obesity since 1980 has appeared in developing countries, particularly in urbanised groups in Oceania, Latin America and North Africa [65].

The primary cause of obesity is an energy imbalance between the consumption and expenditure of calories. While body fat content can be significantly modulated by genetics and maternal as well as peri-natal factors, the current global rise in obesity is predominantly due to a change to a diet consisting of energy-dense foods. These foods tend to be rich in fat and sugars, low in vitamins and other micronutrients, relatively low cost and widely available [65,68]. Thus, over the past two decades, there has been a global escalation in total calorie intake. In addition to this, epidemiological studies show that chronic consumption of high fat diets, high fructose levels (particularly from soft drinks) and regular consumption of fast food elevates the risk and severity of obesity, along with diabetes mellitus and cardiovascular disease [73,74,75]. The impact is particularly seen in indigenous populations as traditionally, indigenous diets are

abundant in vegetables, fruits and fish in contrast to the cheaper, easily accessible and energy-dense Western-style diets [76,77].

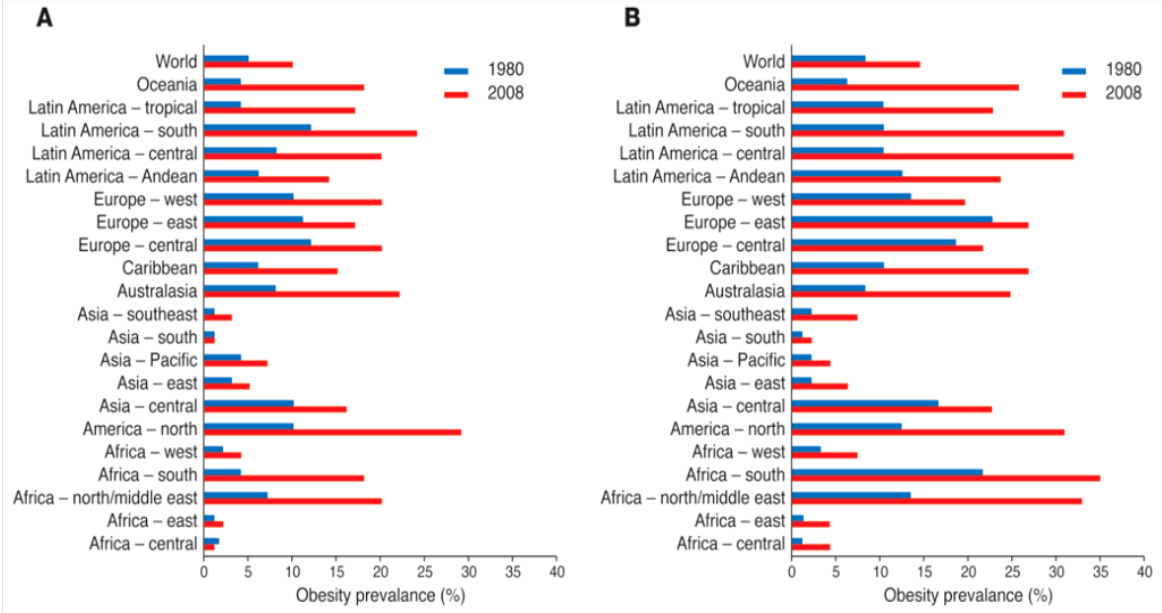

Figure 1.4: Global trends in obesity from 1980 and 2008.
Worldwide obesity prevalence between 1980 (blue) and 2008 (red) in men (A) and women (B). Adapted from reference [65].

1.6.2 Pathogenesis of obesity

Adipose tissue is an active endocrine organ, which primarily consists of cells (adipocytes) that are filled with triglycerides, adipocyte precursors and other stromal cells and resident and infiltrating immune cells, all embedded in collagen network with a rich blood supply [78,79]. The increase in body fat characteristic of obesity may be due to either increases in adipocyte number or cell size. In adipogenesis, mesenchymal stem cells commit to the formation of preadipocytes which undergo a series of cell divisions before proceeding to terminal differentiation and mature adipocytes. Turnover of adipocytes continues into adult life. However, in adult obesity the increase in fat mass is principally attributed to adipocyte hypertrophy rather than hyperplasia (the latter is more typical of pre-pubescent obesity). Adipokines are proteins that are secreted by adipocytes, which work closely to regulate adipose tissue growth and signal other organs to control feeding, energy balance, and other functions.

Lipid droplets are intracellular organelles covered with proteins of the perilipin family, which store neutral lipids in cells [80]. Excess accumulation of intracellular lipids within these organelles has been associated with obesity, diabetes, atherosclerosis and other organ dysfunction [80]. Dysfunction of adiposity in obesity is accompanied with ectopic fat deposition (steatosis), hyperlipidaemia, insulin resistance, diabetes, endothelial dysfunction, cardiovascular complications and other metabolic diseases [78,81].

Monogenic syndromes, rare chromosomal abnormalities, complex molecular interactions between the brain and other organs, and eating disorders have all been proposed as causal agents of obesity [82]. In addition to these, the discovery of leptin was a significant breakthrough in understanding energy homeostasis and its dysregulation in obesity [83]. Leptin is an adipokine which acts on the hypothalamus to inhibit food intake, increases energy expenditure and decreases body fat. Leptin can also modulate blood pressure, heart rate, immunity, sympathetic activities, intermediary metabolism, reproduction, and bone biology. In addition it is considered to be pro-inflammatory agent [83]. Obesity is associated with elevated serum leptin concentrations but also leptin resistance. Conversely, voluntary weight loss, in particularly where this leads to a decrease in adipose tissue mass, results in reduced circulating leptin levels [84]. When secretion of leptin increases, secretion of another adipokine, adiponectin declines. This suppression of adiponectin is believed to result in metabolic impairment. Reduced levels of adiponectin have been shown to contribute to insulin resistance, as adiponectin receptors in hepatocytes and muscle cells help control β-oxidation of fatty acids, glucose uptake, gluconeogenesis and peroxisome proliferator activated receptor (PPAR)-γ activation [85,86]. Further, a decrease in adiponectin production may provide a mechanistic link between obesity and hypertension. Adiponectin stimulates the activity of endothelial nitric oxide synthase (eNOS), the product of which, nitric oxide ($NO^{\cdot}$), is a key mediator of vascular tone, inflammation and smooth muscle cell proliferation. The activation of eNOS by adiponectin stabilizes eNOS mRNA and eNOS phosphorylation. Plasma adiponectin supplementation in adiponectin-deficient mice has been reported to restore endothelial $NO^{\cdot}$ production and vascular wall tone, enhance smooth muscle cell proliferation and decrease leukocyte adhesion [86].

Obesity can lead to a state of systemic, low-grade inflammation. Pro-inflammatory mediators are able to interfere with insulin signalling pathways, thereby reducing responsiveness in insulin sensitive tissues, a key indication of Type 2 diabetes. The inflammatory responses are likely to mediate: (i) infiltration of adipose tissue by inflammatory cells (including monocyte/macrophages and lymphocytes); (ii) the expansion of adipose tissue itself as this is a source of cytokines in addition to adipokines, and (iii) inflammation of the liver in response to either pro-inflammatory signals delivered by portal circulation or hepatic fat accumulation [87,88,89,90,91].

Adipose tissue macrophages are believed to be the major mediators of the chronic systemic inflammation of obesity as these cells are sources of cytokines (such as IL-6) and reactive oxygen species (ROS). Visceral adipose tissue typically contains greater macrophage numbers than subcutaneous adipose tissue, with this being of potential importance because of the key role accumulation of abdominal fat has upon metabolic dysfunction. A number of cytokines have been shown to invoke insulin resistance [85], and in addition cytokine IL-6 stimulates vascular smooth muscle cell production and secretion of angiotensin (AngII) which is as a potent vasoconstrictor, growth factor and stimulant for the generation of reactive oxygen species (ROS) and inflammatory cytokines [92,93]. Production of TNF-α and ROS can be further provoked by free fatty acids, the levels of which are increased during obesity [85,92]. The increase in vascular ROS and cytokine levels may cause endothelial dysfunction (for example by reducing $NO^{\cdot}$ bioavailability) thereby exacerbating vascular inflammation. Furthermore adipokines (including resistin and possibly lowered levels of adiponectin) have been shown to activate the expression of monocyte adhesion molecules (e.g. intracellular adhesion molecule-1, ICAM-1) by the vascular endothelium, as well as monocyte / macrophage chemotactic protein-1 (MCP-1) and colony stimulating factor-1 (CSF-1) which regulates monocyte-to-macrophage differentiation [85,94]. Oxidative stress in turn, suppresses adiponectin secretion and free fatty acid storage by adipocytes and augments the production of MCP-1 [92], thereby creating a vicious cycle of pro-inflammatory changes.

Resistin is a relatively recently discovered adipokine, the molecular properties of which are still in the process of elucidation [95]. The consequences of increased resistin levels in human obesity remain unclear. Resistin has been reported in *in vitro* studies, to impair endothelial function by reducing the expression of eNOS and enhancing the release of the potent vasoconstrictor endothelin-1 [96,97]. Elevated resistin levels, have

also been shown to induce insulin resistance in mice, with this accompanied by elevated blood pressure and hypertension [95]. Resistin is believed to be secreted mainly by adipose tissue macrophages with higher levels detected in obese humans [98,99]. However, the pathophysiological role of circulating resistin in metabolic disturbances in glucose and lipid metabolism its contribution to the progression of obesity-related hypertension is not well established [95].

1.6.3 Current therapeutic agents and interventions for obesity

Anti-obesity medications are used to decrease mass or reduce the rate of mass gain by suppressing appetite, increasing basal metabolism or reducing caloric absorption. The main pharmaceutical drugs for treating obesity are orlistat, lorcaserin, sibutramine, rimonabant, exantide and pramlintide. These are not usually suitable for long term use due to life-threatening side effects such as elevated blood pressure and heart rate, palpitations, glaucoma, drug addiction, restlessness, depression and insomnia. Although orlistat (Xenical) has been recently authorised by FDA for long term use, it has reported side effects of steatorrhea, stomach pain, and flatulence.

Persistent body mass management via lifestyle modifications (i.e. dietary and physical activity) are logical targets for preventing and treating obesity. However, many overweight or obese individuals report that it is very easy to gain but difficult to lose mass and it is known that anti-obesity drugs are not very effective [100]. Bariatric surgery and laparoscopic banding, initially deliver great and rapid weight reduction however many subjects are confronted with substantial weight regain over time. There is therefore a pressing need for a clearer understanding of the molecular pathways behind energy homeostasis and how obesity affects diabetes, atherosclerosis and other complications.

1.7 Causational and mechanistic links (pathogenesis and manifestations) between obesity, diabetes and atherosclerosis

The growing problem of obesity is linked with multiple morbidities, capable of impairing every body system. Obesity is presently the most prevalent cardiovascular risk factor in individuals with confirmed coronary heart disease [101]. Obese people

have a poor quality of life as well as a shorter life expectancy than individuals of healthy body mass [100,101].

Epidemiological studies have revealed that obesity is a major risk factor for coronary heart disease, atherosclerosis, heart failure, atrial fibrillation, ventricular arrhythmias and sudden death [102,103,104]. It is also considered a predisposing causal factor in hypertension, diabetes mellitus type 2, osteoarthritis, obstruction sleep apnoea, dyslipidaemia, gastroesophageal reflux, non-alcoholic fatty liver disease, renal failure and various types of cancers [100,104].

The association between obesity and different forms of cardiovascular disease is complex, due to the presence of a large cascade of interacting factors. Obesity can induce coronary atherosclerosis through well-established mechanisms, such as dyslipidaemia, hypertension, and diabetes [105,106,107]. However, recent evidence has shown that the association between obesity and cardiovascular disease may also include other factors including subclinical inflammation, neuro-hormonal activation with increased sympathetic tone, high leptin and insulin concentrations, obstructive sleep apnoea, increased release of saturated free fatty acids in addition to increases in the volume/mass of subepicardial and abdominal fat deposits. [107,108,109,110].

The mechanisms by which excess fat causes insulin resistance are complex, and are likely to involve several pathways encompassing cytokines, other inflammatory mediators and adipokines. Insulin resistance precedes type 2 diabetes mellitus which can initiate or accelerate atherosclerotic progression. People with diabetes have a substantially greater risk of atherosclerosis and this is true for both genders [111], the increased occurrence also manifests as an acceleration of the rate of disease progression, as well as increasing size and complexity of atherosclerotic plaques [59,112,113]. It is now accepted that this increase in the prevalence and severity of atherosclerosis in people with diabetes includes mechanisms that involve hyperglycaemia [111,112,114]. Four main mechanisms have been proposed to explain how hyperglycaemia invokes or accelerates diabetic vascular complications: increased glucose flux through polyol-sorbital pathway; the hexosamine pathway; formation of advanced glycation end products (AGE); and activation of protein kinase C (PKC) [115]. Conceivably the four pathways may act together in response to common upstream events, most notably oxidative stress.

1.7.1 The poly-sorbitol pathway

Aldose reductases (AR) catalyse the metabolism of glucose to sorbitol, which is then converted to fructose by sorbitol dehydrogenase in the polyol-sorbitol pathway. These reactions are accompanied by the oxidation of nicotinamide adenine dinucleotide phosphate (NADPH) to $NADP^+$, and reduction of nicotinamide adenide dinucleotide (NAD^+) to hydrogenated NAD (NADH) [48].

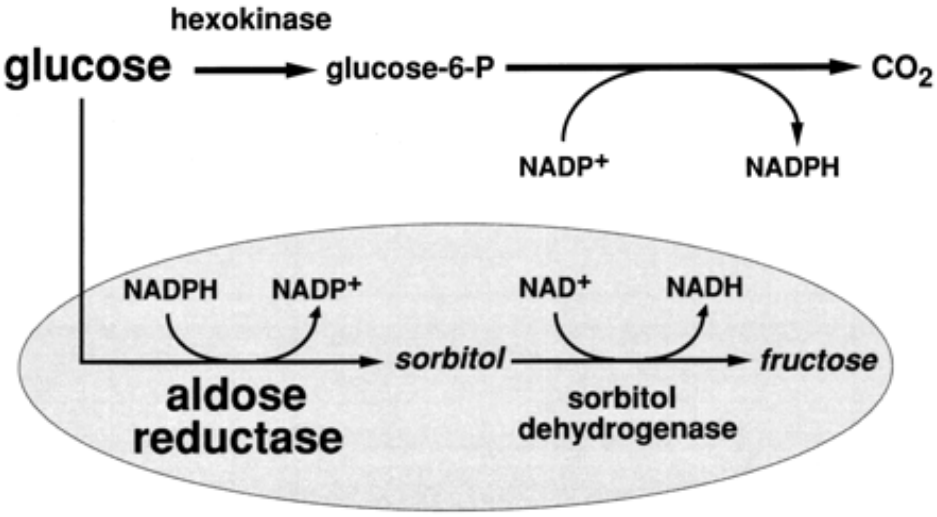

Figure 1.5: Polyol (sorbitol) pathway; glucose-6-P, glucose 6-phosate.
Adapted from reference [116].

High fluxes of glucose through this pathway lead to greater osmotic stress due to increased sorbitol accumulation and reduced radical scavenging capacity due to reduced production of NADPH (an essential co-factor of the antioxidant glutathione peroxidase / reductase system) but also an increase in the cytosolic NADH / NAD^+ ratio and potentially an increase in reductive stress [117,118]. In support of this hypothesis sorbitol and fructose concentrations have been reported to be approximately 9-fold, and the NADH / NAD^+ ratio nearly 4-fold, greater in diabetic hearts [119]. Increased polyol pathway flux may also decrease the production of the antioxidant glutathione by inhibiting glyceraldehyde-3-phosphate dehydrogenase (GAPDH) and elevate triose phosphate concentrations which may leave the cells more prone to oxidative stress and thus promote vascular damage [117]. An *in vivo* study on LDL receptor-deficient diabetic mice showed increased atherosclerotic lesion size when human AR was over expressed in these mice [120]. Inhibition of AR in transgenic rats with over expressed

AR was shown to improve altered glucose metabolism and protect against the progression of long-term diabetic complications [121]. However at this current stage, there is no clinical evidence to support the hypothesis that AR inhibition ameliorates atherosclerosis in people with diabetes, and further studies are required to determine the pathological role of polyol pathway in diabetic atherosclerosis.

1.7.2 The hexosamine pathway

In the hexosamine pathway, fructose-6-phosphate is transformed to glucosamine-6-phosphate and then to uridine diphosphate (UDP)-*N*-acetyl glucosamine via the activity of L-glutamine: D-fructose-6-phophate amidotransferase (GFAT) [122], as shown below. Many substrates for the synthesis of proteoglycans and glycoproteins are generated subsequently.

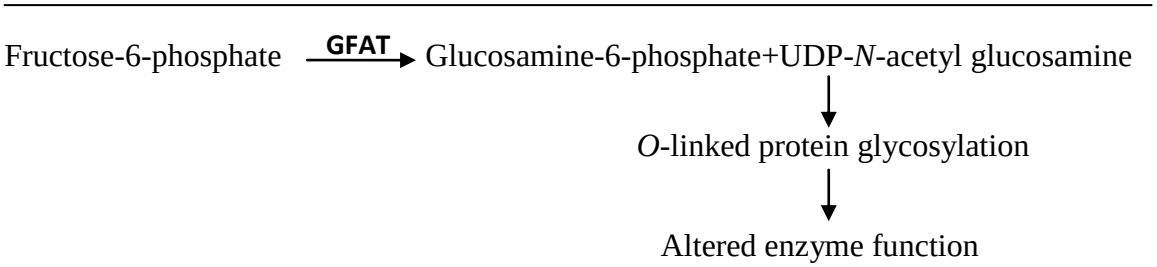

Metabolism of excess glucose via this pathway results in disruption in transcriptional activity and enzyme function. In bovine aortic endothelial cells, increased flux through the hexosamine pathway was found to increase *N*-acetyl glucosamine levels and transcription of pro-inflammatory cytokines, such as transforming growth factor-α (TGF-α), TGF-β1 and plasminogen activator inhibitor-1 (PAI-1) [123]. Although this is one pathway through which hyperglycaemia can initiate and promote atherosclerosis, intraperitoneal administration of glucosamine for 12 weeks to apo $E^{-/-}$ mice was shown to lower atherosclerotic lesion size in the aortic root [124]. Thus the hexosamine pathway may be associated with microvascular diabetic complications but may not have a strong correlation with the development of atherosclerosis. Further studies may clarify the possible mechanistic link between diabetes and atherosclerosis through the hexamine pathway.

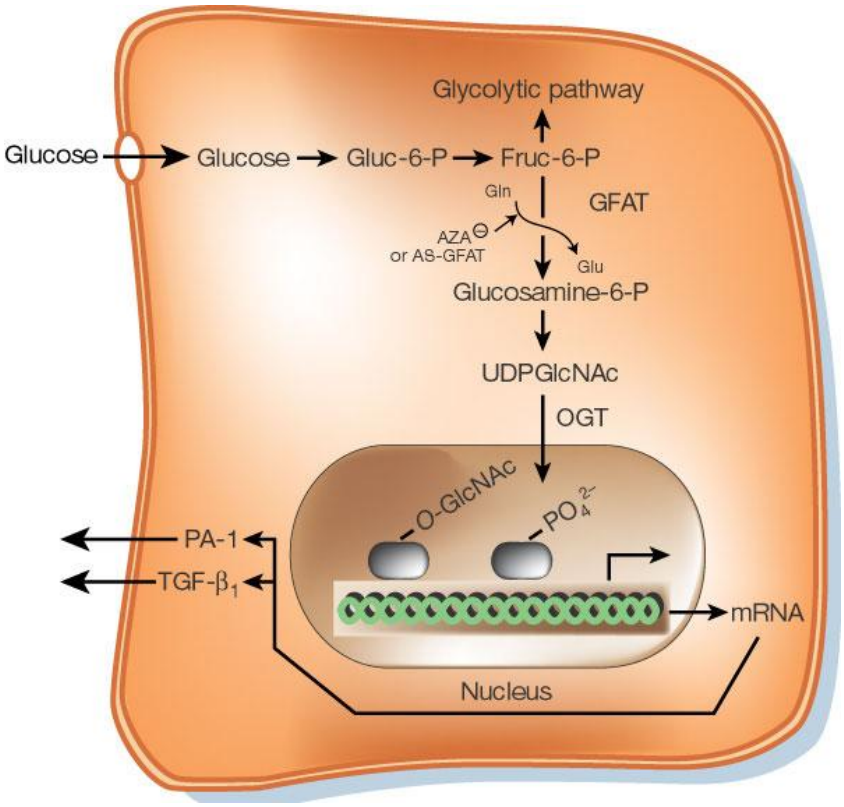

Figure 1.6: The hexosamine pathway.
The glycolytic intermediate fructose-6-phosphate (Fruc-6-P) is converted to glucosamine-6-phosphate by the enzyme glutamine: fructose-6-phosphate amidotransferase (GFAT). Intracellular glycosylation by the addition of *N*-acetylglucosamine (GlcNAc) to serine and threonine is catalysed by the enzyme *O*-GlcNAc transferase (OGT). Increased donation of GlcNAc products to serine and threonine residues of transcription factors such as Sp1, often at phosphorylation sites, increases the production of factors as PAI-1 and TGF-β1. AZA, azaserine; AS-GFAT, antisense to GFAT. Adapted from reference [117].

1.7.3 Protein Kinase C Activation

The protein kinases C (PKC) are a group of enzymes consisting of 12 isozymes. They are important in a variety of cellular activities such as proliferation, contractility, hypertrophy, signal transduction, growth factor transcription and apoptosis [125]. Activation of PKC in diabetes has been implicated in cardiovascular dysfunction by promoting extracellular matrix production, activation of an inflammatory response by cytokine expression and leukocyte adhesion, loss of vascular reactivity, increased endothelial permeability, vascular membrane thickening and angiogenesis [125]. The level of the PKC activator diacylglycerol (DAG) is increased by hyperglycaemia in

endothelial cells by *de novo* synthesis from dihydroxyacetone phosphate (DHAP) and glyceraldehyde-3-phosphate.

DAG may also be indirectly synthesised by the receptor for advanced glycation end products (RAGE) or via the polyol pathway. The activation of the PKCs may lead to numerous proatherogenic effects of these enzymes, such as dysfunction of vascular reactivity and fibrinolysis via elevated plasminogen activated inhibitor-1 (PAI-1) expression and increased redox stress by effects on NADPH oxidases [125]. In hyperglycaemic conditions, PKC also up-regulates adhesion molecules on endothelial cells which would stimulate an inflammatory response. PKC activation in VSMC has been shown to affect mitogenesis, DNA synthesis, and growth factor receptor turnover [126]. PKC activation increases the concentration of transforming growth factor-β which regulates extracellular matrix formation [126]. Inhibition of PKC has been shown to impede or stabilise many vascular abnormalities in diabetes in particularly endothelial dysfunction, a primary initiating factor in atherosclerosis [126].

1.7.4 Oxidative stress

Ninety five percent of oxygen consumption occurs via tetravalent reduction by the cytochrome oxidase system of mitochondria, producing water and ATP. The remaining 5% oxygen is reduced univalently, with electrons added one at a time. This process results in a production of a range of reactive oxygen species (ROS) [48]. ROS consists of free radicals including superoxide, hydroxyl, peroxyl and hydroperoxyl radicals as well as non-radical species such as hydrogen peroxide and hypochlorous acid. Under physiological conditions, any increase in oxidant concentration brings about a compensatory response mediated by several antioxidant enzymes (e.g. superoxide dismutase, catalase, glutathione (GSH) peroxidases, GSH-S-transferases), thiols (e.g. GSH, cysteine, as well as protein-bound thiols) as well as a number of low molecular mass antioxidant compounds including urate, ubiquinol, tocopherol, ascorbate and carotenoids [45, 147].

Oxidative stress can lead to damage to proteins, lipids, carbohydrates and nucleotides including DNA [125] leading to cell dysfunction. ROS may alter endothelial function by peroxidation of membrane lipids, modulated gene expression and by decreasing the bioavailability of $NO^{\cdot}$. The latter may occur as superoxide can react with $NO^{\cdot}$ (at rates comparable to the spontaneous dismutation of superoxide to hydrogen peroxide) and yield the potent oxidant peroxynitrous acid and consequently augmented peroxidation, oxidation of other molecules and protein nitration [127]. ROS are also capable of oxidising LDL [49,128,129,130]. Superoxide and peroxynitrous acid may be critical mediators of pancreatic cell death, potentially leading to atherosclerosis and heart failure [131]. In the context of diabetes, Brownlee has argued that increased mitochondrial production of superoxide under conditions of hyperglycaemia may represent a common underlying mechanism for increased activity of the aldose reductase, hexosamine and PKC pathways [115,117,132]. Thus if oxidative stress does play a key role in the diabetes-induced atherogenesis it would be expected that development and progression of the disease would be inhibited by antioxidant therapies. However, supplementation studies with vitamin C and E and β-carotene have been unsuccessful in confirming the potential retardation of cardiovascular disease progression [133,134].

1.7.5 Glycation, glycoxidation reactions and the formation of advanced glycation end products (AGE)

One of the potentially most important effects of diabetes-induced hyperglycaemia is the non-enzymatic reaction between glucose and proteins leading to the production of advanced glycation end products (AGE) [120]. AGE are adducts that are formed on proteins, lipids or DNA bases after exposure to glucose or reactive aldehydes [135]. The non-enzymatic chemical reaction between glucose and proteins is known as the Maillard or browning reaction, and generates Schiff's base (early glycation products), Amadori products and eventually AGE. Reactive aldehydes such as methylglyoxal, 3-deoxyglucosone and glyoxal, the levels of which are increased in people with diabetes, are key intermediates in the development of "carbonyl stress" and AGE formation [117].

Wolff and Dean have shown that the non enzymatic reaction of sugars with protein entails three processes as follows [136]:

1) Glycation- the non-oxidative, covalent, addition of sugar to the protein;

2) Auto-oxidative glycosylation- free radicals, arising from glucose auto-oxidation, interacting with proteins; and

3) Auto-oxidation of protein-bound sugars produced as a consequence of glycation.

The two auto-oxidative processes are known as glycoxidation and these processes lead to formation of AGE [115]. There is increasing evidence that AGE formation plays a major role in diabetes associated cardiovascular disease and particularly atherosclerosis. The accumulation of AGE is not just a hallmark of hyperglycaemia, as it also entails a combination of metabolic burden (both hyperglycaemia and hyperlipidaemia), oxidative stress and inflammation resulting in detrimental effects on vascular tissue [137].

Alteration of extracellular and intracellular proteins due to AGE formation may distort their role and function by a number of mechanisms including cross-linking of molecules (including these of the extracellular matrix, ECM) structural modifications or adduct formation which leads to a loss of enzyme activity and by binding to the receptors present on various cell types, such as endothelial cells, macrophages and vascular smooth muscle cells which are critical in atherogenesis [120].

Accumulation of AGE has been demonstrated in both the microvascular and macrovascular complications of diabetes, and thus may contribute to progression of atherosclerosis [135]. AGE accumulate with increasing age of the vessel wall and have been noted to accelerate the development of DM, potentially engendering plaque formation by interfering with the function of endothelial cells which line the artery walls [125]. AGE formation can interrupt molecular communication and may modify enzymatic activity and may lead to damaging effects in accelerating atherosclerosis via both non-receptor mediated and receptor-mediated mechanisms [120].

Cross-links may be formed between molecules in the basement membrane of the extracellular matrix and with the receptor for advanced glycation end products (RAGE) [135]. Activation of RAGE by AGE causes up-regulation of the pro-inflammatory transcription factor nuclear factor-κB and thus its target genes [135]. Soluble AGE activates monocytes, and AGE in the basement membrane may disrupt monocyte function and exacerbate the production of reactive oxygen species [132,138,139]. Because of the emerging evidence implicating AGE in damage to the vasculature of

patients with diabetes, a number of different therapies to inhibit AGE are under investigation [135,139].

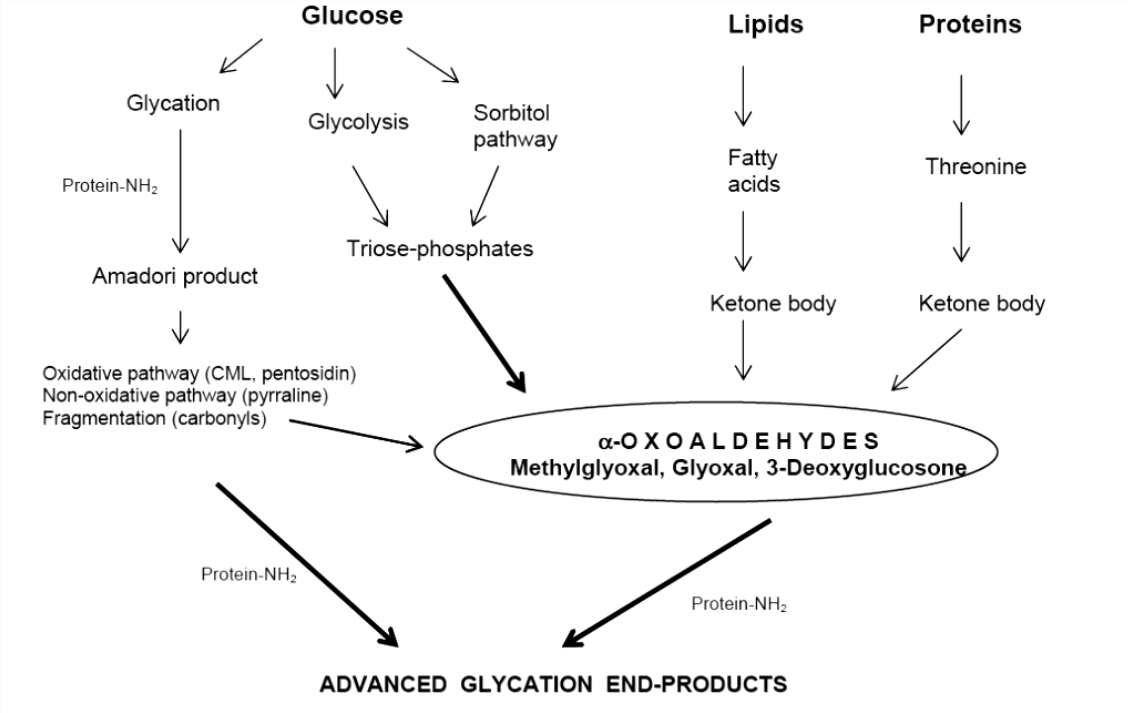

Figure 1.7: Reaction scheme for reactive carbonyl biogenesis.
Adapted from reference [140].

1.7.5.1 Nature and mechanism of formation of AGE

The rate of turnover of glycated or glycoxidised proteins, the extent of hyperglycaemia, the degree of oxidative stress and duration of exposure to these various stimuli, are all critical factors in the formation and accumulation of AGE [115,135,141,142].

The initial step in AGE formation is the reduction of a carbonyl group on (or from a) sugar molecule with protein (or nucleic acid) amino groups, resulting in the formation of chemically-reversible, Schiff base adducts [135]. These Schiff bases can undergo a slow chemical reorganisation (Amadori rearrangement) into a chemically reversible, 1-amino-1-deoxy-2-ketose or ketamine (e.g. fructosyl-lysine or fructosamine). During the Amadori rearrangement, highly reactive species known as α-carbonyls or oxoaldehyde products, such as 3-deoxyglycosone and methylglyoxal (MGO), are generated [143]. Similar reactive carbonyls can be generated as a result of lipid oxidation. The build up of these products is termed carbonyl stress. These α-

dicarbonyls are also capable of reacting with amine, sulfhydryl, and guanidine, functional groups on proteins. Amino acid side chains that react with carbonyls include Lys, Arg, His, Trp and Cys with these reactions contributing to the functional impairment of proteins [144]. Collectively, these reactions lead to denaturation, browning and cross-linking of targeted proteins [141,145]. The reactions between α-dicarbonyls with Lys and Arg functional groups on proteins, result in the production of stable fluorescent and non fluorescent AGE compounds such as N^{ϵ}-(carboxymethyl) lysine (CML), pentosidine, hydroimidazolones, N^{ϵ}-(carboxymethyl) lysine, a homologue of CML; and methylglyoxal lysine dimer (MOLD) [135,145,146]. AGE formation is poorly or non-irreversible due to the highly stable AGE-based crosslinks which are resistant to enzymatic degradation [135,141]. Crosslinking and denaturation of proteins triggered by glycation are common features implicated in aging linked with diabetic, vascular, renal, respiratory, rheumatoid and other chronic disorders [143,147,148].

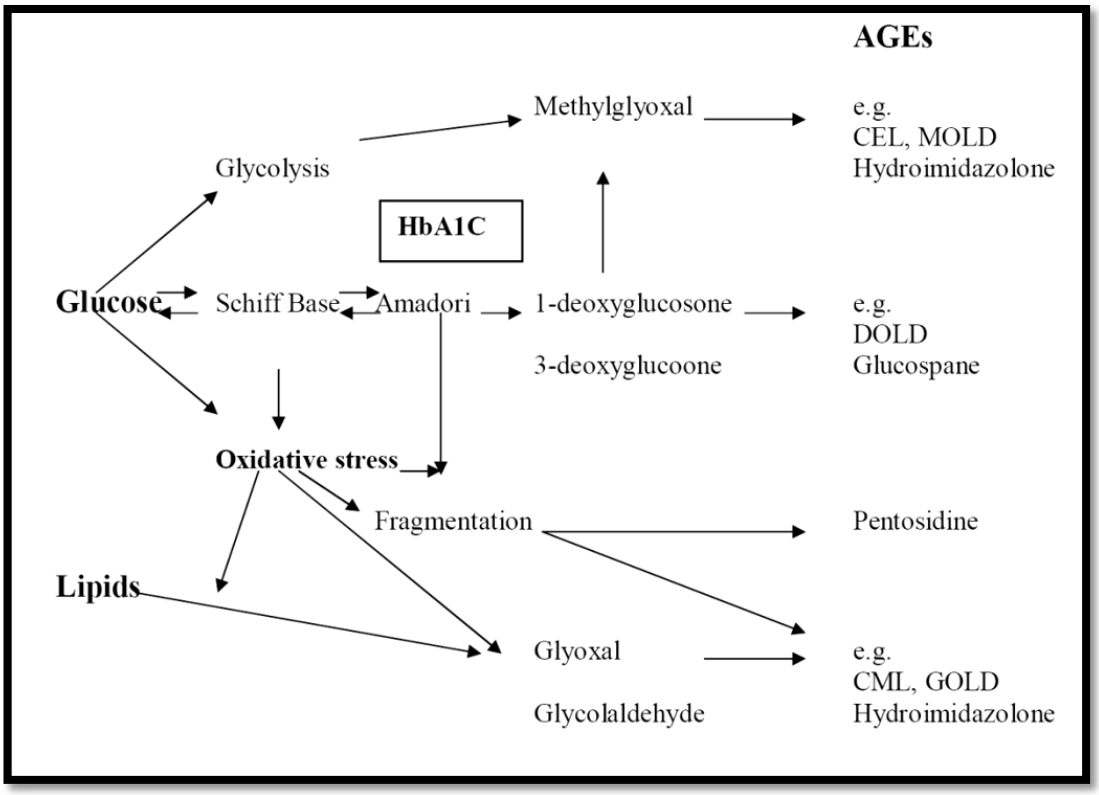

Figure 1.8: Schematic representation of the complex Maillard reaction and formation of some advanced glycation end products.
CEL = carboxyethyllysine; MOLD = methylgloxal lysine dimer; DOLD = 3-deoxyglucosone lysine dimer; CML = carboxymethyllysine; GOLD = glyoxal lysine dimer. Adapted from reference [137].

1.7.5.2 LDL glycation / glycoxidation

Glycation of apolipoprotein component of LDL occurs via Lys, Arg and other residues [149]. The initial reactions result in the formation of Schiff's bases, that may react further to give a more stable fructosamine that is characteristic of early-stage glycated proteins [150]. Chemical modification of Lys residues of apolipoprotein B-100 by the related process of acetylation is known to cause poor recognition by lipoprotein receptors including the native LDL receptor (LDL-R). In contrast these modified species are readily recognised by macrophage scavenger receptors resulting in rapid internalisation of glycated / glycoxidised LDL may further initiate various other processes that are involved in atherogenesis. Glycation of LDL may favour oxidative modifications as glycated LDL can augment inflammatory cell chemotaxis and formation of superoxide radicals by macrophages [150]. In endothelial cells, glycated LDL inhibits shear stress-mediated L-arginine uptake and $NO^{\cdot}$ production, and stimulates secretion of plasminogen-activator inhibitor-1 and prostaglandins, whilst preventing the expression of tissue plasminogen activator [149,150].

There is increasing evidence that AGE play a pivotal role in atherosclerosis and increased AGE accumulation is closely associated with the development of cardiovascular complications of diabetes [137]. AGE-forming reactions can cause modifications to the structure of LDL that are recognised by the scavenger receptors of macrophages. These processes can contribute to a build up of cholesterol and cholesteryl esters within macrophages and foam cell formation [151]. The LDL modifications required for cellular recognition and unregulated uptake are not completely understood and carbonyl stress may play a significant role in facilitating the formation of foam cells and vascular complications of diabetes.

1.7.5.3 Inhibition of glycation and glycoxidation reactions

A number of inhibitors of AGE formation have been identified and more are being developed, which act through preventing glycation / glycoxidation reactions, scavenging the reactive 1,2-dicarbonyls or reversing AGE modifications [135]. Some of these are in advanced clinical trials [152,153,154]. These potential AGE inhibiting drugs include: aminoguanidine, metformin, carnosine, homocarnosine, pyridoxamine, *N*-[2-(hydrazinoiminomethyl)amino)ethyl] acetamide monohydrochloride (ALT-946),

4-oxo-*N*-phenyl-4,5-dihydro-2-[(1-methylethylidene)hydrazino]-5-thiazoleactamide (OBP-9195), alagebrium chloride, and *N*-phenacylthiazolium bromide [155]. Anti-inflammatory drugs such as tenilsetam and aspirin also exhibit AGE-inhibiting properties [154,156]. Antioxidants may also operate as AGE inhibitors, via metal-ion chelation and direct scavenging of free radical species.

Inhibition of glycation and glycoxidation reactions can occur via multiple different modes of action such as: blocking free amino groups on proteins; blocking carbonyl groups on reducing sugars, Amadori products and dicarbonyl intermediates such as methylglyoxal; blocking Amadori products by antibodies with high specificity; chelation of transition metals to prevent glycoxidation; scavenging of free radicals derived from autoxidative glycoxidation; deglycation of Amadori products; reversing AGE accumulation by AGE-cross-link breakers; and inhibiting AGE interaction with RAGE by RAGE blockers [157,158]. In order to carry out such actions, these compounds would require long plasma or tissue half-lives, and minimal side effects, to be of therapeutic use as they would need to be prescribed for long periods due to the slow and chronic progression of the targeted reactions [157]. Inhibition of AGE may be therapeutic significance in numerous diseases and attempts to block the deleterious effects of AGE are still in an experimental phase. Some of the current drugs have harmful side effects as well as beneficial actions [158,159,160,161]; these actions are discussed in greater detail below.

1.7.5.3.1 Aminoguanidine

Aminoguanidine (Pimagedine) has been investigated as a potential therapeutic therapy for the treatment of microvascular complications of diabetes and also as an effective scavenger of methylglyoxal [157]. It removes toxic 1,2 dicarbonyl compounds via conversion to their respective 1,2,4-triazines, which are less toxic compounds. Aminoguanidine has other potential effects in suppressing oxidative stress, via peroxynitrite scavenging and transition metal ion chelation [156]. Several clinical trials have demonstrated the capacity of aminoguanidine to reduce AGE accumulation and the development of the complications of diabetes [158,162]. However the drug has a relatively short half life of four hours which restricts its effectiveness and requires administration in multiple doses over a day. Severe toxicity and adverse reactions were reported in Phase III clinical trials in diabetic recipients, and this material is therefore

unlikely to undergo further trials [163]. A small percentage of the patients developed flu like symptoms, headaches and nausea in human trials. However after a longer duration, macrocytic anaemic was observed in a significant proportion of the patients and antinuclear cytoplasmic antibodies were developed with high doses of aminoguanidine [158].

1.7.5.3.2 Carnosine

Carnosine (β-alanyl-L- histidine) is a naturally occurring dipeptide that contains the β-isomer of alanine (3-aminopropanoic acid) and histidine (2-amino-3-(1H-imidazol-4-yl)propanoic acid). A number of *in vitro* studies have suggested that carnosine has anti-oxidant, anti-ageing, buffering and immune regulation properties [164]. It is synthesised endogenously and is present in high concentrations in skeletal muscle at approximately 5 - 8 mM [165]. Carnosine and associated dipeptides are highly expressed in skeletal muscle, and are detectable in cardiac muscle and brain (particularly in the olfactory lobe). However, it has not been found in the lung, spleen, kidney, adrenal, prostate and thyroid glands, colon or pancreas [166]. In humans intestinal hydrolysis is readily saturated so that a significant proportion of the intact dipeptide is absorbed [167]. Plasma levels of the intact dipeptide are however low or undetectable due to its rapid degradation by the plasma enzyme carnosinase [166]. Carnosine has been proposed to have a number of actions. It is an effective physiological buffer, neuroprotective and neuromodulatory agent, regulates Ca^{2+} sensitivity, has antioxidant activity, and may prevent and or reverse Malliard reaction-type modifications to cell and tissue proteins [168,169,170]. Carnosine has been also detected in the eye lens [171] and potential carnosine-supplementing strategies, via lubricant eye drops containing N-acetylcarnosine (NAC), have been reported to alleviate vision impairment due to Type 1 and 2 diabetes [172,173,174]. NAC eye drops are currently available commercially [175], however the evidence as to whether carnosine delays or attenuates cataractogenesis is preliminary.

1.8 Removal of glycation and glycoxidation products

The maintenance of cellular homeostasis requires cellular organelles to be synthesised and assembled when required, but it is especially critical for these cellular

components to be degraded when they are in excess or damaged. Autophagy is a lysosomal process involved in sustaining cellular homeostasis and it is responsible for the turnover of long lived proteins and organelles that are functionally redundant or damaged. Consequently if the degradation process does not occur efficiently, cellular metabolism may be perturbed and cells may die or transform into a cancerous cell in which growth progresses uncontrollably. Chaperone-mediated autophagy is another lysosomal protein degradation system which is responsible for eliminating cytosolic proteins holding a lysosomal targeting code. This involves detection by a specific chaperone in the cytosol that transports the cytosolic proteins to the lysosomes to be engulfed and degraded [176]. Research on macro autophagy is beginning to highlight the significance of this process in cellular homeostasis in many diseases such as cancer; infectious, neurodegenerative, metabolic and cardiovascular diseases [176].

1.8.1 Proteasomes

The ubiquitin-proteasome pathway is involved in the degradation of short-lived proteins. Proteasomes are very large protein complexes which can be observed in the nucleus and the cytoplasm of eukaryotes [177]. The major role of the proteosome is to degrade unrequired or damaged proteins by proteolysis, with a particular role in degrading short-lived proteins. Proteasomal degradation is the main mechanism by which cells regulate the concentration of specific proteins and degrade misfolded proteins. Proteins targeted for degradation are tagged with ubiquitin, a small protein. A polyubiquitin chain is formed as the initial bound ubiquitin recruits other ligases to append additional ubiquitin molecules [178]. Proteasomes generate peptides of approximately seven to eight amino acids in length, which are further degraded by other peptidases into single amino acids that are utilised in producing new proteins.

The structure of the proteasome is a large complex tube consisting of four stacked rings around a central axis, with each ring comprised of seven separate proteins. The inner two rings are composed of seven β subunits which contain six protease active sites, directed towards the central axis [178]. The outer top and bottom two rings consist of seven α subunits which control the gate by which proteins enter the tube. The regulatory components on the α subunits identify the polyubiquitin tags connected to the protein substrates and initiate the degradation progress [178]. The ubiquitination and proteolytic degradation is known as the ubiquitin-proteasome system (UPS) which is

responsible for the regulation of many essential cellular processes, such as the cell cycle, regulation of gene expression and responses to oxidative stress [178].

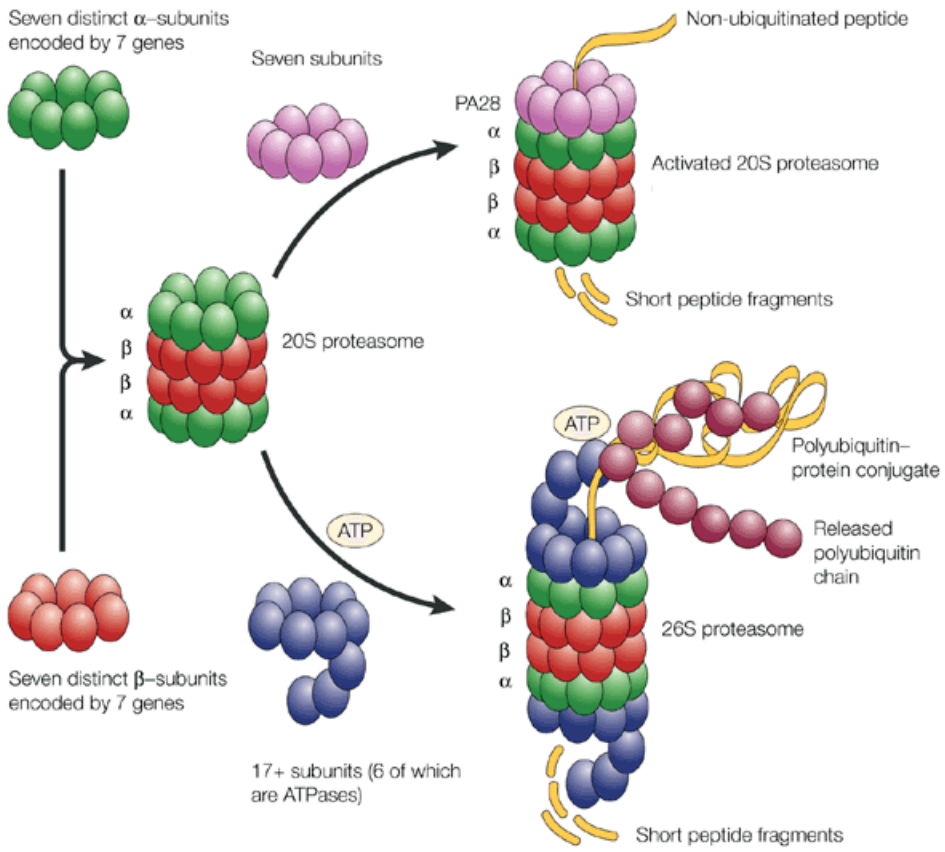

Figure 1.9: The structure of proteasomes and the protein degradation pathway. In the ubiquitin-proteasome pathway, energy from ATP is used to tag an unwanted protein with a chain of ubiquitins marking it for destruction. The protein is then hydrolyzed into small peptide fragments by the proteasome. Adapted from reference [179].

1.8.2 Lysosomes

Lysosomes are single membrane-bound organelles synthesised by the Golgi apparatus that contain, amongst other agents, a large range of hydrolases that degrade endocytosed materials and cellular debris. The approximate size of the lysosome is between 0.1 and 1.2 μm. The name lysosome is derived from the Greek word *'lysis'* means to separate and *'soma'* defining to the body, indicating this organelles' proficiency in degrading a number of biological macromolecules and particles.

The core role of the lysosome is in autophagy as they digest excess or exhausted organelles, food particles, engulfed viruses and bacteria. This occurs as lysosomes fuse with particle-containing vacuoles and discharge their contents into the vacuoles. The digestive enzymes of the lysosomes are optimal at a pH of ~4.5 which is considerably more acidic than the cytosol (pH 7.2). This shift in pH is brought about by the activation of proton pumps that acidify the enclosed compartment leading to the generation of secondary lysosome that degrade the particles. The membrane of the lysosomes protects the cytosol from leakage of hydrolases, peptidases (such as the cathepsin family) and other degradative enzymes as these enzymes are pH sensitive and do not function properly in neutral to alkaline environment.

Cathepsins are lysosomal peptidases categorised in four main classes; aspartic, metalloprotease, serine, and cysteine proteases [180]. Cathepsin D and E are aspartyl proteases, cathepsin III is a metalloprotease, cathepsins A and G are serine proteases, and cathepsin B, C, F, H, I, J, K, L, M, O, P, Q, R, S, T, U, V, W, X, Y and Z are cysteine proteases [181,182,183,184]. Cathepsin B, L and the aspartyl protease cathepin D are the most abundant lysosomal proteases with lysosomal concentrations as high as 1 mM [140].

The main mechanism of action of these proteases involves nucleophilic reaction at the carbonyl-carbon of the amide bond. In the serine and cysteine proteases HO- and HS- side chains, respectively behave as nucleophiles. While in aspartic and metallo-proteases, aspartate residues or metal ions, bind and polarise a water molecule in which the oxygen atom functions as the nucleophile [140,182,185].

1.8.2.1 Lysosomal cysteine proteases

Cysteine-dependent cathepsins have been reported to play a major role in the development and progression of cardiovascular disease. They are implicated as having major roles in ECM remodelling and lipid metabolism [180,181]. Cathepsins have the capability to degrade LDL and decrease cholesterol efflux from macrophages, exacerbating foam cell formation. *In vitro* studies have shown that cathepsins V, K, S, K, L and B possess high elastolytic activity [180,186,187]. Human macrophages secrete cathepsins B, L and S which are found to be localised in macrophage-, smooth muscle cell- and lipid-rich areas in advanced stages of atherosclerosis [180,188]. Cathepsin L

and S were also highly expressed in both human and murine atheroma [187,188,189,190]. Cathepsin B protein levels were increased in atherosclerotic lesions of apo $E^{-/-}$ mice [190], and *in vivo* cathepsin-knockout studies has shown that deficiency of cathepsin K or S reduces atherosclerosis [180,187,191,192,193]. A suppression of cathepsin S was shown to arrest and stabilise atherosclerotic plaque in apo $E^{-/-}$ and LDL-$R^{-/-}$ mice that were fed a high fat diet [192,193,194]. Cathepsin K has been shown to be heavily involved in the turnover of ECM proteins in organs, and this enzyme has been reported to play a significant role in cardiovascular disease, inflammation and obesity [195]. Although the data is still preliminary, cathepsins B, L and S may serve as important biomarkers or imaging tools in the diagnosis of atherosclerosis [180,182].

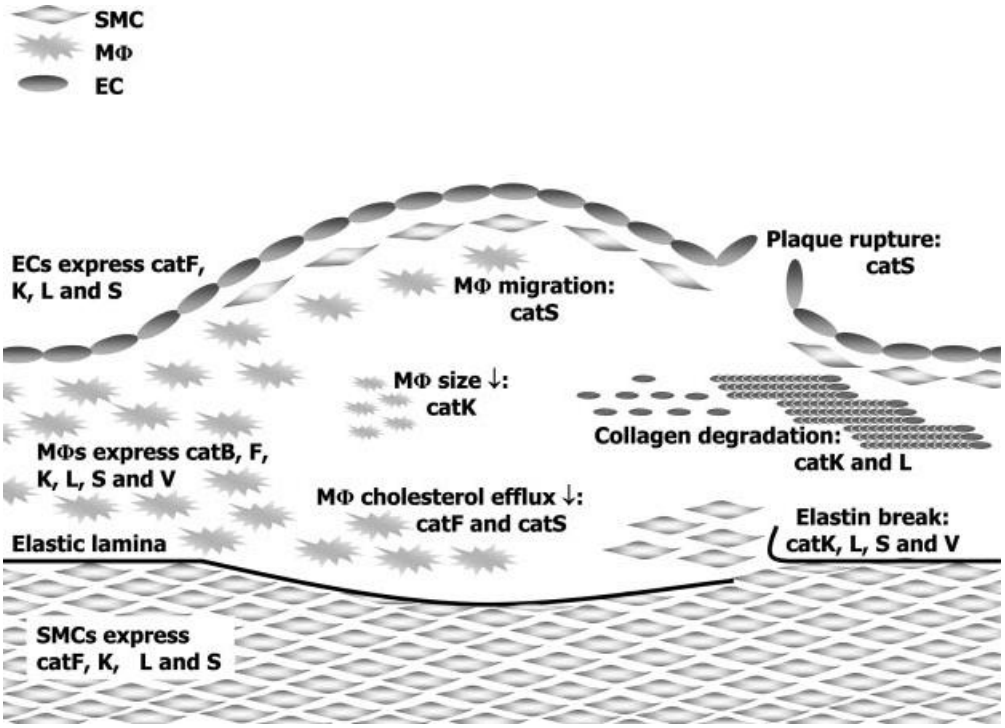

Figure 1.10: Overview of cathepsin expression and activity in atherosclerotic plaque.
Cathepsins are observed in endothelial cells (EC), smooth muscle cells (SMC) and macrophages (M). The ECM consisting of elastin and collagen, is degraded by cathepsin L, K, S and V. Cathepsin S may engender plaque rupture. Cathepsin F and S may influence macrophage foam cell formation by decreasing cholesterol efflux which is counteracted by cathepsin K due to elevation of lipid uptake. Adapted from reference [180].

1.8.2.2 Lysosomal aspartic proteases

The lysosomal aspartic protease Cathepsin D is the major endopeptidase of the lysosomal compartment [184,196]. Cathepsin D has been postulated to play a role in many diseases such as cancer, Alzheimer's disease, and atherosclerosis [197]. A number of studies have found that cathepsin D levels represent an independent prognostic factor in many forms of cancers, and this enzyme is a potential target of anti-cancer therapy [197,198]. It has been shown that expression of cathepsin D is decreased in macrophages of low HDL cholesterol subjects, and thus it may be associated with intracellular metabolism and transport of phospholipids and cholesterol [199]. Cathepsin D may also be significant in LDL degradation. Smooth muscle cells and macrophages generate cathepsins that are able to degrade native but not modified LDL resulting in an accumulation of modified LDL in the vessel wall, engendering foam cell formation and accelerated atherosclerosis [200].

Macrophage lysosomal dysfunction may result from the inactivation of lysosomal cysteine and aspartic proteases with this resulting in impaired degradation of modified proteins and LDL. Hyperglycaemia may also inhibit lipases, rendering these unable to degrade cholesterol esters from the lipoproteins causing accumulation of LDL derived material within the lysosomes. This could lead to cellular cholesterol accumulation generating macrophage foam cells and thus contributing to plaque development due to hyperglycaemia.

1.9 Animal models of macrovascular complications of diabetes and obesity

While T1DM accounts for only around 5% of all DM cases, many of the animal models of diabetes associated atherosclerosis resemble this condition. These animals are produced either by treatment with drugs such as streptozotocin (STZ) or a genetic modification to induce T1DM [201]. T2DM is the main form of DM as it accounts for approximately 95% of DM cases. Most of these T2DM mice have been generated by either a genetic approach or via the use of high fat / sucrose diets [201].

Hyperglycaemia and hyperinsulinaemia are two hallmarks arising from insulin resistance commonly seen in T2DM animal models. Another important manifestation of insulin resistance is dyslipidaemia, marked by an elevation of VLDL, triglyceride levels and a reduction of HDL cholesterol levels, collectively known as the metabolic

syndrome. T1DM have very similar hyperglycaemic complications to T2DM. Therefore a suitable mouse model that closely resembles both types of diabetes in humans and atherosclerosis are required to study mechanistic links and allow the development of strategies to prevent and effectively treat hyperglycaemic complications.

1.9.1 The apolipoprotein E knockout mice

Apolipoprotein E (apo E) is one of several lipoprotein transfer proteins. The main role of this protein is the mediation of receptor-mediated lipoprotein elimination from the blood. Human apo E consist of 317 amino acids, with an 18-amino acid signal peptide arrangement that when cleaved produces the 299-amino acid mature apo E detected in plasma [202]. Apo E is a glycoprotein with a molecular size of around 34 kD that is synthesised in the liver, brain and other tissues in both humans and mice. It serves as the principal ligand for the LDL receptor mediated removal of lipoprotein remnants from the circulation [203]. Apo E was the first lipoprotein transport gene to be deleted via gene targeting in mice. The apo $E^{-/-}$ mouse is amongst the most intensely-expressed phenotypes seen in lipoprotein transport transgenic and gene knockout mice, providing 100% viability of animals lacking apo E [202].

Many studies have used apo $E^{-/-}$ mice to study the pathogenesis and anti-atherogenesis potential of pharmacological interventions. The lesions seen in these mice when fed a high fat Western style diet mimic morphologically the atherosclerotic lesions observed in humans [204,205,206]. Other mouse models of atherosclerosis fail to show the progression of atherogenic stages seen in humans. Significant hypercholesterolaemia develops in apo $E^{-/-}$ mice when fed a low fat chow diet [203]. This finding implies that apo $E^{-/-}$ results in increased sensitivity to dietary fat and cholesterol. Atherosclerosis in the murine aorta was reported to almost have a linear relationship with growth of plaque area and time [207]. Hence the apo $E^{-/-}$ mouse offers many desirable attributes for studying genetic diseases and currently is one of the most appropriate models for atherogenesis.

Many studies have shown that the apo $E^{-/-}$ mice treated with STZ have aortic lesions that are increased in area by greater than fivefold due to the presence of diabetes, which increases serum glucose and cholesterol by up to three fold [205,208,209,210,211]. Similarly, STZ treatment of apo $E^{-/-}$ mice has been shown to

increase the occurrence of premature calcified cartilaginous areas [212]. The use of STZ treatment in apo $E^{-/-}$ mice has also been reported to accelerate atherosclerosis and macrophage-derived foam cell formation via a glucose-dependent mechanism [213].

The STZ-induced atherosclerotic apo $E^{-/-}$ mouse model displays three common features which serve as a useful model in diabetes-associated atherosclerosis. These include the maintenance of hyperglycaemic condition, the presence of accelerated atherosclerosis with increased atherosclerotic regions, and dyslipidaemia with elevated levels of lipoproteins LDL, VLDL, and triglycerides irrespective of feeding chow or a high fat diet.

1.9.2 Animal models of obesity and related metabolic disorders

T2D and insulin resistance are one of the most predominant forms of metabolic disease, and many animal models have been used to examine the pathogenesis of insulin resistance and diabetes-associated metabolic complications.

Models of obesity with T2D are mainly divided into two groups; a mutation in the leptin or leptin receptor gene and polygenic models. Rodents with a mutation, in or deficiency of, the leptin receptor such as the Zucker rats, ob/ob mice, and db/db mice are widely used for T2D research [214]. Db/db mice are the most widely used mice for T2DM research. These mice have a leptin receptor mutation (Lepr (+/+ C57BL/KsJ) that develop T2D, along with increased systolic blood pressure, obesity and hyperlipidaemia, which are also manifested in humans. The db/db mice tend to over consume and do not develop T2D until approximately weeks 9 - 10 and develop more advanced T2D by week 14 with severe hyperglycaemia, requiring insulin injections for survival [215]. By week 20, these mice develop advanced renal dysfunction with declining glomerular filtration rate (GFR) and proteinuria.

The leptin-deficient (ob/ob) or obese mouse develops even more severe renal structural damage and function [216]. However, the db/db mice do not develop atherosclerotic lesions regardless of the manifestations of obesity, hyperlipidaemia, hyperglycaemia, advanced kidney disease and cardiomyopathy [210]. These mice are relatively resistant to the development of atherosclerosis unless they are cross-bred with a vulnerable genetic background, such as the apolipoprotein E-deficient (apo $E^{-/-}$) and LDL receptor (LDL-R) deficient mouse strains [209,210]. Hence, the db/db and ob/ob

leptin deficient mouse models may be more appropriate models for diabetic nephropathy disorders and obesity resulting from T2D.

Obesity models due to leptin signalling abnormalities display microvascular complications that are commonly observed in humans, such as diabetic retinopathy and nephropathy [215,216]. However the major problem with leptin insufficiency or dysfunction, is that this corresponds to only a minority of the obese / diabetic population. This model does not therefore provide the same conditions or circumstances that occur in the majority of T2D [217,218] and obesity cases, and is therefore unable to adequately model obesity-related metabolic disorders.

Polygenic models of obesity with diabetes present a much clearer perspective to the human condition [219]. Particular inbred strains of mice when fed a high fat diet (HFD) show significant obesity, while others experience gene-diet interactions and stay lean [220]. Some strains develop obesity with severe insulin resistance and glucose intolerance, whilst some are obese and resistant to the onset of diabetes. In contrast, some are very susceptible to T2D but do not become morbidly obese [221,222,223]. Polygenic models in rodents fed on a HFD or crossed with other obesity strains, allow access to various diabetic phenotypes, similarly to those detected in humans [219,221,222,223].

The use of a HFD is the most common approach in inducing obesity as it provides a non-leptin-deficient model, a better representation of the current worldwide obesity epidemic [219,224]. Amongst the range of C57 strains, C57/BL/6 mice are the most extensively used to study HFD-induced obesity [220,225,226,227]. This is due to metabolic manifestations which closely resemble the human metabolic syndrome caused by a high HFD consumption [220,221,225]. Sprague Dawley rats are also widely used as a rodent model of HFD-induced obesity, which also mimics the metabolic disorders observed in humans [221].

1.10 Summary and concluding remarks

Cardiovascular-related metabolic disorders are a substantial economic and personal burden in the developing world. Atherosclerosis is the most prevalent type of cardiovascular disease, with a risk of plaque rupture and life-threatening cardiovascular events. Obesity and diabetes exacerbate this risk with perturbations in glucose and lipid

metabolism causing deleterious manifestations in cell and vascular function. The role of hyperglycaemia and hyperlipidaemia in diabetic- and obesity-exacerbated cardiovascular diseases are not yet completely elucidated. Most of the anti-diabetic, anti-lipidaemic and anti-obesity drugs have severe side effects, particularly when these medications are prescribed concurrently over long periods in patients who suffer from a cluster of metabolic disorders. These medications may be effective initially but may cause other effects or lose responsiveness with long term use. Therefore a better understanding and knowledge of the processes which may be occurring in cell culture and animal models are required in order to improve clinical interventions, treatment outcomes and develop suitable pharmaceutical compounds.

1.11 Thesis aims and outline

The research undertaken in this project attempts to investigate some of the molecular mechanisms linking diabetes with atherosclerosis, as well examining potential anti-glycative and antioxidant compounds, which may improve cardiovascular related diseases induced by hyperglycaemia and hyperlipidaemia.

Therefore the aims of this project are:

1) To investigate the impact of high glucose concentrations on macrophage lysosomal function and populations, in a murine macrophage-like cell line (J774A.1) and human monocyte-derived macrophages (HMDM).

2) To examine the potential impairment of lysosomal enzymatic activity and protein levels induced by high glucose during the maturation of human monocytes to HMDM.

3) To assess the possible anti-atherogenic properties of carnosine in a murine type 1 model of diabetes-accelerated atherosclerosis using streptozotocin-treated apo $E^{-/-}$ mice.

4) To examine the potential anti-atherogenic, anti-lipidaemic and anti-inflammatory properties of the stable nitroxide radical TEMPOL in a murine model of obesity and hyperlipidaemia using high fat fed apo $E^{-/-}$ and C57BL/6 mice.

5) To assess the impact of TEMPOL upon macrophage lysosomal function under normal and high glucose concentrations, and assess the potential anti-inflammatory and anti-glycaemic properties of TEMPOL on cytokine expression in hyperglycaemic macrophages.

Chapter 2 describes the experimental materials and methods used in this project. In Chapter 3, the effect of high glucose concentrations upon lysosomes from cell lysates of J774A.1 murine macrophage-like cells and HMDM cell is examined. Chapter 4 extends this work by monitoring the effects of high glucose upon lysosomes during the monocyte to macrophage development in the HMDM cells. The potential anti-atherogenic properties of carnosine and TEMPOL were assessed in *in vivo* animal models in Chapters 5 and 6, respectively. In Chapter 7 the potential protective effects of TEMPOL were examined in hyperglycaemic HMDM cells with lysosomal dysfunction. Finally, a general discussion of the key findings and the prospective future directions for the studies reported in Chapters 3 - 7 is presented in Chapter 8.

CHAPTER 2:

MATERIALS AND METHODS

This chapter describes the overall material and methods used throughout the studies. Each results chapter describes methods relevant to its individual content.

2.1 Materials

Fatty acid free bovine serum albumin (BSA), ethylendiaminetetraacetic acid (EDTA), sodium pyruvate, dimethyl sulfoxide (DMSO), polyoxyethylene 23 lauryl ether (Brig 35), benzamidine, pepstatin A, sodium acetate, triton X-100, E64, sodium dodecyl sulfate (SDS), β-mercaptoethanol, D-mannitol, Tween 20 were from Sigma-Aldrich Pty. Ltd. (Castle Hill, NSW, Australia). Diploma Instant skim milk powder for blocking buffer was purchased from Coles (Parramatta, NSW, Australia). D-(+)-glucose and bromophenol blue sodium salts were obtained from ICN Biomedicals (Aurora, OH, USA). Copper sulfate was purchased from ICN (Seven Hills, NSW, Australia). Sodium chloride, Tris hydrochloride, Tris base, sodium carbonate, glycerol, phosphate buffered saline (20x concentrate, pH 7.5) and glacial acetic acid were from Amresco (Solon, OH, USA). NADH and complete Mini protease inhibitor tablets were purchased from Roche Pty. Ltd (Castle Hill, NSW, Australia). Dithiothreitol (DTT) was purchased from Astral Scientific Pty. Ltd. (Gymea, NSW, Australia).

The substrates used for lysosomal enzyme activities included: Z-Arg-Arg-AMC (for cathepsin B), Z-Phe-Arg-AMC (for cathepsin L) and Z-Val-Val-Arg-AMC (for cathepsin S) which were obtained from Bachem AG, Bubendorf, Switzerland; 7-methoxycoumarin-4-Acetyl-Gly-Lys-Pro-Ile-Leu-Phe-Phe-Arg-Leu-Lys-DNP-D-Arg-amide (for cathepsin D) was purchased from Sigma-Aldrich. Substrates for cathepsins B, L and S were prepared at a concentration of 40 mM in DMSO; while cathepsin D was made up at 8 mM concentration, also in DMSO. These were all stored at -20 ºC.

Agarose gels (1% (w/v) were purchased from Helena laboratories (Mt. Waverly, VIC, Australia).

All solutions were prepared using nanopure water from a Milli Q system (Millipore-Waters, Lane Cove, NSW, Australia) and if necessary treated with washed Chelex-100 resin (Bio-Rad, Reagent Park, NSW, Australia).

All other chemicals were of analytical grade and all solvents were HPLC grade. Methanol, and isopropanol are purchased from EM Science (Gibbstown, NJ, USA) and

hexane was from Sigma-Aldrich. Hydrochloric acid was Analar® grade and purchased from Merck Pty. Ltd. (Kilsyth, Vic, Australia).

2.2 Tissue culture materials

RPMI-1640 medium (with L-glutamine, without glucose and sodium bicarbonate), Dulbecco's phosphate-buffered saline (PBS) pH 7.4 and Dulbecco's modified Eagle's medium (DMEM) were purchased from Sigma-Aldrich. Two mM glutamine was obtained from Thermo Electron (Melbourne, VIC, Australia), 1% (v/v) PenStrep containing 100 units/mL penicillin and 0.1 mg/mL streptomycin from BioWhittaker (Radnor, PA, USA), and 10% (v/v) heat activated (30 min at 60 ºC) human serum (HS) from the Australian Red Cross (Clarence St Blood Bank, Sydney, NSW, Australia) or fetal calf serum (FCS) from JRH Biosciences (Lenexa, Kansas, USA) were added to all media where appropriate. To prepare normal to high glucose conditions, D-glucose (molecular mass = 180.16 g/mol) was added to (glucose-free) media at 5.5, 10, 20 or 30 mM concentrations and then the medium was filter-sterilised by the Bottle Top Vacuum Filter; 0.2 µm pore size, PES Membrane (Corning, NY, USA).

2.2.1 Cell culture

All cells were cultured in 12 well (22 mm diameter wells) or 6 well (35 mm diameter wells) tissue culture plates (Corning, NY, USA), or in Falcon (Becton Dickinson, Franklin Lakes, NJ, USA) 175 or 75 cm^2 tissue culture flasks, in humidified incubators at 37 ºC and 5% (v/v) CO_2.

2.2.2 J774A.1 Mouse macrophage cells grown under normal to high glucose conditions

J774A.1 mouse macrophages (ATCC # TIB-67 and purchased from ATCC™, Manassas, VA, USA) were grown in normal DMEM media (with 5.5 mM glucose content) and used as the control (or normal) glucose condition. Alternatively they were grown in DMEM (with 10% v/v FCS) supplemented with extra 4.5 mmol/L (thus final

glucose concentration was 10 mM), 14.5 mmol/L (20 mM glucose) and 24.5 mmol/L glucose (30 mM glucose) for high glucose conditions. J774A.1 mouse macrophages were incubated in these conditions for 11 days and cells were split every 2 - 3 days. Cell morphology was checked under the microscope then cell pellets were prepared and treated as required.

2.2.3 J774A.1 Mouse macrophage cells for investigation of lysosomal activity

J774A.1 mouse macrophages were grown in 175 cm^2 flasks and supplemented with glucose as previously described. Cells were harvested by scraping using a disposable cell scraper (Greiner Bio-One; Frickenhausen, Germany) and the cell suspension was replated at 1:15 dilution every 2 - 3 days. In order to prepare the cell extracts for lysosomal activity measurements, J774A.1 cells were scraped at confluency and replated into 75 cm^2 Falcon flasks at 0.5×10^6 cell/mL (1 mL/ well) and incubated overnight (16 hr). Cells were washed three times with PBS. Cells were scraped and transferred into a 15 mL Falcon tube. Cell pellets were obtained by centrifugation (Beckman Coulter™, Allegra® X-15R Centrifuge; Palo Alto, CA, USA) at 524 *g* for 5 min at 4 ºC. The supernatant was discarded and the undisturbed cell pellets were snap frozen in liquid nitrogen and stored at -80 ºC for subsequent determination of lysosomal acid lipase (LAL), lysosomal cathepsin B, L, S and D activities.

2.2.4 Human monocyte-derived macrophages (HMDM)

Monocytes were isolated by Mr Pat Pisansarakit from white cell concentrates (provided by the Australian Red Cross), within 24 hrs of collection. The elutriation system consisted of a Beckman Avanti J20-XPI centrifuge equipped with a JE-5.0 elutriation rotor and a 4.2 mL elutriation chamber with a Masterflex (Barrington, IL, USA) peristaltic pump. The elutriation media was pyrogen-free HBSS (Sigma-Aldrich) with phenol red and 0.01% (v/v) EDTA but without Ca^{2+} and Mg^{2+}. First of all the system was rinsed with about 250 mL 70% (v/v) ethanol followed by water, 30% (w/w) H_2O_2, water and finally HBSS. The white cell concentrates were diluted 1:2 in HBSS. Next 30 mL aliquots of diluted white cell concentrate was underlaid with 15 mL Lymphoprep (Fresenius Kabi Norway) and centrifuged at 1900 rpm (2060 *g*), with the brake off, at 21 °C for 40 min. Thereafter, peripheral blood mononuclear cells were

isolated from the Lymphoprep interface, washed once with HBSS and resuspended in 30 mL HBSS. The mononuclear cell suspension was loaded at a rotor speed of 2020 rpm with an initial flow rate of 9 mL/min at room temperature. The flow rate was increased by 1 mL/min every 10 min and the cell fractions from 15, 16, 17, 18 and then a final flow rate of 40 mL/min were collected. The purity of each fraction was routinely determined on smears of the cell suspension prepared using the Cytospin® system (Shandon; Astmoor, Runcorn, England). Cells were stained using Diff Quick staining kits (LabAids Pty. Ltd.; Narrabeen, NSW) according to the manufacturer's instruction. Fractions that were largely pure monocytes were pooled. A viable cell count was subsequently performed using Trypan blue 0.4% (w/v) (Sigma-Aldrich). Cells were diluted to 1×10^6 cells/mL in X-VIVO 10 media (without phenol red or gentamicin; Lonza Australia Pty. Ltd., Mount Waverley VIC, Australia) with no serum and 1 mL was added to each well of 12 well, or 2 mL per well was added to 6 well tissue culture plates. After 1 - 2 hr incubation, the media was replaced with 1 or 2 mL RPMI at the required glucose concentration with 10% v/v HS as previously mentioned. The media was changed 3 days after the elutriation and then every second day afterwards. The health of cells was always checked under the microscope after each media change.

2.2.5 Preparation of human monocyte-derived macrophages (HMDM) matured in normal to high glucose conditions for determination of lysosomal enzyme activities

Monocytes were prepared as previously noted and incubated for 10 - 11 days in RPMI containing normal (5.5 mM) to high (10, 20 and 30 mM) glucose concentrations. This time period results in differentiation into human monocyte-derived macrophages (HMDM) [228]. The health of cells was checked under the microscope before cell harvesting.

Cells were washed three times with PBS. Cells were scraped using the cell scraper and transferred into a 15 mL Falcon tube. Cell pellets were obtained by centrifugation (Beckman Coulter™, Allegra® X-15R Centrifuge) at 931 *g* for 15 min at 4 ºC. The supernatant was discarded and the undisturbed cell pellets were snap frozen in liquid nitrogen and stored at -80 ºC for the determination of LAL, lysosomal cathepsin B, L, S and D activities.

2.3 Lysosomal enzyme activity

2.3.1 Lysosome isolation

Cell pellets (J774A.1 cells or HMDM incubated in normal to high glucose concentrations as previously noted) were resuspended and lysed in 250 µL of nanopure water. The lysate was centrifuged 13.4 x 1000 *g* for 5 min at 4 °C to remove unlysed cells and membrane fractions that may interfere with the assay [229]. The supernatant was transferred to fresh Eppendorf tubes, placed on ice and used immediately for quantification of LAL, cathepsin B, L, S and D activities followed a protein assay.

2.3.2 Determination of cathepsin B and L activity

Cathepsin B activity was measured by continuously monitoring the release of AMC from the peptide substrate Z-Arg-Arg-AMC. Cathepsin L activity was measured by the initial linear increase in fluorescence following the cleavage of AMC from the peptide substrates Z-Phe-Arg-AMC (10 µM). Prior to running the assay, the stock solution was diluted 1000-fold with nanopure water.

20 µL of the lysate was combined with 180 µL of 0.1 M phosphate buffer (NaH_2PO_4 / Na_2HPO_4: pH 5.5) containing 0.005 % (w/v) Brij 35, 2.5 mM EDTA, 2.5 mM DTT, 1 µM pepstatin and 5 mM benzamidine and the cathepsin substrate (10 µM).

The plate was shaken for 30 s prior to analysis to ensure a homogenous mix of the components. Assays were performed in triplicate on 96-well plates at 21 °C with fluorescence changes measured using $\lambda_{excitation}$ 360 nm and $\lambda_{emission}$ 460 nm.

The change in fluorescence was monitored over 10 cycles, with changes in cathepsin B activity monitored every 2 min for 20 min and cathepsin L monitored every minute for 10 min. Fluorescence changes were monitored on either a Cytofluor II fluorescence plate reader or a M2e spectroflurometer.

2.3.3 Determination of cathepsin S activity

To measure cathepsin S activity, a similar procedure to that used for cathepsins B and L was employed except that Z-Val-Val-Arg-AMC was used as the substrate. Before running the assay, the substrate was diluted 50-fold in nanopure water

Cell lysate (50 μL) was added to wells containing 100 μL of 0.2 M phosphate buffer (NaH_2PO_4 / Na_2HPO_4: pH 5.5) containing 5 mM EDTA, 5 mM DDT, 1 μM pepstatin A, 5 mM benzamidine and incubated for 1 hr at 40 ºC in an incubator to inactivate other cathepsins. The plate was then placed on the plate shaker for 5 min at 21 °C. Fluorescence changes were measured immediately after addition of 50 μL of substrate (0.2 mM) using a M2e spectrometer, with measurements made every 5 min for 50 min with $\lambda_{excitation}$ 360 nm and $\lambda_{emission}$ 460 nm at 21 °C [229].

2.3.4 Determination of cathepsin D activity

To measure cathepsin D activity, cell lysate (25 μL) was added to wells containing 100 μL of 0.1 M acetate buffer (CH_3CO_2Na / CH_3COOH, pH 4.2) containing 2.5 mM EDTA, 0.005% (w/v) Brij 35, 5 mM benzamidine and 10 μM E64 (irreversible inhibitor of cysteine proteases) in a 96 well plate. After 5 min activation at room temperature of 21 °C, 50 μL of 7-methoxycoumarin-4-acetyl-Gly-Lys-Pro-IIe-Leu-Phe-Phe-Arg-Leu-Lys-DNP-D-Arg-amide (stock solution 8 mM in DMS0 stored at -20 ºC) at 2 μM was added. Changes in fluorescence were monitored using a M2e Plate Reader spectrometer with $\lambda_{excitation}$ 328 nm and $\lambda_{emission}$ 393 nm with measurements made every 30 s for 6 min.

2.3.5 Analysis of lysosomal cathepsin activity data

Activity of cathepsins was quantified by the initial linear change in fluorescence over time. Nanopure water was used for dilutions, and as negative control (no cell lysate fraction) as this did not result in any change in fluorescence over time. The protein concentrations were determined with other aliquots of the same samples using the Bio-Rad protein assay as described in Section 2.4.1, thereby allowing the lysosomal activity to be expressed relative to the protein concentration.

2.3.6 Determination of lysosomal acid lipase (LAL) activity

LAL activity was quantified using a procedure based on a previously method published [230]. 4-Methylumbelliferone (4-MU) and 4-methylumbelliferyl oleate (4-MUO) were purchased from Sigma-Aldrich. A stock concentration was constituted by dissolving 4-MU (5.676 μM) in hexane and this was further diluted in 4% (w/v) Triton X in order to generate a standard curve from 0 - 2.8 μM of 4-MU. 4-MUO (2.3 μM) was similarly dissolved in hexane and further diluted in 4% (w/v) Triton X (1:100).

In order to determine LAL activity in the J774A.1 cells and HMDM, 25 μL of cell lysate was added to each well followed by 50 μL of prepared 4-MUO in each well. One hundred and twenty five microlitres of prepared assay buffer (0.2 M Na_2Ac, 0.01% v/v Tween 80, pH 5.5) was added to both the standard and cell lysate wells and incubated for 30 min at 37 °C, covered in foil to protect from light. The reaction was stopped with 100 μL of stop buffer (0.75 M Tris, pH 8.0). The fluorescence signal was detected using an M2e plate reader spectrometer with $\lambda_{excitation}$ 360 nm and $\lambda_{emission}$ 460 nm. Fluorescence readings were converted to 4-MU concentrations using the standard curve and expressed as μM of 4-MU formed per min. The 4-MU concentrations were corrected for the protein concentration present in each sample.

2.3.7 Osmotic control

D-Mannitol was used as a control to account for any osmotic effects when cells were exposed to higher glucose levels during the incubation period. J774A.1 cells and HMDM were cultured for 11 days in their media containing 5.5 mM glucose plus 24.5 mM D-Mannitol. Lysosomal activity of cathepsins B, L and LAL activities were determined as described above.

2.4 Protein and enzyme assays

2.4.1 Protein determination

To determine the protein concentration of the cell lysates, the Pierce (Thermo Fisher Scientific, North Ryde, NSW) Bicinchoninic Acid (BCA) Protein Assay was used. One part of Reagent B (4% (w/v) $CuSO_4$) was mixed with 49 parts Reagent A

(sodium carbonate, sodium bicarbonate, BCA and sodium tartrate in 0.1 N NaOH). This method quantifies the reduction of Cu^{2+} by protein to Cu^{1+} under alkaline conditions (Biuret reaction) with colorimetric detection of the Cu^{1+}: BCA complex. Ten µL of sample along with 190 µL BCA working reagent was added in each well of a 96 well plate and incubated at 60 ºC for 30 min. The plate was cooled for 5 min before the absorbance was read at 562 nm on a Tecan Sunrise plate reader (Grödig, Austria). A standard curve obtained using 0 - 50 µg BSA prepared in the same buffer as the samples, was used to calculate the protein concentration, with this expressed as µg/µL.

2.4.2 Cell viability

Lactate dehydrogenase (LDH) is a cytosolic enzyme that is released into the culture medium when plasma membranes are compromised. LDH catalyses the reversible reduction of pyruvate, with NADH as the cofactor.

$$NAD^+ + \text{lactate} \leftrightarrow NADH + \text{pyruvate}$$

In this assay, excess substrate is added to ensure that the enzyme is the limiting factor. NADH loss, which is the proportional to the amount of enzyme present either intracellularly (cell lysate) or extracellularly (cell media), was quantified at 340 nm. Two hundred microlitres of working reagent (0.15 mg/mL NADH and 2.5 mM sodium pyruvate in PBS) was added to 10 µL samples of cell lysate or cell media (after spinning at 353 *g* for 5 min at 4 ºC to remove cellular debris) in each well of a 96-well plate. The absorbance was read every 5 min for 7 cycles on a Tecan Sunrise plate reader. The linear change of absorbance per min was used in the following equation to determine cell viability:

$$\text{Viability (\%)} = [\Delta 340 \text{ nm cell lysate} / (\Delta 340 \text{ nm cell lysate} + \Delta 340 \text{ nm cell media})] \times 100$$

Cells were considered viable if the percentage was > 80% and there was no decrease in the total activity (Δ340 nm cell lysate + Δ340 nm cell media).

2.5 Western blotting to determine protein levels of lysosomal cathepsins B, L, LAL and lysosomal associated marker glycoprotein-1 (LAMP-1)

2.5.1 Antibodies for Western blotting

Mouse polyclonal to LAL, mouse polyclonal antibodies to cathepsin L, rabbit polyclonal to LAMP-1 and rabbit polyclonal to β-tubulin (loading control) were purchased from Abcam (Cambridge, UK) and goat anti-cathepsin B was purchased from Santa Cruz Biotechnology (Santa Cruz, CA, USA). Secondary antibodies of donkey anti-goat IgG-HRP and goat anti-mouse IgG-HRP was purchased from Santa Cruz Biotechnology; donkey anti-rabbit IgG-HRP was purchased from GE Healthcare, Life Sciences, Amersham Biosciences UK Ltd. (Buckinghamshire, UK).

2.5.2 Cell lysis buffer

Cell lysis buffer was premade containing 150 mM NaCl, 50 mM Tris pH 8.0. On the day of the experiment, 0.1% (v/v) Triton-X 100 was added and one mini protease inhibitor cocktail tablet was dissolved into the 7 mL of cell lysis buffer.

Gel loading dye stock 5x was constituted with nanopure water (42.5%), 0.5M Tris pH 6.8 (12.5%), glycerol (20%), 10% w/v SDS (20%) and 0.5% w/v Bromophenol Blue (5%). The premade loading buffer (8 mL) was aliquoted into Eppendorf tubes and stored at -20 °C.

2.5.3 Sample preparation for loading gels

J774A.1 cells or HMDM were washed with PBS and lysed with 1 mL of cell lysis buffer and placed on ice for 15min. The protein concentration of the cell lysates was determined using the BCA protein assay using the cell lysis buffer to dilute the standards. The pre-prepared 5x gel loading dye stock was reconstituted with 5% (v/v) β-mercaptoethanol. Then 5 × complete sample buffer was added to each cell lysate sample to give 1 × final concentration, mixed well and centrifuged briefly to remove particulate matter. Samples were then heated at 95 °C for 5 min, centrifuged briefly to remove precipitated material and placed on ice until loaded onto gels. For investigation of

protein levels of different lysosomal markers, 15 - 30 μL of cell lysate containing 20 - 40 μg protein was loaded into each well.

2.5.4 Gel loading and running to separate proteins by electrophoresis

Four to fifteen percent Tris-HCl gradient SDS-PAGE gels or 4 - 20% mini protean TGX precast gels were purchased from Biorad (Gladesville, NSW, Australia). Two to four gels were assembled into the gel cassettes with these then firmly clamped and placed into a Mini-Protean 3 electrophoresis cell (2 gels) or Mini-Protean Tetra System (4 gels) tank (Biorad). Approximately 1 L of 1 × running buffer prepared from 5 × running buffer (3% w/v Tris base, 14.4% w/v glycine and 0.5% w/v SDS) was inserted into tank and the tank was checked for leaks before filling up the entire tank with running buffer. Five μL of Precision plus protein Kaleidoscope molecular mass standards (Bio-Rad) were included in the first or last lane in each gel. The loaded gels were then run at 125 V for at least 1 hr until the loading bands reached the bottom of the gel. The gels were then separated from the glass and spacer plates, briefly washed in water and then processed further by transferring to nitrocellulose membranes.

2.5.5 Protein transfer to nitrocellulose membranes

Protein transfer from the gels to nitrocellulose membranes was achieved using an iBlot™ Dry Blotting System (Invitrogen Australia Pty Ltd, Mount Waverley, VIC, Australia) with a blotting area of 14 × 8.5 cm suitable for two mini gels. The excess water was removed from gels by gentle shaking of gels and carefully holding the edge. Then two mini gels were placed on the nitrocellulose of an iBlot NC anode stack. Excess water and air bubbles between gel and membrane were carefully removed with a wet roller. A wet filter paper was placed on the gels and excess water and air bubbles were removed as before. On top of this was laid the iBlot cathode stack. The complete apparatus was pressed together by rolling a few times with a dry roller. An iBlot disposable sponge was placed on the lid of the iBlot apparatus and the sandwich assembly was then firmly closed. The transferring of proteins from gels to nitrocellulose membrane was accomplished in 7 min. The sponge, top cathode stack and the wet filter paper were carefully removed and discarded. Any excess of nitrocellulose

membrane around the gels was trimmed and membrane was placed in Tris-buffered saline containing Tween 20 buffer (TBST) with tweezers until Western blotting.

2.5.6 Western blotting

Nitrocellulose membranes with transferred proteins were initially blocked for one hour, using 5% w/v skim milk powder in TBST. This was followed by overnight incubation with the primary antibody (LAMP-1, LAL, cathepsin B or L). For J774A.1 cells the antibodies were used at 1:500 dilution. For HMDM the dilutions for LAMP-1, LAL, cathepin B or L were 1:1000, 1:500, 1:250 or 1:500, respectively.

On the following morning, the membranes were then washed with TBST (5 × 5 min) followed by incubation with the appropriate secondary antibody at 1:2000 dilution in blocking buffer for 1 hr. The membrane was then washed with TBST (4 × 5 min). Donkey anti-rabbit IgG-HRP was used for LAMP-1, goat anti-mouse IgG-HRP was used for LAL or cathepsin L, and donkey anti-goat IgG-HRP was used for cathepsin B.

Freshly prepared ECL Western blotting detection reagent (0.125 mL/cm^2) was added to the membrane and incubated for 1 min at 21 °C. Surface tension holds the reagent on the membrane. The excess of reagent was removed by gentle shaking of the membrane and holding it with tweezers touching the edge against a Kimwipe. Then the membrane was wrapped in polyethylene wrap (Glad wrap™) with bubbles carefully removed. The chemiluminescence was acquired using a Molecular Imager ChemiDoc XRS System (Bio-Rad laboratories, Segrate, Milan, Italy) and Quantity One software, with the focused recorded frozen when a satisfactory image was acquired. The raw images were saved as TIFF files. A blank image was also taken using normal white light exposure.

The acquired images of the scanned membrane were opened using Photoshop and the image adjusted (brightness and contrast) to visualise the bands. LAMP-1 (120 kDa), LAL (45 kDa), procathepsin L (55 kDa), mature cathepsin L (25 kDa), procathepsin B (25 kDa) and mature cathepsin B (20 kDa) were identified by comparison with the manufacturer's guidelines.

2.5.7 Stripping of membrane

The membrane was stripped for 10 min using a Restore PLUS Western Blot Stripping buffer (Thermo Fisher Scientific), and subsequently washed with TBST (4 × 5 min). The stripped membrane was then blocked with blocking buffer for 1 min then probed for β-tubulin (1:1000 in blocking buffer) for 3 hrs. The membrane was then washed with TBST (5 × 5 min), and probed with donkey anti-rabbit IgG-HRP (1:2000 dilution in blocking buffer) for 1 hr. This was followed by washing with TBST (4 × 5 min), addition of the ECL reagent and recording of the membrane image reading as described previously. β-Tubulin was detected by mass at 51 kDa based on the manufacturer's guidelines.

2.5.8 Molecular band analysis

The intensity of each band was quantified using Image J Software (NIH, USA). Briefly, a box was plotted around each band and the same box was copied and pasted for relevant bands on each raw scan of the membrane. For each band the adjusted volume (intensity × mm^2) was calculated. This was the volume (sum of the intensities of the pixels inside the volume boundary × area of a single pixel) minus the local background volume. LAMP-1, LAL, cathepsin B and L levels were expressed relative to β-tubulin.

2.6 *In vivo* animal studies

Histology was conducted on three animal models reported in Chapters 5 and 6.

2.6.1 Materials and solutions for histology

Xylene, Harris' Haematoxylin solution, Eosin Alcoholic 1%, Histolene (100%), and Scott's Blueing Solution were purchased from Fronine Lab Supplies (Riverstone, N.S.W., Australia). DPX Mountant for cover-slipping was purchased from Sigma-Aldrich. Formaldehyde was purchased from Analar® Merk Pty. Ltd. (Kilsyth, Vic, Australia).

2.7 Preparation of tissue samples from diabetic mice

Samples of aortae and brachiocephalic arteries were provided by Dr David van Reyk. The animals were supplied by the Biological Facility of the Heart Research Institute and were maintained and monitored in accordance with the guidelines of Sydney South West Area Health Service Animal Welfare Committee (Protocol number: 2007/002B). Animal housing and care were carried out by Drs. van Reyk, Bronwyn Brown and the staff of the Biological Facility.

Diabetes was induced in male apo $E^{-/-}$ mice at six to seven weeks of age by intraperitoneal injection of streptozotocin dissolved in citrate buffer (pH 4.5) with daily injections of 55 mg/kg for 5 days. Control mice were injected with citrate buffer. These procedures were modified from a previously published method [231].

2.7.1 Animal groups

Mice (n = 80) were maintained for twenty weeks, post-induction of diabetes, with half of the animals receiving carnosine (2 g/L) in their drinking water. Food and water were available *ad libitum*. The groups comprised of control-non supplemented, control-carnosine (β-alanyl-L-histidine) supplemented, diabetic and diabetic-carnosine supplemented as shown in the figure below.

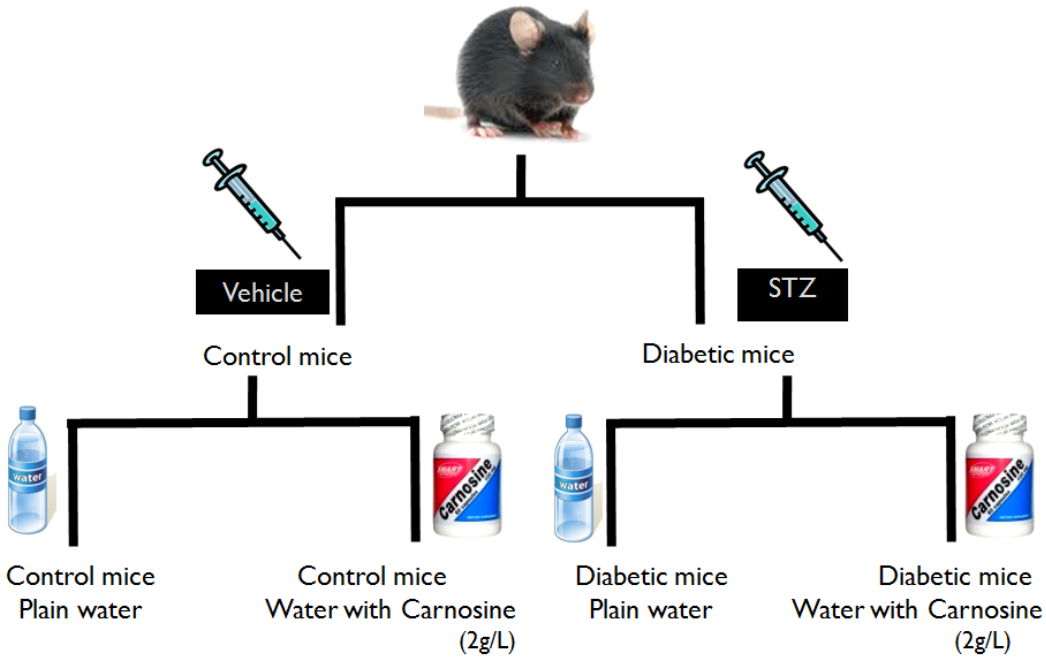

Figure 2.1: Animal model for the carnosine project.

The animal study consisted of 80 apo $E^{-/-}$ mice. The first two comprised of control mice groups (outlined in blue) with and without carnosine in the water. The third and fourth groups comprised of diabetic mice (outlined in orange) that were induced by streptozotocin with and without carnosine in the water.

2.7.2 Sample collection

The mice were sacrificed at approximately 20 weeks after the induction of diabetes by exsanguination via cardiac puncture following anaesthesia using methoxyflurane.

The heart and entire arterial tree were collected for histological analysis based on a method previously published [232]. The arterial tree was flushed by perfusion through the left ventricle, at physiological pressure, with PBS, containing 2 mM EDTA and 20 µM butylated hydroxytoluene, for 4 min followed by fixation by perfusion with 4 % (w/v) paraformaldehyde (pH 7.5) for 6 min. The heart and arterial tree were carefully dissected out and stored in paraformaldehyde. The samples were rinsed in PBS and stored in 70% v/v ethanol. The tissues was then analysed for the plaque areas in the brachiocephalic and the aortic sinus regions with the identity of the samples being coded, to avoid bias by another researcher.

Blood obtained by cardiac puncture was immediately transferred to Eppendorf tubes containing a cocktail of protease inhibitors to prevent clotting and sample degradation (1 μL/mL aprotinin, 0.04 μM D-phenylalanyl-L-prolyl-L-arginine chloromethyl ketone [PPACK; a rapid thrombin inhibitor], 20 μg/mL soybean trypsin inhibitor and 2mM EDTA). Blood glucose concentration were determined using a True Track™ Smart System glycometer (Nipro Diagnostics Inc., Fort Lauderdale, FL, USA), and HbA1c (as a measure of glycated haemoglobin) was determined using AlcNow+ kits (Metrika Inc., Sunnyvale, CA, USA). The remaining blood was spun at 800 *g* for 10 min at 4 °C. The recovered plasma was snap-frozen in liquid N_2 and stored at -80 °C for further analyses, as were the resultant and remaining cell pellets.

2.7.3 Preparation of formalin fixed, paraffin-embedded mouse tissue

The aortic sinus was dissected making a cut perpendicular to the aorta halfway through the heart. The brachiocephalic artery was separated from the aortic arch by dissecting diagonally across the vessel where the artery meets the arch, and embedded in agarose gel. The dissected samples were enclosed in Tissue TEK cassettes and placed in 70% v/v ethanol and taken over the Pathology Department at the University of Sydney for tissue processing overnight through a Tissue-TEK VIP automatic tissue processor (Miles Scientific, Naperville, IL, U.S.A) to dehydrate samples before infusing with paraffin wax. Samples were embedded in paraffin blocks in the desired orientation using a stainless steel mould (Tissue-TEK Dispensing Console, Miles Scientific). These paraffin blocks were taken back to the Heart Research Institute.

2.7.4 Dissection and paraffin embedding of the aortic sinus and the brachiocephalic artery

The whole aortic tree with the heart was carefully removed for morphological and immunohistochemical analyses of the aortic sinus and the brachiocephlic artery. The brachiocephalic artery was separated from the aortic arch dissecting diagonally across the vessel where the artery meets the aortic arch, embedded in agarose gel and cut in a pentagonal shape as shown in Figure 2.2a. The embedded sample in agarose was carefully positioned in between two sponges that were inserted within the top and bottom of the cassette. The dissected samples that were enclosed in cassettes were

labelled with pencil and immersed in 70% ethanol for overnight tissue processing. On the following day the artery was embedded in paraffin blocks with the beginning of the brachiocephalic artery facing the bottom and the right common carotid artery and the right subclavian artery facing the top.

For the aortic sinus, the arterial tree along with the aorta was removed, leaving behind the two atriums attached on top of the whole heart. The second cut was made perpendicular to the aortic root, approximately halfway through the heart and parallel to the two atriums as illustrated in Figure 2.3. The dissected top half of the heart was processed and embedded in paraffin blocks the next day with the aortic opening and the atrium facing the top and the cut end of the heart facing the bottom.

2.7.5 Tissue Sectioning

Plaque area was estimated for the brachiocephalic artery and the aortic sinus. Five micrometer sections of tissue were initially cut on a rotary microtome and floated on a 42 °C water bath. Sections were lifted on to a Superfrost Plus positively-charged glass slides (Menzel-Glaser, Braunschweig, Germany) and air dried before placing in racks to dry overnight at 37 °C.

The first cross section slide of the brachiocephalic artery was taken from the appearance of a complete circular section at the region proximal to the arch. The first section of the aortic slide was taken at the first appearance of the three valve leaflets.

A set of six duplicate (A - F) cross sections were counted and taken at every 100 µm along the brachiocephalic artery and the aortic sinus (refer to Figures 2.2 and 2.3). One set of six duplicate sections (A - F) were stained with Haematoxylin and Eosin (H & E) and photographed using the appropriate magnification (10x for brachiocephalic and 4x magnification for sinus) for plaque area. Total plaque area was calculated across the six sections using Adobe Photoshop CS5 (v12.0).

The other replicate sections were used for immunohistological analysis for α-actin for smooth muscle cells (Slide B), F4/80 for macrophages (Slide C) and picrosirius red for collagen (Slide D).

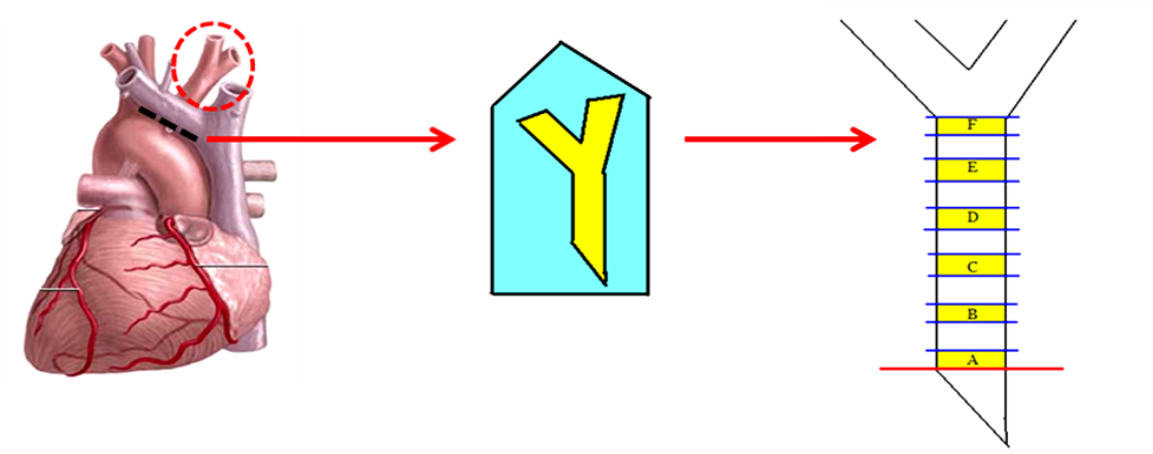

Figure 2.2a: Dissection and tissue sectioning of the brachiocephalic artery.
The brachiocephalic artery was incised from the aorta, fixed in an agarose gel. After the agarose gel had cooled, the sample was cut around the sample in a pentagonal outline as shown in the middle diagram. Two triangular cuts are made on top of the right common carotid artery and the right subclavian artery whilst two parallel cuts are made along the brachiocephalic artery. This allowed the starting point for tissue sectioning to commence from the base of the pentagon. The far right diagram indicates where the duplicate slides of A to F were taken. Slide A was taken where the first full circumference of the artery appeared.

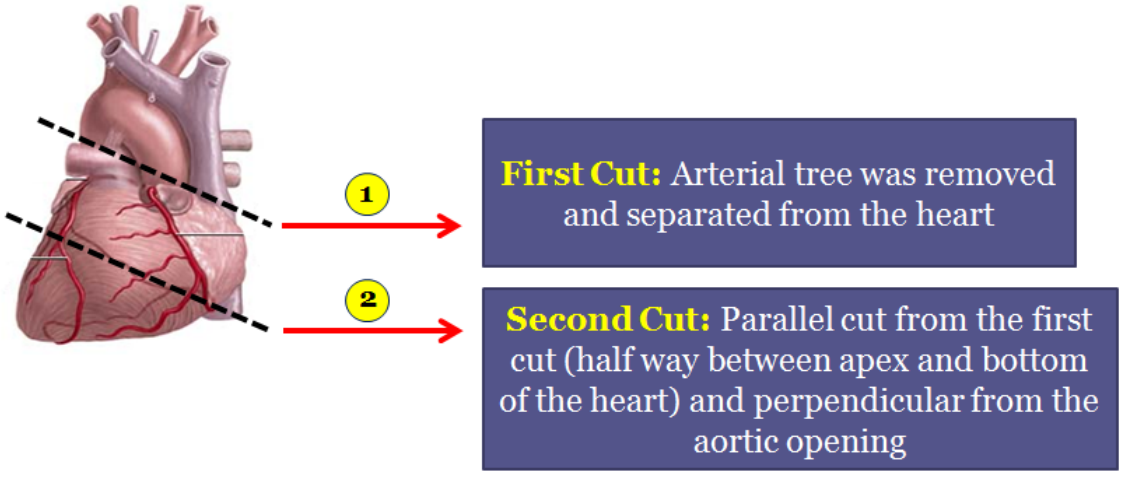

Figure 2.2b: Dissection of the aortic sinus.
The arterial tree was removed and separated from the heart. The second cut was parallel to the first cut and also perpendicular from the aortic opening. The tissues were processed and embedded with the larger cross-section facing the bottom. The sample within the block was sectioned until the leaflets were detected. The first duplicate slide of A was taken at the appearance of all three leaflets of the sinus.

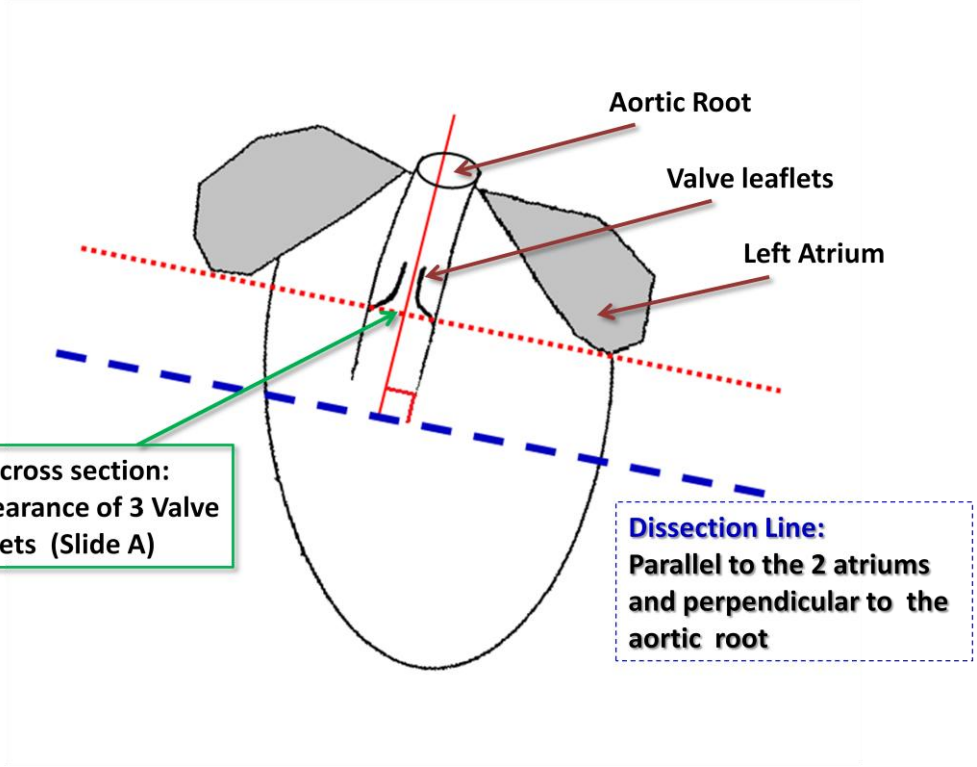

Figure 2.3: Aortic sinus dissections.
This is an anatomical position of the heart in 2D, where two imaginary lines meet perpendicularly from the aortic opening and between the left and the right atriums. The critical dissection (indicated by the broken blue line) takes place midway into the heart, perpendicular to the aortic opening and parallel to the left and right atriums. The first cross section is taken at appearance of three valve leaflets, as outlined in green.

2.7.6 Dewaxing and re-hydration of paraffin-embedded sections

Dewaxing of slides was performed by immersing slides in two changes of xylene for at least 10 min each. Sections were progressively re-hydrated through two changes of 100% ethanol for 2 min each, followed by two changes in 95% v/v ethanol (2 min each) and finally 2 min in 70% v/v ethanol. Sections were then washed in running tap water for at least 2 min.

2.7.7 Haematoxylin and eosin staining (H&E)

Sections were stained in Harris' Haematoxylin for 2 - 3 min. Sections were then washed well under tap water until the water colour was clear. The sections were subsequently dipped three times quickly in an acid alcohol differentiator (conc. HCl

diluted at 1:400 in 70% v/v ethanol) to remove excess blue colouration. After washing in tap water sections were submerged in Scott's Blueing Solution for 30 s. Sections were then checked under the microscope, to determine whether the nuclei were clearly differentiated. If not, the sections were rinsed with water, and re-stained with Harris's Haematoxylin for 30 s, washed under tap water until the water colour was clear, and then submerged in Scott's Blueing Solution for 20 s, washed with water and re-checked under the microscope.

When staining was such that the nuclei were clearly differentiated, the sections were then stained with eosin. Sections were washed in tap water then dipped in 70% v/v ethanol for 30 s and subsequently in two changes of eosin (30 s each). The sections were then washed in two changes of 95% v/v alcohol (30 s each) followed by two more washes in 100% alcohol (30 s each). Slides were then submerged in two changes of histolene (at least 10 min each) before they were mounted with DPX and coverslipped.

2.8 Immunohistochemistry materials and methods

Alkaline phosphatase substrate was purchased from Vector Laboratories Inc. (CA, U.S.A.) One drop from Reagent 1, 2 and 3 were added to 2.5 mL of 100 mM Tris-HCl (pH 8.2 - 8.5) prior to use. PBS 20x conc. (Amresco) was re-constituted to 1x PBS with nanopure water to which PBST 0.1% v/v Tween 20 was added (PBST).

Normal rabbit serum was purchased from Abacus (East Brisbane, Qld, Australia) The powder was reconstituted with 5 mL of nanopure water (as suggested by the product information) in order to yield 100% normal rabbit serum and aliquoted and stored at -20°C. Normal rabbit serum working solution (10% v/v in PBS) was made fresh on the day of experiment.

For the antigen retrieval buffer 5.46 g of sodium citrate tribasic dihydrate (Sigma-Aldrich) was dissolved in 1.5 L of nanopure water. The pH of the solution was measured using a pH meter (PHM 220, Meter Lab®) and adjusted to 6 with 37% w/v HCl (Astral Scientific). The solution was then topped up to 2 L with nanopure water.

2.8.1 Antibodies for immunohistochemistry

Mouse monoclonal α-SM-actin was purchased from Sigma-Aldrich. Rat monoclonal Anti-F4/80 antibody [Cl:A3-1], mouse polyclonal (Alkaline Phosphatase)-IgG isotype control and rat IgG2b, kappa monoclonal [RTK4530]- isotype control were purchased from Abcam.

2.8.2 Plaque composition

Macrophages (Anti-F4/80), smooth muscle cells (α-SM-actin), and collagen (Picrosirius Stain) were identified in paraffin-embedded sections of the brachiocephalic artery and the aortic sinus (refer to Section 2.7.5) taken at 100 μm, 200 μm and 300 μm, from the first complete cross-section of the brachiocephalic and the appearance of three valve leaflets of the sinus. Negative controls without the primary antibody were used for each staining to screen for nonspecific binding which was not evident.

2.8.3 Smooth muscle-α-actin staining

Sections were embedded and deparaffinised as described above. The sections were then rinsed in PBS. Antigen retrieval was achieved by placing the slides in citrate buffer and heating them in the microwave on high power for 15 min. The slides were then rapidly cooled in running tap water and immersed in PBST for 4 min. Sections were encircled with a ImmEdge™ hydrophobic barrier pen (Vector Laboratories Inc., Burlingane, CA, U.S.A.) to reduce the volume of reagents required. Normal rabbit serum working solution was added to the samples which were incubated for 4 hr at 21 °C in a closed slide sorter. The slides were then briefly rinsed in PBST. The alkaline phosphatase-conjugated anti-α-SM-actin monoclonal antibody (1/100 dilution in TBS, Sigma-Aldrich) was applied overnight at 4 °C with damp paper towels inside the slide sorter.

The following day samples were rinsed in Tris-HCl (200 mM Tris, pH 8.3) for 5 min. The samples were recircled with the hydrophobic barrier pen. The Vector Red Substrate (Alkaline Phosphatase Substrate Kit, Vector Laboratories Inc.) was freshly prepared in Tris-HCl buffer at room temperature as previously described. The prepared substrate was added to the samples and incubated for 10 min. The colour development

was halted by immersing the slides in Tris-HCl buffer for 5 min. Sections were rinsed briefly in water before counterstaining in Harris' Haematoxylin and Scott's blueing solution as previously described.

2.8.4 De-hydration of paraffin-embedded sections for immunohistochemistry

After the completion of counterstaining with Harris's Haematoxylin and Scott's blueing solution, the sections were then taken through two changes of 70% v/v ethanol (30 s each), followed by 95% v/v (2 min each) and 100% absolute alcohol (5 min each) and submerged in histolene for at least 10 min each. Slides that were cleared with histolene and mounted with aqueous mounting medium (Aquamount, BDH Laboratory Supplies, Poole, England, U.K.).

2.8.5 F4/80 macrophage staining

Paraffin embedded sections were prepared as described above, however no antigen retrieval was performed. Normal rabbit serum working solution was added to the samples which were incubated for 4 hrs at 21 °C with the slide sorter closed. The samples were then briefly rinsed in PBST. The anti-F4/80 antibody [Cl:A3-1] (1:100 dilution in PBS, Abcam) was applied overnight at 4 °C with damp paper towels inside the slide sorter.

The following day the samples were rinsed with TBS for 1 min. The samples were then recircled with the PAP-pen and incubated for 1 hr at 21 °C with goat anti-Rat H & L (AP) secondary antibody (Abcam) diluted 1:200 in PBS. The slides were then immersed in Tris-HCl buffer for 5 min.

The Vector Red Substrate was freshly prepared in Tris-HCl buffer at room temperature 21 °C as described above. The prepared substrate was added to the samples and incubated for 20 min. The colour development was halted by immersing the slides in Tris-HCl buffer for 5 min. The sections were then rinsed briefly in water before counterstaining, dehydration and mounting as described.

2.8.6 Cholesterol clefts

Lipid filled areas appeared white as a result of the sample delipidation. These delipidated areas were clearly differentiated from macrophages that were stained pink. The quantification of these areas was carried out using a modification of previously published methods [233,234].

2.8.7 Determination of plaque lipid

The lipid content was measured from the F4/80 stain (Slide C), which were used to quantify the area occupied by macrophages. The lipid content was assessed as extracellular lipid pools which appeared as white areas within atherosclerotic plaque sections following the F4/80 staining with graded ethanol concentration, which solubilises the lipid. These delipidated white areas were clearly differentiated from macrophages that were stained pink as shown in Panel A in Figure 2.4. The images for the aortic sinus were retaken one valve leaflet at a time, at a higher magnification of 10x as the program could not accurately detect the specific areas of interest.

All the images were colour deconvoluted and filtered, as previously described. The area of interest was saturated with red as indicated in Panel B in Figure 2.4. The total area of interest within the plaque was outlined and calculated as displayed in Panel C in Figure 2.4. The amount of red marked within the plaque equates to the extracellular lipid pool quantified.

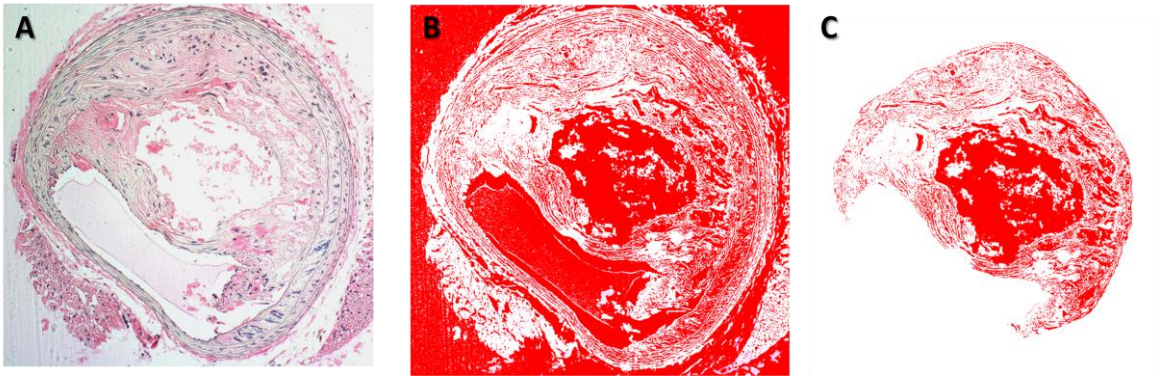

Figure 2.4: Estimation of extracellular lipid content of atherosclerotic plaques. Extracellular lipid content of atherosclerotic plaques was estimated by measuring the white area on a section stained with F4/80 as shown on Panel A. The image was filtered via the Image J program in order to quantify the lipid areas. The white areas were selected and saturated with red, leaving the remaining segments white as seen in Panel B. The plaque area was carefully outlined as shown in Panel C. The amount of red corresponds to the original extracellular lipid pool, which was calculated and expressed as a percentage of total plaque area.

2.9 Materials for picrosirius staining

2.9.1 Picrosirius for collagen staining

Paraffin embedded sections were dewaxed and taken through rehydration as previously described. The sections were stained using picrosirius red solution (0.5 g of Sirius Red (Sigma-Aldrich) dissolved in 500 mL of saturated aqueous solution of picric acid (Sigma-Aldrich) for 1 hr). The slides were then washed in two changes of acidified water (glacial acetic acid 1:400 in nanopure water; Astral Scientific) by vigorous shaking to remove any excess red dye from the sections. The slides were dehydrated in three changes of 100% ethanol (2 min each). The sections were cleared with histolene and coverslipped as previously described.

2.9.2 Compositional analysis of atherosclerotic plaques

Duplicate images obtained from each slide were captured digitally using an IX71 Olympus microscope (North Ryde, NSW, Australia). Measurements of smooth muscle cell, macrophage, lipid and collagen areas were quantified using the Image J program (NIH, Bethesda, MD, USA).

All the images that were taken for smooth muscle cells, macrophages and collagen, were initially separated into three colours (blue, green and pink) using the "Colour Devolution" function within the Image J program. The pink deconvoluted image was then filtered by the "Multi-thresholder" function in order to detect the specific stain of interest, which was marked with red. The amount of red marked equates to the area of interest that was quantified. The α-actin, F4/80, lipid or collagen content were expressed as a percentage of total plaque area for each image produced.

2.10 Preparation of tissue and plasma samples from high fat diet fed mice for the 4-hydroxy-2,2,6,6-tetramethylpiperidin-1-oxyl (TEMPOL) study

Heart and plasma samples were obtained from Prof. Jim Mitchell (Radiation Biology Branch, Center for Cancer Research, National Cancer Institute, Bethesda, MS, U.S.A.) from C57/B6 (n = 28) and apo $E^{-/-}$ (n = 38) mice. The two animal types each comprised of four groups. In each case two groups were fed a chow diet with or without TEMPOL (10 μg/g) supplemented into the food. The remaining two groups were fed a high fat diet (refer to Figure 2.4) with and without TEMPOL placed into the food. The chow diet consisted of 5% kcal of fat whilst the high fat diet consisted of 60% kcal from fat (refer to Table 2.1 below).

	Chow	**High Fat Diet**
Protein	**0.936**	**0.82**
Fat	**0.405**	**3.28**
Carbohydrate	**1.96**	**1.43**
Total (kcal/g):	**3.301**	**5.49**

Table 2.1: Caloric profile between chow and high fat diet in terms of protein, fat and carbohydrate in kcal/g.

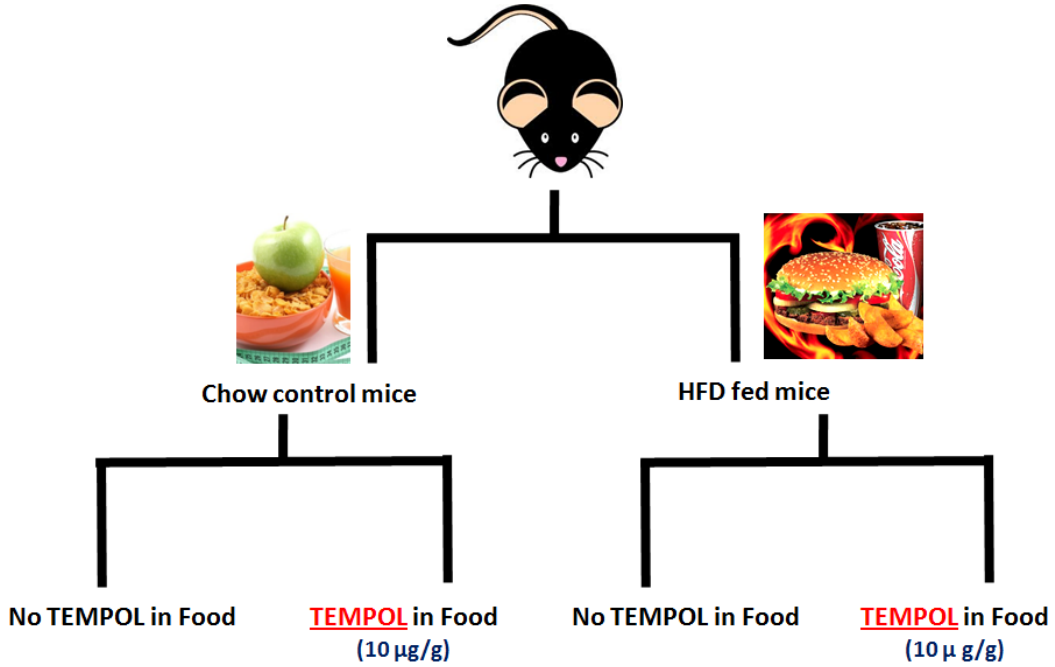

Figure 2.5: Animal model for TEMPOL study.
C57B/6 wild type and the apo $E^{-/-}$ mice were each divided into four groups comprising of Chow control mice with and without TEMPOL included in the food or high fat diet fed mice with and without TEMPOL included in the food.

2.10.1 Tissue processing and dissection for TEMPOL project

The heart was sampled for histological analysis based on a previously method published [233]. The heart was dissected out and stored in paraformaldehyde. The samples were rinsed in PBS and stored in 70% v/v ethanol. The aortic sinus was dissected as described above by making a cut perpendicular to the aorta halfway through the heart. The dissected samples were enclosed in cassettes and placed in 70% ethanol and then processed at the Pathology Department, University of Sydney, where the tissues were embedded in paraffin blocks. These paraffin blocks were then sectioned and stained with haematoxylin and eosin as previously described for plaque area.

2.10.2 Histological sectioning for TEMPOL project

The glass slides were pre-labelled from 1 - 25 for each sample. The sections for slide 1 were taken at the appearance of the first valve leaflet, and the rest of the

remaining sections were taken in sequentially labelled 2 - 25. Each slide consisted of three sections.

2.10.3 Analysis of plaque for TEMPOL project

Three slides arbitrarily labelled A, B and C were taken for plaque analysis. The first appearance of all three leaflets was chosen for Slide A and the first disappearance of all three leaflets were taken for Slide C. Slide B was taken in the middle of Slide A and C.

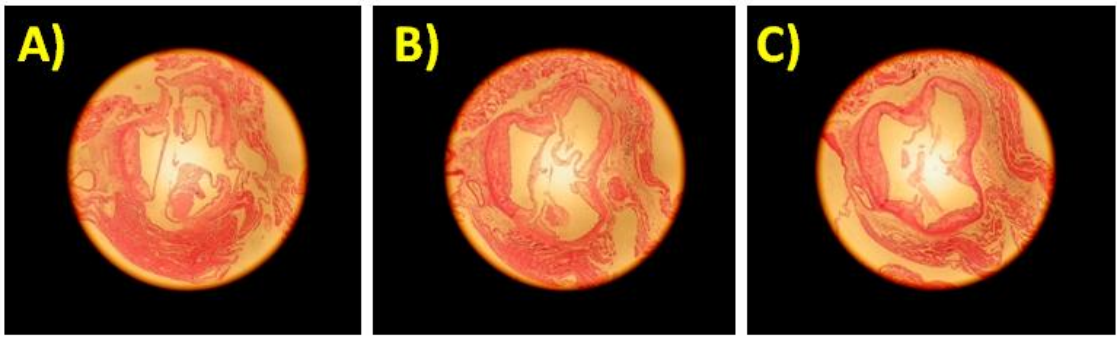

Figure 2.6: Representative images of 3 cross-sections (A - C) taken from the aortic sinus.
The first appearance of three leaflets was chosen for Slide A. The first disappearance of all three leaflets was taken for Slide C. Slide B was taken in the middle of Slide A and C.

2.11 Lipid analysis in plasma for TEMPOL animal work

The frozen plasma samples were obtained by the National Cancer Institute and stored at -80°C until analysis at the Heart Research Institute. Plasma samples were then given to a blinded observer for determination of triglycerides (TG), total cholesterol (TC), low-density lipoprotein-cholesterol (LDL-C) and high-density lipoprotein cholesterol (HDL-C).

2.11.1 Triglyceride determination

A standard curve (0 to 300 mg/mL) was generated using materials supplied with the Triglyceride kit from Wako Diagnostics (Osaka, Japan). The plasma was diluted in 1 in 5 with TBS. Initially 10 μL of prepared standards, along with 190 μL of colour reagent was applied to a 96-well plate in triplicate. The plate was incubated at 37 °C for 5 min in the M2e Spectrometer, shaken for 5 s before reading the absorbance at 600 nm. Values were read from the standard curve for each sample and converted to mmol/L.

2.11.2 Cholesterol determination

A standard curve for cholesterol (0 to 200 mg/mL) was generated using the materials supplied with the Total Cholesterol kit (Wako Diagnostics). The standards and the samples (1 in 5 dilutions in TBS) were prepared as described in the previous section with the absorbance measured at 505 nm. Values were calculated from the standard curve generated for each sample.

For HDL analysis, low density lipoproteins were precipitated from the plasma prior to analysis. Specifically 25 μL of undiluted serum from each mouse to be tested along with 25 μL of polyethylene glycol (PEG) solution (200 mg/mL in nanopure water; Sigma-Aldrich) were added to each Eppendorf tube and vortexed. The solution was allowed to stand for 20 min to allow the apolipoprotein B protein to precipitate then centrifuged at 13 000 rpm (15 700 *g*) for 20 min in a microcentrifuge. The supernatant, which contained the HDL-C, was quickly transferred to a fresh tube. The precipitate (LDL-C) was discarded. The HDL-C was measured for total cholesterol and then corrected for the dilution by the PEG solution.

LDL-C (mmol/L) levels were determined as shown in the formula below.

$$\text{LDL-C} = \text{Total Cholesterol} - \{\text{HDL-C} + (\text{Triglycerides}/5)\}$$

2.11.3 Materials for mouse cytokine, chemokine and adipokine measurements

Mouse Quantikine ELISA kits were purchased from R & D systems (Mineapolis, MN, U.S.A) for determining tumour necrosis factor-alpha (TNF-α), monocyte chemostatic protein-1 (MCP-1), leptin and resistin levels in mouse serum.

The murine MPO ELISA kit was purchased from Hycult Biotech, Inc. (Uden, Netherlands). The mouse IL-6 ELISA kit was purchased from Ray Biotech, Inc. (Norcross, GA, U.S.A.). The AssayMax mouse Adiponectin Kit was purchased from AssayPro (St. Charles, MO, U.S.A.). The mouse serum amyloid A (SAA) ELISA kit was purchased from Tridelta Development Ltd. (County Kildare, Ireland). Reagents supplied by the manufacture were brought to 21 °C before the commencement of the specified procedure.

For the Quantikine ELISA kits, mouse plasma was diluted as required by the assays: TNF-α (no dilution), MCP-1 (1:2), leptin (1:10), resistin (1:30) with the Calibrator Diluent specific to serum/ plasma samples. Standards were also prepared according the manufacturer's guidelines; TNF-α (0 - 700 pg/mL), MCP-1 (0 - 1000 pg/mL), leptin (0 - 4000 pg/mL) and resistin (0 - 2000 pg/mL).

Initially 50 µL of assay diluent was inserted in each well with 50 µL of the prepared samples / standards and incubated for 2 hrs at 21 °C, on the plate shaker. Each well was then manually aspirated and washed 4 - 5 times with 400 µL of washing buffer. 100 µL of conjugate was added and incubated for 1 to 2 hrs at 21 °C. The wells were washed again 4 - 5 times and 100 µL of substrate solution prepared by mixing equal volumes of Colour Reagent A and B from the kit. The plate was mixed and incubated for 30 min in darkness. The appearance of the blue-green colour reaction was stopped by adding 100 µL of Stop Solution. The optical density of each well was read by the spectrometer at 450 nm and 570 nm. The subtraction of the two measurements corrected for optical imperfections in the plate.

For the determination of MPO, IL-6, adiponectin and SAA levels in the plasma, enzyme linked immunosorbent assays were used in a similar manner to the Quantikine ELISA kits. The cytokine of interest within the standards and mouse plasma was determined using a sandwich ELISA in which the material was immobilized antibody and biotinylated polyclonal antibody of interest, which in turn is recognised by a streptavidin-peroxidase conjugate. The unbound material was then washed away and the peroxidase enzyme substrate tetramethylbenzidine (TMB) added. Colour development was stopped by the addition of oxalic acid. The absorbance was then measured with a spectrometer at 450 nm and 570 nm. The subtraction of the two measurements corrected for optical imperfections in the plate.

A standard curve was generated by plotting the absorbance (linear) versus the corresponding concentrations of the mouse MPO standards. The mouse plasma was diluted as required (MPO (1:4), IL-6 (1:6), Adiponectin (1:400), SAA (1:200)) with the supplied Diluent Buffer in Eppendorf tubes and vortexed. 50 – 100 µL of reconstituted standard, plasma samples and controls were transferred into appropriate wells and incubated for 1 to 2.5 hrs at 21 °C. After the first incubation, the wells were washed 4 to 5 times in a similar manner as previously described. 50 – 100 µL of Biotinylated Tracer Antibody was added to each well and further incubated for 1 hr at 21 °C. After the washing step, streptavidin-peroxidase conjugate (50 – 100 µL) was added to each well and incubated for 30 – 60 min at 21 °C. The solution was then discarded from the wells and washed, then 50 – 100 µL of TMB was added to each well and incubated for 10 – 30 min at 21 °C protected from light. The stop solution (50 – 100 µL) was then added to stop colour development. The absorbance was then read at 450 nm and 570 nm to correct for optical imperfections.

2.12 TEMPOL *in vitro* work

Human monocytes were matured into macrophages in media containing 5.5 or 20 mM glucose as previously described with and without the addition of 100 µM 4-hydroxy-2,2,6,6-tetramethylpiperidin-1-oxyl (Sigma-Aldrich). Lysosomal acid lipase (LAL) and cathepsin B and L activities enzymatic assays were assessed as described in Sections 2.2 and 2.3.

2.12.1 Cytokine expression

To examine cytokine expression by normal and hyperglycaemic cells, HMDM was stimulated with lipopolysaccharide (LPS; Sigma-Aldrich) from *Escherichia coli* in order to induce cytokine secretion. On day 10 of the maturation period, the cells were stimulated with 0, 25 and 50 ng/mL of LPS and further incubated for 24 hrs. On the following day cell media was collected and transferred to Eppendorf tubes and centrifuged at 2000 rpm (400 *g*) for 5 min at 4 °C to remove cell debris. The supernatant was then transferred to fresh Eppendorf tubes, aliquoted and stored at -80 °C. Each well was washed 3 times with PBS and 1 mL of nanopure water was added to each well and

the plate placed on ice to induce cell lysis. The cells were then scraped and transferred to Eppendorf tubes and stored at -20 °C before protein analysis.

2.12.2 ELISA for human C-Reactive Protein (CRP), TNF-α and Macrophage Inhibitory Protein (MIP-1α)

The levels of C-Reactive Protein (CRP), TNF-α and Macrophage Inhibitory Protein (MIP-1α) secreted into the media were determined by using Quantikine Human ELISA sandwich kits (R and D systems). Media samples were diluted with the supplied Calibrator Diluent specific for cell culture; 1:100 for MIP-1α, 1:200 for CRP and 1:10 for TNF-α.

Standards were prepared according to the manufacturer's guidelines. 50 – 100 µL of assay diluent was added to each well, then 50 – 100 µL of the reconstituted samples and standards was added and incubated for 1 – 2 hrs at 21 °C. Each well was then manually aspirated and washed 4-5 times with 400 µL of washing buffer. 200 µL of conjugate was added and incubated for 1 – 2 hrs at 21 °C. The wells were then washed 4 to 5 times and 200 µL of substrate solution prepared by mixing equal volumes of Solution A and Solution B from the kit. The plate was mixed and incubated for 20 – 30 min in darkness. The colour reaction was stopped by adding 50 µL of stop solution. The optical density of each well was read by the spectrometer at 450 nm and 570 nm, with subtraction used to correct for optical imperfections in the plate.

2.13 Statistical analyses

Data are expressed as mean ± standard error of the mean (SEM) in this thesis and results are from at least 4 - 6 separate experiments, consisting of samples assayed in triplicate.

Statistical analyses were undertaken using Prism 5.03 (GraphPad software, San Diego, CA, USA). For pair comparisons, paired or unpaired t tests were employed. For multiple comparisons, one way analysis of variance (ANOVA) with Tukey's Multiple Comparison test was used to assess differences. Two-way ANOVA with Bonferroni's post hoc test was applied when two different conditions were applied such as glucose and time intervals. Differences were considered statistically significant when $p < 0.05$.

CHAPTER 3:

INHIBITION OF LYSOSOMAL FUNCTION IN MACROPHAGES INCUBATED WITH ELEVATED GLUCOSE CONCENTRATIONS

3.1 Introduction

Atherosclerosis is a progressive vascular disorder leading to cerebro- and cardiovascular diseases and still remains the principal cause of mortality and morbidity in the world [235]. People with diabetes have a 2 to 4 fold elevated risk of cardiovascular disease compared to people without diabetes. Multiple studies indicate that this enhanced disease incidence cannot be solely explained by well-established cardiovascular risk factors, and are consistent with chronically elevated blood glucose levels contributing to an increased incidence of atherosclerosis [236].

In atherosclerosis macrophages are present within the inflamed artery wall and utilise multiple pathways including scavenger receptor mediated endocytosis, to remove damaged cells and tissue components, including modified low-density lipoproteins [237]. These materials are trafficked through the endo-lysosomal system for degradation, but under circumstances where the LDL are resistant to degradation, and / or lysosomal degradative function is impaired, they could accumulate with pathological consequences [238]. Thus altered lysosomal function is a potential route to lipoprotein-derived intracellular accumulation of lipid and protein, and the generation of lipid-laden ("foam") cells. Foam-cells are a major contributor to atherogenesis and atherosclerotic progression. Earlier onset and the rate of atherosclerotic progression are enhanced in DM along with chronically elevated level of AGE, glycated proteins and glucose.

Evidence from both cellular and *in vivo* studies, is consistent with lysosomal lipid accumulation [239,240]. Modified and native proteins are catabolised by the proteasomal and lysosomal systems, with the former primarily responsible for degradation of intracellular species, whereas the latter handles both extra- and intra-cellular materials [241]. The lysosomal system of human monocyte-derived macrophages utilises multiple proteases including cysteine- (e.g. cathepsins B, L and S) and aspartate dependent (e.g. cathepsin D) enzymes. Both proteasomal [242] and lysosomal [243] enzyme activities can be modulated by *in vitro* incubation of cell lysates or proteasomal fractions with reactive aldehydes or pre-glycated proteins. For the lysosomal enzymes, the cysteine proteases were most markedly affected with this attributed to modification of the active site cysteine [243].

In the light of this data, we hypothesised that maturation of human monocytes into macrophages in, or exposure of a murine macrophage-like cell line to, elevated glucose would result in altered lysosomal function.

3.2 Aims

The aim of the studies reported here was to investigate whether high glucose concentrations alter enzymatic activities associated with lysosomal protein and lipid metabolism. The impact of high glucose concentrations upon macrophage lysosomal function and population was examined in murine macrophage-like cell line J774A.1, and human monocyte derived macrophage (HMDM) cells incubated in normal (5.5 mM) and higher (10, 20 and 30 mM) glucose concentrations, with the activities of lysosomal cathepsin enzymes (cathepsins B, L, S and D), lysosomal acid lipase activity (LAL) and lysosomal number quantified.

3.3 Methods

Murine J774A.1 macrophage-like cells were incubated, and primary human monocytes were matured into macrophages in the presence of 5.5, 10, 20 or 30 mM glucose for 11 days as detailed in Section 2.2. The activity of lysosomal cysteine proteases B, L and S, and the aspartic protease cathepsin D, along with lysosomal acid lipase (LAL) were quantified by fluorescence spectroscopy as described in Section 2.3 to 2.4. Lysosomal numbers were quantified by Western blotting for LAMP-1 protein (relative to tubulin) levels as detailed in Section 2.5 to 2.5.8.

The lysosomal activities were corrected for the protein concentration in the lysates for each sample. The data (mean ± SEM, from 5 to 6 independent experiments each with triplicate samples) for the lysosomal activities from higher glucose treatments (10 to 30 mM) was expressed as a percentage of the 5.5 mM glucose condition.

For multiple comparisons one-way ANOVA with Tukey's multiple comparison tests were used. Gel analysis was carried out using Image J analysis software. Significance was assumed at $p < 0.05$.

3.4 Results

3.4.1 Effects of incubation of J774A.1 and HMDM in high glucose concentrations for 11 days on cell viability

The cell viability was measured as a marker for potential cytotoxicity in the J774A.1 and HMDM cells incubated in the normal 5.5 mM and 30 mM glucose conditions as outlined in Section 2.4.2, as elevated glucose levels might cause damage to the cells.

Initial experiments examined the minimum and maximum concentrations of glucose used: 5.5 mM and high 30 mM. The overall cell viability observed was greater than 90% in both the J774A.1 (90.6 ± 0.9%) and HMDM (98 ± 0.8%) cells as shown in Figure 3.1. There were no statistical differences noted between the two glucose treatment groups for the J774A.1 or HMDM cells using Student's t- tests. These results indicated the absence of cytotoxicity in either case. In the light of these data intermediate concentrations of glucose were not investigated.

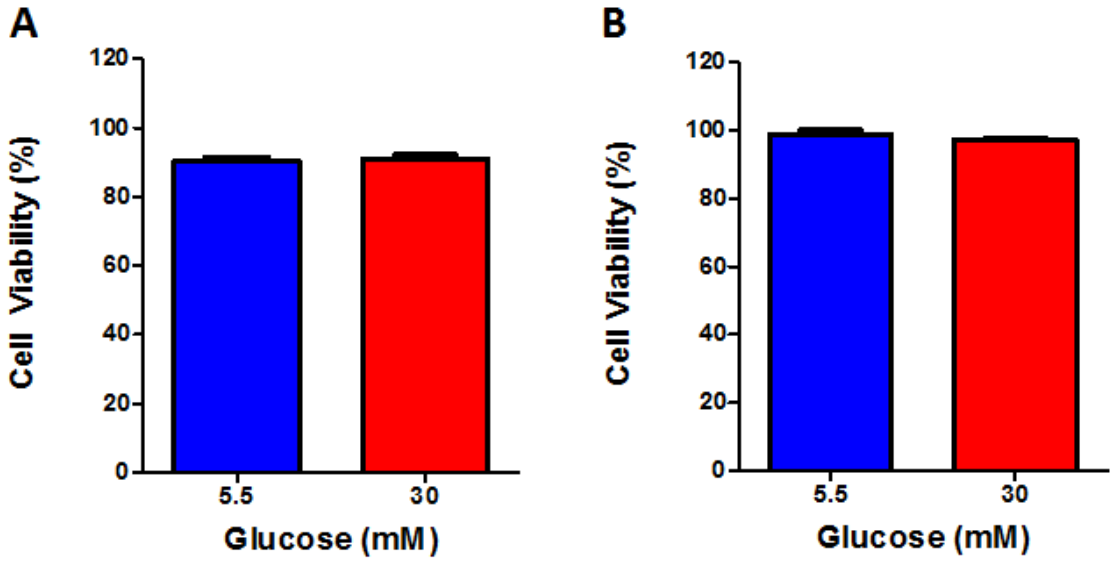

Figure 3.1: Cell viability of J774A.1 and HMDM cells incubated in normal (5.5 mM) and high (30 mM) glucose conditions for 11 days.
Measurement of cell viability for J774A.1 cells (Panel A) and human monocyte-derived macrophages (HMDM) (Panel B) in the normal 5.5 and high 30 mM glucose concentrations of glucose. Data (mean ± SEM) are expressed as a percentage from 6 independent experiments using separate cell donors (HMDM) or separate cultures of J774A.1 cells.

3.4.2 Protein content of J774A.1 and HMDM cells incubated in varying glucose concentrations for 11 days

Protein levels were assessed to confirm the cell viability results and to establish that high glucose levels did not affect cell confluency in the case of the J774A.1 and HMDM cells. The protein levels of the cells incubated in the normal (5.5 mM) to high (10 to 30 mM) glucose concentrations were determined by the BCA protein assay by use of a standard curve generated using BSA as discussed in Section 2.4.1.

There were no statistical differences in protein content observed across the glucose treatments for either J774A.1 or HMDM cells using a repeated measures one-way ANOVA with Tukey's post hoc multiple comparison's test (Figure 3.2). These results suggest that high glucose conditions do not affect the protein levels or cell confluency in the J77A.1 or HMDM cells.

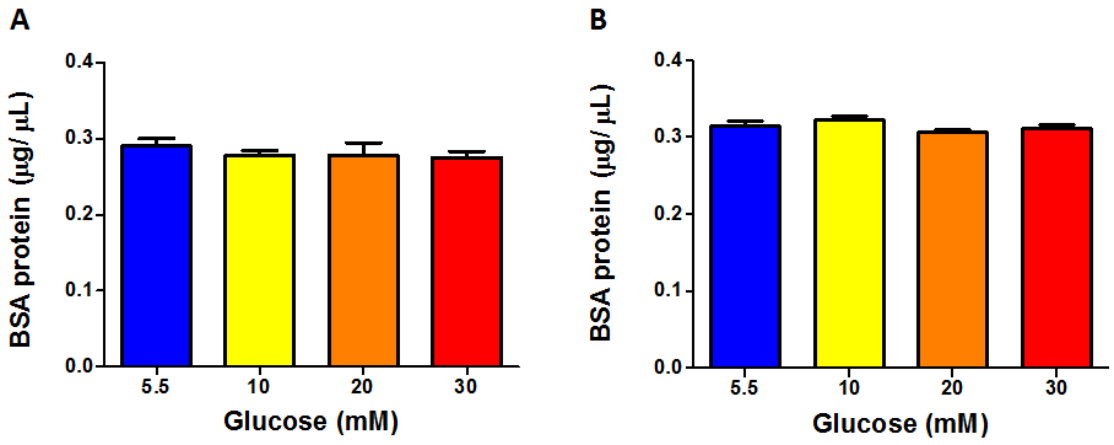

Figure 3.2: Protein levels in J774A.1 and HMDM cells incubated in various concentrations of glucose (5.5, 10, 20 and 30 mM) for 11 days.
Measurement of protein levels in J774A.1 cells incubated (Panel A), and maturation of human monocytes to macrophages (HMDM) (Panel B), in various concentrations of glucose (5.5, 10, 20 and 30 mM glucose). Data (mean ± SEM) are expressed in µg/µL equivalent of BSA protein from 6 independent experiments using separate cell donors (HMDM) or separate cultures of J774A.1 cells.

3.4.3 Effect of high glucose concentrations on activity and level of lysosomal cathepsin enzymes

Lysosomal activity was determined in cell lysates prepared from J774A.1 cells and HMDM cells that were incubated in normal 5.5 mM and higher glucose concentrations (10, 20 and 30 mM) for 11 days (see Sections 2.2.2, 2.2.4, 2.2.5). The cell extracts for lysosomal activity measurements were collected and snap frozen in liquid nitrogen and stored at -80°C as described in Section 2.2.3 for J774A.1 cells and Section 2.2.5 for HMDM cells.

The cell lysates obtained were then resuspended in nanopure water followed by centrifugation at 13 400 *g* for 5 min at 4°C to remove unlysed cells and membrane fractions that may interfere with the assay as described in Sections 2.2.3 and 2.3.1. The supernatant was then transferred to fresh tubes to measure the activity of lysosomal enzymes, and protein content by use for the BCA protein assay (see Section 2.4.1).

To determine the activity of lysosomal cathepsin enzymes, release of AMC from the peptide substrates was monitored using a fluorescence plate reader ($\lambda_{excitation}$ 360 nm and $\lambda_{emission}$ 460 nm) as discussed in Sections 2.3.2 to 2.3.5. The substrates for cathepsin B, L, S and D were Z-Arg-Arg-AMC, Z-Phe-Arg-AMC, Z- Val-Val-Arg-AMC and 7-methoxycoumarin-4-acetyl-Gly-Lys-Pro-IIe-Leu-Phe-Phe-Arg-Leu-Lys-DNP-D-Arg-amide, respectively. The buffer pH used to achieve maximum activity for each cathepsin was 6, 5.5, 7.5 and 4.2 for cathepsin B, L, S and D, respectively. To ensure that the activities measured were specific to particular enzymes, specific assay inhibitors were included in the buffer to suppress the activities of other cathepsins. For example, in buffers for assessment of cysteine protease activity, pepstatin A was added to inhibit aspartate proteases such as cathepsin D, and in buffers for determination of cathepsin D activity, E64 was added to inhibit cysteine proteases.

In order to determine lysosomal cathepsin activities, the initial linear region of plots of florescence against time were used as shown in Figure 3.3a and b. Nanopure water was used for dilutions, and served as the negative control (no cell lysate fraction) in each case. In these cases there was no change in fluorescence over time as shown by the black squares in Figure 3.3a and b.

The protein concentration was determined in remaining portions of the same cell lysate samples as described in Section 2.4.1, thereby allowing the lysosomal activity to

be corrected for the protein concentration (μg/μL) of the cell lysate used for each measurement. The corrected data were expressed as a percentage of the lysosomal activities determined for the normal (5.5 mM) glucose condition.

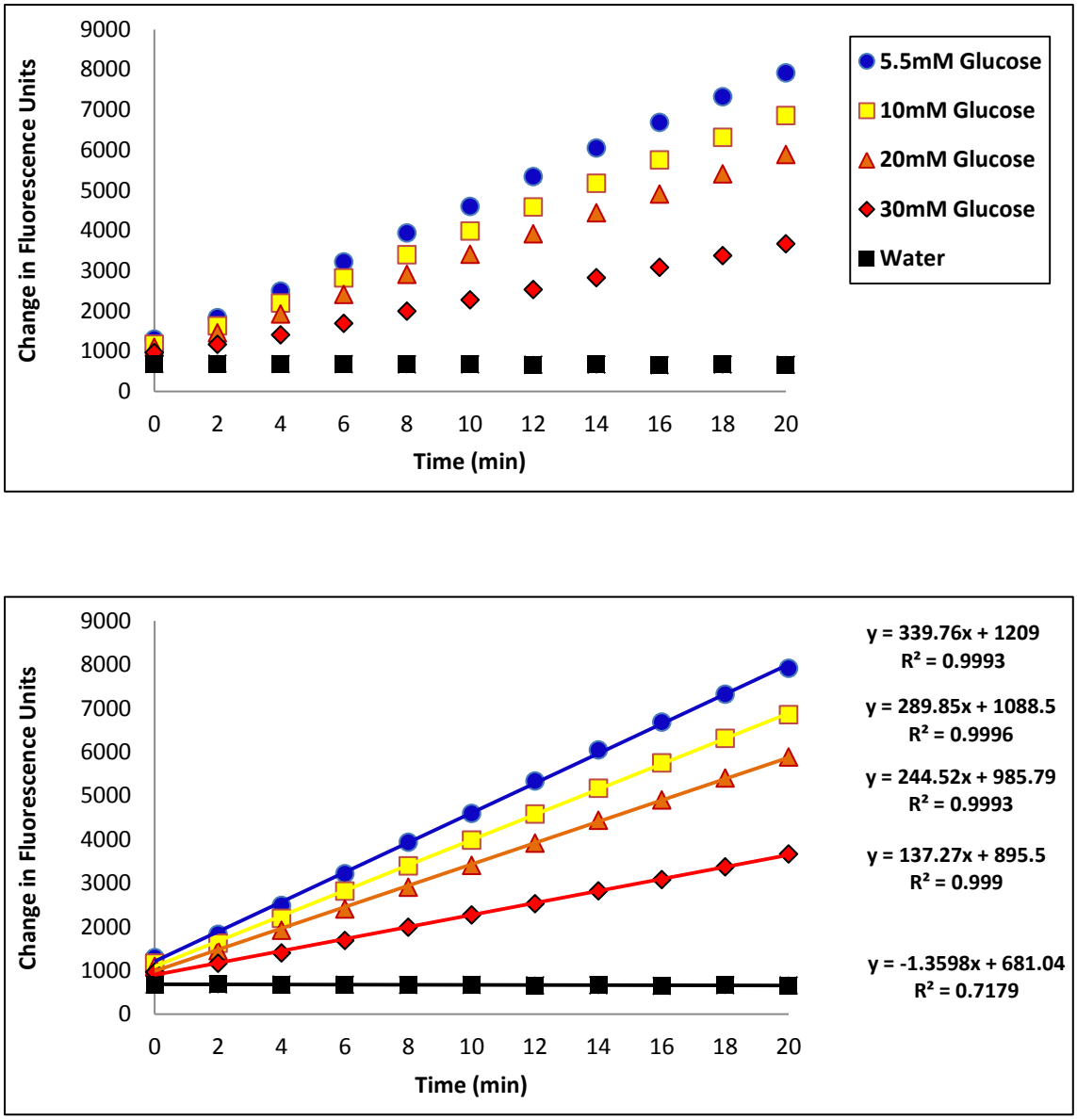

Figure 3.3: Changes in fluorescence in cell lysate fractions of HMDM matured in normal 5.5 mM or 10, 20 and 30 mM glucose concentrations followed by addition of cathepsin B substrate.

Representative data are presented for cells matured in normal 5.5 mM and higher (10 - 30 mM) glucose concentrations. The changes in fluorescence emission followed a linear relationship as shown on the bottom graph. The black squares represent the negative control (no cell lysate) which showed no change in fluorescence over time.

3.4.3.1 Effects of lysosomal cathepsin activity in J774A.1 cells incubated in normal and high glucose concentrations

The lysosomal cathespsin B, L, S and D enzymatic activities were investigated in the J774A.1 cells to examine the impact of high glucose concentrations upon lysosomal function. Incubation of J774A.1 cells in high glucose concentrations for 11 days modulated the activities of all of the lysosomal cathepsin enzymes examined (Figure 3.4). Cells incubated in elevated glucose concentrations showed significantly less cathepsin B activity for the 10 mM condition (73.2 ± 6.6%, $p < 0.01$), the 20 mM condition (58.2 ± 8.5%, $p < 0.001$) and the 30 mM condition (50 ± 6.4%, $p < 0.001$) than cells incubated in 5.5 mM glucose (activity taken as 100%) using repeated measures one-way ANOVA with Tukey's post hoc multiple comparison's test. A statistical significance was also observed between the 10 and 30 mM glucose conditions ($p < 0.05$).

Cathepsin L activity also showed a significant decrease in cells incubated in 10 mM (68.6 ± 7.6%, $p < 0.05$), 20 mM (53.9 ± 7.6%, $p < 0.01$) and 30 mM (37.1 ± 6.7, $p < 0.001$) glucose as compared to the 5.5 mM glucose concentration (values taken as 100%). A statistical significance was also observed between the 10 and 30 mM glucose conditions ($p < 0.05$).

Cathepsin S activity was significantly decreased in cells incubated in 10 mM (67 ± 4.3%, $p < 0.001$), 20 mM (47.8 ± 5.8%, $p < 0.001$) and 30 mM (23.4 ± 2.5%, $p < 0.001$) glucose when compared to the 5.5 mM glucose condition (100%). Differences were also observed for the 20 and 30 mM glucose conditions ($p < 0.001$) versus the 10 mM glucose condition, and also between the 20 and 30 mM glucose conditions ($p < 0.01$).

Cathepsin D activity was significantly lower in cells incubated in 10 mM (75.1 ± 4.1%, $p < 0.01$), 20 mM (64.6 ± 3%, $p < 0.001$), 30 mM (42.5 ± 5.6%, $p < 0.001$) glucose compared to the 5.5 mM glucose concentrations (100%). Lower cathepsin D activity was detected for the 30 mM when compared with 10 mM ($p < 0.01$) and 20 mM ($p < 0.05$) glucose conditions.

In summary the results showed decreased cathepsin B, L, S and D activities in the J774A.1 cells incubated in high concentrations of glucose when compared to the normal glucose concentration.

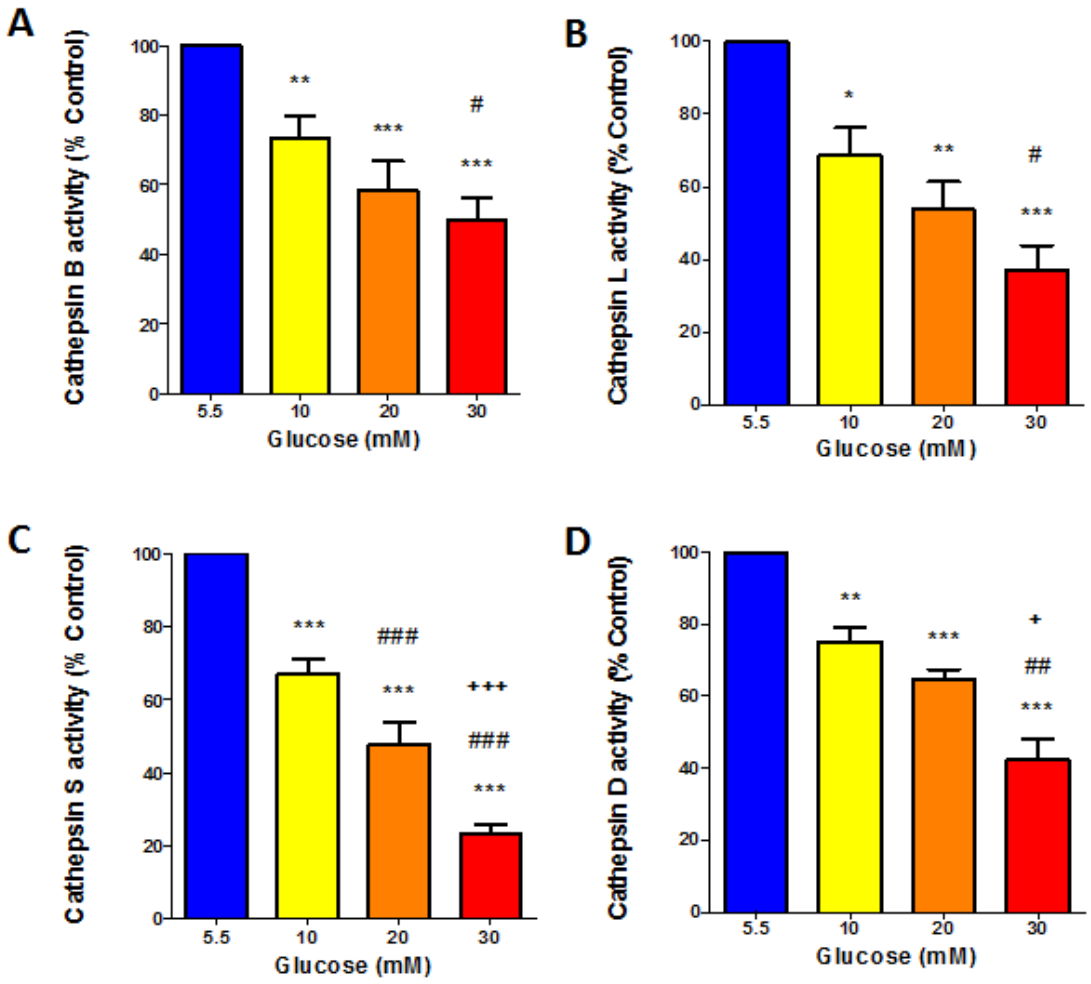

Figure 3.4: Lysosomal cysteine and aspartic cathepsin activities in J774A.1 cells incubated in various concentrations of glucose (5.5, 10, 20 and 30 mM) for 11 days. Data (mean ± SEM, from n = 5 independent experiments using different passages) are reported as the linear change in fluorescence intensity with time, as a percentage of the 5.5 mM glucose condition, corrected for protein levels. Panels A, B, C and D represent cathepsin B, L S and S activities, respectively. Statistical significant differences were carried out by one-way ANOVA followed by Tukey's post-hoc test. * $p < 0.05$, ** $p < 0.01$ and *** $p < 0.001$ when compared to the 5.5 mM glucose condition. # $p < 0.05$, ## $p < 0.01$ and ### $p < 0.001$when compared to the 10 mM glucose condition. + $p < 0.05$ and +++ $p < 0.001$ when compared to the 20 mM glucose condition.

3.4.3.2 Effects of lysosomal cathepsin activity in HMDM incubated in normal and high glucose concentrations

As inhibition of lysosomal cathepsin activities was observed in the murine J774A.1 cells that were treated with high glucose levels, the potential detrimental impact of high glucose levels upon lysosomal cathepsin activity was also investigated in the HMDM cells that were matured in the normal (5.5 mM) and high 10, 20 and 30 mM glucose conditions.

HMDM incubated with elevated glucose concentrations showed significantly less cathepsin B activity in the 10 mM (49 ± 3.4%, $p < 0.001$), 20 mM (43.1 ± 8.9%, $p < 0.001$) and 30 mM (36.9 ± 9.5, $p < 0.001$) glucose conditions, than cells incubated in 5.5 mM glucose (100%) using repeated measures one-way ANOVA with Tukey's post hoc multiple comparison's test.

Cathepsin L activity also showed a significant decrease in cells matured in 10 mM (71 ± 4.1%, $p < 0.05$), 20 mM (50.5 ± 11.1%, $p < 0.01$) and 30 mM (35.5 ± 9.3%, $p < 0.001$) glucose concentrations as compared with 5.5 mM glucose (100%). A statistical significance was also observed between the 10 and 30 mM glucose conditions ($p < 0.05$).

Cathepsin S activity was decreased significantly in cells matured in 10 mM (61.3 ± 9.9%, $p < 0.01$), 20 mM (31.6 ± 8.6%, $p < 0.001$) and 30 mM (27.5 ± 8.8%, $p < 0.001$) glucose when compared to the 5.5 mM glucose concentration (100%). Statistical significance were also observed between the 20 ($p < 0.05$) and 30 mM ($p < 0.01$) glucose conditions versus the 10 mM condition.

Cathepsin D activity showed a significant decrease in cells matured in 20 mM (55.2 ± 11.3%, $p < 0.01$) and 30 mM (47.5 ± 8.6%, $p < 0.01$) glucose concentrations as compared with normal glucose concentrations (100%). Although there was lower cathepsin D activity in the 10 mM glucose (80.1 ± 7%) condition, this was not statistically significant when compared to the 5.5 mM condition.

Overall, maturation of HMDM in high glucose concentrations for 11 days suppressed the activity of lysosomal cathepsin B, L, S and D enzymes (Figure 3.5) when compared to the normal glucose concentrations with this effect seen even at 10 mM glucose for cathepsins B, L and S.

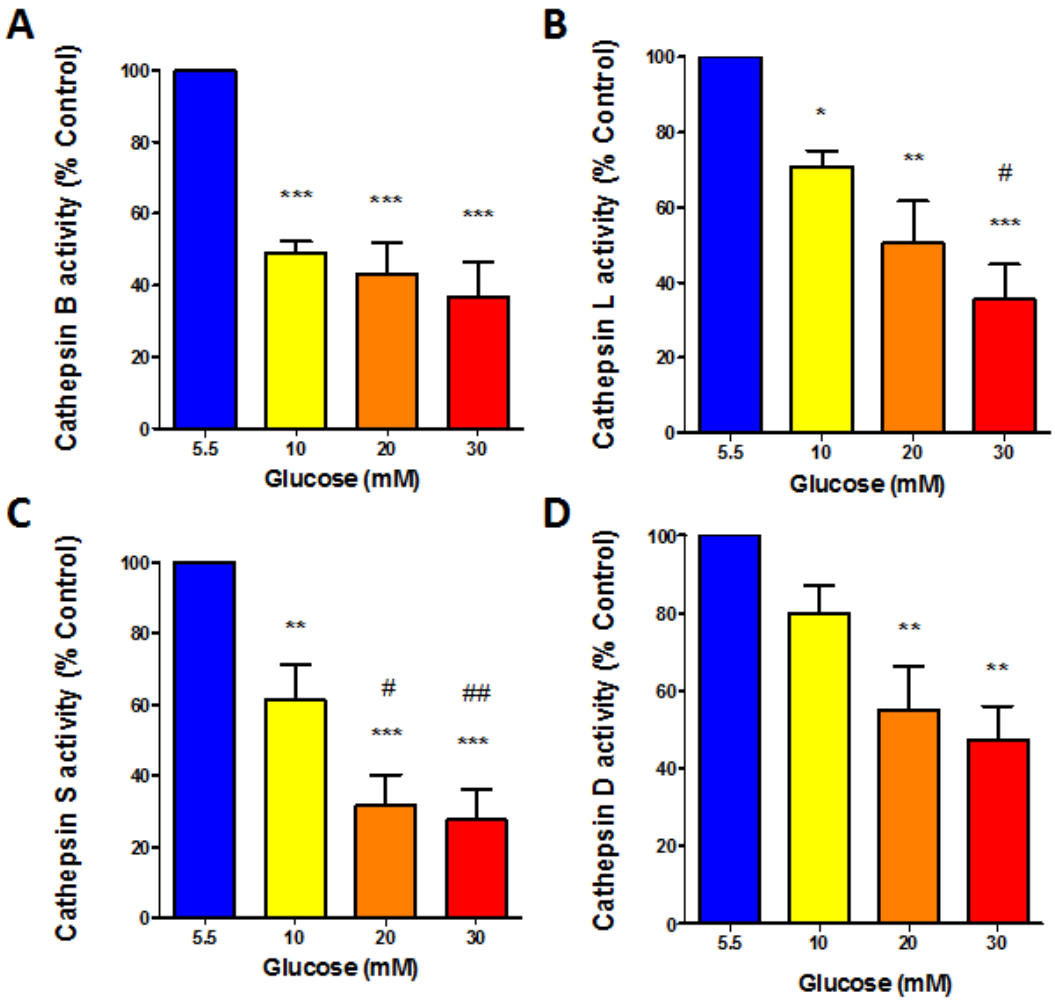

Figure 3.5: Lysosomal cysteine and aspartic enzyme activities in HMDM cells matured in various concentrations of glucose (5.5, 10, 20 and 30 mM) for 11 days. Data (mean ± SEM, from n = 5 independent experiments using different donors) are reported as a percentage of the 5.5 mM glucose condition, corrected for protein levels. After incubation for 11 days the cells were lysed and cathepsin activity quantified using specific pro-fluorescent substrates as described in Section 3.4. Panels A, B, C and D represent cathepsin B, L S and S activities, respectively. Statistical significant differences were carried out by one-way ANOVA followed by Tukey's post-hoc test. * $p < 0.05$, ** $p < 0.01$ and *** $p < 0.001$ when compared to the 5.5 mM glucose condition. # $p < 0.05$ and ## $p < 0.01$ when compared to the 10 mM glucose condition.

3.4.4 Effects of normal and high glucose concentrations on lysosomal acid lipase activity (LAL) in J774A.1 and HMDM cells

LAL is the sole lysosomal hydrolase for endocytosed cholesteryl esters and triglycerides [230]. Given the role of lipoprotein-derived cholesterol and triglycerides in foam cell formation it was therefore of interest to determine whether cells incubated in high glucose concentrations also demonstrated impaired LAL activity. Using cell lysates from HMDM and J774A.1 cells that were exposed to varying glucose levels, LAL activity was assessed by using the pro-fluorescent probe, 4-methylumbelliferyl oleate (4-MUO) which is cleaved to the fluorescent species 4-methylumbelliferone (4-MU); this material was subsequently quantified as described in Section 2.3.6.

Incubation of J774A.1 and HMDM cells in high glucose concentrations for 11days modulated the activities of the lysosomal acid lipase (LAL) activities within the macrophages examined (Figure 3.6). J774A.1 cells incubated in high glucose concentrations for 11 days showed significantly lower levels of LAL activity for the 10 mM (77.1 ± 4.3%, $p < 0.05$), 20 mM (63.3 ± 7.9%, $p < 0.001$) and 30 mM conditions (51.6 ± 8%, $p < 0.001$) than cells incubated in 5.5 mM glucose (activity set as 100%) using repeated measures one-way ANOVA with Tukey's post hoc multiple comparison's test. A statistical significance was also observed between the 10 and 30 mM glucose conditions ($p < 0.01$).

Maturation of HMDM in elevated glucose concentrations also suppressed LAL activity (Figure 3.6) when compared to the 5.5 mM glucose concentrations. Thus HMDM incubated in high glucose concentrations showed significantly less LAL activity in the 10 mM (54.3 ± 5.6%, $p < 0.001$), 20 mM (49.9 ± 5.3%, $p < 0.001$) and 30 mM glucose condition (41.7 ± 5.7%, $p < 0.001$) than cells incubated in 5.5 mM glucose (100%) using repeated measures one-way ANOVA with Tukey's post hoc multiple comparison's test. A statistically significant difference was also observed between the 10 and 30 mM glucose conditions ($p < 0.05$).

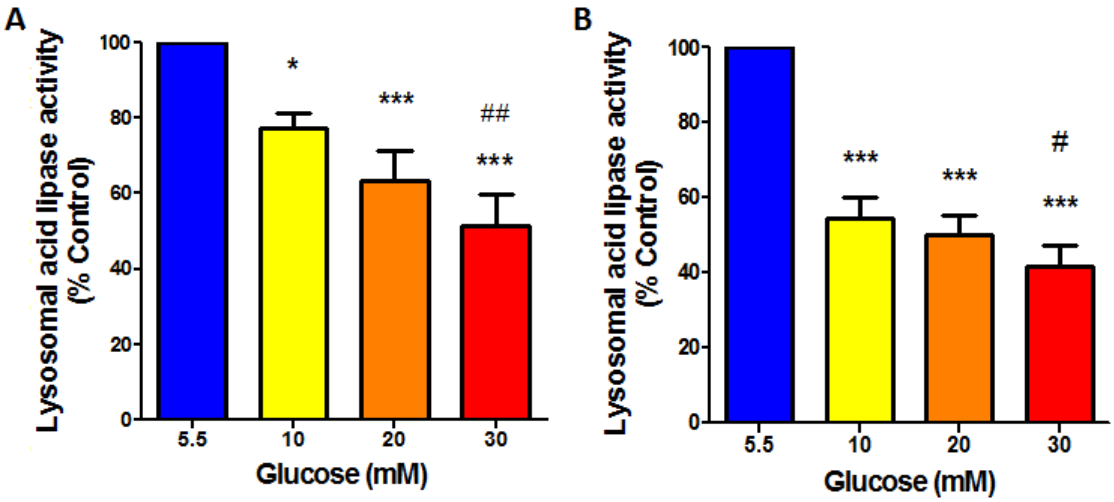

Figure 3.6: Lysosomal acid lipase (LAL) activity in J774A.1 and HMDM cells incubated in various concentrations of glucose (5.5, 10, 20 and 30 mM) for 11 days. The effect of incubation of murine macrophage-like J774A.1 cells (Panel A) and maturation of human monocytes to macrophages (HMDM) (Panel B) in various concentrations of glucose (5.5, 10, 20 and 30 mM glucose) on the activity of LAL is presented. Data (mean ± SEM) are reported as a percentage of the 5.5 mM glucose condition, corrected for protein levels from 6 independent experiments using separate cell donors (HMDM) or separate cultures (J774A.1 cells). Statistically significant differences were assessed by one-way ANOVA followed by Tukey's post-hoc test. * $p < 0.05$ and *** $p < 0.001$ when compared to the 5.5 mM glucose condition. # $p < 0.05$ and ## $p < 0.01$ when compared to the 10 mM glucose condition.

3.4.5 Effect of high concentrations of mannitol on J774A.1 and HMDM incubated for 11 days

High levels of glucose may induce osmotic stress upon cultured cells and this may explain the results presented above. In order to differentiate between the effects of higher osmotic pressure and other effects of high glucose levels, J774A.1 or HMDM cells were exposed to the normal (5.5 mM) or high (30 mM) glucose conditions, or 5.5 mM glucose with 24.5 mM mannitol (as a high osmotic pressure treatment) for 11 days as stated in Section 2.3.7. Cells were collected and lysed, and the activities of lysosomal cathepsins B, L and LAL were measured as described in Sections 2.3, 2.3.1, 2.3.2, 2.3.5 and 2.3.6.

There was a significant reduction in cathepsin B (48.6 ± 4%, $p < 0.001$), L (67.6 ± 5.5%, $p < 0.001$) and LAL (75.5 ± 5.9%, $p < 0.01$) activities in the 30 mM glucose condition treated J774A.1 cells when compared to the 5.5 mM condition (100%) consistent with the data reported earlier. Significantly greater cathepsin B (90.1 ± 2.9%, $p < 0.001$), L (101.2 ± 4.5%, $p < 0.01$) and LAL (97.6 ± 4.1%, $p < 0.01$) activity was observed in the glucose + mannitol-treated cells when compared to the 30 mM glucose treated J774A.1 cells. There were no statistically significant changes in lysosomal activities observed between incubation with 5.5 mM versus the cotreatment with 5.5 mM glucose and 24.5 mM mannitol (Figure 3.7).

For the HMDM cells a reduction in cathepsin B (37 ± 10.3%, $p < 0.001$), L (35.7 ± 9.7%, $p < 0.001$) and LAL (38.4 ± 10.6%, $p < 0.001$) activities were observed in the HMDM that were incubated with high glucose conditions compared to cells matured in 5.5 mM glucose consistent with the data reported in Figure 3.5. However, no significant difference in lysosomal enzyme activity was found for the glucose + mannitol treated cells when compared to the cells matured in 5.5 mM glucose. However, significantly greater cathepsin B (95.5 ± 1.4%, $p < 0.001$), L (93.1 ± 1.1%) and LAL (99.8 ± 7.5%, $p < 0.001$) activities were detected in the osmotic control when compared to the high glucose condition in the HMDM cells.

The addition of mannitol at a concentration which gave an equivalent osmotic pressure to 30 mM glucose did not result in a reduction of lysosomal activities as there were no statistically significant changes in the lysosomal activities when compared with the cells incubated with 5.5 mM glucose. In contrast with this, cells exposed to 30 mM glucose (positive control) clearly showed the expected inhibition of lysosomal cathepsins B, L and acid lipase activities based upon the results presented earlier.

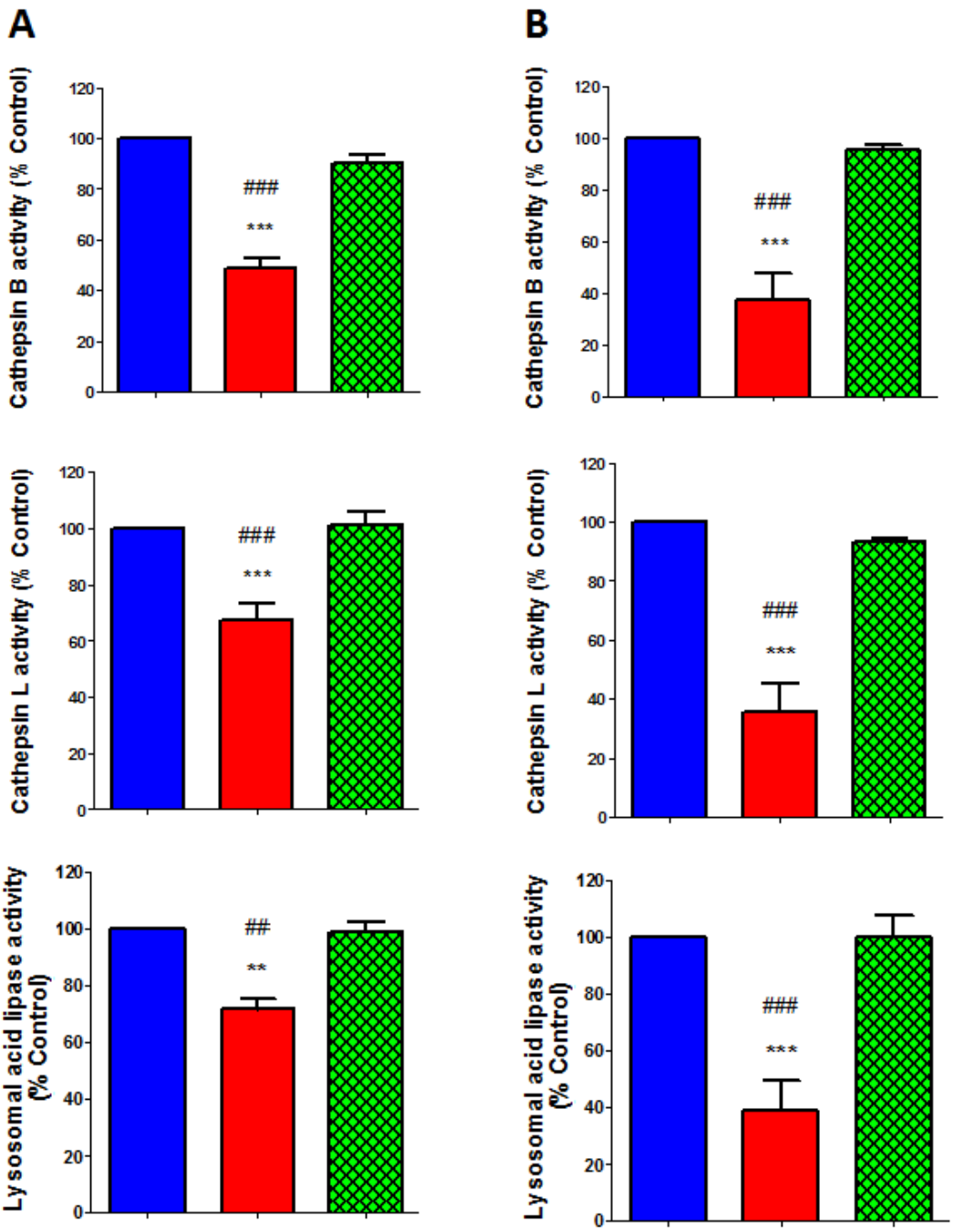

Figure 3.7: **Lysosomal enzymatic activities in J774A.1 and HMDM cells incubated in the normal (5.5 mM), high (30 mM) glucose and 5.5 mM glucose + 24.5 mM mannitol (osmotic control) conditions for 11 days.**

Macrophages were exposed to 5.5 mM glucose, 30 mM glucose or 5.5 mM glucose + 24.5 mM mannitol (osmotic control). Panel A) J774A.1 and Panel B) HMDM. Each panel displays the lysosomal enzymatic activities of cathepsins B, L and LAL. Statistical significant inhibition of lysosomal activities were observed for the 30 mM glucose conditions at ** $p < 0.01$, and *** $p < 0.001$ against the normal glucose conditions and ## $p < 0.01$, ### $p < 0.001$ versus the osmotic control. No differences were detected between the 5.5 mM and 5.5 mM glucose + 24.5 mM mannitol conditions.

3.4.6 Western blot analysis of lysosomal associated marker protein-1 (LAMP-1) levels

Exposure to high glucose decreased the activity of multiple lysosomal enzymes critical for the metabolism of low-density lipoproteins (LDL). This decrease in lysosomal activities observed in the macrophages incubated with high glucose conditions could be due to (i) inhibition of enzyme function or inactivation of the enzymes; (ii) a reduction in lysosomal population; or (iii) changes in protein expression. To examine the potential differences in lysosomal number in cells incubated in high glucose concentrations, LAMP-1 expression was assessed in macrophages that were incubated/matured in the normal 5.5 mM or 10 - 30 mM high glucose conditions.

Cell lysates were collected from J774A.1 and HMDM cells after 11 days and subjected to Western blotting for the determination of LAMP-1 levels under various glucose concentrations as detailed in Sections 2.5 - 2.5.8. The LAMP-1 protein was detected at 120 kDa and β-tubulin was used as a loading control (band detected at 51 kDa) and the data was expressed relative to β-tubulin and as a percentage of the data for the 5.5 mM glucose condition.

J774A.1 cells incubated in high glucose concentrations for 11 days showed significant decreases in LAMP-1 levels for the 20 mM (61.6 ± 7%, $p < 0.05$) and 30 mM glucose concentration (47.7 ± 7.5%, $p < 0.01$) when compared to cells incubated in 5.5 mM glucose (values taken as 100%) using repeated measures one-way ANOVA with Tukey's post hoc multiple comparison's test. A statistical significance was also observed between the 10 (86.7 ± 9.3%, $p < 0.05$) and 30 mM glucose conditions.

Maturation of HMDM in elevated glucose decreased LAMP-1 protein levels (Figure 3.8) when compared to the normal glucose concentrations. HMDM incubated with high glucose showed significantly less LAMP-1 protein in the 20 mM (66.2 ± 10.9%, $p < 0.05$) and 30 mM (48.8 ± 11.4, $p < 0.001$) glucose conditions when compared to cells incubated in 5.5 mM glucose concentrations (100%) using repeated measures one-way ANOVA with Tukey's post hoc multiple comparison's test. A statistical difference was also observed between the 10 mM (79.9 ± 6.6 %, $p < 0.05$) and 30 mM glucose conditions.

LAMP-1 protein levels were significantly diminished in the 20 and 30 mM glucose conditions, for both the J774A.1 and HMDM cells (Figure 3.8). Decreased

LAMP-1 protein expression at higher glucose concentrations may be indicative of a decrease in lysosomal population which may be a potential contributing factor for the loss of lysosomal activity observed in macrophages incubated under the highest (20 and 30 mM) glucose concentrations.

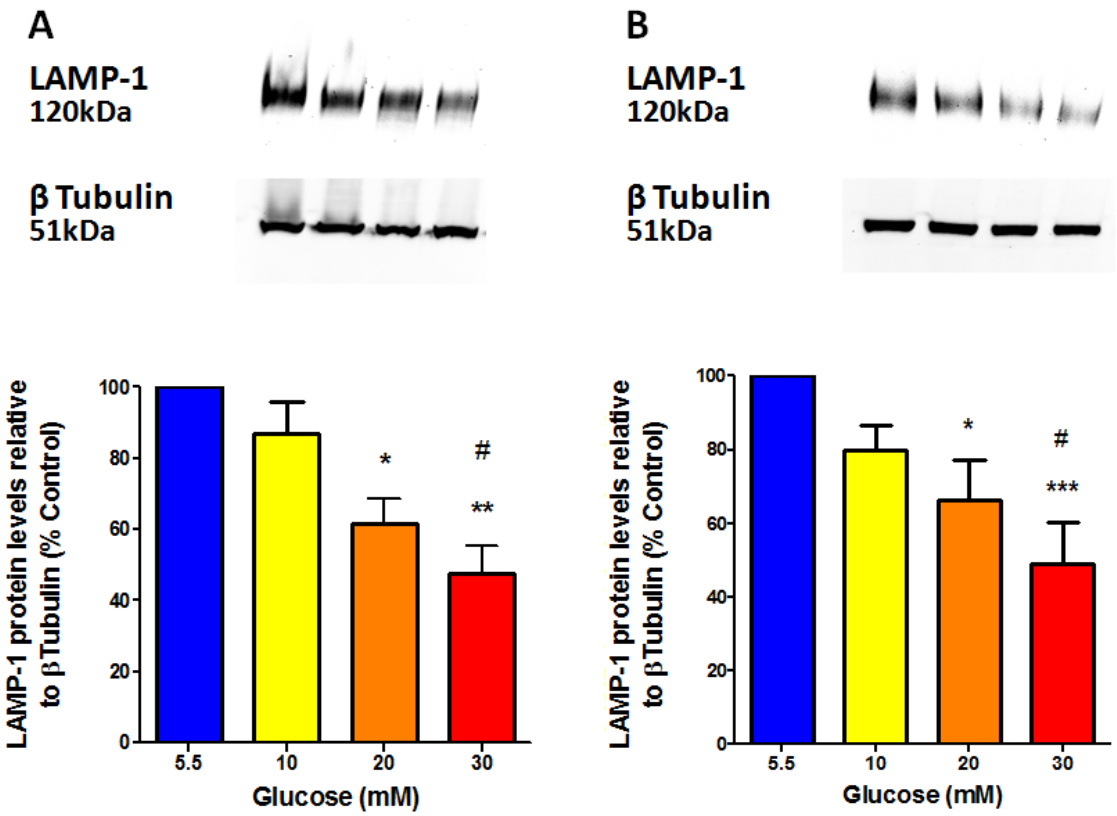

Figure 3.8: Quantification of LAMP-1 levels by Western blotting for J774A.1 and HMDM cells incubated in various concentrations of glucose (5.5, 10, 20 and 30 mM) for 11 days.

The top panels represent representative Western blots of LAMP-1 and corresponding β-tubulin (loading control) from Panel A) J774A.1 and, Panel B) HMDM cells, incubated in (left to right) 5.5, 10, 20 or 30 mM glucose. The lower panels display the ratio of the band intensities of LAMP-1 relative to β-tubulin for the different glucose conditions as a percentage of the 5.5 mM glucose control. Data in lower panels are mean ± SEM from 5 passages of J774A.1 cells or 5 individual donors (HMDM). Statistical analyses were carried out using one-way repeated measures ANOVA with Tukey's post-hoc test. * Indicates $p < 0.05$, ** $p < 0.01$ relative to the 5.5 mM glucose condition. # $p < 0.05$ between the 10 and 30 mM glucose conditions.

3.4.7 Pilot studies on aryl sulfatase activity, visualisation of lysosomes with LysoTracker and cathepsins B, L, S and D protein levels in J774A.1 and HMDM that were incubated in 5 and 30 mM glucose.

Freshly isolated human monocytes were incubated in 5 and 30 mM glucose for 11 days to allow maturation into macrophages J774A.1 cells were cultured in a similar manner in order to determine: the aryl sulfatase activity levels, lysosomal numbers using LysoTracker® Red DND-99; and the protein levels of cathepsins B, L S and D. The studies reported in this section were carried out by Dr Fatemeh Moheimani as reported in her PhD thesis and the result were subsequently published in *Atherosclerosis* [244].

Western blot analyses were carried out to examine potential differences in cathepsin B, L S and D protein levels, using the 5 and 30 mM conditions; intervening levels were not examined in these pilot studies. For cathepsin B from HMDM, two bands at 25 (mature single chain) and 21 kDa (two-chain active form) were detected (Figure 3.9). For the J774A.1 cells a single band was detected at 25 kDa. The proenzyme (45 kDa) was not detected in either case. No significant differences were detected between the two conditions for either the individual species, or the total protein.

For cathepsin L from HMDM, three bands were detected at 24 kDa (two-chain form), 30 kDa (single chain form) and 42 kDa (procathepsin) (Figure 3.9). A significant decrease of approximately 50% in the 30 kDa band was detected for the 30 compared to 5 mM glucose condition, but the intensities of the other two bands individually and the sum of all three forms, were not significantly different. No bands were detected for the J774A.1 cells, with a wide range of antibody dilutions, consistent with a low level of this enzyme being present.

A single band was detected for cathepsin S with both cell types at 24 kDa (active single side chain). For the HMDM cells exposed to 30 mM glucose, the intensity of the band was significantly less (by around 90%) compared to the 5 mM condition. For the J774A.1 cells no significant differences were detected between the two conditions.

For HMDM cells and cathepsin D, three bands were detected at 22 (light chain), 29 (heavy chain) and 50 kDa (dimer). A significant decrease in band intensity of

approximately 50% was detected for the 50 kDa for the 30 mM condition, but no significant differences were detected for the other two bands, or the total protein.

For the J774A.1 cells two bands were detected at 31 kDa and 25 kDa. The former was invariant whereas the much weaker 25 kDa band showed a significant increase (approx. 80%) for the 30 versus 5mM condition. The total protein was significantly lower for the 30 mM condition.

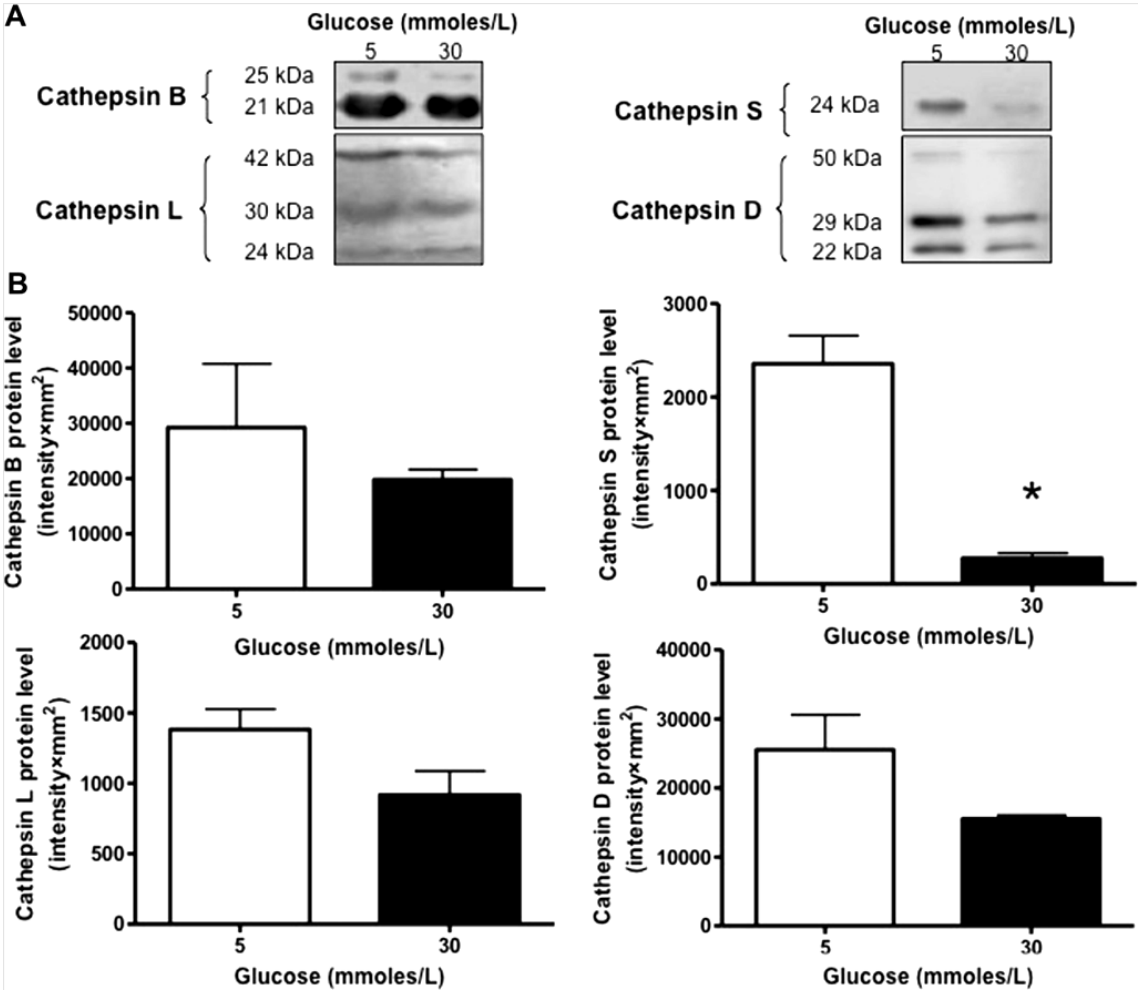

Figure 3.9: Protein levels of cathepsins B, L, S and D in HMDM cells exposed to 5 or 30 mM glucose as determined by Western blotting.
For each cathepsin representative Western blots (Panel A) and image analysis of total protein levels (i.e. sum of all bands) (Panel B) are given. Data are mean ± SEM from three independent blots obtained from separate experiments. Silver stained gels (not shown) showed identical loading in each lane. For assignment of bands see text. Statistical analyses were carried out using Student's t test, with * indicating significant differences at the $p < 0.05$ level.

Aryl sulfatase activity is commonly used for monitoring lysosomal populations. The aryl sulfatase activity in lysates from HMDM and J774A.1 cells exposed to 30 mM

glucose was significantly decreased ($p < 0.05$) when compared to the 5 mM condition as shown in Figure 3.10, and this decrease is consistent with the LAMP-1 data reported earlier in Figure 3.8.

LysoTracker Red is a weakly-basic cell-permeable fluorescent amine dye that accumulates in lysosomes; as such it can be used to assess lysosomal numbers. Fluorescent ($\lambda_{excitation}$ 577nm, $\lambda_{emission}$ 590 nm) and bright field images of HMDM and J774A.1 cells stained with this dye under identical conditions, showed more intense red fluorescence in cells incubated in 5 versus 30 mM glucose (Figure 3.11). The reduction in arylsulfatase activity and visualisation of lysosomes by LysoTracker® Red DND-99 observed in the high glucose conditions in both cell types may indicate a decrease in lysosomal population.

These preliminary data indicate that maturation of HMDM in high glucose concentrations results in a decrease of overall lysosomal number, a reproducible reduction in cathepsin (cysteine and aspartate) protein levels and a marked suppression of lysosomal cathepsin enzyme activities. These data complement and extend the results reported previously in Sections 3.4.3.2 and 3.4.4.

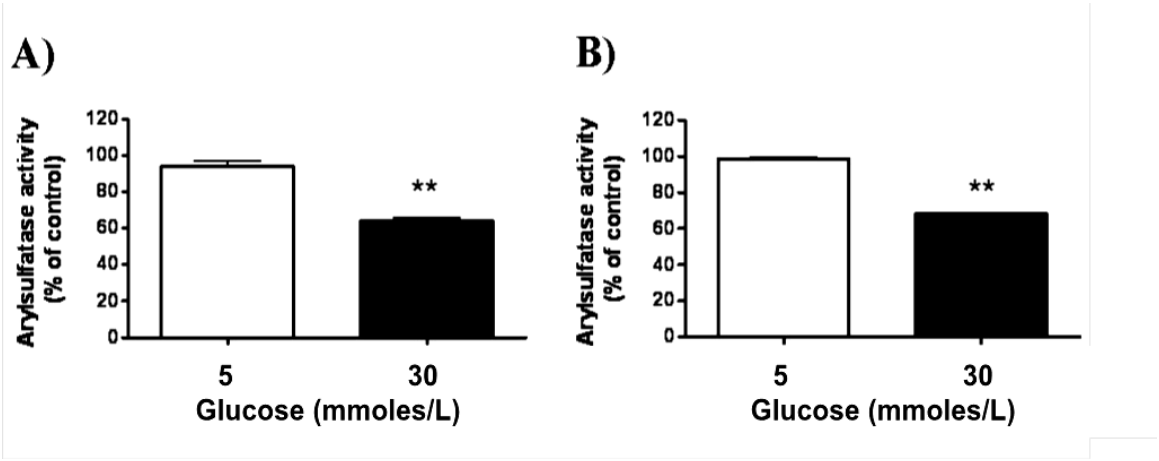

Figure 3.10: Effect upon lysosomal aryl sulfatase activity of maturation of human monocytes to macrophages (HMDM) (Panel A) or incubation of murine macrophage-like J774A.1 cells (Panel B) in 5 versus 30 mM glucose.
After incubation for 11 days in the stated level of glucose, the cells were lysed, and aryl sulfatase activity quantified. Data are mean $\pm$ SEM, from n = 4 independent experiments using separate donors (for HMDM) or separate cultures (for J774A.1 cells), and are reported as the change in absorbance with time, arising from cleavage of the added substrate as a percentage of the value determined for the 5 mM glucose condition, corrected for protein levels in the lysates. Statistical analyses were carried out using paired Student's t-test: ****** $p < 0.01$ when compared to the 5 mM glucose condition.

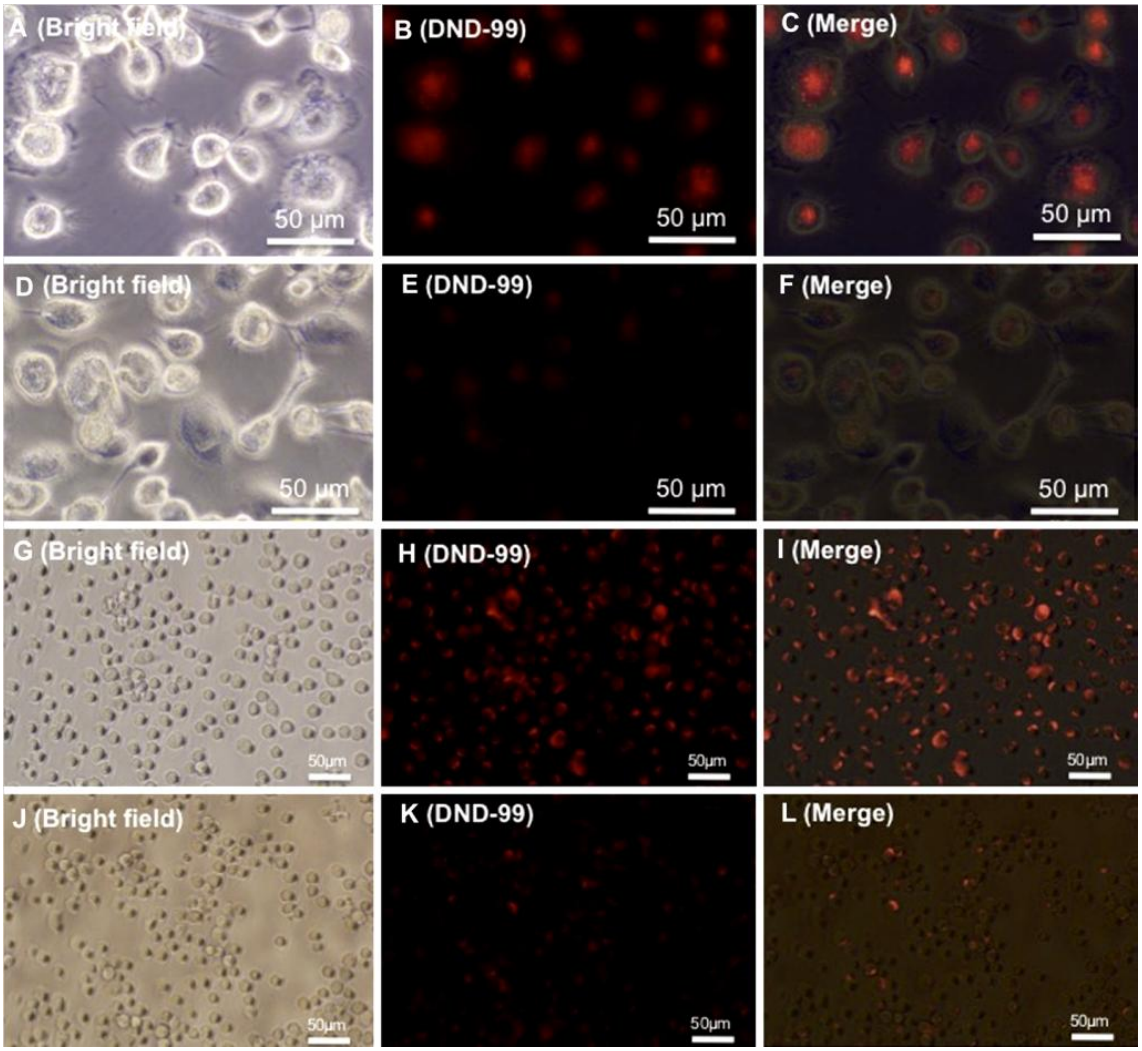

Figure 3.11: Representative photomicrographs of HMDM (Panels A to F) and J774A.1 (Panels G to L) cells incubated under normal or high glucose concentrations and stained with LysoTracker® Red DND-99.

Photos A - C and G - I are of cells incubated in 5 mM glucose, and D - F and J - L cells incubated in 30 mM glucose for 9 to 11 days. DND-99 (50 nM) was added to cells for 30 min and images were obtained using bright field (A, D, G, J), and a fluorescent filter ($\lambda_{excitation}$ 530 - 550 nm and $\lambda_{emission}$ 575IF) exposed for 1 - 2 s (B, E, H, K). The bright field and fluorescent images were used to generate the merged images in Panels C, F, I, and L. Data are representative of 3 independent experiments for each cell type, with ~50 images captured from cells in 6-well plates.

3.5 Discussion

This study shows that exposure of both HMDM and a murine macrophage-like cell line (J774A.1), to extended periods of high glucose concentrations results in significant reductions in lysosomal function as evidenced by changes in the activity of multiple cathepsin enzymes and lysosomal acid lipase. These enzymes play a critical role in protein catabolism (cathepsins) and hydrolysis of endocytosed neutral lipids (cholesteryl esters and triglycerides; LAL). Significant decreases in some of the enzyme activities were detected with 10 mM glucose, with a greater loss detected at higher levels. Glucose concentrations of this magnitude are commonly encountered in people with poorly controlled diabetes. Levels of up to 30 mM have been reported [245] but are not commonplace. Analogous changes were not detected in osmotic control experiments using a mixture of 5.5 mM glucose and 24.5 mM mannitol.

The changes in enzyme activity that occurred at the highest glucose concentrations (20 and 30 mM) were accompanied by changes in LAMP-1 protein level as evidenced by Western blotting. These results confirm the earlier findings of Moheimani *et al*. [244] for 30 mM glucose as evidenced by reduced accumulation of LysoTracker® Red DND-99 and decreased arylsulfatase activity. Thus lysosomal enzyme activity was found to be sensitive to high glucose levels below those that lead to reductions in protein expression and lysosomal number. A previous study has also reported decreased cathepsin (but not D) activity in endothelial progenitor cells exposed to high glucose [246].

Multiple mechanisms may act in parallel or synergistically to give these alterations. It has been reported that lysosomal cysteine protease activity can be decreased by exposure to reactive aldehydes and glycated proteins as a result of modification of the active site Cys of cathepsins B, L and S [243]. Reactive aldehydes, including methylglyoxal and glyoxal, are formed at elevated levels in cells exposed to high glucose, as a result of glucose autoxidation and increased triose phosphate pathway flux, with decomposition of the triose phosphates yielding methylglyoxal [247]. Oxidative stress and oxidised proteins arising from high glucose concentrations can also modulate lysosomal enzyme activities directly [229]. Although direct enzyme inactivation may explain the decreased activity of cathepsins B, L and S, this may be of lesser significance for cathepsin D, which has an active site Asp residue that is unlikely to be modified by glucose or reactive aldehydes. However, lysosomal protease activity

is dependent on a reaction cascade that generates the functional enzymes from proenyzmes, so alterations to cahtepsin B, L or S activity may subsequently modulate cathepsin D activation [229].

Exposure of cells to high glucose generates glycated proteins, advanced glycation end products (AGE) and protein aggregates [115]. The proteasome is the major complex that degrades most modified cytosolic proteins, and hence it might be expected that AGE-modified and aggregated proteins would be catabolised by this complex. However evidence exists for cross-talk between the proteasome and the endo-lysosomal systems, as well as direct trafficking of modified proteins to lysosomes [241]. The presence of modified proteins in the lysosomes may affect enzyme function directly, and or lysosomal properties that result in changes in protein level and enzyme activities for example by increasing the fragility of lysosomal membranes [248], and changes in intra-lysosomal pH [249], as these enzymes typically require acidic pHs [250]. It is likely that multiple mechanisms are involved, as these processes may occur concurrently and be interdependent.

Little previous data is available on changes in LAL activity. Mononuclear leukocytes from newly-diagnosed subjects with Type 1 of Type 2 diabetes have been reported to have unchanged activity compared to controls [251]; LAL activity was decreased in the Type 1, but not Type 2, subjects after insulin therapy. An earlier study reported an increase in LAL activity in subjects with Type 2 diabetes after insulin treatment [252]. People with autosomal recessive genetic traits resulting in Wolman's disease, and Cholesteryl Ester Storage Disease [253,254] have a deficit in LAL activity with this resulting in substantial cholesteryl ester (and to a lesser extent triglyceride) accumulation within cells [253], and accelerated atherosclerosis [255]. Whether this is due to the defect in lysosomal function, or associated hyperlipidaemia, is not known. Modified, including glycated, LDL particles may also directly modulate LAL activity and expression in human vascular endothelial and smooth muscle cells, with this occurring via the LXR signalling pathway [256].

Clinical studies have reported increased lysosomal activity in human atherosclerotic lesions. Thus subjects with atherosclerosis and diabetes have elevated levels of plasma cathepsin D and S [257], monocyte cathepsin D activity [258], neutrophilic lysosomal activity [259] and myocardial levels of cathepsin L [260]. However, these represent data from an expanded population of activated inflammatory

cells, and not lysosomal function on a per cell basis as examined here. Furthermore while increased intracellular levels of oxidised proteins can induce elevated lysosomal cathepsin expression and activity, this may not equate to an increase in modified protein degradation [241]. Increased cathepsin expression and activity may merely be (an unsuccessful) response to the accumulation of damaged materials.

The changes in enzyme activity may result from a decreased clearance of both native and modified (glycated / glycoxidised / oxidised) proteins, including those internalised by endocytosis, or trafficked intracellularly. A previous study has reported that pyrraline-modified albumin is cleared by macrophage-like (P388D1) cells at a slower rate than unmodified protein [261], but no changes in lysosomal activity were detected. As cathepsin enzymes play a key role in the turnover of internalised LDL in arterial wall macrophages, the data obtained in the current study may be of significance in diabetes-induced atherosclerosis, with decreased cathepsin activity resulting in an accumulation of native or modified apolipoprotein B-100 protein [262] and cholesteryl esters and triglycerides. A decreased turnover may also result in a vicious cycle of increasing organelle dysfunction, as the level of modified material increases; the consequences of such accumulation have been reviewed [239,263].

3.6 Conclusions

The studies reported in this chapter indicate that the maturation of human monocytes to macrophages over a period of 11 days in high glucose concentrations (20 - 30 mM) resulted in a significant reduction in lysosomal number, as indicated by the LAMP-1, cathepsin protein levels and arylsulfatase activities. There was a marked inhibition of lysosomal cathepsin B, L S, D and an inhibition of acid lipase activities with increasing glucose concentrations (10 - 30 mM) versus the normal 5.5 mM glucose condition at the end of the maturation period. However it is not known when this disruption begins to impede lysosomal function during the maturation period, as only macrophages after complete maturation were assessed. Thus a major limitation to this study is the use of the single time point of 11 days. In the following chapter the time course of inhibition of lysosomal function in maturing monocytes incubated in 20 mM glucose was investigated at multiple time points.

CHAPTER 4:

LYSOSOMAL DISRUPTION DURING MATURATION OF HUMAN MONOCYTES TO MACROPHAGES IN PRESENCE OF ELEVATED GLUCOSE

4.1 Introduction

A number of studies have detected elevated levels of oxidised LDL in atherosclerotic plaques [264,265,266], however the mechanism by which this accumulation occurs is unclear. Changes in protease and possibly lipase activity may alter or inhibit the activity of the removal systems for damaged lipoproteins which may play a role in diabetes-associated cardiovascular diseases. Such accumulation may arise as a result of impairment of proteolysis and lipolysis processes such as those mediated by lysosomes [242,244]. Lysosomal enzymes have been shown to be susceptible to modulation by *in vitro* incubation with reactive aldehydes or preglycated proteins, both of which would be elevated in diabetes [243]. In the previous chapter, elevated glucose levels were shown to have a dose dependent inhibitory effect on lysosomal number, multiple cathepsins and acid lipase activities in fully-differentiated macrophages. These lysosomal functional changes may affect the capacity of macrophages to catabolise modified (lipo) proteins and enhance accumulation of lipids seen in diabetes associated atherosclerosis. In the light of this data, the aim of the studies reported in this chapter was to explore at what point during the maturation of monocytes to macrophages in 20 mM glucose this perturbation in lysosomal function occurs.

4.2 Aims

To examine the impairment of lysosomal cathepsins and acid lipase activity and protein levels during the *in vitro* maturation of human monocytes to HMDM under conditions of high and normal glucose.

4.3 Methods

Human monocytes isolated from buffy coats of healthy donors were matured into macrophages over 10 days as detailed in Section 2.2.4. Maturation in 5.5 mM glucose was compared to that in 20 mM glucose. The cell pellets were obtained on days 2, 4, 6, 8 and 10 as described in Section 2.2.5, to determine the lysosomal activities of cathepsins B, L and LAL as detailed in Sections 2.3, 2.3.2 and 2.3.6.

In separate experiments, the cells were harvested on days 2, 4, 6, 8 and 10 and lysates prepared for Western blotting in order to quantify cathepsins B and L and LAL

protein levels as detailed in Sections 2.5 - 2.8. Lysosome numbers was estimated using lysosomal-associated membrane glycoprotein-1 (LAMP-1) expression. Lysosomal protein levels were quantified relative to β-tubulin as loading control.

4.3.1 Statistical Analysis

Lysosomal activities from the cells of different donors were determined. The values were adjusted to the protein content of the sample and the results were then expressed as a percentage of that determined for cells incubated in 5.5 mM glucose after two days *in vitro*. Two-way ANOVA analysis was used followed by a Bonferroni's post hoc test (against time points and glucose concentrations). Differences were assumed to be statistically significant at $p < 0.05$.

4.4 Results

4.4.1 Protein content in monocytes that were matured in normal and high glucose conditions

The protein content was measured in monocytes as they were developing into macrophages to determine the rate of cell growth and examine whether this was different between the two glucose conditions. This was determined by the BCA protein assay as detailed in Section 2.4.1. There was an overall increase in protein content as the monocytes developed into macrophages in both the normal ($p < 0.001$) and high glucose ($p < 0.001$) treated monocytes, using two-way ANOVA followed by Bonferroni's post-hoc test. However, there were no statistical differences in the protein content observed in the monocytes matured to HMDM in the normal 5.5 mM and high 20 mM glucose conditions during the maturation period.

4.4.2 Lysosomal cathepsin B and L activity during maturation

The data presented in the previous chapter is consistent with the inhibition of cathepsin B and L activities in human monocytes matured for 10 - 12 days in medium containing 20 mM glucose [244]. Whether this inhibition was also present at earlier time points during the maturation process was investigated in the current study.

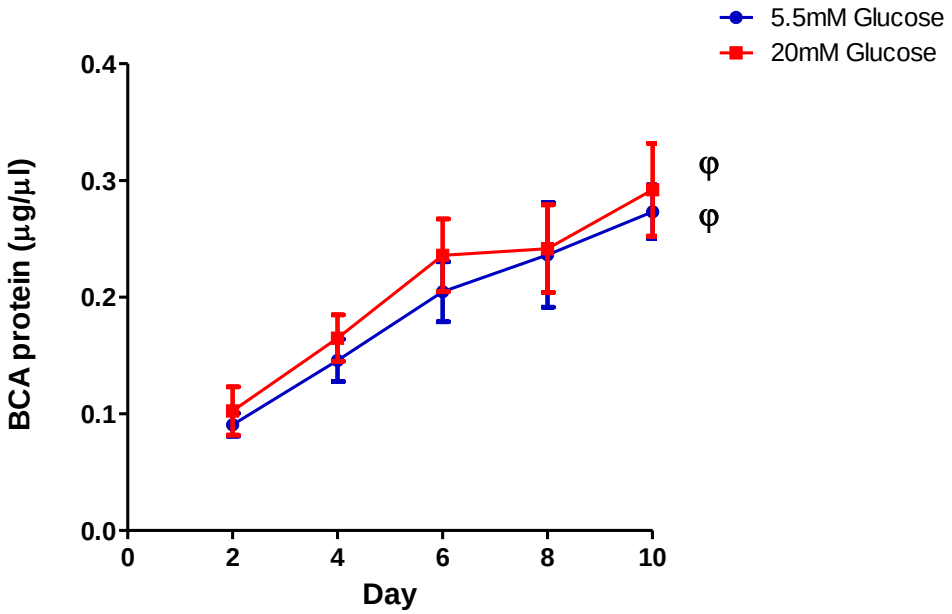

Figure 4.1: Measurement of cellular protein levels during maturation of human monocytes in normal versus high glucose concentrations.
Monocytes were matured in media with either 5.5 mM (blue line) or 20 mM (red line) glucose. Data (mean ± SEM) is expressed in µg/µL from 5 independent experiments using separate cell donors. **φ** indicates a significance ($p < 0.001$) by two-way ANOVA followed by Bonferroni's post-hoc test in protein levels between day 2 and day 10.

Cathepsin B activity (assessed as described in Chapter 3) was found to increase during monocyte maturation to macrophages. There was an overall increase in lysosomal cathepsin B activity as the monocytes developed into macrophages in both the normal ($p < 0.001$) and high glucose ($p < 0.001$) conditions (Figure 4.2; Panel A). At each time point cathepsin B activity was significantly lower for the cells matured under the high glucose condition.

Cathepsin L activity was observed to increase during monocyte maturation to macrophages. The activity of lysosomal cathepsin L increased as the monocytes developed into macrophages in both the normal ($p < 0.001$) and high glucose ($p < 0.001$) concentrations (Figure 4.2; Panel B). The cathepin L activity was significantly lower in the cells matured under the high glucose condition compared to 5.5 mM glucose for each time point assessed.

Overall the monocytes incubated in high glucose showed lower levels of lysosomal cathepsin B and L activity at all the time points examined during the maturation process to macrophages.

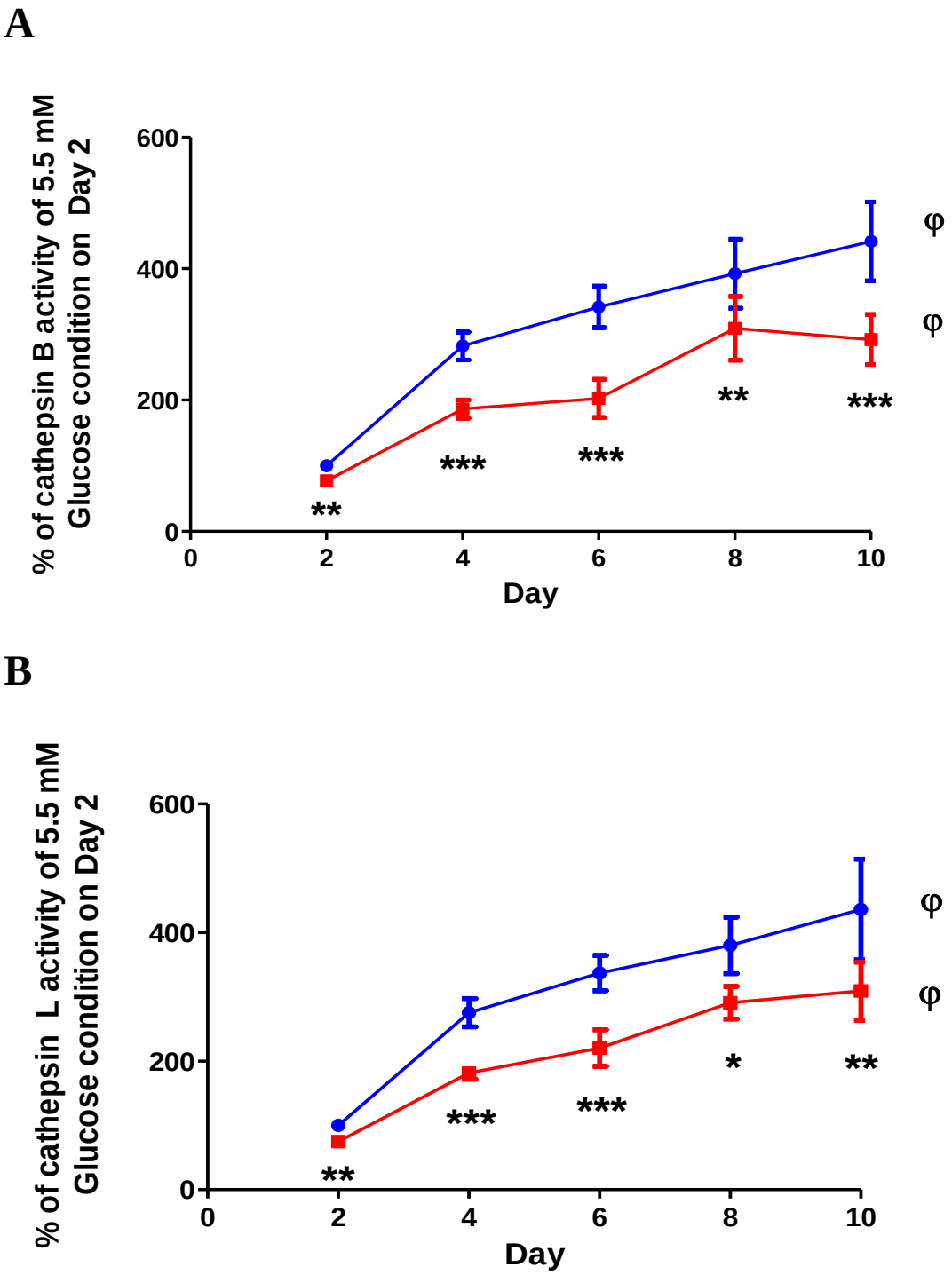

Figure 4.2: Maturation of human monocytes in high glucose decreases the activity of cathepsin B (Panel A) and L (Panel B) compared to normal glucose concentrations.

Lysosomal cathepsin B and L activities were measured in human monocytes that were matured in media with either 5.5 mM (blue line) or 20 mM (red line) glucose for up to 10 days. Data (mean ± SEM) are expressed relative to the 5.5 mM glucose condition on Day 2. Samples were collected from 5 independent experiments using separate cell donors. Asterisks indicate a significant decrease in enzyme activity compared to control (5.5 mM glucose condition) by two-way ANOVA followed by Bonferroni's post-hoc test; * $p < 0.05$, ** $p < 0.01$, *** $p < 0.001$. **φ** indicates a significance ($p < 0.001$) in activity between day 2 and day 10.

4.4.3 Lysosomal acid lipase (LAL) activity during maturation

LAL is the sole lysosomal hydrolase for endocytosed cholesteryl esters and triglycerides [230]. In the previous chapter it was demonstrated that there was an impairment of LAL activity in human monocytes matured for 10 - 12 days in medium containing 20 mM glucose [244]. The current study examined whether this inhibition was also present at earlier time points during the maturation process.

LAL activity was measured, as described in the previous chapter, in the normal and high glucose conditions in the monocytes during the maturation period from days 2 to 10. There was no statistical increase in LAL activity as the monocytes developed into macrophages in either the normal or high glucose treated cells. In the case of the cells incubated in 5.5 mM glucose there was an increase in LAL activity between day 2 and 4 although this did not reach significance ($p > 0.05$). Between days 4 and 10, the LAL activity remained unchanged. In contrast for the cells treated with 20 mM glucose no increase in LAL was seen, and at each time point from day 4 to day 10 the LAL activity was significantly lower for the high glucose treated cells.

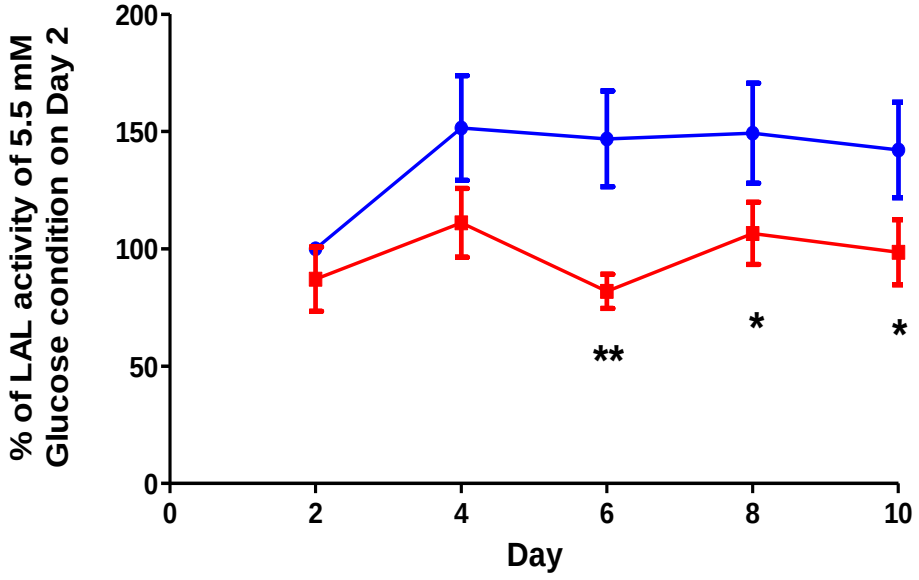

Figure 4.3: LAL activity during monocyte maturation at different time points. Lysosomal acid lipase (LAL) activity measured in human monoctyes that were matured in media with either 5.5 mM (blue line) or 20 mM (red line) glucose for up to 10 days. Data (mean ± SEM) are expressed relative to the activity detected for the 5.5 mM glucose condition on Day 2. Data was obtained from 5 independent experiments using separate cell donors. Asterisks indicate a significant decrease in enzyme activity compared to control (5.5 mM glucose condition) by two-way ANOVA followed by Bonferroni's post-hoc test; * $p < 0.05$, ** $p < 0.01$.

4.4.4 Protein levels of cathepsin B

The protein levels of procathepsin and mature cathepsin B were assessed to determine whether the changes in activity detected during the maturation process arose from changes in protein synthesis or processing during the maturation process. This was determined for monocytes that were incubated in the normal 5.5 mM and high 20 mM glucose concentrations and collected on every second day, by Western blotting (as described in Section 2.5.1 - 2.5.8). The cathepsin B proenzyme was detected at 37 kDa and the activated cathepsin B was observed at 25 kDa via Western blotting. Cathepsin B protein levels were expressed relative to β-tubulin levels, which was detected at 51 kDa.

The total cathepsin B protein levels were calculated by the addition of procathepsin B and activated cathepsin B protein levels that were expressed relative to β-tubulin levels. When the ratio of procathepsin to activated cathepsin B protein levels were analysed, it was observed that the ratio of procathepsin B declined as the activated cathepsin B progressively increased. The normal and high glucose treated monocytes followed the same trend and ratio as shown in Figure 4.4.

When the protein levels were assessed relative to β-tubulin levels, procathepsin levels declined as activated cathepsin B protein levels increased during monocyte maturation to macrophages in the normal glucose conditions only. There were no significant changes observed in the procathepsin and activated cathepsin B protein levels from days 2 to 10 in the monocytes that were incubated with high glucose. Treatment with high glucose resulted in decreased levels of procathepsin ($p < 0.05$) and activated cathepsin B ($p < 0.01$) protein with this difference being significantly lower at day 10 only (as shown in Figures 4.5 and 4.6 respectively).

The activity values for cathepsin B that were reported in Section 4.4.2 were also assessed relative to activated cathepsin B protein levels to determine whether there was a change in lysosomal activity compared to the amount of protein present in the monocytes. Overall, there was a decrease in lysosomal activity when compared to protein levels expressed from days 2 and 4, which continued throughout the maturation process (refer to Panel B in Figure 4.6) though this was not statistically significant. However there were no differences in ratio of cathepsin B activity over protein levels in the two glucose conditions.

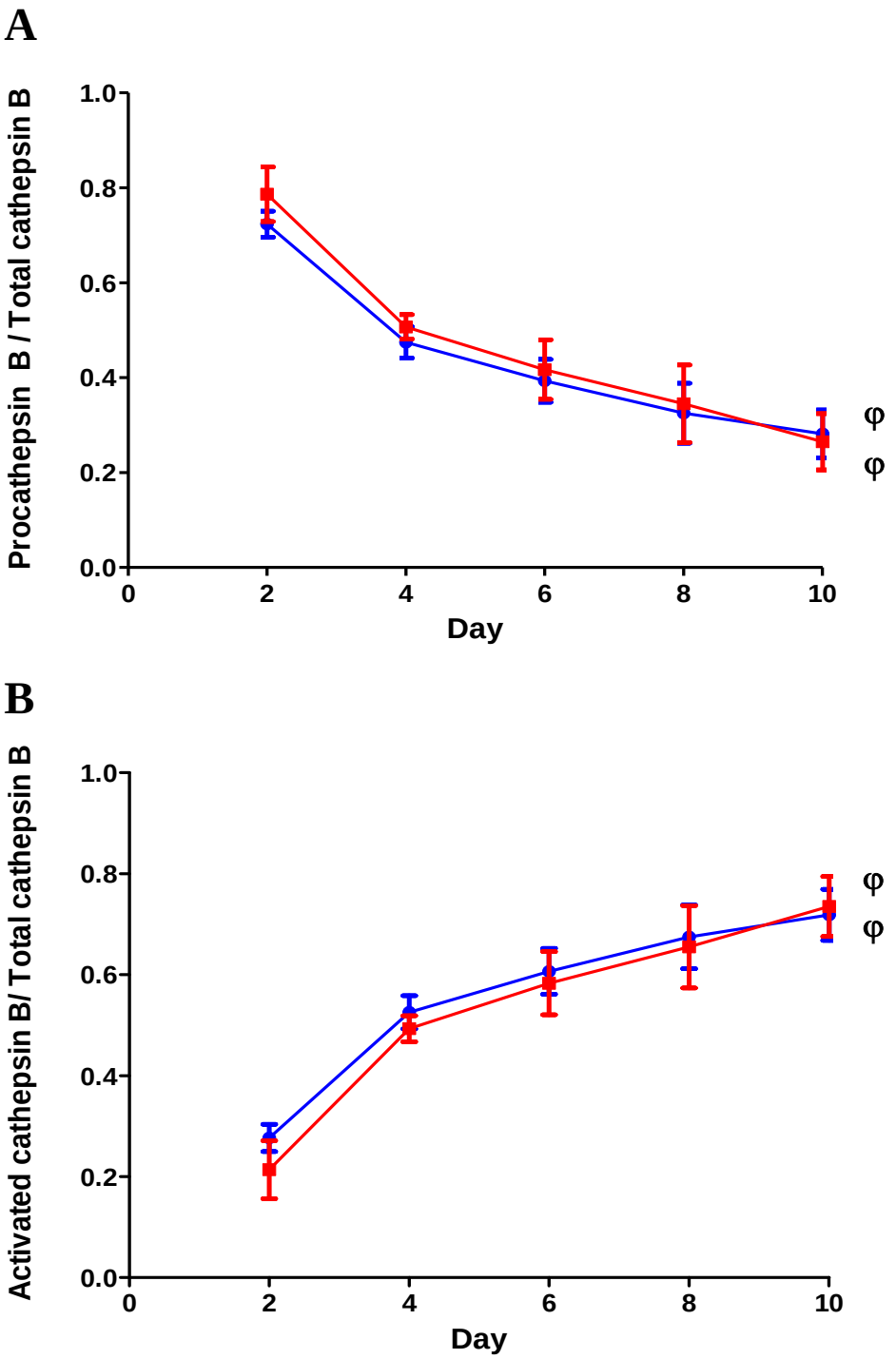

Figure 4.4: Procathepsin and activated cathepsin B over the total cathepsin protein levels during monocyte maturation at different time points.

Procathepsin B (Panel A) and activated cathepsin B (Panel B) protein levels were measured and quantified over the total cathepsin B protein levels in human monocytes that were matured in media with either normal (5.5 mM; blue line) or high (20 mM; red line) glucose for up to 10 days. Pooled data (mean ± SEM; from 5 independent experiments using separate cell donors) for procathepsin and activated cathepsin B protein levels are presented in Panels A and B, respectively. Statistical analysis was carried out using two-way ANOVA followed by Bonferroni's post-hoc test; **φ** indicates a significance ($p < 0.001$) difference between the values obtained at days 2 and 10.

A

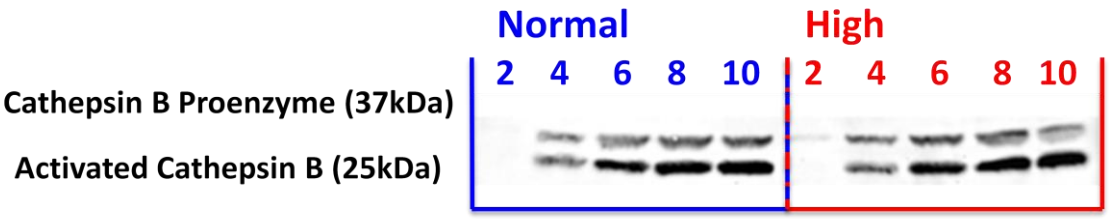

B

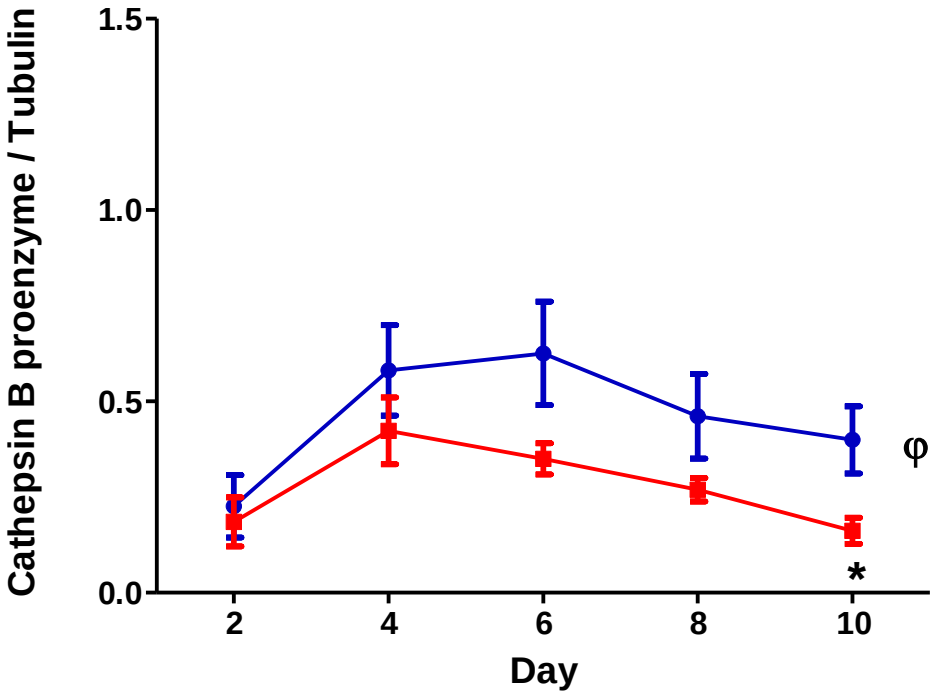

Figure 4.5: Cathepsin B protein levels during monocyte maturation at different time points.

Procathepsin B (37 kDa) and activated cathepsin B (25 kDa) protein levels were measured in human monocytes that were matured in media with either normal (5.5 mM; blue line) or high (20 mM; red line) glucose for up to 10 days. Panel A shows the results from one representative Western blotting experiment at the indicated time points from a total of five. Pooled data (mean ± SEM; from 5 independent experiments using separate cell donors) for procathepsin B protein levels (expressed relative to β-tubulin) is presented in Panel B. Statistical analysis was carried out using two-way ANOVA followed by Bonferroni's post-hoc test; * $p < 0.05$ between the two glucose concentrations. **φ** indicates a significant ($p < 0.001$) difference between the values obtained at days 2 and 10.

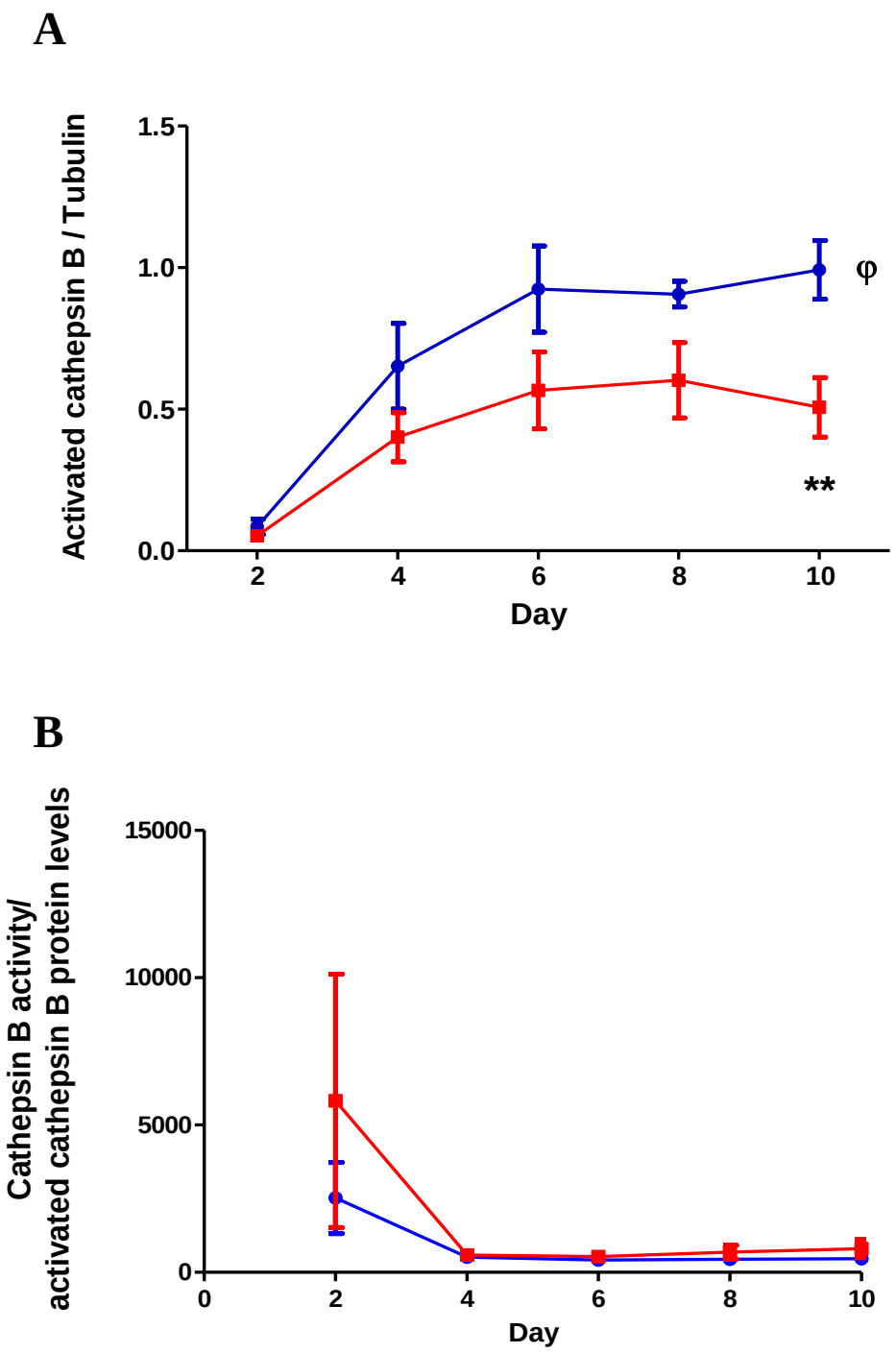

Figure 4.6: Activated cathepsin B protein levels and cathepsin B activity versus protein levels during monocyte maturation at different time points.

Activated cathepsin B (25 kDa) protein levels were measured in human monocytes that were matured in media with either normal (5.5 mM; blue line) or high (20 mM; red line) glucose for up to 10 days (as shown in Panel A). In Panel B the activity of lysosomal cathepsin B was assessed over the activated cathepsin B protein levels. Pooled data (mean ± SEM; from 5 independent experiments using separate cell donors) for activated cathepsin B protein levels (expressed relative to β-tubulin) and activity versus protein levels are presented in Panels A and B, respectively. Statistical analysis was carried out using two-way ANOVA followed by Bonferroni's post-hoc test; ** $p < 0.01$ between two glucose concentrations. **φ** indicates a significance ($p < 0.001$) difference between the values obtained at days 2 and 10.

4.4.5 Protein levels of cathepsin L

The protein levels of procathepsin and mature cathepsin L were assessed to determine whether changes in activity detected during the maturation process affected the synthesis of cathepsin L and the conversion of the pro to active forms. This was examined via Western blotting (as detailed in Sections 2.5.1 - 2.5.8) from monocytes that were incubated in the normal 5.5 mM and high 20 mM glucose conditions and collected on every second day throughout the maturation period. The procathepsin L protein was detected at 55 kDa and the mature cathepsin L was observed at 25 kDa via Western Blotting. These protein levels were expressed relative to β-tubulin levels which were detected at 51 kDa.

The total cathepsin L protein levels were calculated by the addition of procathepsin L and mature cathepsin L protein levels that were expressed relative to the β-tubulin levels. When the ratio of procathepsin and activated cathepsin L protein levels was analysed, the ratio of procathepsin L declined as the mature cathepsin L progressively increased as monocytes developed into macrophages, regardless of the different glucose conditions, as shown in Figure 4.7.

When the protein levels were assessed relative to β-tubulin levels, procathepsin levels declined as the mature cathepsin L protein levels increased during monocyte maturation to macrophages in the normal glucose conditions only (as shown in Figure 4.8 and 4.9 respectively). There were no significant changes observed in the procathepsin and mature cathepsin L protein levels from days 2 to 10 in the monocytes that were incubated with high glucose. There were no statistical differences in procathepsin L levels between the two glucose concentrations during the maturation period; however treatment with high glucose significantly lowered mature cathepsin L ($p < 0.05$) protein levels at day 10.

The activities of cathepsin L that were reported in Section 4.4.2 were also assessed relative to the level of mature cathepsin L protein to determine whether there was a change in lysosomal activity compared to the amount of protein in the monocytes exposed to high glucose conditions. Overall, there was reduction in lysosomal activity relative to protein levels expressed for days 2 and 4 ($p < 0.001$) in the two glucose conditions, which continued throughout the maturation process (refer to Panel B in Figure 4.9). However there were no differences in the ratio of cathepsin L activity over protein levels between the normal and high glucose concentrations for the cells.

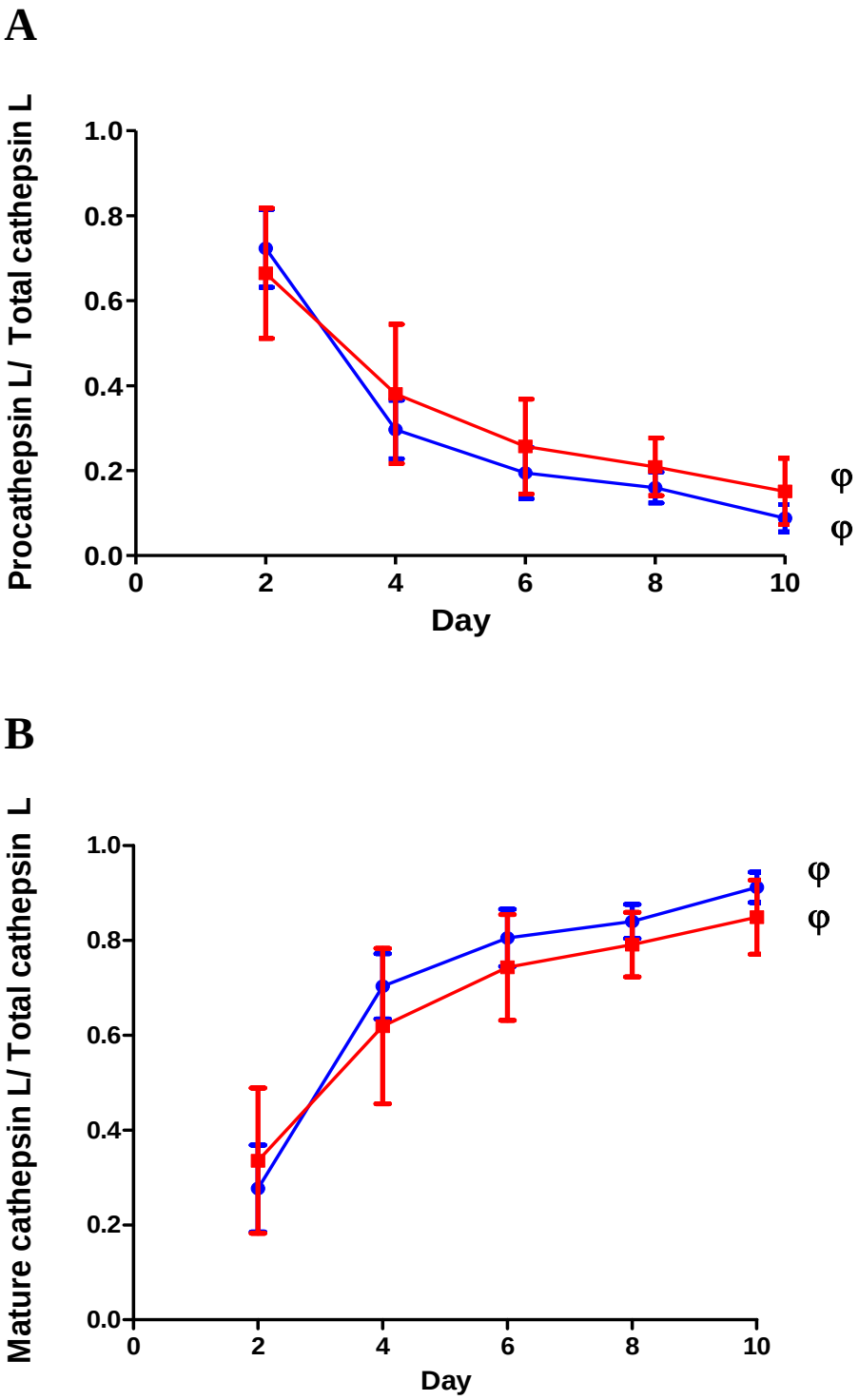

Figure 4.7: Procathepsin and activated cathepsin L over the total cathepsin protein levels during monocyte maturation at different time points.

Procathepsin L (Panel A) and activated cathepsin L (Panel B) protein levels were measured and quantified over the total cathepsin L protein levels in human monocytes that were matured in media with either normal (5.5 mM; blue line) or high (20 mM; red line) glucose for up to 10 days. Pooled data (mean ± SEM; from 5 independent experiments using separate cell donors) for procathepsin and mature cathepsin L protein levels are presented in Panels A and B, respectively. Statistical analysis was carried out using two-way ANOVA followed by Bonferroni's post-hoc test; **φ** indicates a significance ($p < 0.001$) difference between the values obtained at days 2 and 10.

A

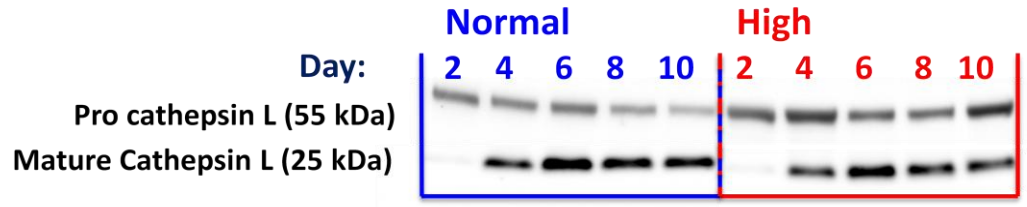

B

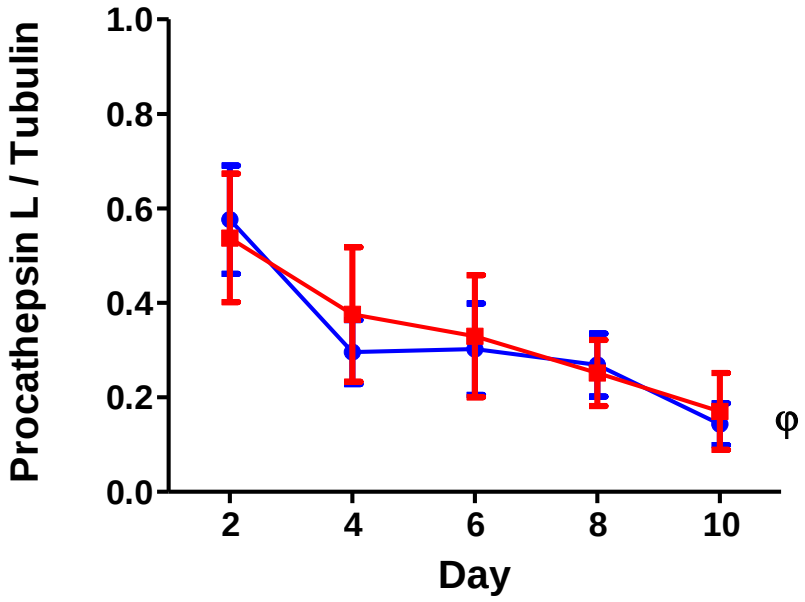

Figure 4.8: Cathepsin L protein levels during monocyte maturation at different time points.

Procathepsin L (55 kDa) and mature cathepsin L (25 kDa) levels were measured in human monocytes that were matured in media with either normal (5.5 mM; blue line) or high (20 mM; red line) glucose for up to 10 days. Panel A shows the results from one representative experiment from a total of five. Pooled data derived from procathepsin and mature cathepsin L (mean ± SEM; from 5 independent experiments using separate cell donors) are expressed relative to β-tubulin levels as presented in Panel B, respectively. Statistical analysis was carried out using two-way ANOVA followed by Bonferroni's post-hoc test; **φ** indicates a significant difference ($p < 0.001$) between days 2 and 10.

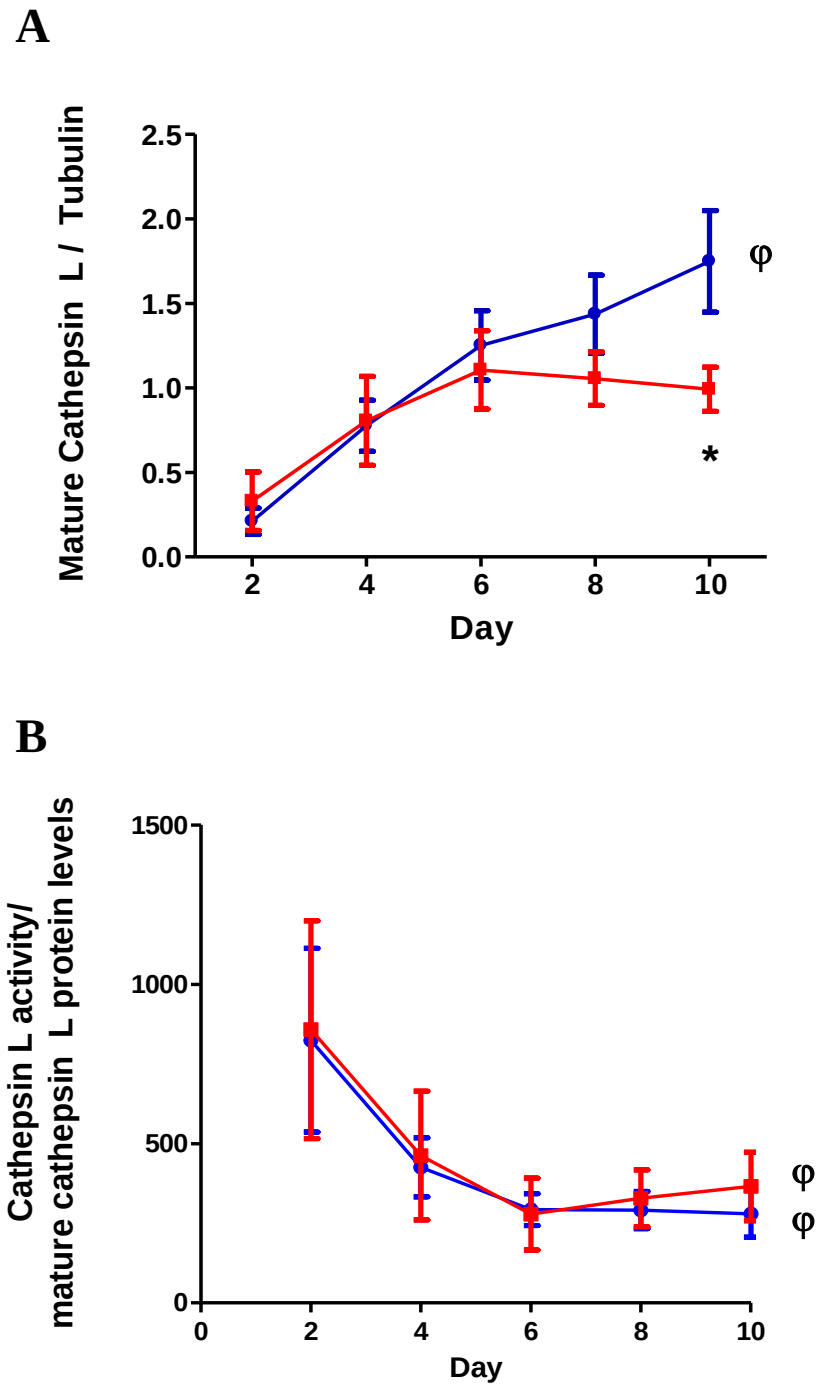

Figure 4.9: Mature cathepsin L protein levels and cathepin L activity versus protein levels during monocyte maturation at different time points.

Mature cathepsin L (25 kDa) levels were measured in human monocytes that were matured in media with either normal (5.5 mM; blue line) or high (20 mM; red line) glucose for up to 10 days (as shown in Panel A). The activity of lysosomal cathepsin L was assessed over the activated cathepsin B protein level as shown in Panel B. Pooled data derived from procathepsin and mature cathepsin L (mean ± SEM; from 5 independent experiments using separate cell donors) are expressed relative to β-tubulin levels as presented in Panels A and B, respectively. Statistical analysis was carried out using two-way ANOVA followed by Bonferroni's post-hoc test; * $p < 0.05$ between the two glucose concentrations. φ indicates a significant difference ($p < 0.001$) between days 2 and 10.

4.4.6 Protein levels of LAL

The protein levels of LAL were assessed to determine whether the changes in activity detected during the maturation process arose from changes in protein synthesis during the maturation process. Therefore LAL protein levels were assessed by Western blotting (as described in Sections 2.5.1 - 2.5.8) to determine whether high glucose affected synthesis of LAL during the maturation process. This was examined in monocytes that were incubated in the normal 5.5 mM and high 20 mM glucose concentrations, with samples collected every second day between days 2 to 10. The LAL protein was detected at 45 kDa and was expressed relative to β-tubulin levels which were detected at 51 kDa via Western Blotting.

There were no changes in LAL protein levels during the maturation process for cells incubated in either 5.5 mM or 20 mM glucose. The protein levels of LAL were generally lower for cells matured under 20 mM glucose most notably at day 10 but this did not reach statistical significance ($p > 0.05$) (refer to Figure 4.10).

The activity of LAL that was reported in Section 4.4.3 was also assessed relative to LAL protein expression to determine whether there was a change in lysosomal activity relative to the amount of protein that was present in the monocytes. Overall, there were no changes in the lysosomal activity relative to the protein levels during the maturation period (refer to Figure 4.11) and no differences between the two glucose treatments.

A

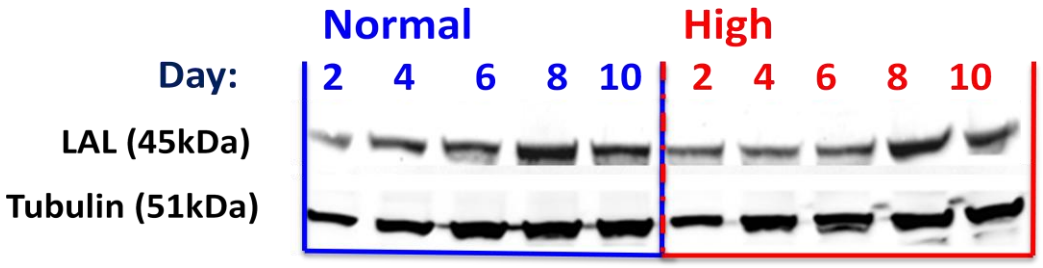

B

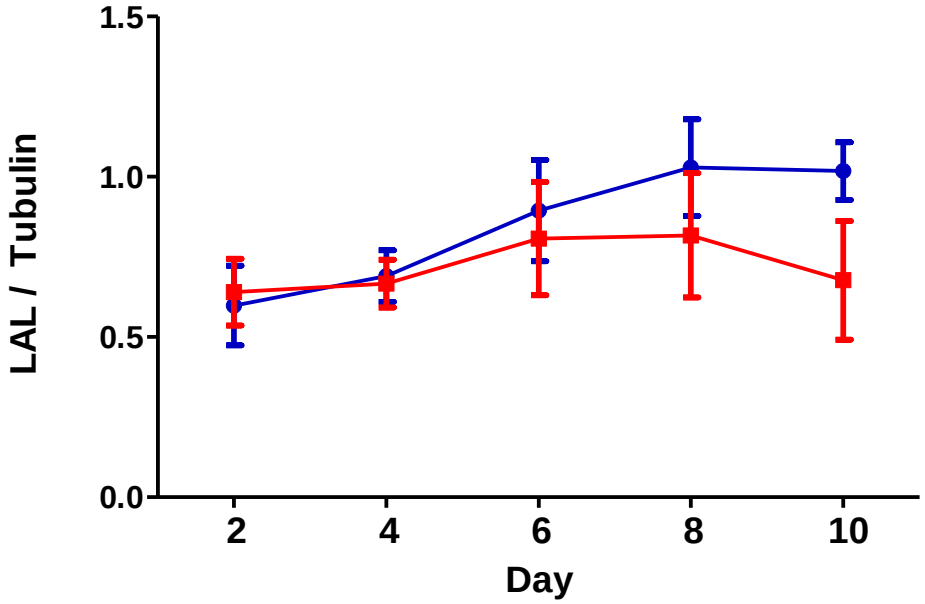

Figure 4.10: LAL protein levels during monocyte maturation at different time points.

LAL (45 kDa) protein levels were measured in human monocytes that were matured in media with either normal (5.5 mM; blue line) or high (20 mM; red line) glucose for up to 10 days. Panel A shows the results from one representative experiment from a total of five. Pooled data (mean ± SEM; from 5 independent experiments using separate cell donors) for LAL protein levels (expressed relative to β-tubulin) derived from 5 individual donors is presented in Panel B. Statistical analysis was carried out using two-way ANOVA followed by Bonferroni's post-hoc test; no statistical differences were detected.

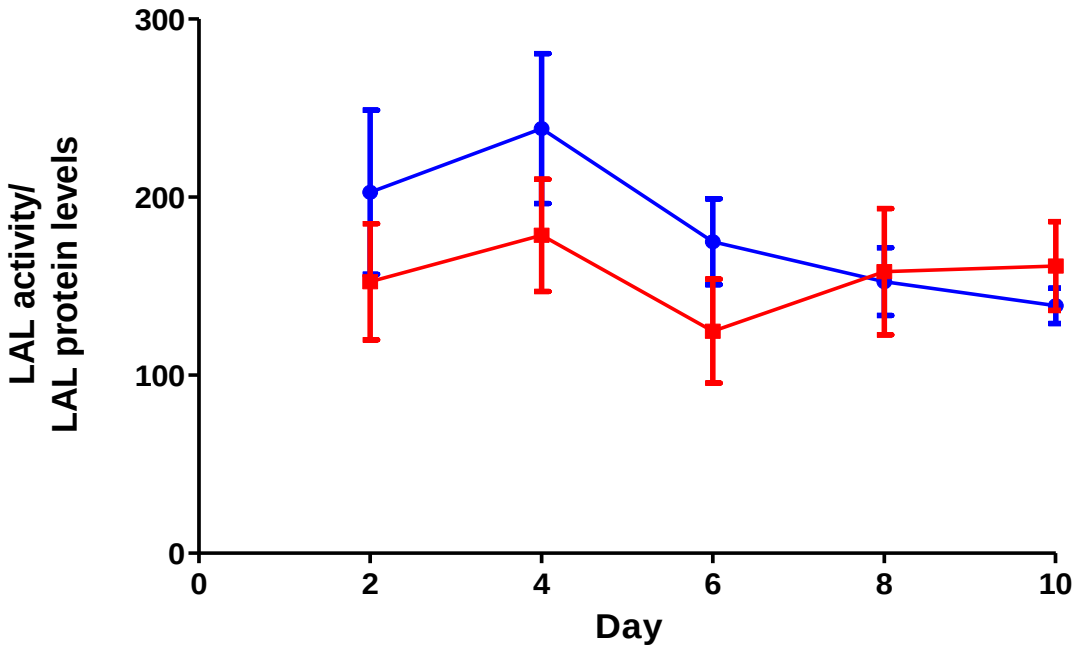

Figure 4.11: LAL activity relative to protein levels during monocyte maturation at different time points.
The LAL activity and LAL (45 kDa) protein levels were measured in human monocytes that were matured in media with either normal (5.5 mM; blue line) or high (20 mM; red line) glucose for up to 10 days. Pooled data for LAL activity relative to protein expression (mean ± SEM; from 5 independent experiments using separate cell donors). Statistical analysis was carried out using two-way ANOVA followed by Bonferroni's post-hoc test, and showed no statistical differences.

4.4.7 Protein levels of LAMP-1

The protein levels of LAMP-1 were assessed as a measure of any change in lysosomal number during the maturation process; the data presented in the previous chapter indicated that LAMP-1 levels were significantly reduced on treatment with high glucose (20 mM) for 11 days in HMDM [244]. The LAMP-1 protein band was detected at 120 kDa and expressed relative to β-tubulin which was detected at 51 kDa.

There was an overall increase in LAMP-1 protein levels in both the normal glucose ($p < 0.001$) and high glucose conditions ($p < 0.001$) during the maturation period (Figure 4.8). There were no statistical differences in LAMP-1 levels between the two glucose concentrations during the maturation period from days 2 to 8, although the results for the high glucose-treated cells trended to lower values. However by day 10 the LAMP-1 levels were significantly lower for the high glucose-treated HMDM ($p < 0.05$).

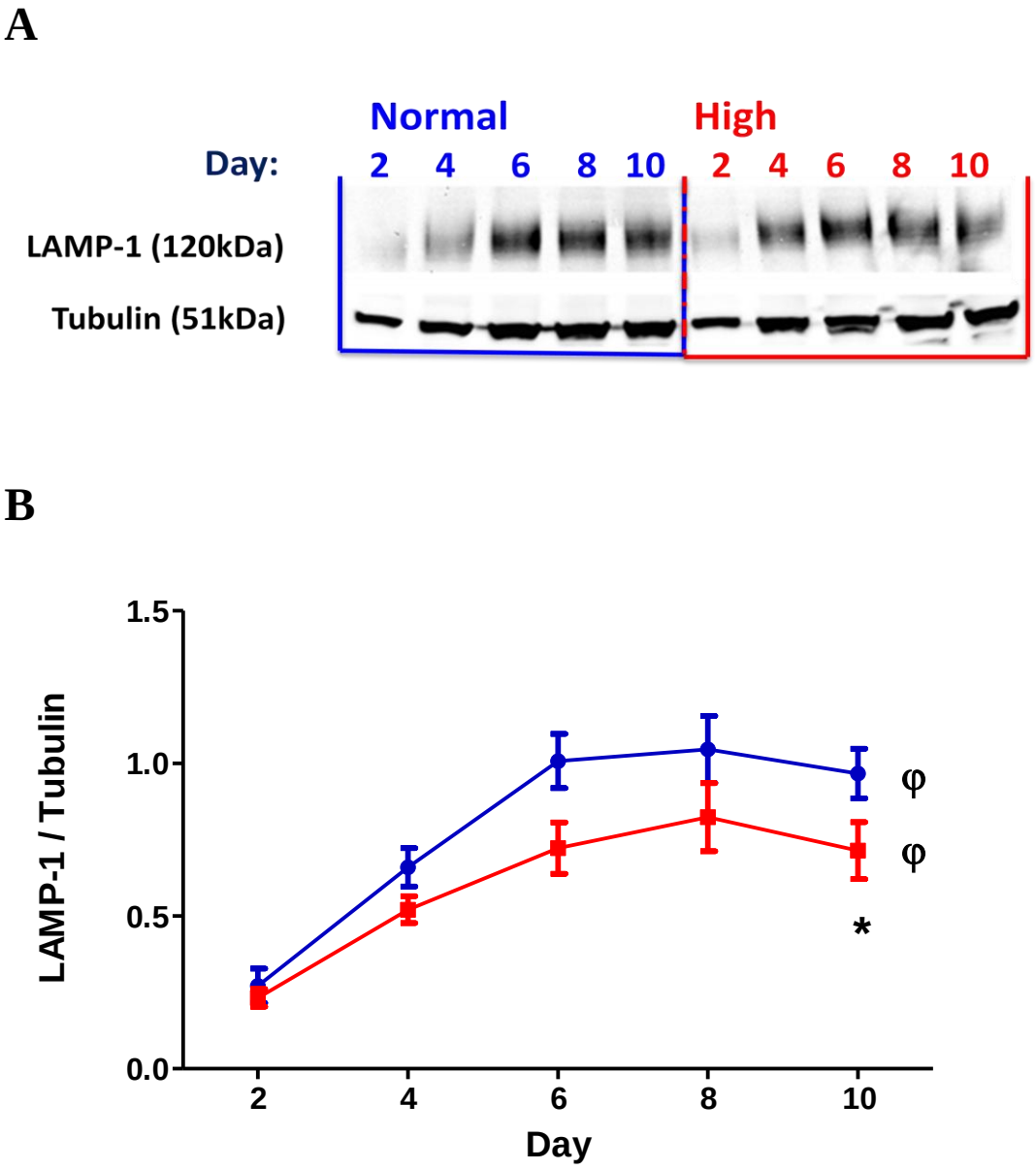

Figure 4.12: LAMP-1 protein levels during monocyte maturation.
LAMP-1 (120 kDa) protein levels were measured in human monocytes matured under normal (5.5 mM; blue line) or high (20 mM; red line) glucose concentrations for up to 10 days. Panel A shows the results from one representative Western blotting experiment from a total of five. Pooled data (mean ± SEM; from 5 independent experiments using separate cell donors) for LAMP-1 levels (expressed relative to β-tubulin) are presented in Panel B. Statistical analysis was carried out using two-way ANOVA followed by Bonferroni's post-hoc test; * $p < 0.05$ between the two glucose concentrations. **φ** indicates a significant difference ($p < 0.001$) between the data obtained at days 2 and 10.

4.5 Discussion

This study examined changes in lysosomal protease and lipase activity and protein levels as well as lysosomal number in human monocytes as these were matured *in vitro* to macrophages. It was found that exposure of human monocytes to chronic high glucose concentrations resulted in an impairment of protease activity as monocytes matured to macrophages. The magnitude of the glucose-induced changes was most pronounced at the final time point examined.

The studies reported in the previous chapter showed a significant reduction in lysosomal cathepsin B, L and LAL activities in macrophages matured in 20 mM glucose compared to the 5.5 mM condition [244]. Significant reductions in cathepsin B and L enzymatic activities were detected for cells matured under the high glucose conditions from as early as two days *in vitro*. The high glucose condition also reduced the LAL enzymatic activity in the maturing monocytes from day six onwards.

Independent of the glucose treatment, maturation *in vitro* was associated with a decline in pro-cathepsin enzyme levels, with a parallel increase in active enzyme levels for both cathepsins B and L both individually and when expressed relative to the total cathepsins. The impact of high glucose upon protein levels differed between the two cathepsins. With cathepsin B there was a trend towards lower levels from day 2 although this was only statistically significant at day 10. In contrast to this a decline in cathepsin L protein levels in the high glucose-treated cells was discernible after day 6 although it was also only statistically significant at day 10. When comparing these results with those for cathepsin activity, it would seem that impact of high glucose upon monocyte/macrophage proteolytic activity may involve both inactivation as well as a reduction in protein synthesis. However this was not seen in a previous study by Moheimani [244], where HMDM were incubated with 5 or 30 mM glucose concentrations and the differences were not statistically different. In the current study the procathepsin and the mature/ activated form of cathepsin B and L were investigated and were quantified relative to β-tubulin levels, commonly used as a loading control to account for differences in protein loading. This is important as the total protein levels steadily increased throughout the whole maturation process.

In contrast to the cathepsins, there was no significant increase in LAL protein levels during the maturation process and exposure to high glucose did not have a statistically significant impact upon these levels. Here again these results are in contrast

to what was seen with the LAL activity levels where maturation under the high glucose condition had a significant inhibitory effect. These data therefore suggest that the major effect of high glucose levels is to inactivate LAL.

There was reduction in activity relative to the amount of the protein expressed for cathepsin L, and to a lesser degree cathepsin B over the maturation period when the individual lysosomal activities were assessed relative to the corresponding protein levels in both glucose conditions. However the differing glucose treatments did not cause any changes in LAL activity when compared to protein expression during the maturation process. A similar loss in activity was detected on incubation of glyceraldehyde-3-phosphate dehydrogenase with reactive aldehydes and protein-bound carbonyls along with concurrent loss of thiol groups. This loss in activity has been reported to be due to reaction of the free or protein-bound carbonyls with the thiol groups of the enzyme [267]. Reactive aldehydes and protein-bound carbonyls have also been shown to inhibit lysosomal cysteine proteases B, L and S due to the loss of the cysteine residue within the active site in a macrophage cell line [243]. Inactivation of these enzymes induced by oxidative/ carbonyl stress may contribute to the accumulation of modified proteins and lead to cellular dysfunction in a number of diseases.

The significant increase in lysosomal number (as represented by a significant increase in LAMP-1 protein levels) during monocyte maturation paralleled the changes for the two cathepsins as well as the trend seen for LAL protein. Here again a significant impact upon LAMP-1 levels of the high glucose levels were only seen at day 10. The decrease in LAMP-1 levels observed at the end of the maturation period was similar to that observed in the previous chapter for HMDM that were incubated in 20 mM glucose [244].

A number of previous studies have proposed a major role for lysosomes in diabetes-associated complications. A reduction in lysosomal proteolytic activity has been reported to be reduced by glycated proteins [229,242,243]. Lysosomal cathepsin B and L activity has also been reported to be impeded by proteins containing hydroperoxide groups with this ascribed to oxidation of the active site Cys residues of these enzymes [229,243]. Advanced glycation end products (AGEs) which are known to be elevated in diabetes have also been shown to have inhibitory effects on both proteasome activity [242] and on lysosomal cathepsin activities [268,269]. These deleterious effects of AGE products on proteasomal and lysosomal function may

influence the turnover of both intracellular and extracellular proteins [268]. A reduction in intracellular protein turnover was also shown by Xian et al [270]. Suppression of cathepsin mRNA expression may play a role in reduced lysosomal activities, with a previous study having reported time and dose dependent decreases in the activities of cathepsins B, L and H after incubation with AGEs [271]. The inhibitory effects of high glucose on mRNA levels were not assessed for the monocytes/ macrophages examined in the current studies. A study by Moheimani *et al.* has shown that macrophage scavenger receptor mRNA and protein levels can be perturbed by high glucose in HMDM, however these changes did not affect cholesterol and cholesteryl ester accumulation, or ester type in these human macrophages [272]. The studies reported above confirm that hyperglycaemia may be a contributory factor in the increased occurrence and the acceleration of atherosclerosis in people with diabetes.

The degradation of a complex mixture of AGE-modified proteins might be a multifactorial process involving several proteases and peptidases and lysosomal activities [243,273]. In particular the proteasome and the endosomal lysosomal systems involved in the catabolism of modified and damaged proteins may act synergistically [243,269]. Lysosomal proteolytic enzymes appear to be essential for the survival of cells during the maturation of monocytes to macrophages which may provide insight into how accumulation of AGEs and their deleterious effects can be reduced by lysosomal enzymes [269]. In the circumstances of diabetes where the current studies have demonstrated impaired lysosomal function, and previous studies have shown the deleterious impact of AGE-modified proteins upon the same functions [243,269,274], one important contributor to the increased prevalence and rate of progression seen in people with diabetes could be impact of chronic hyperglycaemia upon macrophage function.

Further investigations should be carried out to determine whether stimulation of lysosomal cathepsins or acid lipase activities modulates lipid cholesterol and cholesteryl ester accumulation, which may be a base for developing new pharmaceuticals for the prevention / alleviation of diabetes-associated cardiovascular diseases. Therefore, as to whether therapies designed to promote lysosomal function could have a synergistic effect to those that alleviate the hyperglycaemia of diabetes remains to be investigated.

Given the current findings, agents that could reduce the hyperglycaemia and glycative damage that characterises diabetes mellitus may be protective of macrophage

degradative function and potentially anti-atherogenic in the case of diabetes-accelerated atherosclerosis. The following chapter presents an investigation as to whether carnosine (which has putative hypoglycaemic and anti-glycative activities) can prevent or inhibit atherosclerotic plaque development in a model of diabetes-accelerated atherosclerosis: apo $E^{-/-}$ mice in which diabetes is induced by treatment with streptozotocin.

4.6 Conclusion

Increased lysosomal cathepsin and acid lipase activities, as well as protein levels and lysosomal number were observed during *in vitro* maturation of monocytes to macrophages. This has implications for clinical studies that generally rely on blood monocytes as a marker of tissue-dwelling macrophage function. Chronic exposures to high glucose during the maturation lead to impaired lysosomal proteolytic and lipase levels as well as total lysosome numbers. Shorter term exposure was found to inhibit lysosomal enzyme activity independent of any effect upon protein levels. These results suggest several mechanisms by which high glucose can lead to an impairment of macrophage degradative activity. These functional changes may affect the capacity of macrophages to catabolise modified (lipo) proteins during the maturation process and enhance the lipid accumulation seen in diabetes-associated atherosclerosis.

CHAPTER 5:

INVESTIGATIONS OF THE POTENTIAL PROTECTIVE EFFECT OF CARNOSINE IN A MURINE APO $E^{-/-}$ MODEL OF DIABETES-INDUCED ATHEROSCLEROSIS

5.1 Introduction

Cardiovascular disease is a major complication of diabetes and several studies have demonstrated that people with diabetes have 2 - 4 fold greater risk of cardiovascular disease compared to people without diabetes [111]. Diabetes has also been identified as an independent risk factor for cardiovascular- associated mortality [112]. Evidence suggests that the high incidence of cardiovascular disease amongst people with diabetes cannot be solely explained by well-established cardiovascular risk factors and that the chronically elevated blood glucose levels in diabetes contributes to the increased incidence of atherosclerosis [114,275].

The major impact of diabetes on cardiovascular health has led to extensive investigations of therapies designed to prevent, inhibit or reverse diabetes-associated atherosclerosis with many of these studies carried out in experimental animals such as mice. Mouse models of this disease include the streptozotocin-treated apo $E^{-/-}$ mouse [276,277]. Studies using this model, as well as clinical reports, are consistent with a role for increased production of AGE, mediated by protein glycation / glycoxidation and oxidative stress, in the development and progression of diabetes-accelerated atherosclerosis [278].

Carnosine (β-alanyl-L-histidine dipeptide) is an endogenous dipeptide present at high concentrations in skeletal muscle [279]. A number of functions have been ascribed to carnosine including: as a buffer; as a regulator of Ca^{2+} sensitivity, as an antioxidant, or as an agent which could both prevent and reverse glycative and glycoxidative modifications to cell and tissue components [279,280]. Previous *in vitro* studies have shown that carnosine was effective at blocking pro-atherosclerotic AGE formation on low-density lipoproteins [281]. Recently Meini *et al*. [282] have demonstrated an anti-atherosclerotic activity of D-carnosine octylester in fat-fed apo $E^{-/-}$ mice. Carnosine has also been shown to block increases in plasma triglycerides and cholesterol in fat-fed, non-diabetic, C57BL/6 mice [283]. As an endogenous peptide, carnosine has been shown to be safe and effective for oral delivery. It is absorbed as the intact dipeptide and hydrolysis in the intestinal mucosa is readily saturable [284]. However while it would be expected that intact dipeptide should be detectable in blood, plasma carnosine levels in humans are low or undetectable due to the rapid hydrolysis of carnosine in plasma induced by the enzyme carnosinase (e.g. [279,284]). Synthetic derivatives have however been developed that are much less susceptible to such hydrolysis (e.g.

[285,286,287]) and may therefore have therapeutic potential. By contrast, chronic supplementation of rodents with carnosine results in a persistent and significant elevation of plasma and tissue carnosine levels (e.g. [283,288,289]). Thus, chronic supplementation of rodents with carnosine provides an appropriate model to examine potential *in vivo* effects of carnosine (or its derivatives) as anti-oxidative / anti-glycative agents. The current study assesses, *in vivo*, the anti-atherogenic potential of chronic supplementation of streptozotocinF-treated apo $E^{-/-}$ mice with carnosine.

5.2 Aims

To determine whether carnosine prevents or reverses atherosclerotic lesion formation and progression caused by prolonged periods of high blood glucose *in vivo*, using streptozotocin-treated diabetic apo $E^{-/-}$ gene knock-out mice as a model of diabetes-associated atherosclerosis.

5.3 Methods

5.3.1 Animal model design

Mice (n = 80) were maintained for 20 weeks, post-induction of diabetes, with the grouping as shown in Figure 5.1 that is; (i) control (vehicle-dosed); (ii) control mice receiving carnosine (2 g/L) in their drinking water; (iii) diabetic (streptozotocin-dosed) mice; and (iv) diabetic mice receiving carnosine in their drinking water. At the time of sacrifice, blood was collected for quantification of blood glucose and glycated haemoglobin, and plasma was prepared for assessment of carnosine, total cholesterol and triglyceride levels. The details and source of the animals used in this study are outlined in Sections 2.7 and 2.7.1.

Induction of diabetes; care and monitoring of the animals; determination of body mass, blood glucose and glycated haemoglobin level; sample collection, fixation and store; and determination of plasma carnosine levels were undertaken by Dr David van Reyk and Dr Bronwyn Brown. Plasma cholesterol and triglyceride analyses were carried out by Ms Liming Hou of the Lipid Group of the Heart Research Institute.

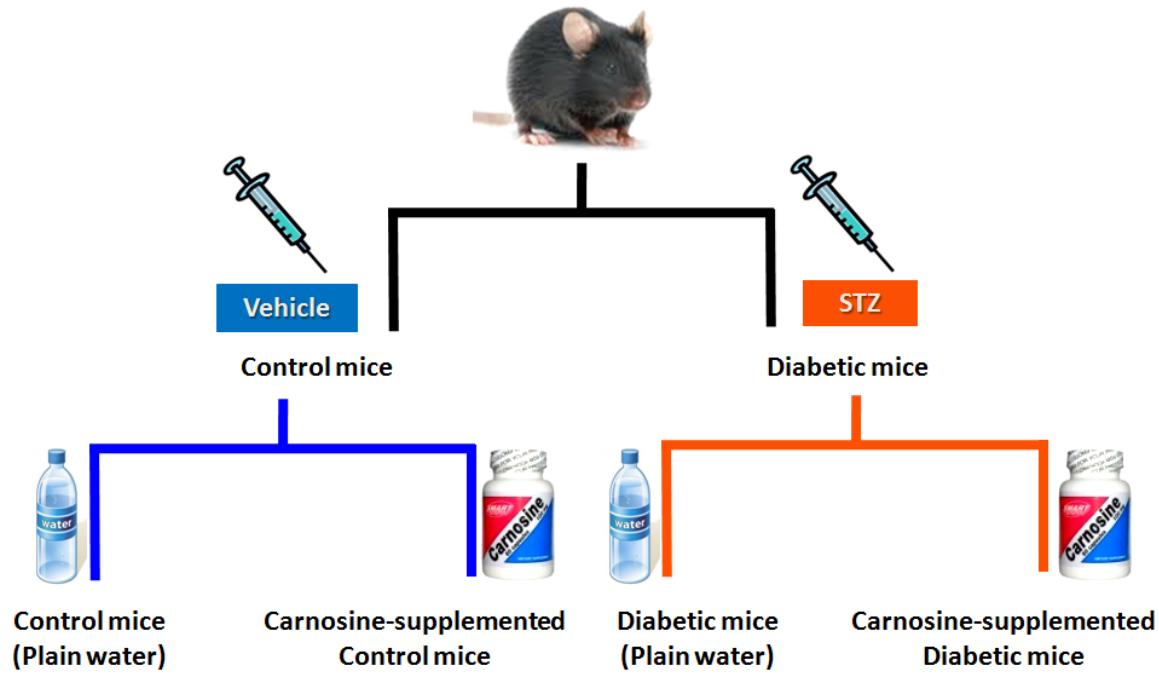

Figure 5.1: Experimental Plan.
The first two groups comprised of vehicle-dosed control mice groups (outlined in blue) with and without carnosine supplemented in their water. The third and fourth groups comprised of streptozotocin induced diabetic mice (outlined in orange) with and without carnosine supplemented in the water respectively.

5.4 Results

5.4.1 Induction of diabetes with STZ treatment

Diabetes was confirmed by significant increases in blood glucose and glycated haemoglobin as shown in Figure 5.2 (reproduced with permission from Dr van Reyk). A wide range of blood glucose levels was observed amongst the mice, a blood glucose level of 18 mM was chosen to distinguish between those with and without diabetes. This cut-off was supported by glycated haemoglobin levels and body mass determinations. Thus mice with blood glucose levels < 18mM (for STZ-treated mice) or above this level (for vehicle-treated mice) were omitted from the data set. This cut-off is similar to that used previously for this model (19.2 mM; [276]). To ensure this decision did not have a major effect on the conclusions drawn, the data sets were also censored at 20, 16, 14 and 12 mM blood glucose and reanalysed. Each cut-off gave broadly

consistent results, indicating that the choice of 18 mM did not affect the conclusions, nor was the level of blood glucose used as an indicator of diabetes induction, critical to the effects detected.

Using this cut-off to distinguish between control mice (CTL) and those with diabetes (DIAB), the latter had a significantly lower body mass at time of sacrifice with a significant elevation of blood glucose, glycated haemoglobin, total cholesterol and triglycerides levels as presented in Table 5.1 (reproduced with permission from Dr van Reyk). These data are in accord with previous studies [276,290,291].

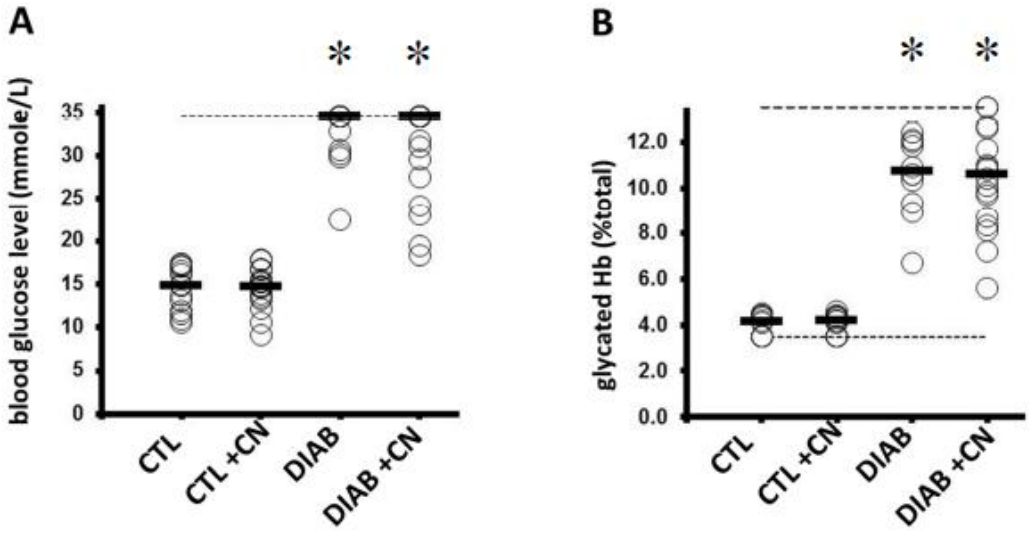

Figure 5.2: Blood glucose levels (A) and glycated haemoglobin levels (B), at the time of sacrifice, for control (CTL) and diabetic (DIAB) apo $E^{-/-}$ mice with (+CN) or without carnosine supplementation.

Individual determinations (n = 12 - 18) are presented, together with the median value (horizontal bar). Out of range results (> 33 mmoles/L for blood glucose; and < 4% or >13% for glycated haemoglobin) are represented as markers placed on the dashed line that delimits the range of detection. A number of the animals with diabetes have superimposed data points. *: significantly different ($p < 0.05$) from the control group at the same level of carnosine supplementation using rank-transformed data.

	Control	Control with CN	Diabetic	Diabetic with CN
Mass (g)	27.8 ± 0.6	29.9 ± 0.5	24.6 ± 0.9*	24.2 ± 0.5*
Total cholesterol (mmoles/L)	9.6 ± 0.5	9.0 ± 0.3	14.6 ± 2.1*	15.2 ± 0.7*
Triglycerides (mmoles/L)	1.1 ± 0.1	0.8 ± 0.1$^{\#}$	1.7 ± 0.2*	1.3 ± 0.1*$^{\#}$

Table 5.1: Mean body mass, total cholesterol and triglyceride plasma levels, estimated at the time of sacrifice, for non-diabetic (control) and diabetic apo E$^{-/-}$ mice with or without carnosine (CN) supplementation.

Results are expressed as mean ± standard error of the mean (SEM) for 12 - 19 mice per group. *: significantly different ($p < 0.05$) from control group at the same level of carnosine supplementation. $^{\#}$: significantly different ($p < 0.05$) from the non-supplemented group matched for glycaemic status using transformed data.

5.4.2 Efficacy of carnosine supplementation

Plasma-derived low molecular mass filtrates (< 3000 Da) were obtained by centrifugation (13 400 *g*, 30 min, 4°C) using Pall Nanosep 3000 MWCO filters (Ann Arbor, MI, USA) after. Carnosine was quantified by HPLC, after pre-column derivatisation with *o*-phthaldialdehyde (with 5% v/v 2-mercaptoethanol), against authentic standards [18].

Low levels of plasma carnosine were detected reproducibly in the non-supplemented mice, with supplementation significantly increasing this value as presented in Figure 5.3 (reproduced with permission from Dr van Reyk and Dr Brown). There was however substantial variation amongst individual mice in both supplemented groups.

Supplementation with carnosine had no effect on blood glucose or glycated haemoglobin levels, final body mass or plasma total cholesterol levels (Table 5.1). However, for mice with the same glycaemic status (CTL or DIAB), triglycerides were significantly lower in the carnosine supplementation groups.

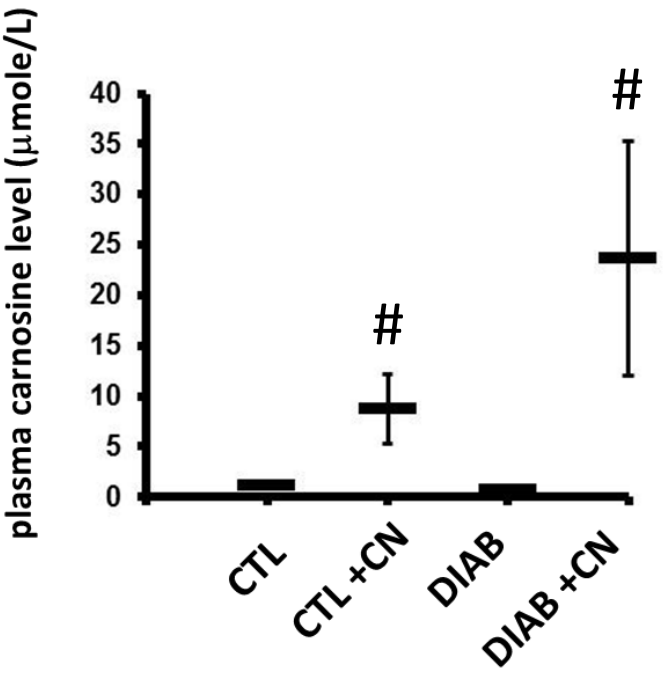

Figure 5.3: Plasma carnosine levels (µmoles/L), at the time of sacrifice, for control (CTL) and diabetic (DIAB) apo $E^{-/-}$ mice with (+CN) or without carnosine supplementation.
Data are presented as the 95% confidence interval together with the mean (n =12 - 18). #: significantly different ($p < 0.05$) from the non-supplemented group matched for glycaemic status using General Linear Model on the natural log-transformed data.

5.4.3 Morphometry of atherosclerotic plaques in the brachiocephalic artery

Six sections (A - F) were prepared for estimation for atherosclerotic lesion size in the brachiocephalic artery. One set of the six duplicate sections (A - F) was stained with Haematoxylin and Eosin (H & E) for general morphology in order to determine plaque areas, as described in Section 2.7.7 and displayed in Figure 5.4. The images were captured digitally with an IX71 Olympus microscope (North Ryde, NSW, Australia) for morphometric analysis for the following areas within the outlined boundaries of the brachiocephalic artery: total cross-sectional area, lumen, plaque and the cross-sectional area within the internal elastic intima as illustrated in Figure 5.5.

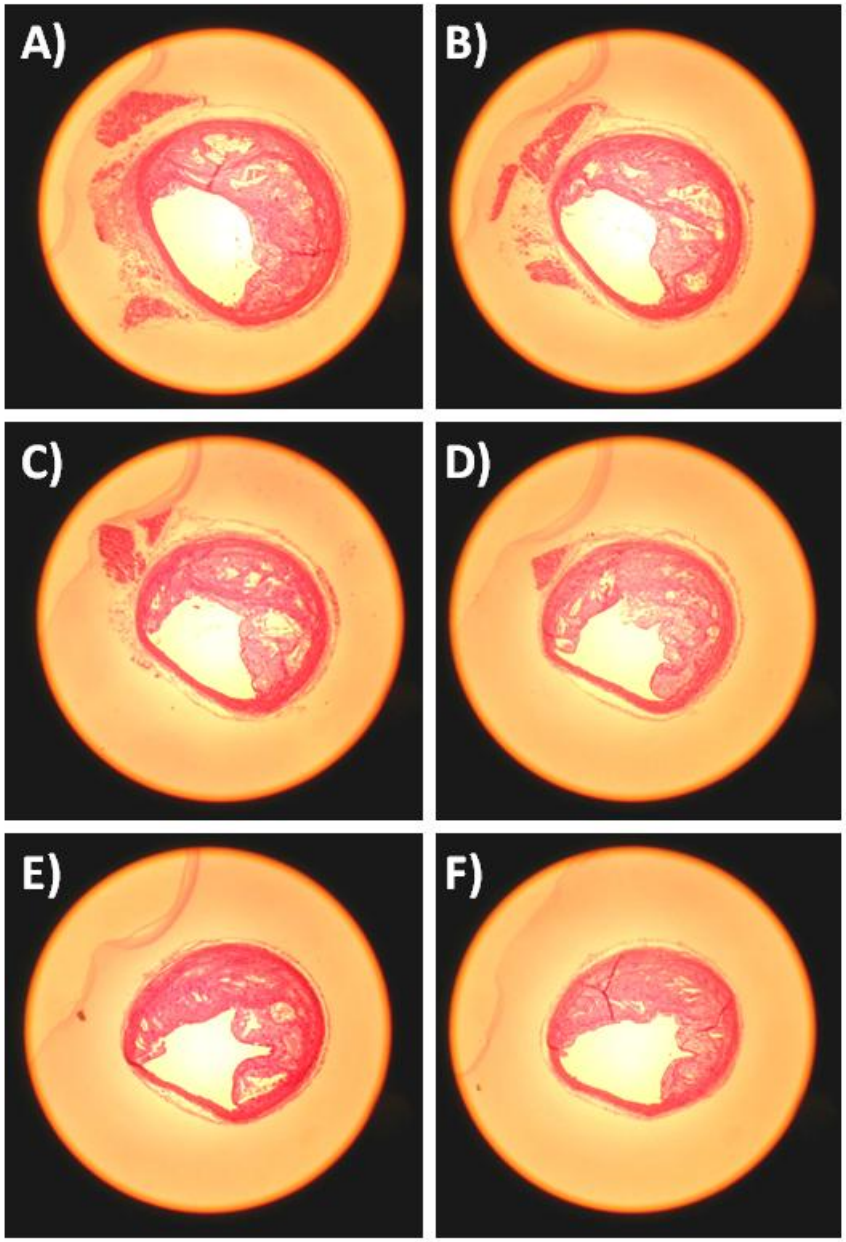

Figure 5.4: Representative images of 6 cross sections (A - F) taken from the brachiocephalic artery.

5 µm sections were taken from the brachiocephalic artery commencing when the first entirely circular cross-section appeared for Slide A. Duplicate sections were taken every 100 µm until six sections in total had been obtained from A to F. Sections were stained with H&E and photographed using a 20x objective.

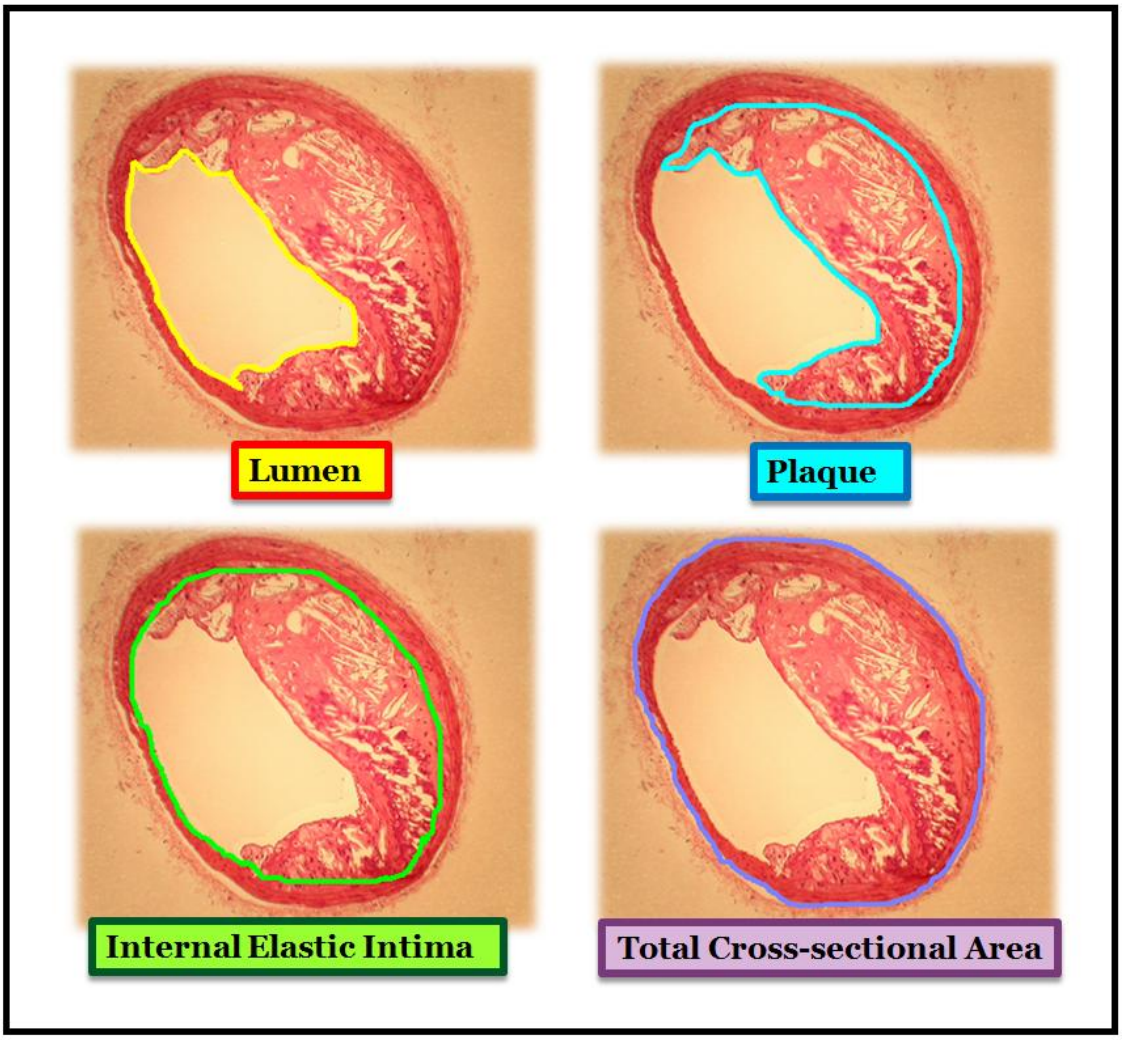

Figure 5.5: Calculation of plaque morphometry in the brachiocephalic artery. Morphometry was performed on the cross-sections of the brachiocephalic artery. For the brachiocephalic artery the following measurements were made; internal area of lumen, plaque, internal elastic intima and total cross-sectional area.

The arteries from the diabetic mice contained more plaque than the non-diabetic mice ($p < 0.05$) in both the non-carnosine and carnosine supplemented groups as shown in Figure 5.6 (Panel A). There were significant increases in plaque area in the diabetic control (60.9 ± 4.8 ($x10^3$) μm^2, $p < 0.05$) when compared to the non-diabetic control mice (44.9 ± 4.7 ($x10^3$) μm^2). Diabetic mice supplemented with carnosine (57.2 ± 3.6 ($x10^3$) μm^2, $p < 0.05$) also had more plaque than the control supplemented carnosine mice (40.4 ± 4.7 ($x10^3$) μm^2).

When the plaque areas are expressed relative to the total area there was a higher percentage observed in the diabetic control (41.8 ± 2.9 %, $p < 0.05$) than the non-diabetic control mice (33.5 ± 2.8 %) as shown in Figure 5.6 (Panel C). There was also a greater plaque percentage in the diabetic supplemented carnosine mice (41.6 ± 1.5 %, $p < 0.05$) when compared to the control supplemented carnosine mice (31 ± 3.5%).

The area enclosed within the internal elastic intima and the area of the lumen were also measured in order to determine whether there were any differences between the morphological structure of the diabetic and non-diabetic mice with and without carnosine supplementation. There was a smaller ratio of lumen area over the total area observed in the diabetic mice supplemented with carnosine (30.9 ± 1.4, $p < 0.05$) than the non-diabetic mice supplemented with carnosine (39 ± 2.9) as presented in Figure 5.7 (Panel A). There were no statistical differences observed when the internal elastic intima areas were analysed over the total area as shown in Figure 5.7 (Panel B).

Overall the diabetic mice had a greater extent of atherosclerotic plaque and a decreased lumen size as a percentage of total area in the brachiocephalic artery than the non-diabetic mice. Carnosine supplementation had no effect upon the increased plaques and smaller lumen sizes in these mice.

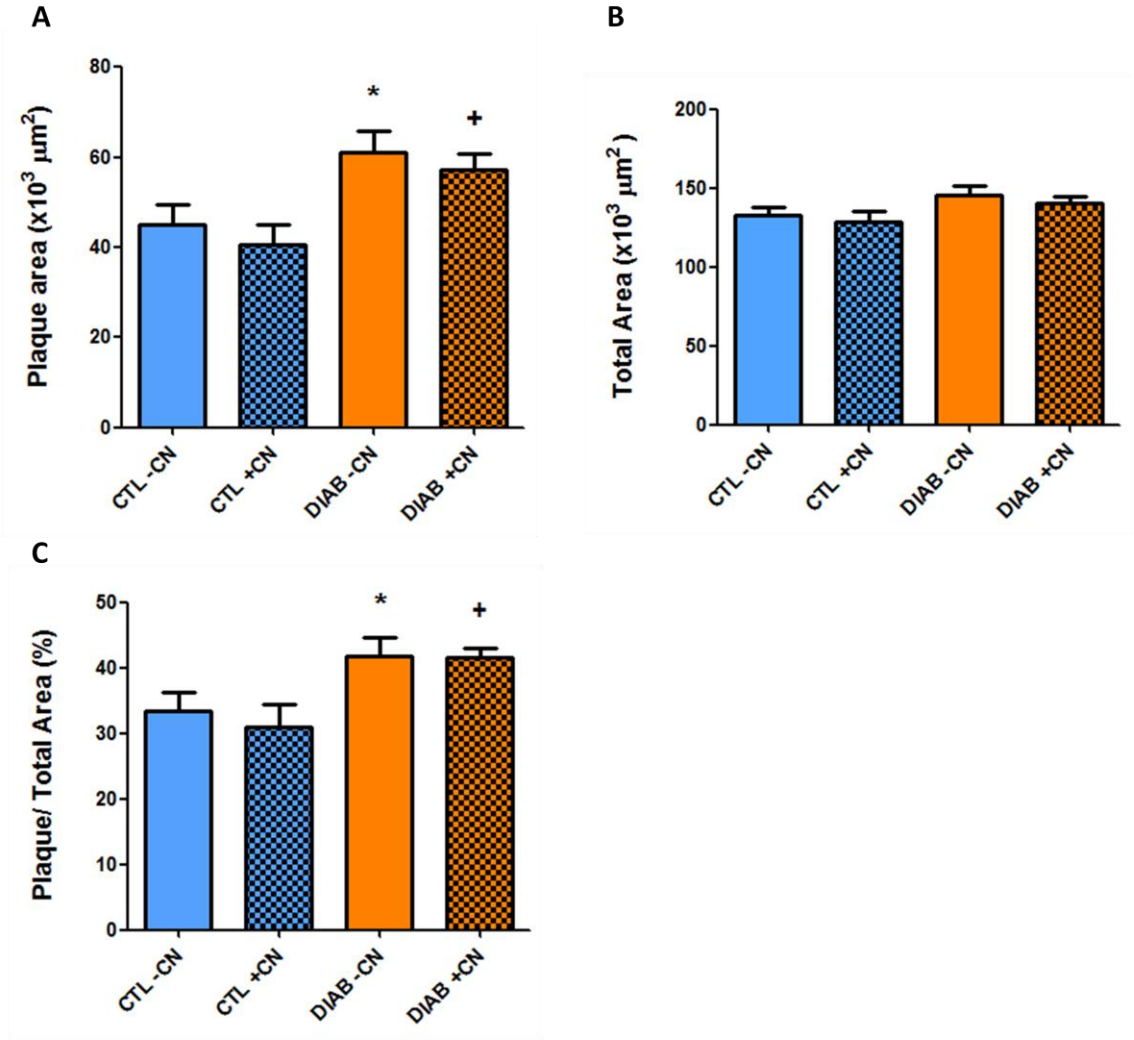

Figure 5.6: Plaque morphometry in brachiocephalic artery for plaque area (Panel A), total area (Panel B) and percentage of plaque compared to total arterial cross-sectional area (Panel C) in control (CTL) and diabetic (DIAB) apo $E^{-/-}$ mice with or without carnosine (+/- CN) supplementation.

Plaque and total cross sectional areas of the artery were determined in the brachiocephalic artery are calculated as (x10³) µm² in Panels A and B. Plaque is expressed as a percentage over the total area in Panel C. Statistical significance was achieved at * $p < 0.05$ versus control (CTL - CN), + $p < 0.05$ versus control supplemented with carnosine (CTL + CN) using two-way ANOVA followed by Bonferroni's post-hoc test. Values are expressed as mean ± SEM.

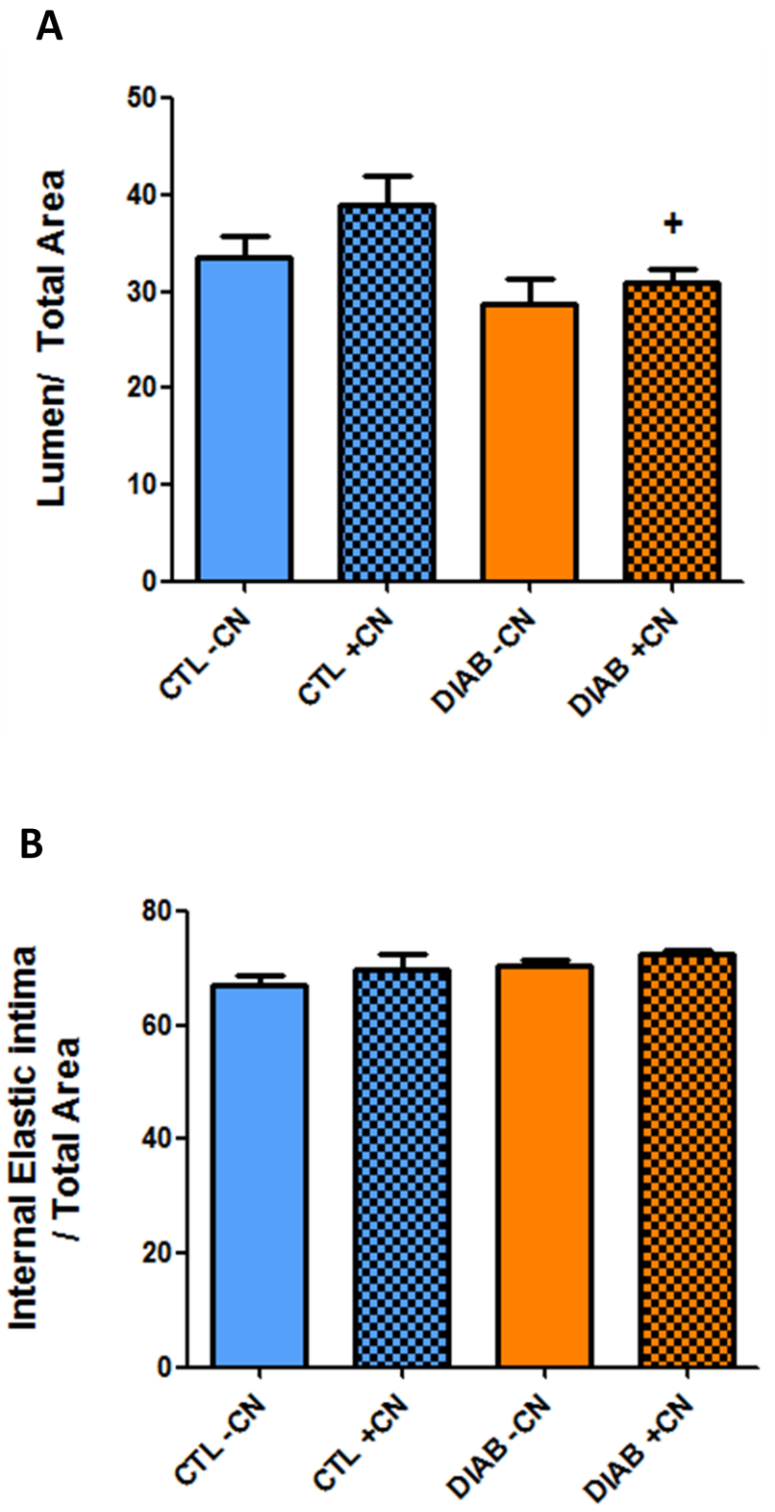

Figure 5.7: Ratio of lumen (Panel A) and internal elastic intima areas (Panel B) over the total cross-sectional area of the brachiocephalic artery in control (CTL) and diabetic (DIAB) apo $E^{-/-}$ mice with or without carnosine (+/- CN) supplementation.

Lumen and internal elastic intima areas of the artery were determined in the brachiocephalic artery and the ratio was calculated over the total cross-sectional area. Statistical significance was achieved at + $p < 0.05$ versus control supplemented with carnosine (CTL + CN) using two-way ANOVA followed by Bonferroni's post-hoc test. Values are expressed as mean ± SEM.

5.4.4 Plaque area in aortic sinus

Six duplicate (A - F) cross-sections were taken along the aortic sinus and were imaged and morphometric measurements were performed with image analysis software as described in Section 5.3.3 to 5.3.4 and shown in Figure 5.8. The areas within the outlined boundaries of the aortic sinus were examined across the six duplicates (A - F) cross-sections in order to determine total plaque and cross-sectional area as illustrated in Figure 5.9.

There were significant increases in plaque area in the diabetic supplemented carnosine group (43.3 ± 4.9 ($x10^3$) μm^2, $p < 0.01$) when compared to the control supplemented carnosine mice (24.9 ± 3.2 ($x10^3$) μm^2) as shown in Figure 5.10 (Panel A). There were no statistical significant differences in the average cross-sectional total areas of the aortic sinus observed across the groups as shown in Figure 5.10 (Panel B).

When plaque area was analysed over the total arterial cross-sectional area there was a higher percentage plaque area observed in the diabetic mice supplemented with carnosine (28.9 ± 2.4 %, $p < 0.001$) when compared to the control supplemented carnosine mice (18.1 ± 1.6%). There was a lower percentage of plaque seen in the control supplemented carnosine mice than the control mice (26.2 ± 1.5%, $p < 0.05$) as shown in Panel C of Figure 5.10.

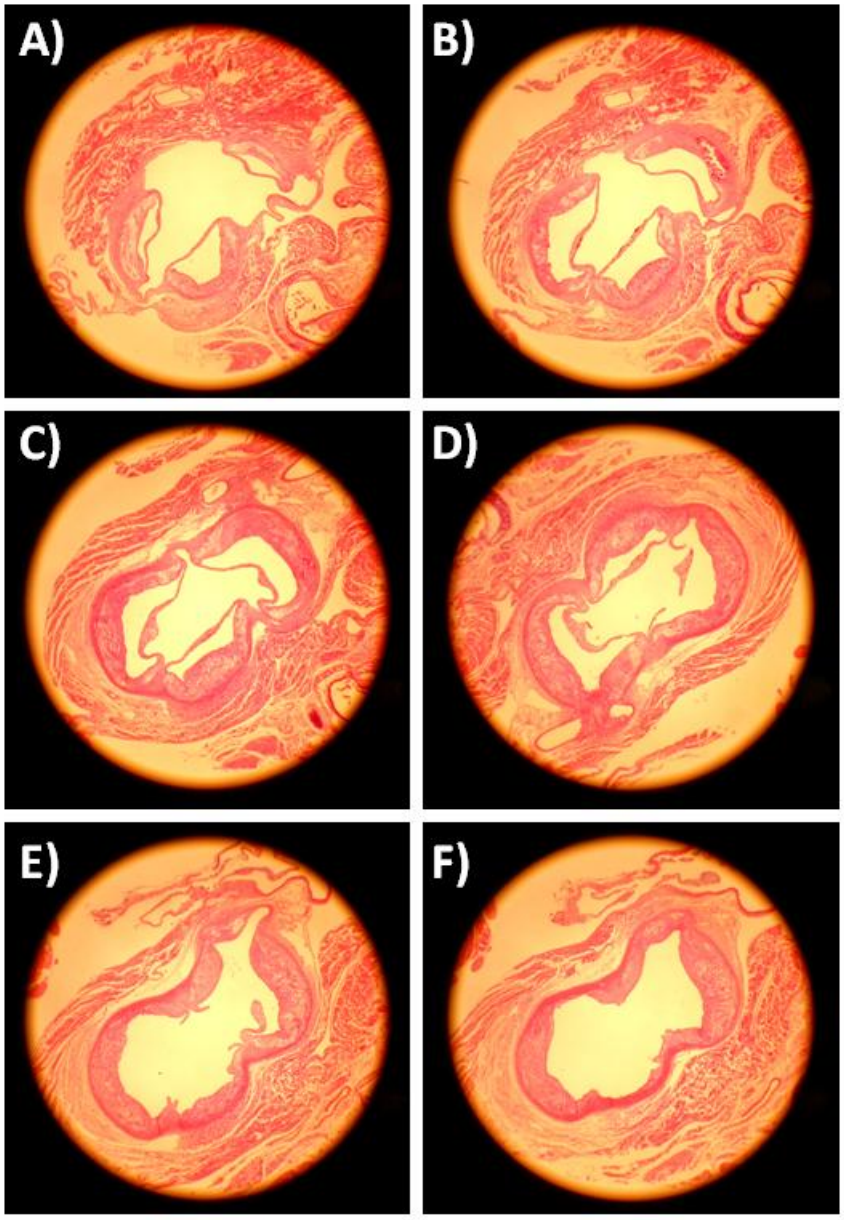

Figure 5.8: Representative images of 6 cross-sections (A - F) taken from the aortic sinus.

5 µm sections were taken from the appearance of the three valve leaflets for Slide A. Duplicate sections were taken every 100 µm until six sections in total had been obtained. Sections were stained with H&E and photographed using a 10x objective.

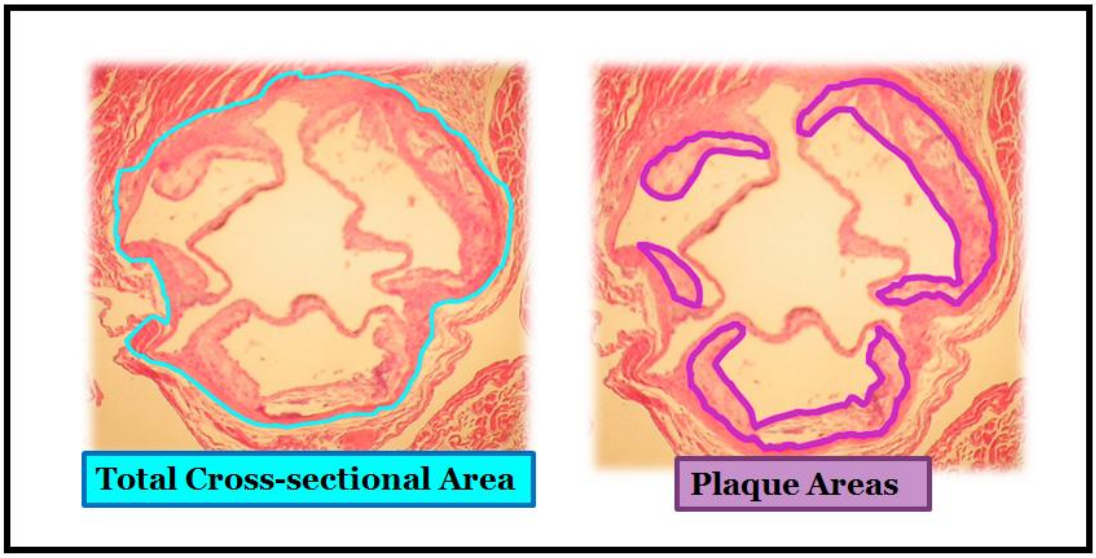

Figure 5.9: Calculation of plaque morphometry in the aortic sinus.
Morphometry was performed on the cross-sections of the aortic sinus. For the aortic sinus, the total surface cross-sectional area and plaque areas were measured.

Overall the diabetic mice had a greater extent of atherosclerotic plaque formation than the non-diabetic mice for groups on the same supplementation regime. Ingestion of carnosine did not result in a significant reduction in plaque size for the diabetic animals.

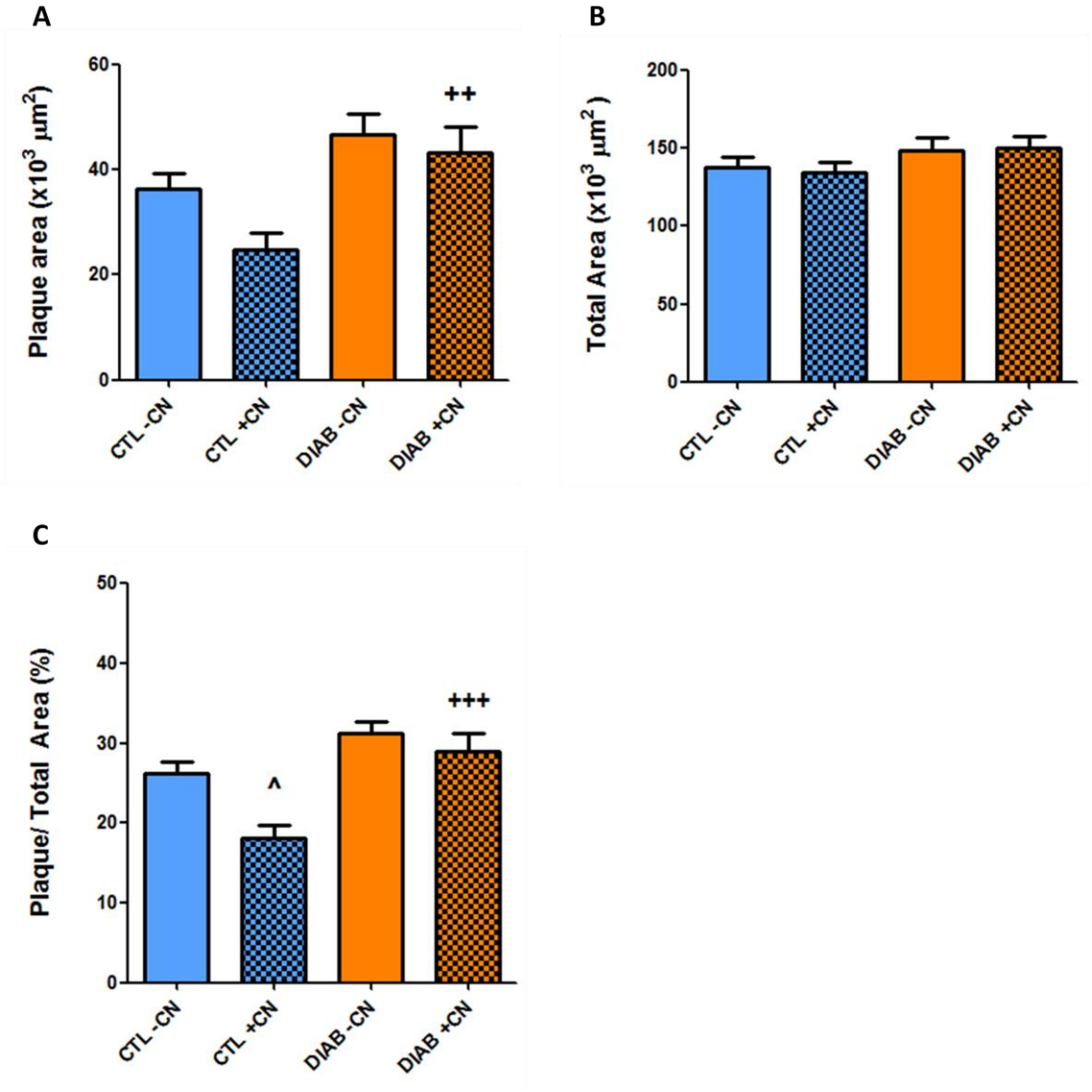

Figure 5.10: Plaque morphometry in the aortic sinus for plaque area (Panel A), total area (Panel B) and percentage of plaque on total area (Panel C) in control (CTL) and diabetic (DIAB) apo $E^{-/-}$ mice with or without carnosine (+/- CN) supplementation.

Plaque and total cross sectional areas within the leaflets were determined for the aortic sinus are calculated as (x10³) µm² in Panels A and B. Plaque is expressed as a percentage over the total area in Panel C. Statistical significance was achieved at ++ $p < 0.01$, +++ $p < 0.001$ versus control supplemented with carnosine (CTL + CN) and ^ $p < 0.05$ versus the control (CTL – CN) using two-way ANOVA followed by Bonferroni's post-hoc test. Values are expressed as mean ± SEM.

5.4.5 Smooth muscle cells in fibrous cap in the brachiocephalic artery

Immunostaining for α-actin was examined as a marker for the degree of smooth muscle cell infiltration of the plaque, to determine whether carnosine had any effect on plaque stability. The plaques were examined using the same sets of samples as described previously (refer to Sections 2.8.3 and 2.8.4). The fibrous caps of the atherosclerotic plaques were observed to contain α-actin expressing cells with these primarily detected in the regions of the cap directly beneath the endothelium as shown in Figure 5.11.

As shown in Figure 5.12 (Panel A), there were no differences in absolute levels of α-actin staining between the diabetic and control mice in the absence of carnosine supplementation. However, there was a greater extent of α-actin staining in the carnosine-supplemented diabetic (1.5 ± 0.3 ($x10^3$) μm^2, $p < 0.05$) than the carnosine-supplemented control (0.7 ± 0.2 ($x10^3$) μm^2) mice. Carnosine-supplemented diabetic mice had more levels of α-actin than the diabetic (0.5 ± 0.2 ($x10^3$) μm^2, $p < 0.05$) mice.

A higher plaque area was observed in the diabetic (47.2 ± 4.2 ($x10^3$) μm^2, $p < 0.05$) than the control mice (34 ± 3.2 ($x10^3$) μm^2) without carnosine supplementation as shown in Figure 5.12 (Panel B). No statistical differences were seen between the two carnosine supplemented groups. When the area of α-actin staining was analysed over the plaque area, there was a higher, statistically significant, percentage of α-actin staining observed in the carnosine-supplemented diabetic (4.2 ± 0.8 %, $p < 0.05$) than the diabetic mice (1.5 ± 0.6 %; and refer to Panel C in Figure 5.12).

Although there were no statistical differences detected in α-actin levels between the control and diabetic mice, when comparing the two diabetic groups, carnosine supplementation was associated with higher absolute levels and percentage of α-actin immunostaining in the brachiocephalic artery.

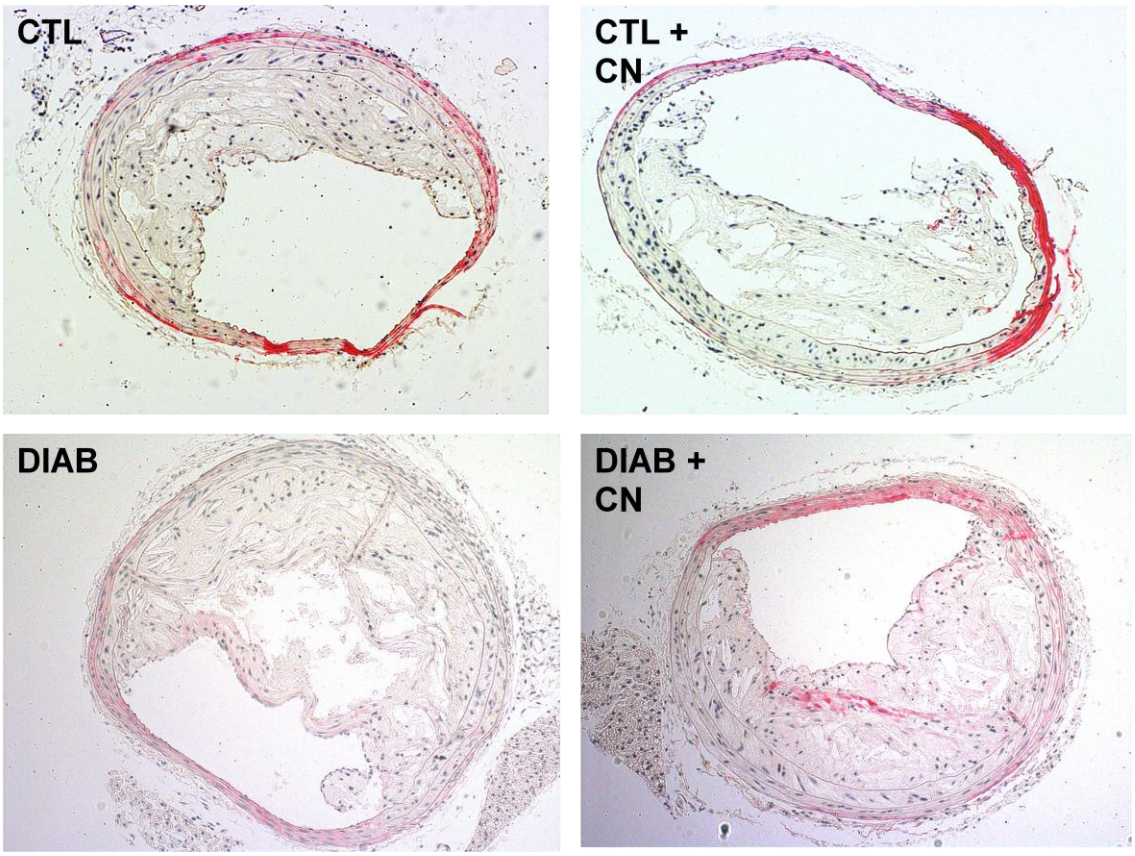

Figure 5.11: Representative sections showing α-SM-actin staining in the brachiocephalic artery in control (CTL) and diabetic (DIAB) apo $E^{-/-}$ mice with or without carnosine (+/- CN) supplementation.

Representative image of sections from the brachiocephalic artery stained for α-actin (red staining) produced by smooth muscle cells. The red staining was quantified and expressed as a percentage of the total plaque area. For illustration purposes the slides were captured using a Carl Zeiss microscope and a 20x objective lens.

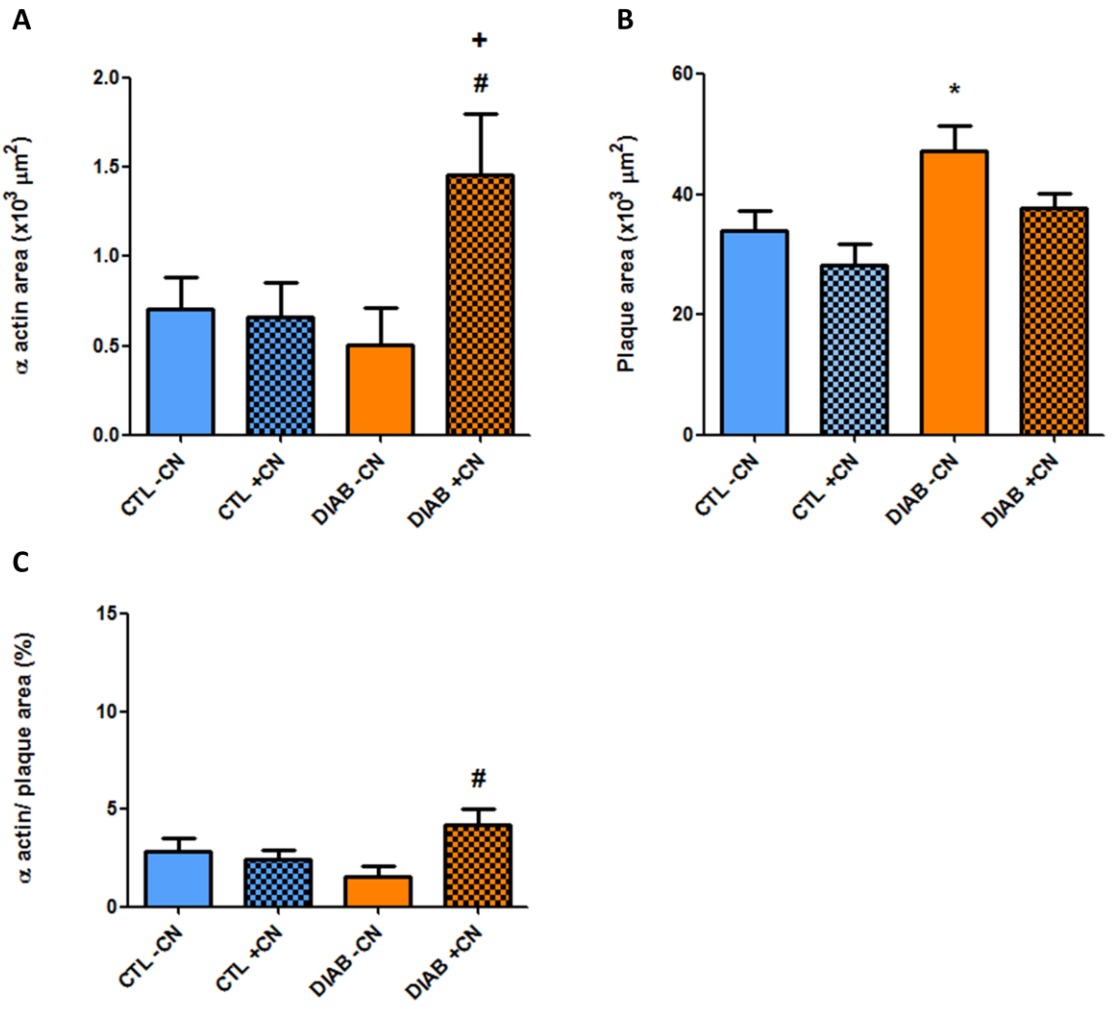

Figure 5.12: α-SM-actin staining of the fibrous cap in the brachiocephalic artery for α-actin area (Panel A), plaque area (Panel B) and percentage of α-actin on total area (Panel C) in control (CTL) and diabetic (DIAB) apo $E^{-/-}$ mice with or without carnosine (+/- CN) supplementation.

The area of α-actin staining and plaque area determined for the brachiocephalic artery sections are calculated as (x10³) µm² in Panels A and B. The area stained by α-actin is expressed as a percentage over the plaque area in Panel C. Statistical significance was achieved at * $p < 0.05$ versus control (CTL - CN), + $p < 0.05$ versus control supplemented with carnosine (CTL + CN) # $p < 0.05$ versus the diabetic (DIAB) apo $E^{-/-}$ mice using two-way ANOVA followed by Bonferroni's post-hoc test. Values are expressed as mean ± SEM.

5.4.6 Smooth muscle cells in the aortic sinus

The fibrous caps were examined for α-actin staining arising for smooth muscle cells in the aortic sinus at 100 μm from the first appearance of the three valve leaflets as described in Sections 2.8.3 and 2.8.4. Representative images of the fibrous caps of the atherosclerotic plaques contained α-actin expressing cells which were stained red are shown in Figure 5.13.

As shown in Figure 5.14 (Panel A), there were no statistical differences in absolute levels of α-actin staining between the control and the diabetic mice in the absence of carnosine supplementation. However there was a significant increase in α-actin staining in the carnosine-supplemented diabetic mice (1.5 ± 0.3 ($x10^3$) μm^2, $p < 0.05$) when compared to the carnosine-supplemented control mice (0.6 ± 0.1 ($x10^3$) μm^2).

A significant increase in plaque size was detected in the diabetic (21.6 ± 1.5 ($x10^3$) μm^2, $p < 0.001$) when compared to the control mice (14.5 ± 2.9 ($x10^3$) μm^2) as shown in Figure 5.14 (Panel B). A similar trend for plaque area was seen in the carnosine-supplemented diabetic (18.1 ± 1.2 ($x10^3$) μm^2, $p < 0.001$) than the carnosine-supplemented control mice (11.9 ± 1.2 ($x10^3$) μm^2). There were no statistical differences detected across the groups when the area of α-actin was expressed as a percentage of the plaque area as shown in Figure 5.14 (Panel C). When α-actin staining was expressed as a percentage of the total plaque area, carnosine-supplementation was associated with an increase in the percentage area positive for α-actin for both control and diabetic mice; however this increase did not reach statistical significance at this site.

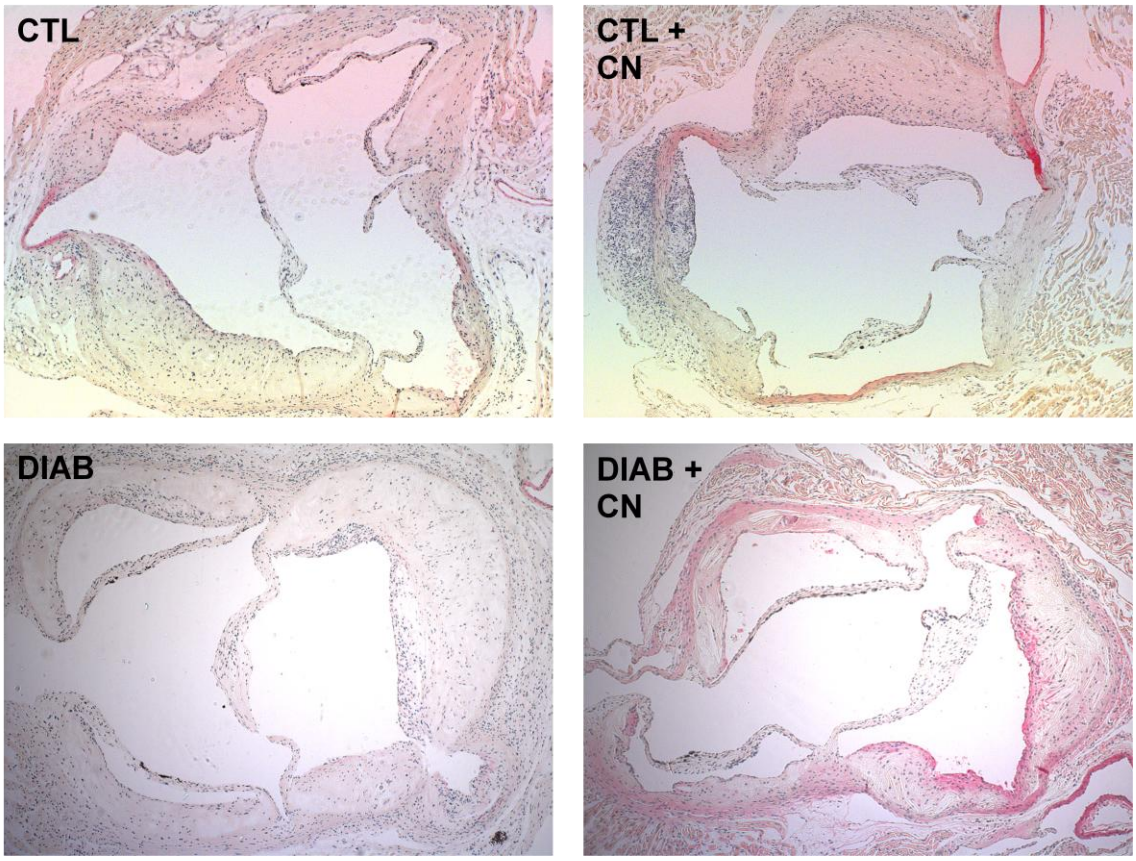

Figure 5.13: Representative sections showing α-SM-actin staining in the aortic sinus in control (CTL) and diabetic (DIAB) apo $E^{-/-}$ mice with or without carnosine (+/- CN) supplementation.

Representative images of sections taken from the aortic sinus stained for α-actin to detect smooth muscle cells which appear as red staining. The area of red was calculated over the plaque area and expressed as a percentage of α-actin content within the plaques formed. For illustration purposes the slides were captured by use of a Carl Zeiss microscope.

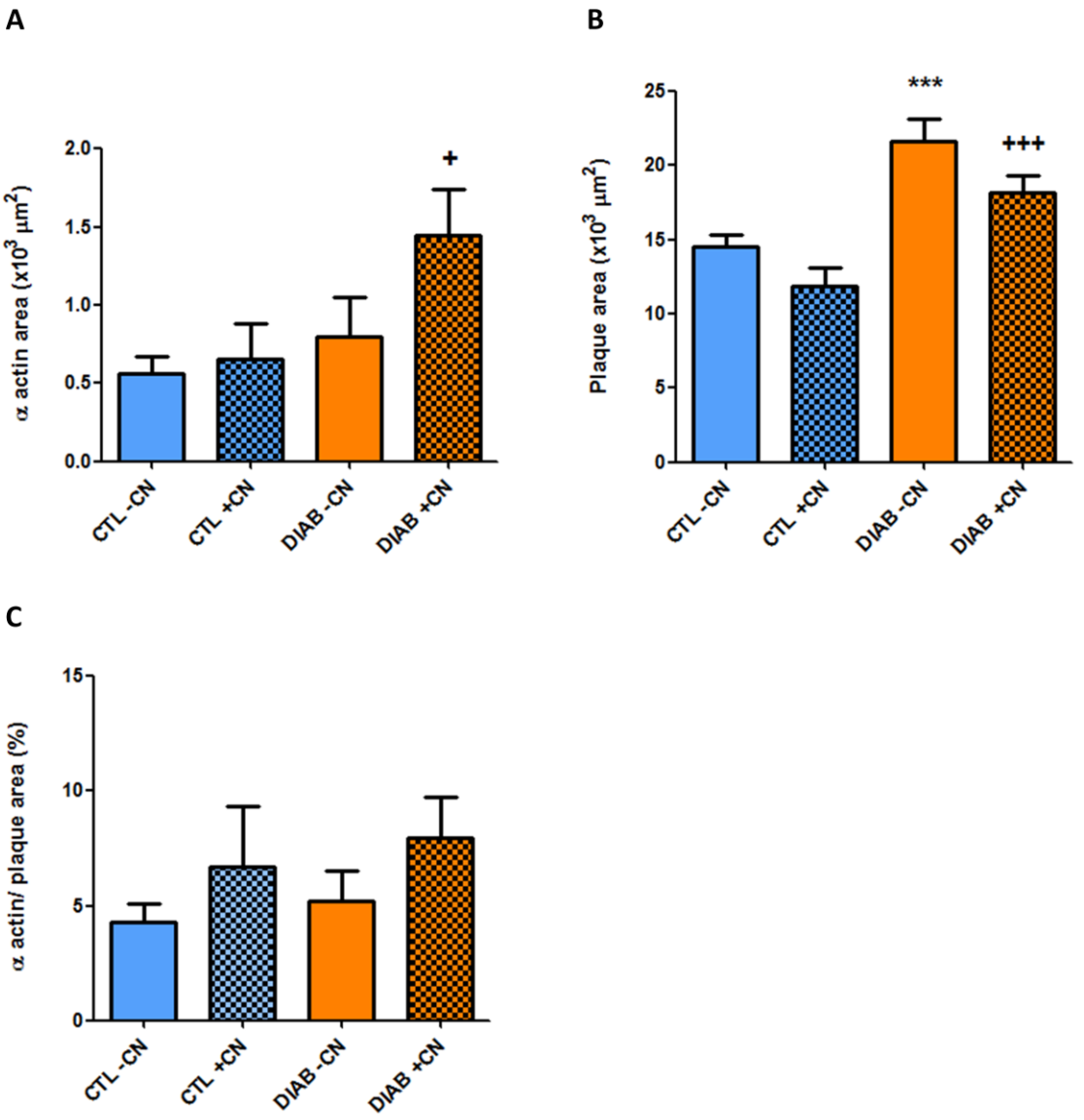

Figure: 5.14: α-SM-actin staining of the fibrous cap in the aortic sinus for α-actin area (Panel A), plaque area (Panel B) and percentage of α-actin on total area (Panel C) in control (CTL) and diabetic (DIAB) apo $E^{-/-}$ mice with or without carnosine (+/- CN) supplementation.

The α-actin and plaque areas that were determined in the aortic sinus are calculated as (x10³) µm² in Panels A and B. The area stained by α-actin is expressed as a percentage over the plaque area in Panel C. Statistical significance was achieved at *** $p < 0.001$ versus control (CTL - CN) and + $p < 0.05$, +++ $p < 0.01$ versus control supplemented with carnosine (CTL + CN) apo $E^{-/-}$ mice using two-way ANOVA followed by Bonferroni's post-hoc test. Values are expressed as mean ± SEM.

5.4.7 Macrophages in plaque within the brachiocephalic artery sections

In the brachiocephalic artery, the presence of macrophages in the plaques was assessed by probing for the murine macrophage marker F4/80 at 200 μm from the first complete circumference of the vessel as described in Sections 2.8.5. The macrophages were stained pink as shown in Figure 5.15 and the area occupied by these cells was quantified in order to investigate the composition of the atherosclerotic plaque formed in the diabetic and non-diabetic mice that were treated with and without carnosine.

There was no increase in the areas that were stained for macrophages in the diabetic mice versus the non-diabetic mice regardless of carnosine supplementation as shown in Figure 5.16 (Panel A). There was a significant increase in plaque area in the vessels from the diabetic mice (38.1 ± 3.3 ($x10^3$) μm^2, $p < 0.01$) than the control mice 22.3 ± 3.5 ($x10^3$) μm^2) and higher plaque size in carnosine-supplemented diabetic (33.1 ± 3.6 ($x10^3$) μm^2, $p < 0.01$) than carnosine-supplemented control mice (17.4 ± 3.1 ($x10^3$) μm^2) as presented in Figure 5.16 (Panel B).

When F4/80 staining was expressed as percentage of total plaque area diabetic mice were associated with decrease in percentage positive for F4/80 than the control mice regardless of carnosine-supplementation, however this decrease did not reach statistical significance. There were no statistical differences achieved when the area of F4/80 was analysed over the total plaque area as shown in Figure 5.16 (Panel C). Supplementation with carnosine did not therefore appear to affect the macrophage content within the plaques formed in the brachiocephalic artery.

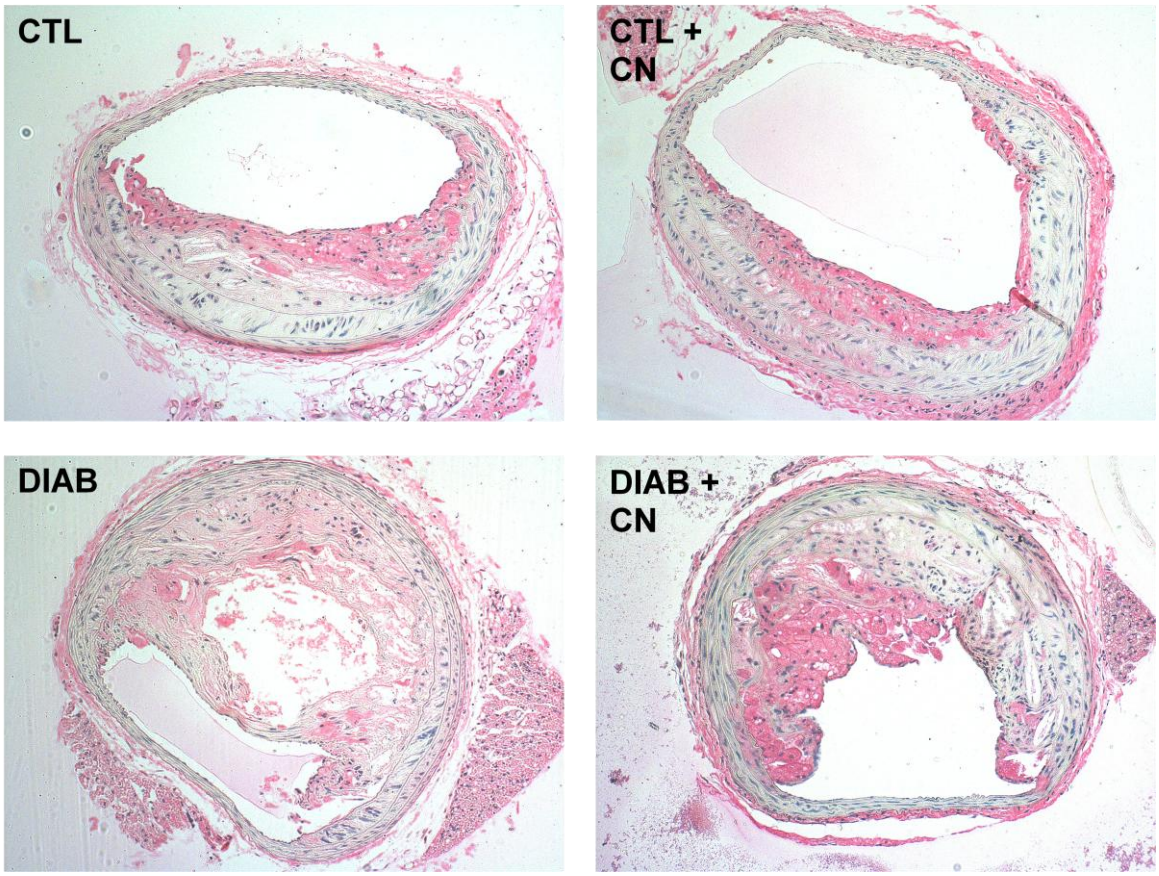

Figure 5.15: Representative sections showing F4/80 staining in the brachiocephalic artery in control (CTL) and diabetic (DIAB) apo $E^{-/-}$ mice with or without carnosine (+/- CN) supplementation.

Representative sections taken from the brachiocephalic artery were stained with F4/80 to detect for macrophages which appeared as pink colouration. The area of pink staining was calculated over the plaque area and expressed as a percentage of F4/80 staining within the total plaques formed. For illustration purposes the slides were captured by Carl Zeiss microscope using a 20x objective lens.

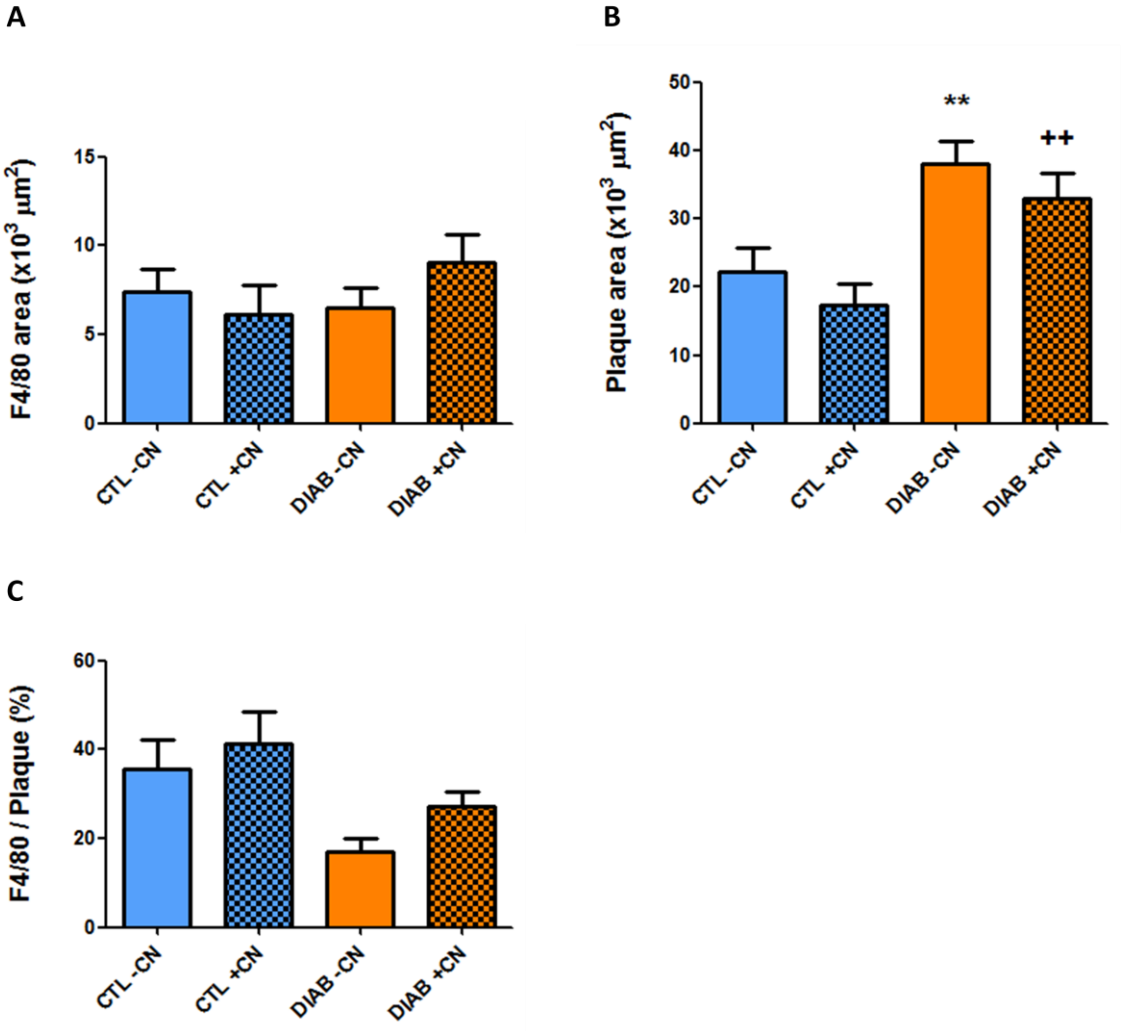

Figure 5.16: F4/80 staining for macrophages in the brachiocephalic artery for F4/80 area (Panel A), plaque area (Panel B) and percentage of F4/80 on total area (Panel C) in control (CTL) and diabetic (DIAB) apo $E^{-/-}$ mice with or without carnosine (+/- CN) supplementation.

The F4/80 and plaque areas that were determined in the brachiocephalic artery are calculated as (x10³) µm² in Panels A and B. The area stained by F4/80 is expressed as a percentage over the plaque area in Panel C. Statistical significance was achieved at ** $p < 0.01$ versus control (CTL - CN) and ++ $p < 0.01$versus control supplemented with carnosine (CTL + CN) apo $E^{-/-}$ mice using two-way ANOVA followed by Bonferroni's post-hoc test. Values are expressed as mean ± SEM.

5.4.8 Macrophages in plaque within aortic sinus sections

In order to examine the composition of the plaque generated in the diabetic and non-diabetic mice with and without carnosine-supplementation, the presence of macrophages within the plaques of the aortic sinus was examined by probing for the murine macrophage marker F4/80 at 200 μm from the first appearance of three valve leaflets as described in Sections 2.8.5. The macrophages were stained pink within the atherosclerotic plaques formed within the valve leaflets of the aortic sinus as shown in Figure 5.17.

There were no statistical differences observed in the areas that were stained for macrophages in the diabetic mice versus the non-diabetic mice regardless of carnosine supplementation as shown in Figure 5.18 (Panel A). There were a significant increase in plaque size in the valve leaflets from the diabetic (21.8 ± 1.6 ($x10^3$) μm^2) than the control mice (15.3 ± 1.2 ($x10^3$) μm^2, $p < 0.01$) as presented in Figure 5.18 (Panel B). There was a smaller area of plaque in the carnosine-supplemented control (11.5 ± 1 ($x10^3$) μm^2, $p < 0.05$) than the control mice. There was a significant decrease in plaque size observed in the carnosine-supplemented diabetic (15.1 ± 1.1 ($x10^3$) μm^2, $p < 0.001$) than the diabetic mice.

When the F4/80 was expressed as a percentage of total plaque area there was a higher percentage of F4/80 staining observed in the carnosine treated mice compared to its respective control as shown in Figure 5.18 (Panel C). The carnosine-supplemented control mice (44.4 ± 4.3 %, $p < 0.05$) possessed higher macrophage content than the control mice (31.8 ± 3.7%). There was an increased percentage of F4/80 staining observed in the carnosine-supplemented diabetic (41.3 ± 3.7 %, $p < 0.05$) than the diabetic mice (22.7 ± 3.1 %, $p < 0.01$).

Although diabetic mice had greater plaque areas, the absolute area stained for macrophages was not significantly different to the control mice. However there was a percentage increase of macrophages on total plaque areas observed in the aortic sinus for the carnosine-supplemented mice in both the diabetic and non-diabetic groups.

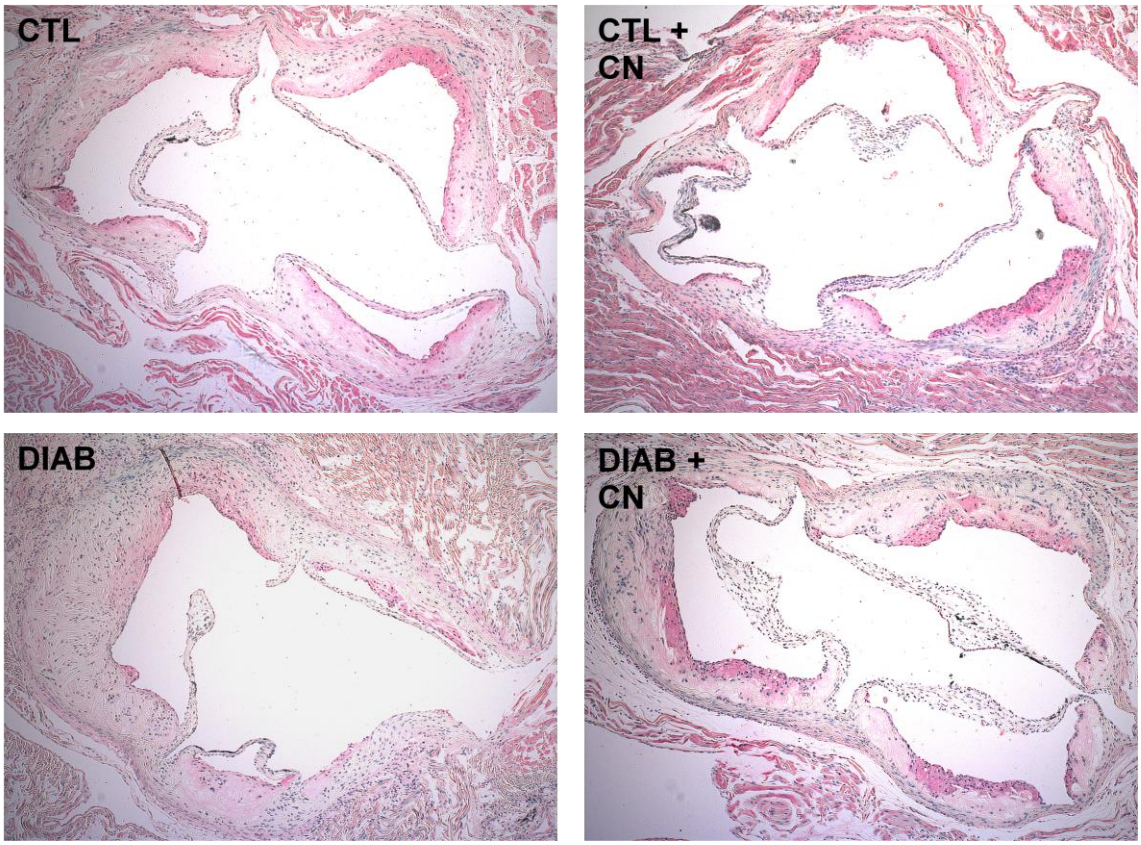

Figure 5.17: Representative sections showing F4/80 staining in the aortic sinus in control (CTL) and diabetic (DIAB) apo $E^{-/-}$ mice with or without carnosine (+/- CN) supplementation.

Representative sections taken from the aortic sinus were stained with F4/80 to detect for macrophages which appeared as pink colouration. The area of pink staining indicating the presence of F4/80 macrophages was expressed as a percentage over the total plaque formed. For illustration purposes the slides were captured by Carl Zeiss microscope using the 10x objective lens.

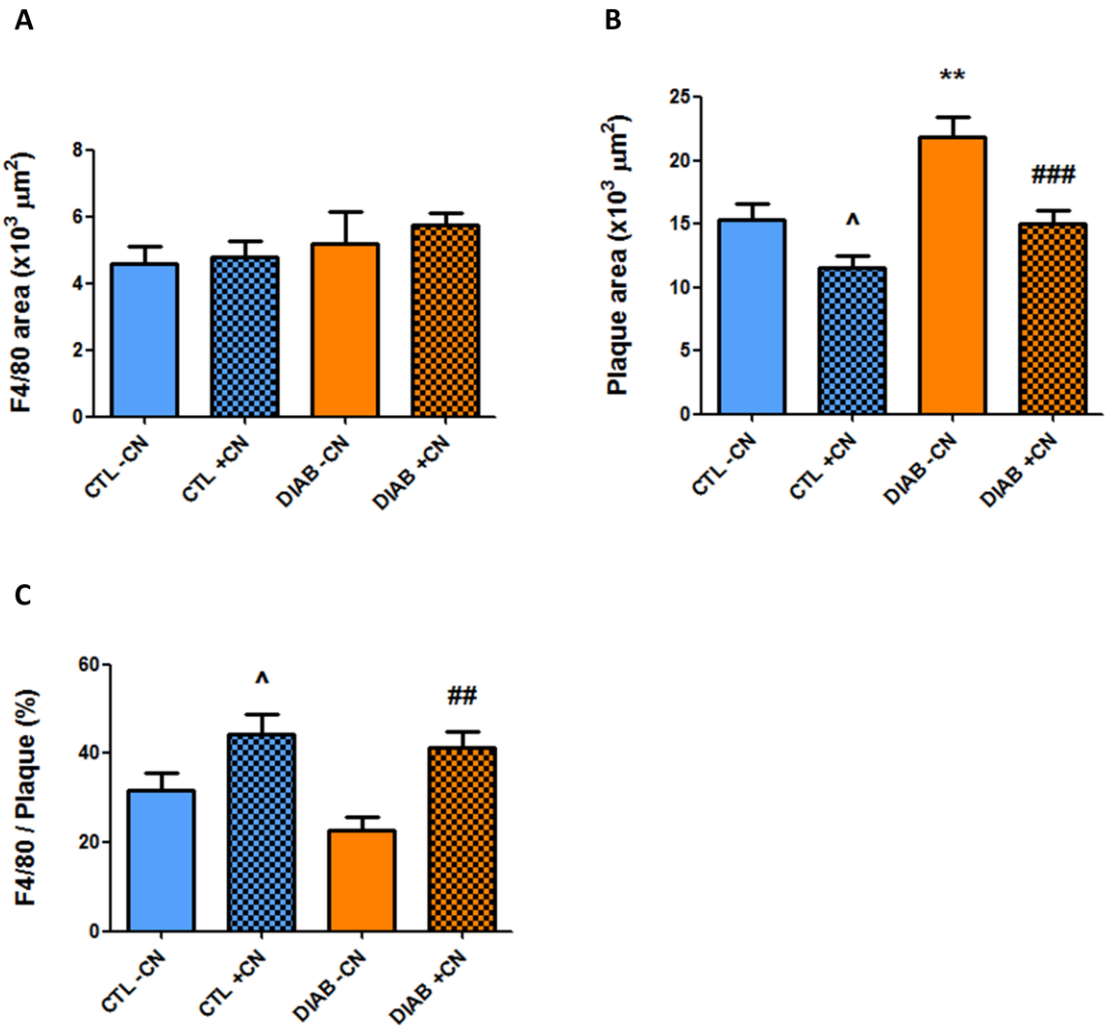

Figure 5.18: F4/80 staining for macrophages in the aortic sinus for F4/80 area (Panel A), plaque area (Panel B) and percentage of F4/80 on total area (Panel C) in control (CTL) and diabetic (DIAB) apo $E^{-/-}$ mice with or without carnosine (+/- CN) supplementation.

The F4/80 and plaque areas that were determined in the aortic sinus are calculated as (x10³) µm² in Panels A and B. The area stained by F4/80 is expressed as a percentage over the plaque area in Panel C. Statistical significance was achieved at ** $p < 0.01$ versus control (CTL - CN), ^ $p < 0.05$ versus control supplemented with carnosine (CTL + CN) and ## $p < 0.01$, ### $p < 0.001$ versus diabetic (DIAB) apo $E^{-/-}$ mice using two-way ANOVA followed by Bonferroni's post-hoc test. Values are expressed as mean ± SEM.

5.4.9 Lipid content of plaque within the brachiocephalic artery

The extracellular lipid content of the plaques was determined in the brachiocephalic artery as detailed in Sections 2.8.6 and 2.8.7. The lipid content was examined to determine the nature and progression of the atherosclerotic plaque generated in the non-diabetic and diabetic mice with and without carnosine-supplementation.

Plaques from diabetic mice (7.5 ± 1.2 ($x10^3$) μm^2, $p < 0.001$) contained significantly larger extracellular lipid pools than for the control mice (1.3 ± 0.3 ($x10^3$) μm^2). Most notably the extracellular lipid content from the carnosine-supplemented diabetic mice (2.8 ± 0.5 ($x10^3$) μm^2, $p < 0.001$) was significantly lower than for the un-supplemented diabetic mice as shown in Figure 5.19 (Panel A).

When the lipid area was expressed as a percentage of total plaque area that was measured from the F4/80 stained lesion samples as shown in Figure 5.17 (Panel B), the plaques from the diabetic mice ($20.5 \pm 2.7\%$) contained a significantly greater lipid percentage than the control ($6 \pm 1.2\%$, $p < 0.001$) mice. However, a significant decrease in lipid percentage was detected for the carnosine-supplemented diabetic mice ($8.2 \pm 1\%$, $p < 0.001$) when compared to the diabetic mice.

Overall the lesions analysed from the diabetic mice had a higher area occupied by lipid pools and a greater percentage of extracellular lipid compared to control mice brachiocephalic artery samples. There was significantly greater lipid deposition observed in the diabetic than both the non-diabetic control and carnosine supplemented mice and this elevation was significantly attenuated in the diabetic mice that were supplemented with carnosine.

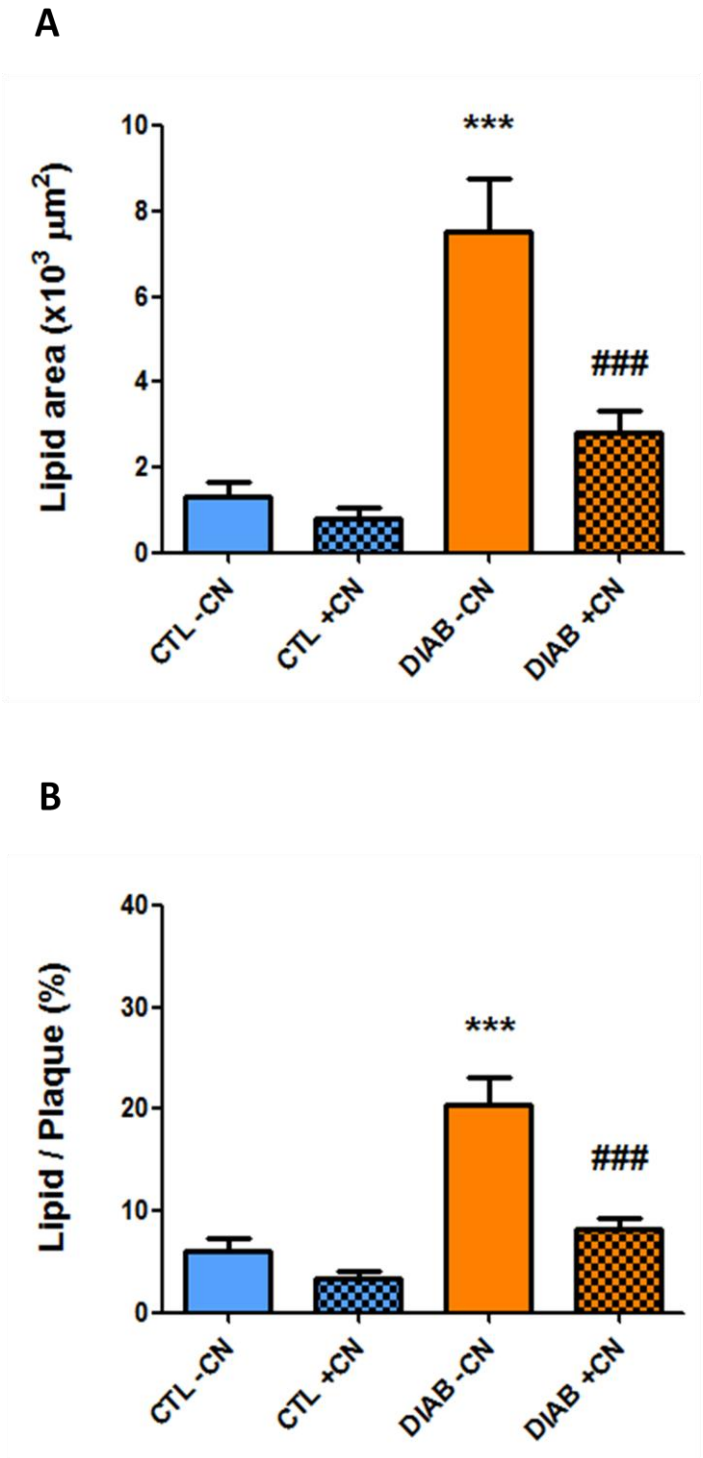

Figure 5.19: Comparison of extracellular lipid pools in the brachiocephalic artery determined as absolute lipid area (Panel A) and percentage area occupied by lipid compared to total plaque area (Panel B) in control (CTL) and diabetic (DIAB) apo $E^{-/-}$ mice with or without carnosine (+/- CN) supplementation.

The lipid area that was determined in the brachiocephalic artery is calculated as ($x10^3$) μm^2 in Panel A. The area occupied by lipid is expressed as a percentage over the total plaque area in Panel B. Statistical significance was achieved at *** $p < 0.001$ versus control (CTL – CN) and ### $p < 0.01$ versus diabetic (DIAB) apo $E^{-/-}$ mice using two-way ANOVA followed by Bonferroni's post-hoc test. Values are expressed as mean ± SEM.

5.4.10 Lipid content in plaque within aortic sinus

The extracellular lipid content of the plaques was determined in the aortic sinus sections in an analogous manner to that described in the previous section. The diabetic mice (7.6 ± 0.7 (x10³) μm²) contained a significantly higher extracellular lipid content than the control mice (2.2 ± 0.3 (x10³) μm², $p < 0.001$) as shown in Figure 5.20 (Panel A). Most notably the extracellular lipid content for the carnosine-supplemented diabetic mice (2.4 ± 0.3 (x10³) μm², $p < 0.001$) was significantly less than the diabetic mice.

The lesion area occupied by extracellular lipid was expressed as a percentage of total plaque area as displayed in Figure 5.20 (Panel C). The diabetic mice (30.2 ± 1.6%) contained greater percentage lipid content when compared to the control mice (14.5 ± 1.7%, $p < 0.001$). The carnosine-supplemented diabetic mice (13.2 ± 1.6%, $p < 0.001$) contained significantly less percentage lipid content than the non-supplemented diabetic mice. Overall the diabetic mice had a greater extent of extracellular lipid and a higher percentage area occupied by extracellular lipid in the aortic sinus sections than the control mice. This elevation was however significantly attenuated in the diabetic mice that were supplemented with carnosine.

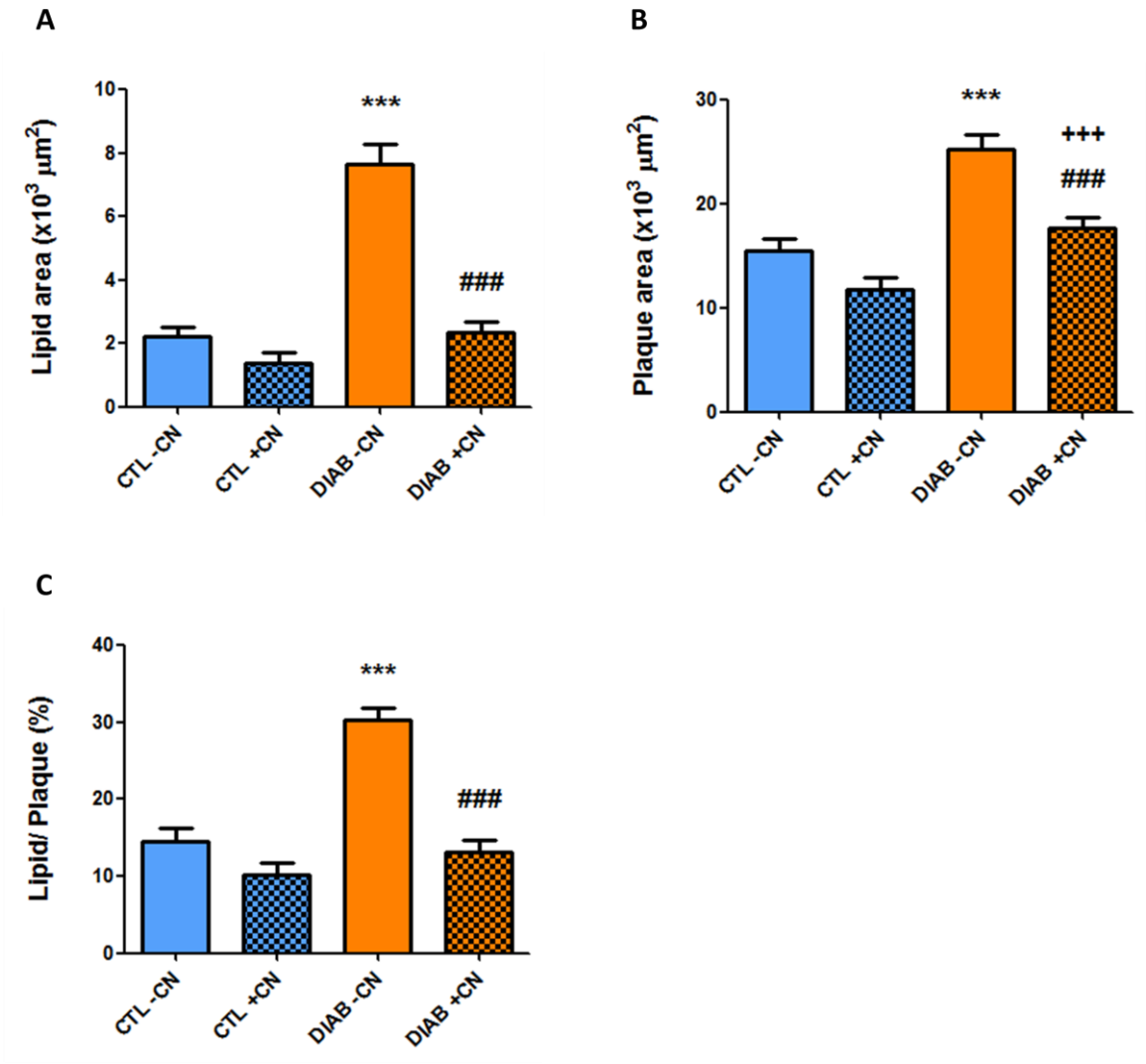

Figure 5.20: Comparison of extracellular lipid pools in the aortic sinus. Absolute lipid area (Panel A), plaque area (Panel B) and percentage of area occupied by extracellular lipid when compared to the total lesion area (Panel C) in control (CTL) and diabetic (DIAB) apo $E^{-/-}$ mice with or without carnosine (+/- CN) supplementation.

The lipid and plaque areas that were determined in the aortic sinus are calculated as ($x10^3$) µm² in Panels A and B. The area quantitated for lipid is expressed as a percentage over the plaque area in Panel C. Statistical significance was achieved at *** $p < 0.001$ versus control (CTL - CN), +++ $p < 0.001$ versus control supplemented with carnosine (CTL + CN) and ### $p < 0.01$ versus diabetic (DIAB) apo $E^{-/-}$ mice using a two-way ANOVA followed by Bonferroni's post-hoc test. Values are expressed as mean ± SEM.

5.4.11 Collagen content of plaques within the brachiocephalic artery

The collagen content of the plaques was examined to provide information on the potential stability of the plaques that were formed in the diabetic and non-diabetic mice that were treated with or without carnosine. The composition of collagen was examined at 300 μm from the first complete circumference of the brachiocephalic artery as described in Sections 2.91. The collagen was stained with picrosirius red as shown in Figure 5.21.

Although, there were no differences observed in collagen content between the diabetic and the control mice, there was an increase in collagen content observed in the carnosine-supplemented diabetic mice (23.7 ± 1.7 ($x10^3$) μm^2) when compared to the carnosine-supplemented control mice (15.7 ± 2.3 ($x10^3$) μm^2, $p < 0.05$). There was also significantly greater collagen content determined in the carnosine-supplemented diabetic than the diabetic mice (15.9 ± 1.2 ($x10^3$) μm^2, $p < 0.05$).

There was a higher absolute amount of plaque observed in the diabetic control (44 ± 3.4 ($x10^3$) μm^2) than the control mice (32.6 ± 3.1 ($x10^3$) μm^2, $p < 0.05$). A greater extent of plaque was also detected in the diabetic mice supplemented with carnosine (39.2 ± 2.7 ($x10^3$) μm^2) than the control supplemented carnosine mice (27.3 ± 3.5 ($x10^3$) μm^2, $p < 0.05$). When the collagen area was expressed as percentage of total plaque area there were no statistical differences between the diabetic and control groups. However, the carnosine-supplemented diabetic mice contained higher collagen content ($60.3 \pm 3.4\%$) than the corresponding non-supplemented diabetic mice ($37.5 \pm 2.8\%$, $p < 0.001$) as shown in Figure 5.22.

Overall the carnosine-supplemented diabetic mice contained greater absolute collagen content than the carnosine-supplemented control and diabetic mice. Furthermore the diabetic mice that were supplemented with carnosine contained a higher collagen percentage than the diabetic control in the brachiocephalic artery suggesting that these lesions might be of greater stability than those in the non-supplemented animals.

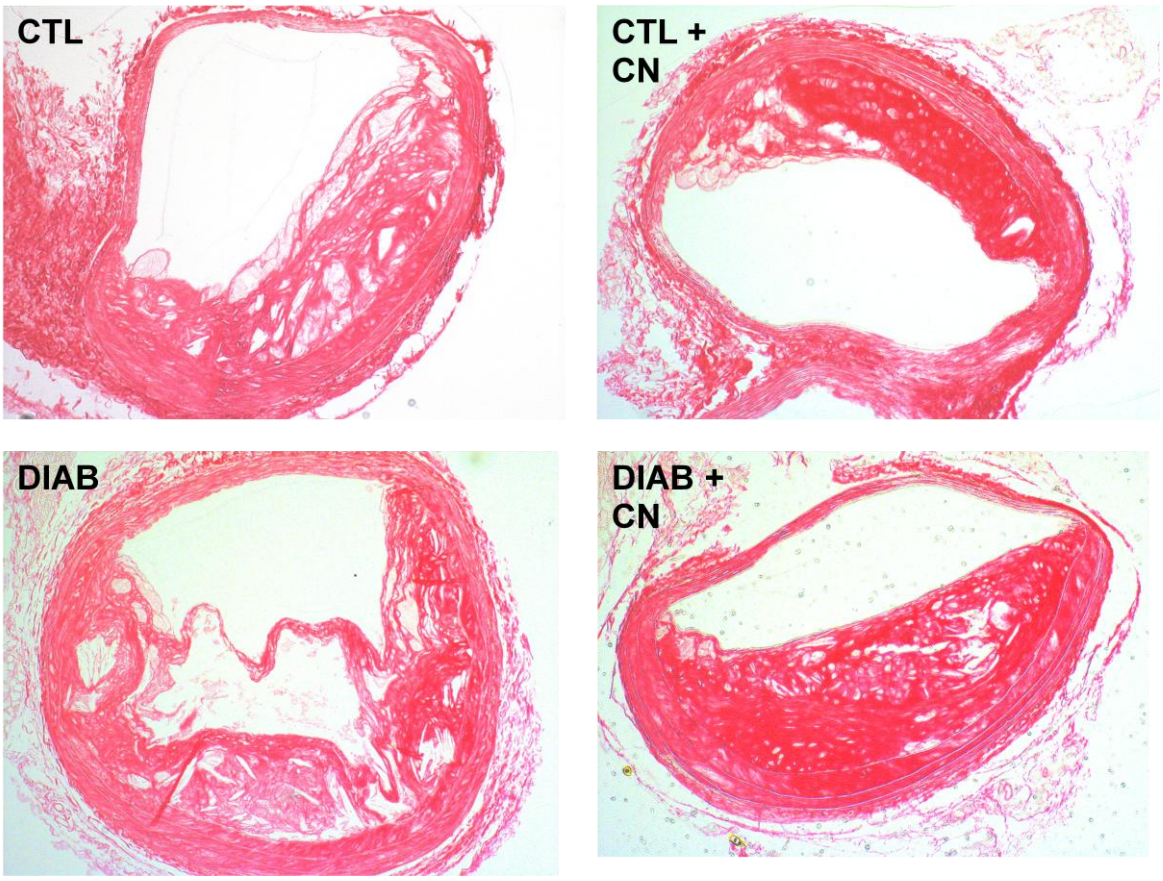

Figure 5.21: Representative images of atherosclerotic plaques stained with picrosirius red in the brachiocephalic artery cross sections of control (CTL), control + carnosine (CTL + CN), diabetes (DIAB) and diabetes + carnosine (DIAB + CN) mice.

Positive staining for collagen is depicted in red. The area of red was calculated over the plaque area and expressed as a percentage of collagen content within the plaques formed. For illustration purposes the slides were captured by a Carl Zeiss microscope using the 20x objective lens.

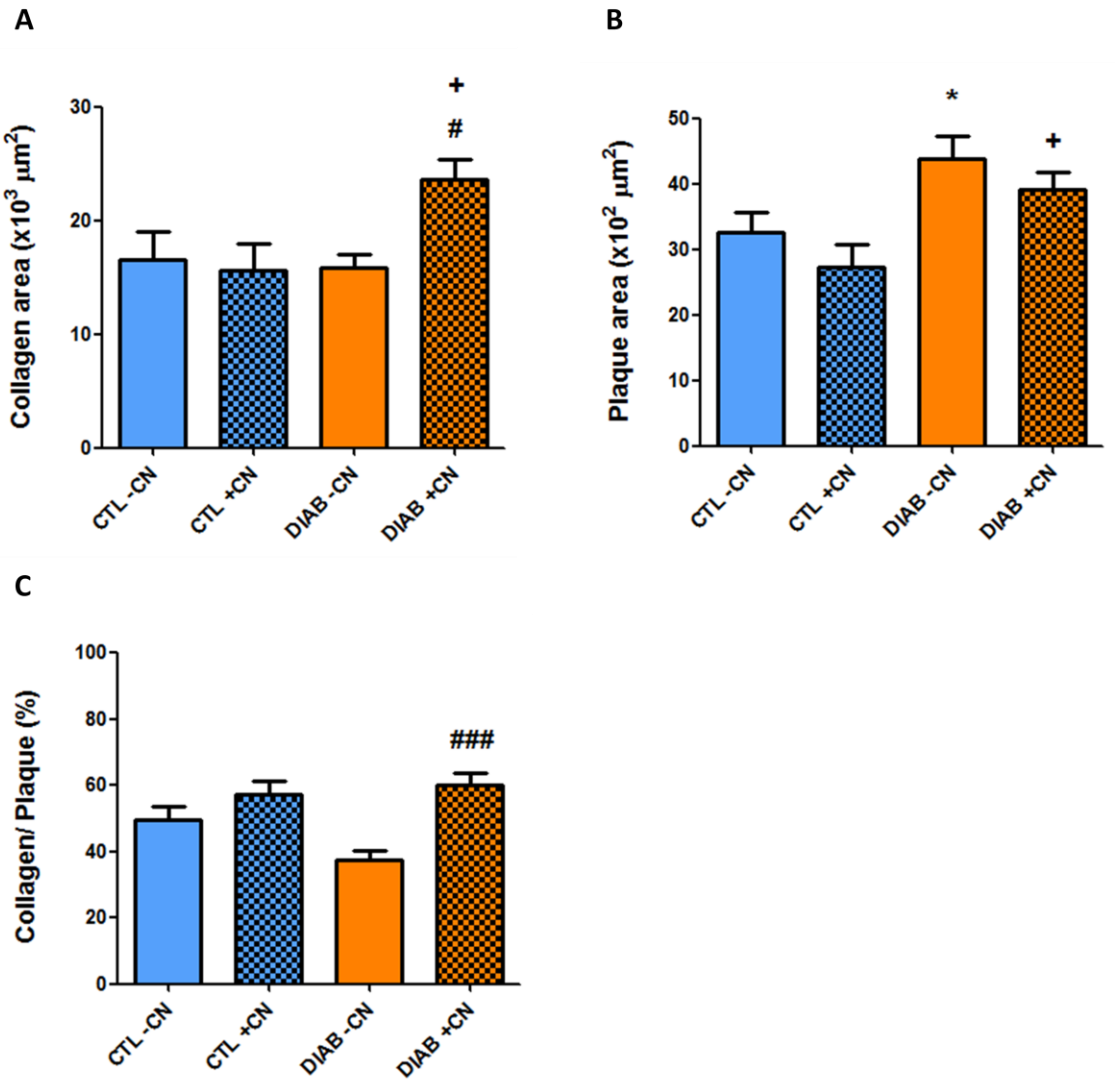

Figure 5.22: Comparison of collagen content within plaques in the brachiocephalic artery. Absolute collagen area (Panel A), plaque area (Panel B) and percentage of collagen expressed relative to the total plaque area (Panel C) in control (CTL) and diabetic (DIAB) apo $E^{-/-}$ mice with or without carnosine (+/- CN) supplementation.
The collagen and plaque areas that were determined in the brachiocephalic artery are calculated as (x10³) µm² in Panels A and B. The area quantitated for collagen is expressed as a percentage over the plaque area in Panel C. Statistical significance was achieved at *$p < 0.05$ versus control without carnosine (CTL - CN), + $p < 0.05$versus control supplemented with carnosine (CTL + CN) and # $p < 0.05$, ### $p < 0.001$ versus diabetic (DIAB) apo $E^{-/-}$ mice using two-way ANOVA followed by Bonferroni's post-hoc test. Values are expressed as mean ± SEM.

5.4.12 Collagen in plaque within the aortic sinus

The collagen content was also examined via picrosirius red stain at 300 μm from the first appearance of the three value leaflets in the aortic sinus as described in Section 2.9.1 and shown in Figure 5.23. Although there were no statistical differences in collagen content between the diabetic and the control mice, a significantly greater absolute area of collagen staining was seen in the carnosine-supplemented diabetic (11 ± 0.9 ($x10^3$) μm^2) than the carnosine-supplemented control mice (7.9 ± 0.8 ($x10^3$) μm^2, $p < 0.05$).

There was higher plaque observed in the diabetic (22.8 ± 1.5 ($x10^3$) μm^2) than the control (13.8 ± 1 ($x10^3$) μm^2, $p < 0.001$). This was also detected with the carnosine-supplemented diabetic mice (17.2 ± 1.1 ($x10^3$) μm^2) when compared to the carnosine-supplemented control mice (11.4 ± 1 ($x10^3$) μm^2, $p < 0.001$). Less plaque was observed in the carnosine-supplemented diabetic mice ($p < 0.01$) than its respective control.

When the collagen area was expressed as percentage of total plaque, a significantly lower percentage of collagen was observed in the diabetic mice (42.7 ± 3.6%) than the control (67.7 ± 2.6%, $p < 0.001$) mice. This was also the case in the diabetic groups where the diabetic mice had significantly less percentage collagen content than the carnosine-supplemented diabetic mice (63.9 ± 3%, $p < 0.001$) as shown in Figure 5.24.

Overall lesions from the carnosine-supplemented diabetic mice appear to have significantly higher collagen content than those of the diabetic mice. When the collagen content was examined over the plaque area, the diabetic mice had the lowest percentage of collagen in the aortic sinus. There was a lower percentage of collagen observed in the diabetic group than the non-diabetic control group, and this decrease in collagen content seen in the diabetic mice was significantly attenuated by carnosine.

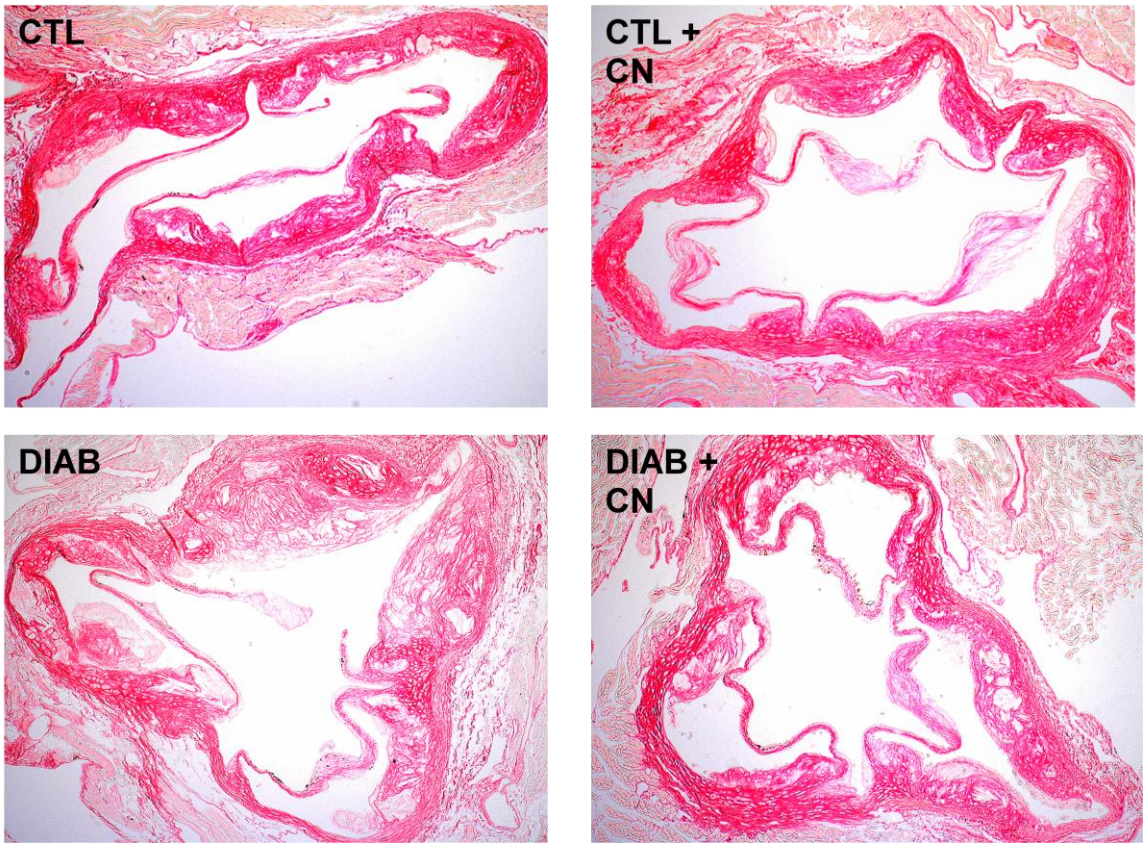

Figure 5.23: Representative images of atherosclerotic plaques stained with picrosirius red in the aortic sinus cross sections of control (CTL), control + carnosine (CTL + CN), diabetes (DIAB) and diabetes + carnosine (DIAB + CN) mice.

Positive staining for collagen is depicted in red. The area of red was calculated over the total plaque areas and expressed as a percentage of collagen content within the plaques formed. For illustration purposes the slides were captured using a Carl Zeiss microscope with a 10x objective lens.

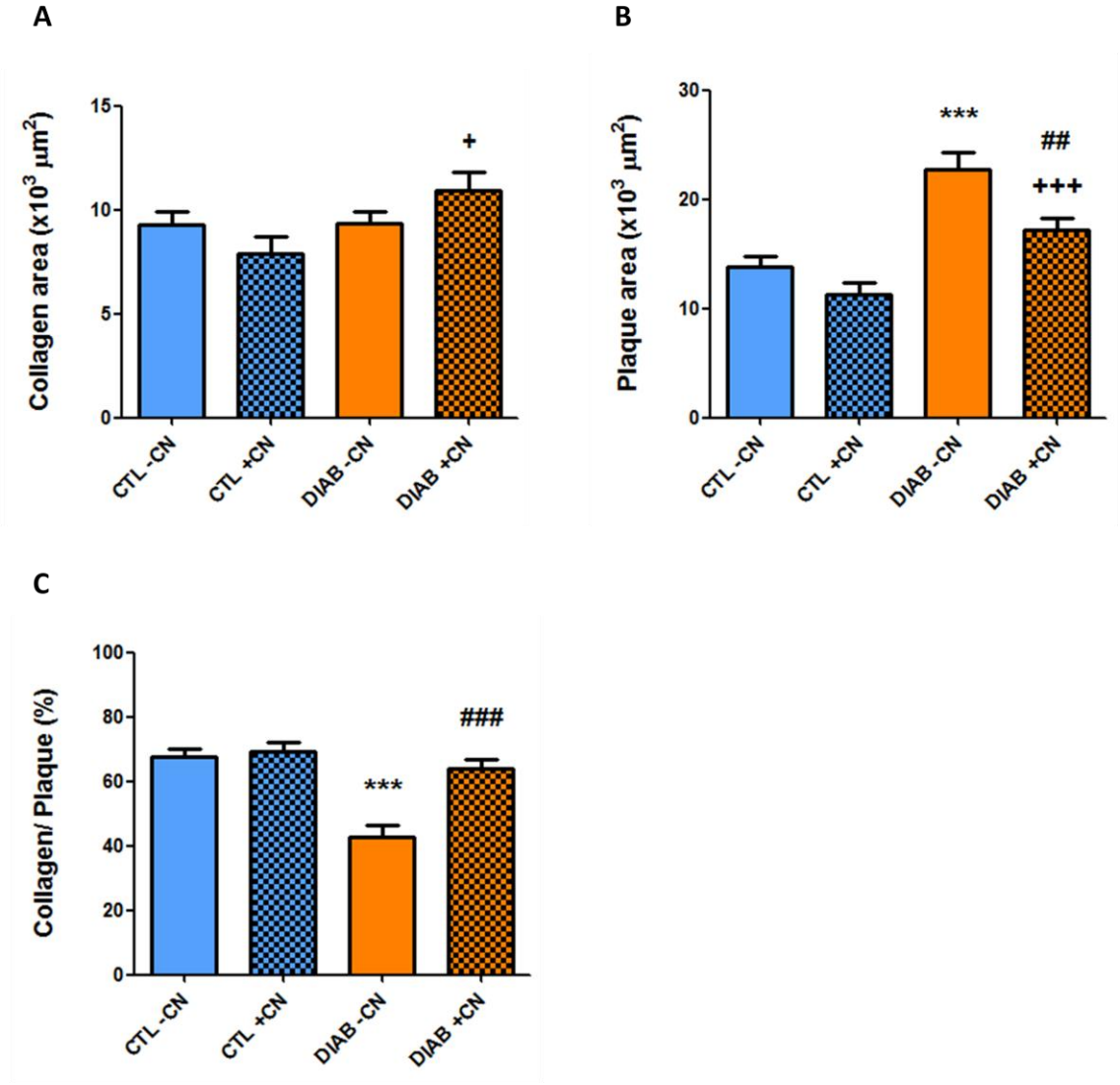

Figure 5.24: Comparison of collagen within plaques in the aortic sinus. Absolute collagen area (Panel A), plaque area (Panel B) and percentage of collagen expressed relative to the total plaque area (Panel C) in control (CTL) and diabetic (DIAB) apo $E^{-/-}$ mice with or without carnosine (+/- CN) supplementation.

The collagen and plaque areas that were determined in the aortic sinus are calculated as ($x10^3$) µm² in Panels A and B. The area quantitated for collagen is expressed as a percentage over the plaque area in Panel C. Statistical significance was achieved at *** $p < 0.001$, + $p < 0.05$, +++ $p < 0.001$ versus control supplemented with carnosine (CTL + CN) and ## $p < 0.01$, ### $p < 0.001$ versus diabetic (DIAB) apo $E^{-/-}$ mice using two-way ANOVA followed by Bonferroni's post-hoc test. Values are expressed as mean ± SEM.

5.5 Discussion

The antioxidant / anti-glycative activity of carnosine has been investigated extensively given the therapeutic potential that such actions could have in diseases where oxidative and / or glycative damage contributes to pathogenesis and disease progression. As an endogenous product, carnosine can be administered safely. Rodents provide an ideal model to assess the effects of carnosine, as chronic supplementation results in a sustained elevation in blood carnosine levels. The hyperglycaemic component of atherosclerosis was investigated using a mouse model of diabetes that was induced by streptozotocin in apo $E^{-/-}$ mice. This treatment increased blood glucose, haemoglobin Alc, total cholesterol and triglycerides in the mouse plasma, and the diabetic mice had a significantly greater plaque burden than the non-diabetic mice resulting in a smaller lumen size in the artery.

Direct administration of carnosine to humans results in only transient increases in plasma levels [288]. However, previous studies (e.g. [288,289]) and the current study have demonstrated that there is a significant increase in plasma carnosine levels in rodents if the animals are continuously supplemented with carnosine via their drinking water. The levels achieved in the current study are higher than those reported by Lee *et al*. [288] (who used Balb/cA mice), probably due to the higher dose employed in the current study. In contrast to these findings, Aldini et al. [289] using Zucker rats, demonstrated significant increases in plasma and kidney carnosine levels with chronic supplementation with D- but not L- carnosine. Thus the capacity to establish and maintain significantly high circulating levels of L-carnosine varies from species to species. In our study, a wider range of plasma carnosine levels was detected amongst the diabetic animals when compared to those for the matched control group, with this likely to be due to the characteristic polydipsia of diabetes with a three-fold higher level of water consumption observed in the diabetic animals.

In this study, prolonged carnosine administration did not significantly modulate multiple disease parameters in the mice with diabetes including blood glucose levels. Lee *et al.* [288] demonstrated a significant reduction in blood glucose levels after four weeks of carnosine supplementation in mice with diabetes. Transient hyperglycaemia induced by 2-deoxy-D-glucose in Wistar rats has also been shown to be inhibited by intravenous and intraperitoneal delivery of carnosine [292]. The effect of carnosine in the latter study was restricted to submicro- and in some circumstances subnanomolar

concentrations. Whilst it has been repeatedly demonstrated that plasma levels of reactive aldehydes (e.g. methylglyoxal and glyoxal) are elevated in people with diabetes, the determination of plasma aldehyde levels is problematic. Values for methylgloxal can range from 0.2 - 120 and 0.5 - 400 μM in normoglycaemic and people with diabetes, respectively [293,294,295,296]. As these aldehydes react rapidly with proteins [297] these low concentrations are not unexpected. Thus the levels of plasma carnosine achieved by supplementation in this study, and another [288], may be within the range that would lead to effective aldehyde scavenging *in vivo*. In contrast to these studies, we did not find any hypoglycaemic effect of carnosine supplementation in the animals with diabetes, and this is supported by the absence of a carnosine-associated decrease in glycated haemoglobin. We conclude that the chronic high dose supplementation of carnosine used here does not have the more transient and low dose effects of carnosine upon blood glucose previously demonstrated.

Whilst carnosine supplementation had no effect upon diabetes-induced hypercholesterolaemia in the diabetic mice, supplementation significantly reduced plasma triglyceride levels. This effect was also seen with carnosine-supplemented control mice. This differential effect upon the two classes of lipids was also found by Lee et al. [288] where both doses of carnosine (0.5 and 1.0 g/L) blunted the increase in heart and liver triglyceride levels in diabetic mice, while for cholesterol levels a significant effect was only seen with the higher dose of carnosine. In contrast, supplementation of hyperlipidaemic (but not hyperglycaemic) Zucker rats with either L- or D-carnosine resulted in matched and significant decreases in both plasma cholesterol and triglyceride levels [289]. Similarly both carnosine and histidine (at 1g/L of drinking water) blocked increases in plasma triglycerides and cholesterol in fat-fed, non-diabetic, C57BL/6 mice [283]. Thus while carnosine has been consistently demonstrated to have a cross-species hypotriglyceridaemic action this is not the case for modulation of blood cholesterol levels.

Further port mortem studies were carried out to examine the anti-atherogenic potential of carnosine as plasma triglyceride levels were significantly decreased in the diabetic mice that were supplemented with carnosine. Analysis of atherosclerotic lesions and disease progression using this model of diabetes-associated atherosclerosis is commonly determined by *en face* analysis of total aortic plaque area. However we chose to restrict our analysis to a more detailed examination of the brachiocephalic artery and aortic sinus given the propensity of these sites for the development of

advanced, rupture-prone, lesions in this strain of mouse [277]. Induction of diabetes resulted in a significant increase in plaque area at both sites. The plaques in the diabetic mice was shown to consist of large pools of deposited lipids extracellularly in the subendothelial space with lower levels of macrophages and decreased level of collagen with this potentially weakening the structure of the lesion and heightening the risk of plaque rupture [50,298].

Despite the triglyceride-lowering effects of carnosine, supplementation did not lead to a significant reduction in plaque area compared to the un-supplemented mice matched for glycaemic status. This data is in agreement with Nestel *et al.* [291] who showed that dietary supplementation of diabetic apo $E^{-/-}$ mice with conjugated linoleic acid did not lead to a decrease in aortic plaque area although there was a substantial lowering of plasma triglycerides. Using the same model Levi *et al.* [299] have demonstrated a decrease in aortic sinus plaque area in mice treated with PPARγ-agonist rosiglitazone, while drug treatment resulted in an elevation of blood triglycerides and cholesterol levels. Thus the modulation of diabetes-induced hypertriglyceridaemia in this particular animal model does not appear to have a consistent impact on gross plaque characteristics. Our results are in contrast to the recent demonstration that supplementation of fat-fed apo $E^{-/-}$ with D-carnosine octylester resulted in a reduction in plaque area [282]. In common with the study of Menini *et al*., carnosine supplementation did lead to changes in plaque composition, specifically a reduction in the area occupied by lipid matched by an increase in that occupied by collagen. Cholesterol cleft formation and lipid deposition in atherosclerotic plaque reflects the severity and progression of the arterial disease and such lipid-enriched lesions are prone to plaque rupture [298]. In particular lesion rupture has been associated with a thinning of the fibrous cap and decreased collagen formation [300,301,302]. This shift in plaque composition from a lipid rich environment to a collagen rich area is thought to reduce the risk of plaque rupture [303]. Given the increasing costs, both personal and economic, of the complications of diabetes mellitus there is a strong drive to develop treatments to alleviate, delay and hopefully prevent these complications.

Carnosine and its analogues have recently been shown to have both anti-hyperlipidaemic, anti-atherosclerotic, hepato- and renal-protective actions in models of obesity-associated complications [282,283,288,289]. Our current study is the first to demonstrate that this well-tolerated dipeptide may also have a significant impact in the treatment of the complications of diabetes. While it had been conceived that carnosine's

anti-atherogenic action would be mediated by its well-characterised anti-glycative / glycoxidative activities, this study found carnosine-linked improvements in lipid parameters. Thus while hyperglycaemia is a key agent of atherogenesis and atherosclerotic progression in diabetes, it must be remembered that, at least in the case of Type 2 diabetes, hyperlipidaemia is also likely to have critical pathological role.

5.6 Conclusion

Prolonged carnosine supplementation has been shown to have a significant impact on the progression of the atherosclerosis in a well-established model of diabetes-associated atherosclerosis. Diabetic mice had a greater extent of plaque formation in the brachiocephalic artery and aortic sinus compared with their non-diabetic littermates. There were no significant differences in the plaque area when carnosine-supplemented mice were compared with mice on plain water and matched for glycaemic status.

However potential anti-atherosclerotic effects of carnosine were found when plaque composition was investigated. When compared to the other treatments there were significantly increased numbers of smooth muscle cells (as evidenced by the extent of α-actin staining) in the plaques of the carnosine treated diabetic mice. There was a significant decrease in macrophage cell numbers in the diabetic mice in the brachiocephalic and the aortic sinus. This can be potentially rationalised by the significantly higher extracellular lipid content in the same plaques with these lipid levels being the result of macrophage foam cell death and lysis. Conversely, carnosine supplementation resulted in greater levels of collagen in the plaque although this was not consistently linked to an increase in smooth muscle cell staining. It is clear that cell populations within the lesions of the carnosine treated animals and particularly these with diabetes are altered and this may result in greater lesion stability as judged by greater collagen and less extracellular lipid.

The hypolipidaemic effect of carnosine did not affect plaque area in the diabetic mice. However, carnosine does seem to have played an important role in reducing extracellular lipid deposition possibly as a result of a decrease in macrophage apoptosis and / or necrosis which are known to result in extracellular lipid accumulation [50], slowing down atherosclerotic plaque progression by significantly modulating the composition of the plaques, engendering plaque stability. On the basis of this data it

would appear that supplementation with carnosine may be of benefit in the treatment of atherosclerosis including that associated with diabetes.

These studies are extended in the following chapter where another anti-lipidaemic agent was also examined using apo $E^{-/-}$ mice but where atherosclerosis was driven by high fat-feeding. The focus of the following chapter concentrates on the hyperlipidaemic manifestations that were initially observed in the diabetic mice, in apo $E^{-/-}$ and wild type C57BL/6 mice that were fed a high fed diet to induce obesity. The anti-oxidant and anti hyperlipidaemic properties of TEMPOL was investigated using this high fat obesity animal model to further examine whether TEMPOL reverses the atherosclerosis.

CHAPTER 6:

INVESTIGATION OF THE IMPACT OF TEMPOL UPON ATHEROSCLEROSIS, LIPID PROFILE AND CYTOKINE EXPRESSION IN A MURINE OBESITY MODEL

6.1 Introduction

Dyslipidaemia plays a major role in the majority of cardiovascular disorders including atherosclerosis [304,305,306]. Total blood cholesterol and LDL-cholesterol (LDL-C) are classified as independent risk and graded factors for cardiovascular disease (CVD) and meet the criteria for causality related to CVD risk [304]. The causality between saturated fat consumption, blood cholesterol levels, and CVD mortality has been identified from various genetic, animal study, experimental pathology and epidemiological investigations [304,305,307,308,309,310,311,312,313,314,315,316]. There are several mechanisms postulated for the role of triglycerides in CVD, such as smooth muscle damage and impaired vascular repair, or that excess triglycerides in lipoproteins may result in abnormal transport, but the association between hypertriglyceridaemia and CVD remains controversial [317,318,319,320]. Elevated triglyceride levels may be a warning sign and indicate a need to investigate other metabolic manifestations such as central obesity, hypertension, low HDL-C and glucose intolerance [305,321,322].

The prevalence and impact of dyslipidaemias and metabolic disorders has led to extensive investigations of therapies designed to prevent, inhibit or reverse cardiovascular related diseases [304]. Many studies have shown therapeutic reduction of these lipid fractions via pharmaceutical or surgical interventions are strongly associated with improved measures [323,324,325,326,327,328]. However, prevention of the development of obesity, through promotion of healthy eating practices and increased physical activity, remains critical to reducing the occurrence of dyslipidaemia and excess body weight gain in the community [5,309,329]. Treatments that arrest gain in body fat and / or promote body fat loss (including pharmaceuticals and surgical procedures) provide critical support where management of body mass remains refractory to behavioural modifications alone [327]. Pharmaceuticals also provide tools to investigate the mechanisms that underlie obesity, and one example of such a compound is TEMPOL which has known impacts upon body weight gain, sensitivity to radiation and tumourigenesis [330,331,332,333,334,335].

TEMPOL (4-hydroxy-2,2,6,6-tetramethylpiperidine-N-oxyl; $C_9H_{18}NO_2$) is a cell permeant nitroxide, whose structure is shown in Figure 6.1. It has a well characterised superoxide dismutase-mimetic activity (which is thought to be basis of its previously demonstrated hypotensive effects) and is capable of reacting, and thus detoxifying, a

number of free radicals and reactive oxygen species [336,337,338,339,340,341,342,343,344,345,346,347]. Previous work from James Mitchell (National Cancer Institute) has shown for C3H male and female mice, rendered obese by feeding with a Western-style high fat diet, that administration of TEMPOL (10 mg/g of food) had a profound inhibitory effect upon weight gain. This compound also prevented obesity induced changes in leptin levels and decreased age-related spontaneous tumour incidence [330]. TEMPOL has been found to reduce irradiation induced salivary gland hypofunction (xerostomia) and alopecia in numerous brain, head and neck cancer murine models [331,332]. Phase I and II clinical trials for safety, pharmacokinetics and preliminary efficacy for the prevention of alopecia induced by whole brain radiotherapy have been reported, and this compound is under consideration for phase III trials [333,334,335].

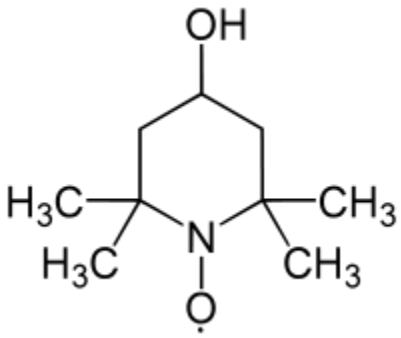

Figure 6.1: Chemical structure of TEMPOL.
TEMPOL is also referred to as 4-Hydroxy-TEMPO, and 4-hydroxy-2,2,6,6-tetramethylpiperidin-1-oxyl.

The potential protective effects of TEMPOL have also been examined in the cardiovascular and diabetes area and research has shown that it can prevent the production of hepatic reactive oxygen species induced by diabetes [345]. Antihypertensive effects of TEMPOL have been revealed in cell signalling and animal models [336]. Several studies have shown TEMPOL lowers blood pressure of rodents that were made hypertensive [337,346,347]. Prolonged lowering of blood pressure by TEMPOL has been related to an enhancing effect of this compound on the production or the action of endogenous nitric oxide ($NO^{\cdot}$) [336,338]. TEMPOL has also been reported to work as a vasodilator, and has been shown to exhibit protective effects upon

vessels and the endothelium in hypertensive rats [337,338,339,346,347] and also in small arteries from visceral fat of obese patients [348].

Endothelial dysfunction is an early event in atherogenesis and further alterations occur to the endothelial layers of the arterial wall with the progression and severity of atherosclerosis [349,350,351,352,353]. In the previous chapter a model of diabetes-associated atherosclerosis was investigated using apo $E^{-/-}$ mice in which diabetes was induced using the pancreatic toxin streptozotocin. Induction of diabetes was associated with larger plaque volume as well as dramatic changes in artery wall composition with noticeable lipid accumulation and significantly lower collagen content. The impact of the anti-glycative / anti-oxidative agent carnosine upon plaque morphology was characterised as a shift to a more stable phenotype with an increased collagen content and decreased extracellular lipid. This was associated with a significant decrease in blood triglyceride levels. However, hyperglycaemic manifestations (elevated blood glucose and glycated Hb levels) in the diabetic mice were not arrested by carnosine.

The current chapter focuses on the potential modulation of hyperlipidaemia and the vascular lipid accumulation of atherosclerosis, a critical component to the progression of this disease, in the absence of diabetes. Although there are many reported studies on the hypotensive and cardio-protective vascular functions of TEMPOL upon the endothelium, arteries and blood vessels, the potential anti-atherogenic action of TEMPOL remains poorly characterized. Therefore the study reported in this chapter assesses the potential anti-atherogenic actions of TEMPOL in a murine model of high fat fed atherosclerosis and obesity.

6.2 Aims

The overall aims of this study were firstly to determine whether TEMPOL prevents or attenuates atherosclerotic plaque development in obesity-associated atherosclerosis, and secondly to examine if TEMPOL reverses or suppresses obesity-associated hyperlipidaemia, and / or systemic inflammation.

6.3 Experimental methods

6.3.1 Animal model design

Heart and plasma samples were obtained from Prof. Jim Mitchell from the National Cancer Institute (United States) from apo $E^{-/-}$ (n = 38) mice and the parent strain C57BL/6 (n= 28) as outlined in Section 2.10. For each strain (i.e. apo $E^{-/-}$ and C57BL/6) there were four groups. The first two groups consisted of mice fed a regular chow diet with and without TEMPOL (10 mg/g) placed into the food whilst the third and fourth groups comprised of a high fat diet with and without TEMPOL included in the food as shown in Figure 6.2. Five animals were allocated in each group for the chow fed mice with or without TEMPOL supplementation for both animal types. For the apo $E^{-/-}$ mice, 13 mice were dedicated to the HFD and 15 were allocated to the HFD with TEMPOL supplemented group. For the C57BL/6 parent strain, 8 mice were placed into the HFD and 10 were allocated to the HFD with TEMPOL supplemented group. The composition of the chow and high fat diets are detailed in Table 2.1 under Section 2.10.

6.3.2 Histology procedures

The histological analysis of the aortic sinus was undertaken as detailed in Sections 2.7.5 to 2.7.7 and 2.10.1 to 2.10.3 from sample preparation, through to tissue sectioning and haematoxylin staining. Three slides (which contained 3 sections) were chosen for plaque analysis as described in Sections 2.10.2 and 2.10.3. The first triplicate section was taken at the first appearance of the three valve leaflets of the sinus. The third slide was taken from the first disappearance of all three valve leaflets. The second slide was taken between the first and third sections. The three chosen slides were stained with Haematoxylin and Eosin (H & E) as detailed in Section 2.7.7 and later photographed using the appropriate magnification as shown in Figure 2.6. The total surface area and plaque were determined using Adobe Photoshop as shown in Figure 5.5.

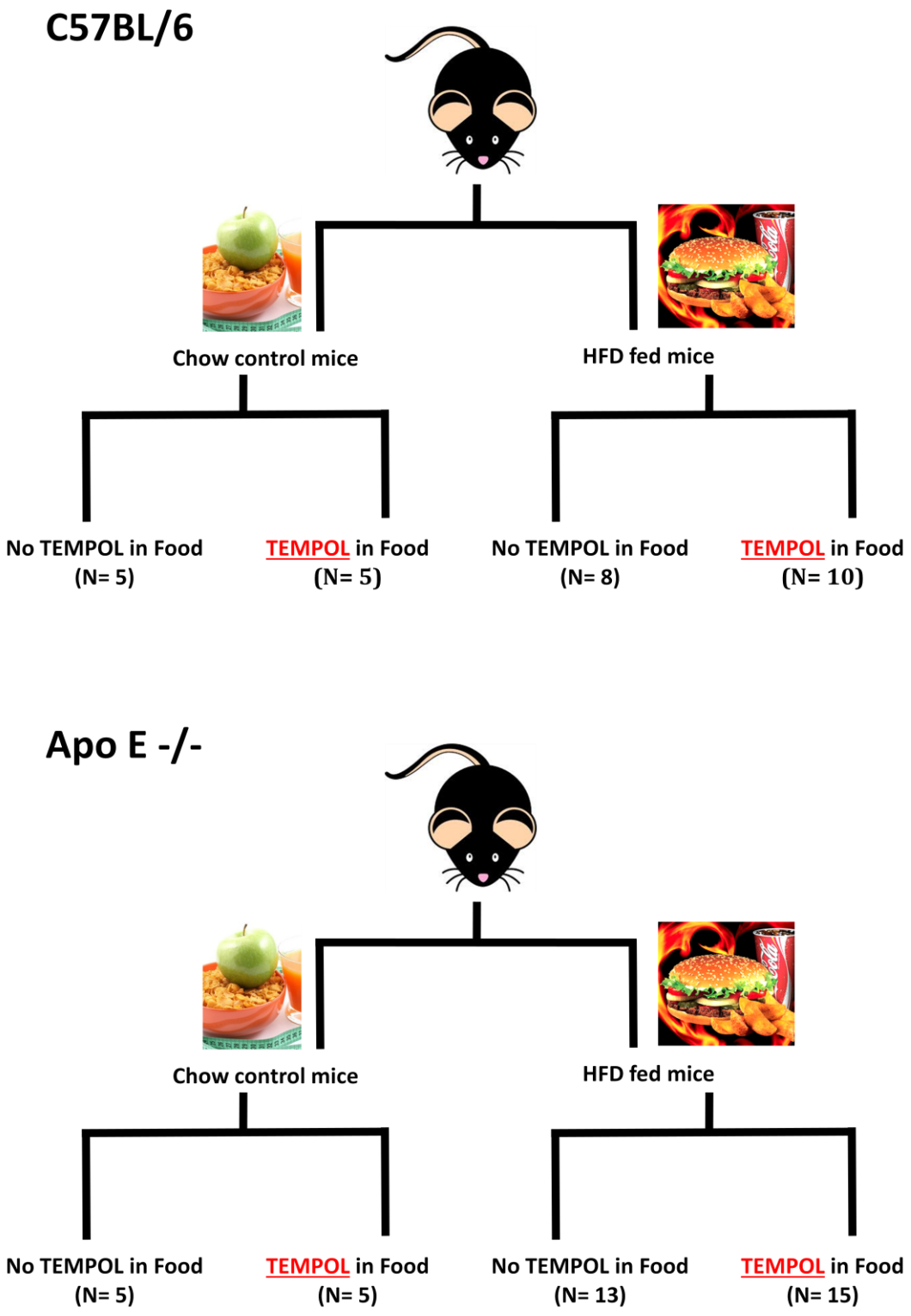

Figure 6.2: Animal model for TEMPOL study.
C57BL/6 wild type and the apo $E^{-/-}$ mice were divided into four groups comprising of chow control mice with and without TEMPOL administered in the food, and high fat diet fed mice with and without TEMPOL inserted in the food.

6.3.2 Plasma analysis

The mouse plasma samples were analysed as described in Sections 2.11 to 2.11.2 for triglycerides, total cholesterol, HDL-cholesterol and LDL-cholesterol. Cytokine, inflammatory agents and adipokine measurements were also examined as detailed in Sections 2.11.3. Statistical analysis was carried out by using two-way ANOVA analyses followed by a Bonferroni's posthoc test.

6.4 Results

6.4.1 Effects of TEMPOL upon body mass in apo $E^{-/-}$ and parent strain C57BL/6 mice

The animal husbandry was carried out at the National Cancer Institute (Bethesda, MD, USA) as outlined in Section 2.10. The body masses of the mice were closely monitored for 20 weeks. The body masses of the HFD fed mice increased considerably in comparison to the chow fed mice regardless of TEMPOL supplementation in both animal types. However treatment with TEMPOL resulted in significantly lower gain in mass for the HFD mice. Notably the body mass of the TEMPOL-treated HFD mice was similar to that of the non-HFD fed mice (Figure 6.3).

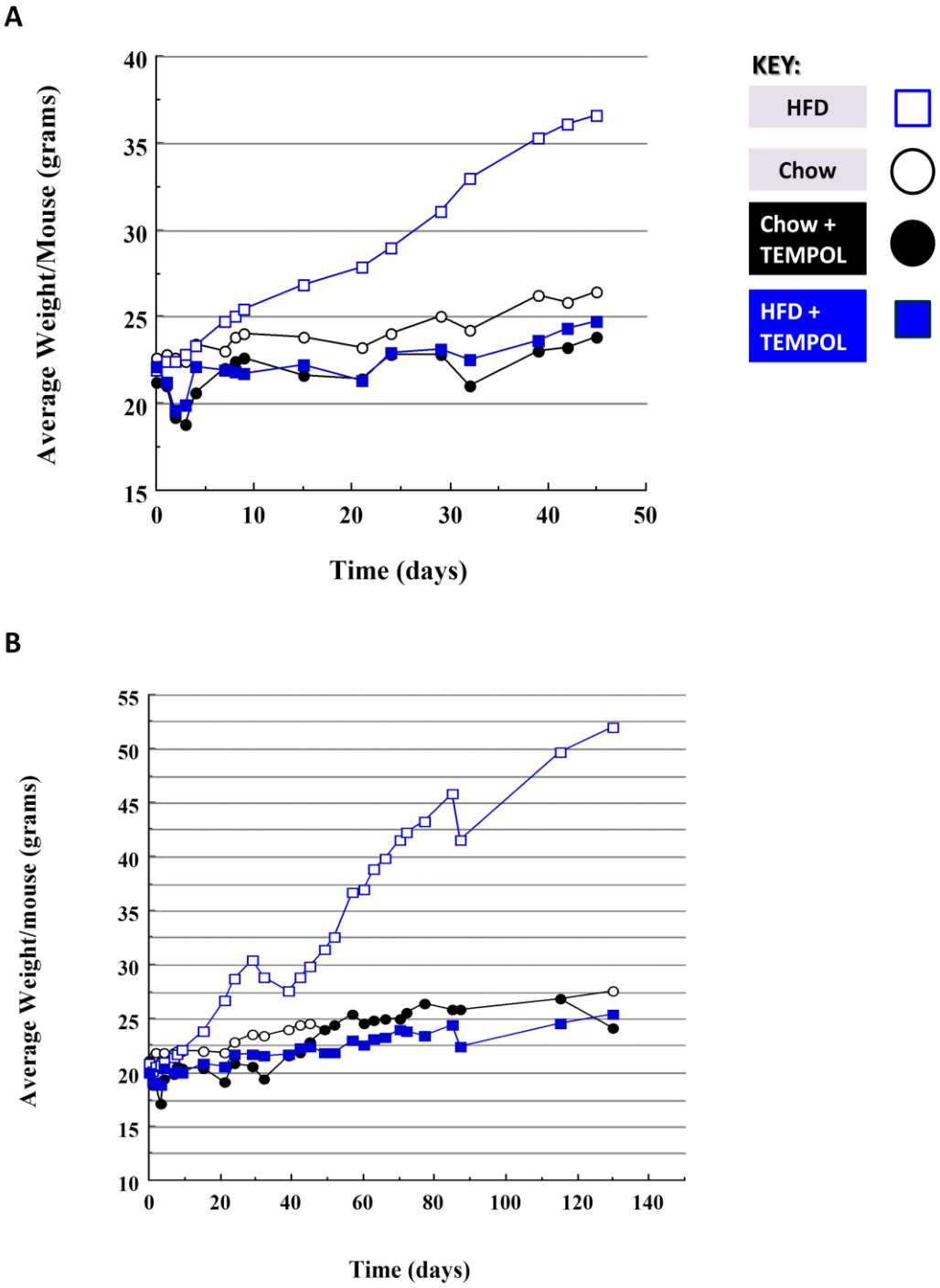

Figure 6.3: Average body mass of apo $E^{-/-}$ (Panel A) and C57BL/6 (Panel B) mice during the intervention phase during which the mice were fed normal chow or HFD with or without TEMPOL supplementation.

The mean body mass (g) of the mice from each group during the intervention period of 7 weeks is displayed for apo $E^{-/-}$ (Panel A) and 20 weeks for C57BL/6 (Panel B) mice.

6.4.2 Morphometry of atherosclerotic plaques in the aortic sinus

The heart samples from the different experimental groups outlined above were supplied by the National Cancer Institute. As each of these was provided without an intact arterial tree, only the aortic sinus was available for plaque analysis. This was analysed in order to determine whether TEMPOL inhibited or delayed the progression of atherosclerosis.

Three triplicate cross-sections were taken along the aortic sinus and morphometric measurements were performed for each mouse as described in Sections 2.10.1 to 2.10.3. Atherosclerotic plaques were observed in the apo $E^{-/-}$ mice however no atherosclerosis was detected in the aortic sinus in the parent strain mice regardless of their diet and body mass gain (Figure 6.4).

The aortic sinuses from the HFD fed mice (10.8 ± 0.7 ($x10^3$) μm^2) contained less plaque than for the chow control mice (17.1 ± 2.9 ($x10^3$) μm^2, $p < 0.05$). In contrast the HFD supplemented mice with TEMPOL (12.1 ± 1.2 ($x10^3$) μm^2, $p < 0.01$) contained a lower plaque area than the chow fed animals supplemented with TEMPOL (20.5 ± 1.8 ($x10^3$) μm^2, $p < 0.01$) mice as shown in Figure 6.5 (Panel A).

There were no statistical differences in the total cross-sectional areas of the aortic sinus as shown in Figure 6.5 (Panel B). When the plaque was examined over the total area as presented in Figure 6.5 (Panel C), there were no statistical differences in plaque percentage between the chow ($16.5 \pm 2.8\%$) and HFD ($11.8 \pm 0.8\%$) fed apo $E^{-/-}$ mice. A lower plaque percentage was seen in the HFD mice supplemented with TEMPOL ($12.3 \pm 1.1\%$, $p < 0.01$) than the chow with TEMPOL ($20.6 \pm 1.3\%$, $p < 0.01$) supplemented apo $E^{-/-}$ mice.

Although TEMPOL effectively suppressed HFD induced gain in body mass, in both apo $E^{-/-}$ mice and the parent strain, it did not appear to suppress atherosclerotic development in the apo $E^{-/-}$ mice. The plaques measured in the aortic sinuses in both groups of chow-fed mice (that is with or without TEMPOL) mice were significantly larger than for the HFD apo $E^{-/-}$ mice, matched for TEMPOL treatment. No atherosclerosis was detected in the aortic sinuses taken from the parent strain C57BL/6 mice.

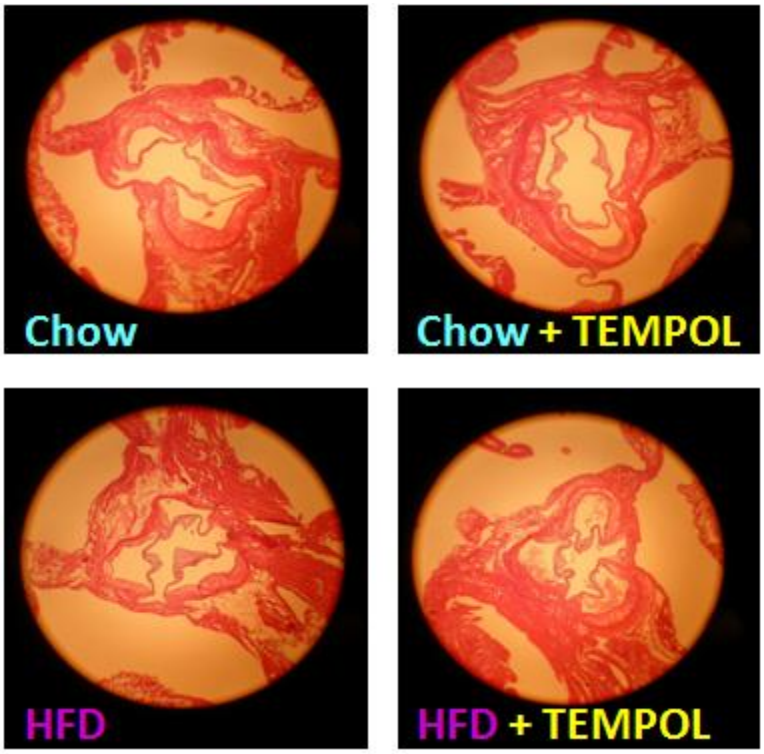

Figure 6.4: Representative sections of the aortic sinus stained with H & E from chow and high fat diet (HFD) fed apo $E^{-/-}$ mice with or without TEMPOL supplementation.

Sections taken from the aortic sinus were stained with H & E and photographed using the 10x objective to determine the degree of plaque formation within the valve leaflets. The total plaque area was analysed over the total area and expressed as a percentage.

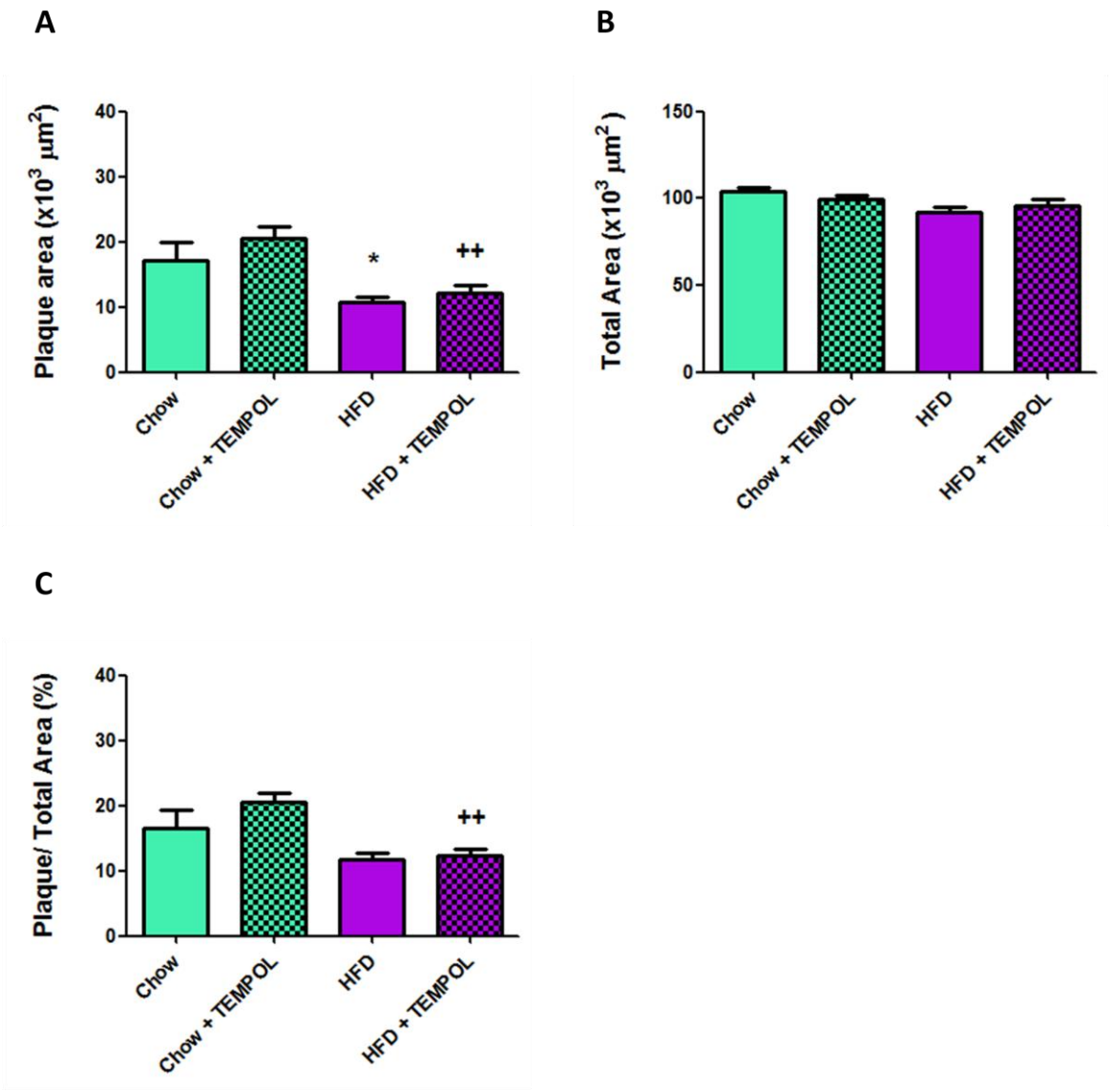

Figure 6.5: Plaque morphometry in the aortic sinus for plaque area (Panel A), total area (Panel B) and percentage of plaque on total area (Panel C) in apo $E^{-/-}$ mice that were fed either a chow or HFD, with or without TEMPOL supplementation.
Plaque and total cross sectional areas within the leaflets were determined in the aortic sinuses and expressed as (x10³) µm² in Panels A and B. Plaque is expressed as a percentage over the total area in Panel C. Statistical significance was achieved at * $p < 0.05$ versus the chow control and ++ $p < 0.01$ versus the chow supplemented with TEMPOL mice using two-way ANOVA analysis followed by Bonferroni's post hoc test. Values are expressed as mean ± SEM.

6.4.3 Effects of TEMPOL upon plasma triglyceride levels in the treatment groups

Hypertriglyceridaemia is associated with an increased risk of cardiovascular disease and commonly seen in people with lipid abnormalities, visceral obesity, metabolic syndrome and type 2 diabetes [354]. Triglyceride levels were measured in plasma from all mice as described in Section 2.11.1 to determine whether TEMPOL had an effect upon the lipid profile in mice that became obese via consumption of a high fat fed diet.

The measured plasma triglyceride levels were significantly higher for the HFD fed apo $E^{-/-}$ mice (2 ± 0.1 mmol/L) than the chow control (0.8 mmol/L, $p < 0.001$). HFD fed TEMPOL mice (0.6 mmol/L, $p < 0.001$) showed lower triglyceride levels than the HFD fed mice as shown in Panel A of Figure 6.6.

Triglyceride levels were significantly elevated in the high fat fed C57BL/6 mice (0.8 mmol/L) than the chow control animals (0.5 ± 0.1 mmol/L, $p < 0.001$). HFD fed mice that were supplemented with TEMPOL (0.5 mmol/L, $p < 0.001$) showed lower triglyceride levels than the HFD fed mice. Lower levels of triglycerides were also detected in the chow fed mice administered TEMPOL (0.3 mmol/L, $p < 0.05$) when compared to the HFD fed mice supplemented with TEMPOL mice as shown in Panel B of Figure 6.6.

Overall, the HFD fed mice had higher triglyceride levels than the non-HFD fed mice in both animal types, and TEMPOL significantly attenuated this elevation. The triglyceride levels in the plasma of the HFD mice administered TEMPOL were similar to that of the non-HFD fed mice as shown in Figure 6.6.

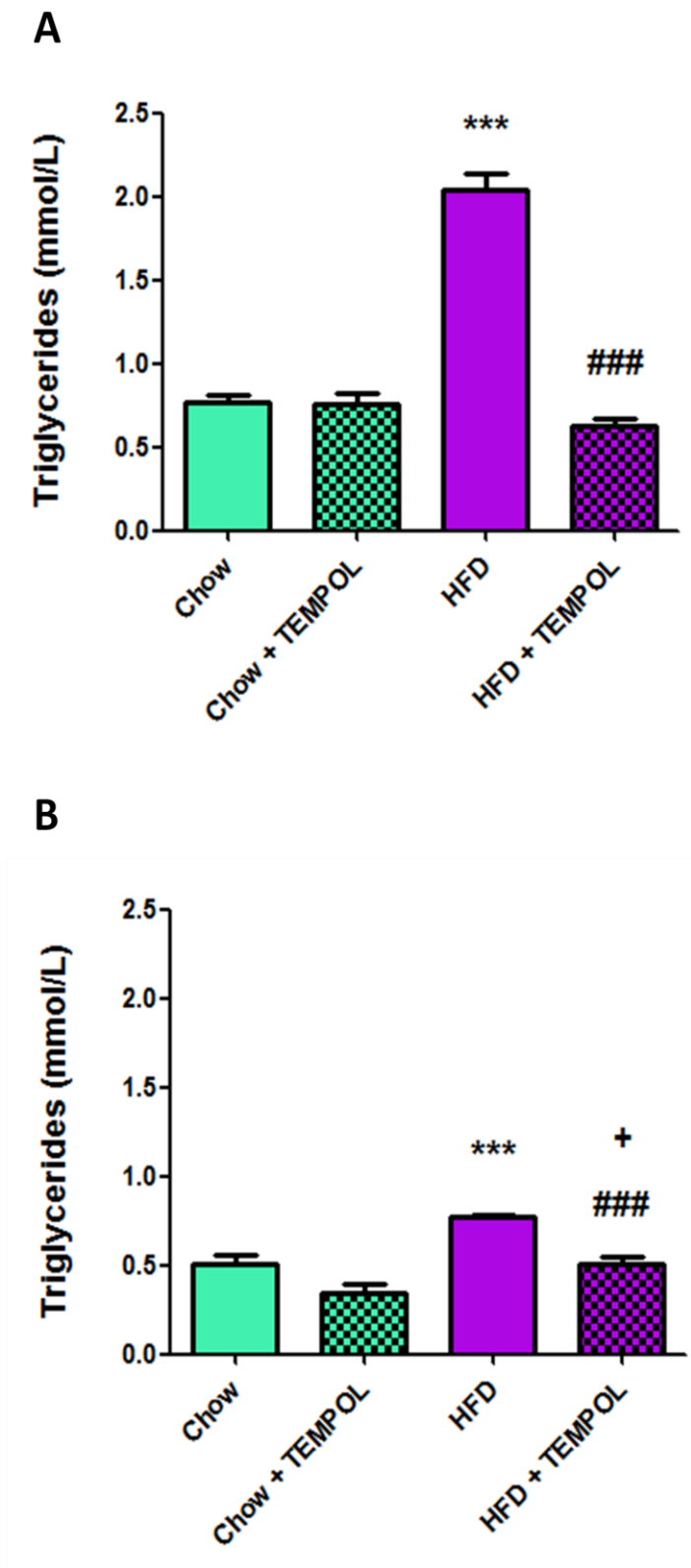

Figure 6.6: Plasma triglyceride levels for apo $E^{-/-}$ (Panel A) and C57BL/6 (Panel B) mice.

Triglyceride levels (mmol/L) were measured in mice that were fed a chow or a high fat diet (HFD) with or without TEMPOL supplementation. Statistical significance is achieved at *** $p < 0.001$ versus chow control, + $p < 0.05$ versus chow with TEMPOL and ### $p < 0.001$ versus HFD fed mice using two-way ANOVA analysis followed by Bonferroni's post-hoc test. Data are expressed as mean ± SEM.

6.4.4 Effects of TEMPOL upon plasma total cholesterol in apo $E^{-/-}$ and parent strain C57BL/6 mice

Hypercholesterolaemia is a major risk factor for CVD [310,311] and was assessed to determine whether TEMPOL treatment could also modulate cholesterol levels as seen with the triglyceride levels in the HFD mice. Total cholesterol levels were measured in the mouse plasma as described in Section 2.11.2.

Total cholesterol levels were significantly elevated in the high fat fed apo $E^{-/-}$ mice (4.6 ± 0.2 mmol/L) when compared to the chow control mice (2.8 ± 0.1 mmol/L, $p < 0.001$) as shown in Panel A of Figure 6.7. The HFD fed TEMPOL mice (2.7 ± 0.1 mmol/L, $p < 0.001$) had lower cholesterol levels than the HFD and the chow supplemented with TEMPOL (3.8 ± 0.5 mmol/L, $p < 0.01$) mice. The chow control mice had lower cholesterol levels than the chow supplemented with TEMPOL mice ($p < 0.05$).

HFD fed C57BL/6 mice had higher total cholesterol levels (4.2 ± 0.2 mmol/L) compared to the chow control (1.9 ± 0.1 mmol/L, $p < 0.001$). HFD fed mice supplemented with TEMPOL (2.7 ± 0.1 mmol/L, $p < 0.001$) exhibited lower cholesterol levels than the HFD fed mice. Total cholesterol levels were statistically higher in the HFD mice supplemented with TEMPOL than the chow mice supplemented with TEMPOL (1.5 ± 0.1 mmol/L, $p < 0.001$) as shown in Panel B of Figure 6.7.

Overall, high fat-feeding resulted in a significant increase in total plasma cholesterol levels for both the apo $E^{-/-}$ and parent strains, and TEMPOL significantly attenuated this elevation. The total cholesterol levels in the plasma of the HFD mice administered TEMPOL were similar to those of the chow-fed mice as shown in Figure 6.7.

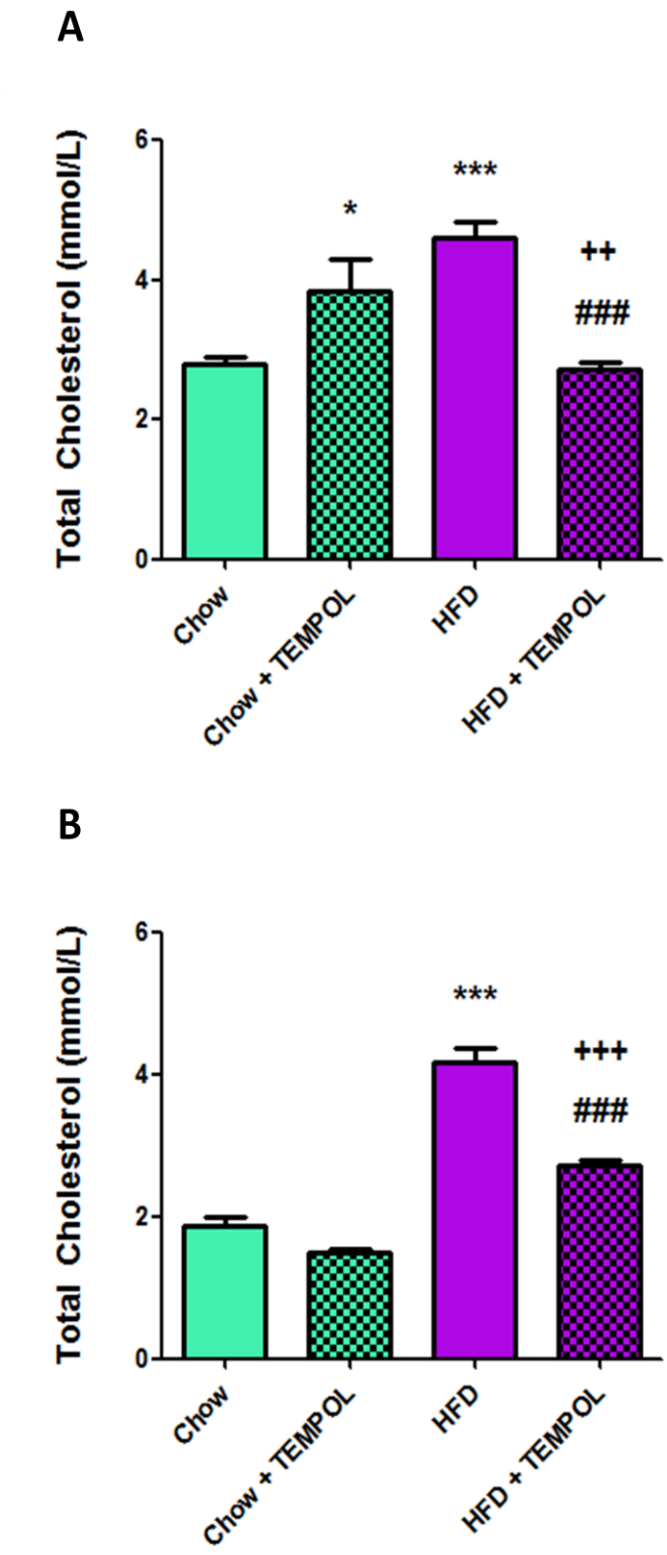

Figure 6.7: Plasma total cholesterol levels for apo $E^{-/-}$ (Panel A) and C57BL/6 (Panel B) mice.

Total cholesterol levels (mmol/L) were measured in mice that were fed a chow or a high fat diet (HFD) with or without TEMPOL supplementation. Statistical significance was achieved at * p <0 .05, *** p < 0.001 versus chow, ++ p < 0.01, +++ p < 0.001, +++ p < 0.001 versus chow administered TEMPOL mice, ### p < 0.001 versus HFD using two-way ANOVA analysis followed by Bonferroni's post-hoc test. Values are expressed as mean ± SEM.

6.4.5 Effects of TEMPOL upon plasma high density lipoprotein-cholesterol (HDL-C) levels in apo $E^{-/-}$ and parent strain C57BL/6 mice

High density lipoproteins are believed to have cardio-protective effects as they mediate cholesterol efflux and reverse cholesterol transport, which is critical in limiting the number of lipid-laden foam cells that contribute to atherosclerosis [355,356]. Many cohort and case-control studies have reported a negative correlation between HDL concentrations and the occurrence of atherosclerotic disease, and HDL-C is involved in protection against the pathogenesis of atherosclerosis [304,305,306]. HDL-C levels were therefore measured in the mouse plasma as described in Section 2.11.2 to determine whether TEMPOL could modulate HDL-C levels in obese mice that consumed a HFD.

HFD fed apo $E^{-/-}$ mice had higher HDL-C levels (0.4 mmol/L) than the chow control mice (0.1 mmol/L, $p < 0.001$). HFD mice supplemented with TEMPOL (0.1 mmol/L, $p < 0.001$) had lower HDL-C levels than the HFD fed mice as shown in Panel A of Figure 6.8.

HDL-C levels were significantly elevated in the HFD fed C57BL/6 mice (1.4 ± 0.1 mmol/L) compared with the chow control fed mice (0.6 ± 0.1 mmol/L, $p < 0.001$). HFD mice supplemented with TEMPOL (0.9 mmol/L, $p < 0.001$) exhibited lower HDL-C levels than the HFD fed mice. Lower levels of HDL-C (0.6 mmol/L, $p < 0.001$) were observed in the chow supplemented TEMPOL mice when compared to the HFD mice supplemented with TEMPOL as shown in Panel B of Figure 6.8.

Overall high fat feeding was associated with elevated HDL-C in both mouse strains, and this elevation was attenuated by TEMPOL. The HDL-C levels in the plasma of the HFD administered TEMPOL mice were similar to that of the non-HFD fed apo $E^{-/-}$ mice.

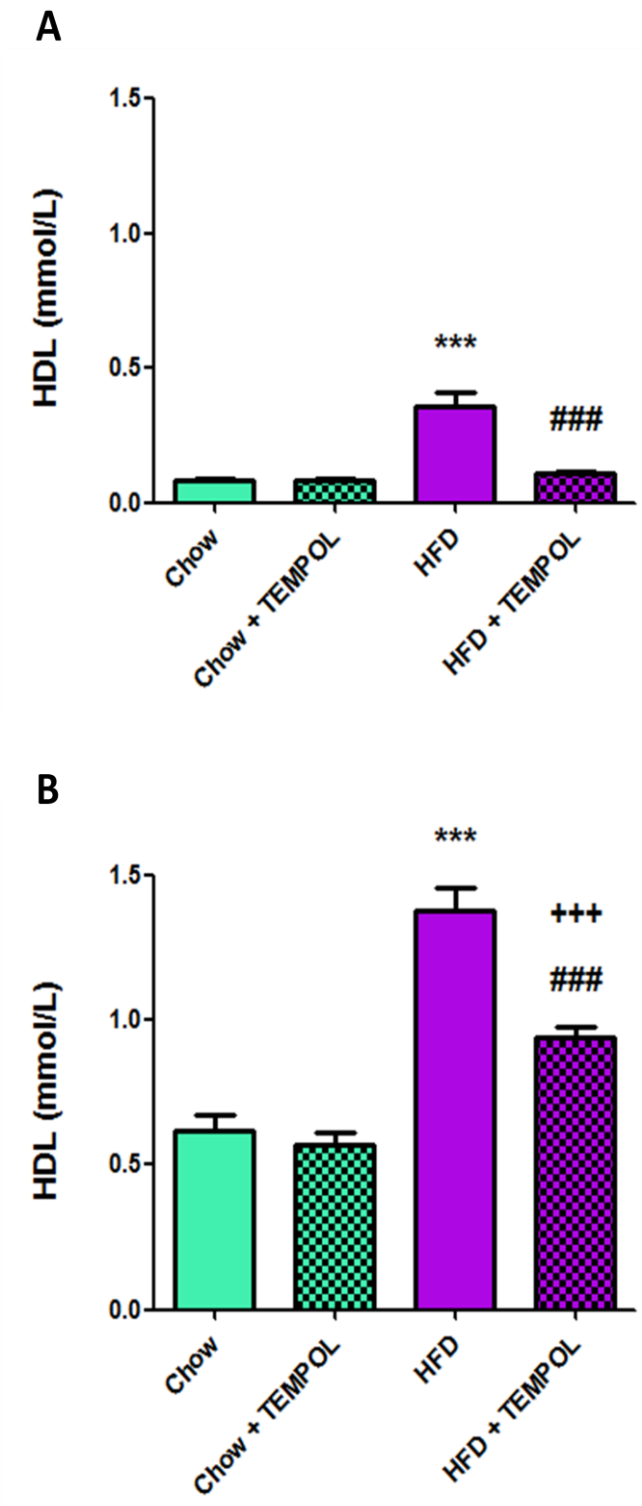

Figure 6.8: Plasma HDL-C levels for apo $E^{-/-}$ (Panel A) and C57BL/6 (Panel B) mice.

HDL-C levels (mmol/L) were measured in mice that were fed a chow or a high fat diet (HFD) with or without TEMPOL supplementation. Statistical significance was achieved at *** $p < 0.001$ versus chow, +++ $p < 0.001$ versus chow administered TEMPOL and ### $p < 0.001$ versus HFD fed mice using two-way ANOVA analysis followed by Bonferroni's post-hoc test. Data are expressed as mean ± SEM.

6.4.6 Effects of TEMPOL upon plasma low density lipoprotein-cholesterol (LDL-C) in apo $E^{-/-}$ and parent strain C57BL/6 mice

Total blood cholesterol and LDL-cholesterol (LDL-C) are classified as independent risk and graded factors for cardiovascular disease (CVD) and meet the criteria for causality related to CVD risk [304]. Increased levels of LDL-C are associated with the progression of atherosclerosis, metabolic dysfunction and obesity [357,358,359]. LDL-C levels were therefore measured in the mouse plasma as described in Section 2.11.2 to determine whether TEMPOL had an effect upon LDL-C levels in mice that consumed a HFD.

LDL-C levels were significantly higher in the HFD fed apo $E^{-/-}$ mice (4.3 ± 0.2 mmol/L) when compared to the chow control (2.7 ± 0.1 mmol/L, $p < 0.001$) as shown in Panel A of Figure 6.9. The HFD mice supplemented with TEMPOL (2.6 ± 0.1 mmol/L, $p < 0.001$) had lower LDL-C levels than the HFD fed mice. Lower levels of LDL-C were observed in the chow fed mice than the chow supplemented with TEMPOL mice (2.7 ± 0.1 mmol/L, $p < 0.05$). There were statistically lower LDL-C levels in the HFD supplemented with TEMPOL than the chow supplemented with TEMPOL mice ($p < 0.01$).

The HFD fed C57BL/6 mice had higher LDL-C levels (2.8 ± 0.2 mmol/L) than the chow control (1.2 ± 0.1 mmol/L, $p < 0.001$) as shown in Panel B of Figure 6.9. HFD mice supplemented with TEMPOL (1.8 ± 0.1 mmol/L, $p < 0.001$) had lower LDL-C levels than the HFD fed mice. Lower levels of LDL-C were also detected in the chow mice supplemented with TEMPOL (0.9 mmol/L, $p < 0.001$) than the HFD fed mice supplemented with TEMPOL.

Overall high fat feeding was associated with elevated LDL-C levels in both strains of mice, and TEMPOL significantly attenuated this elevation. The LDL-C levels in the plasma of the HFD mice administered TEMPOL were similar to those of the non-HFD fed apo $E^{-/-}$ mice.

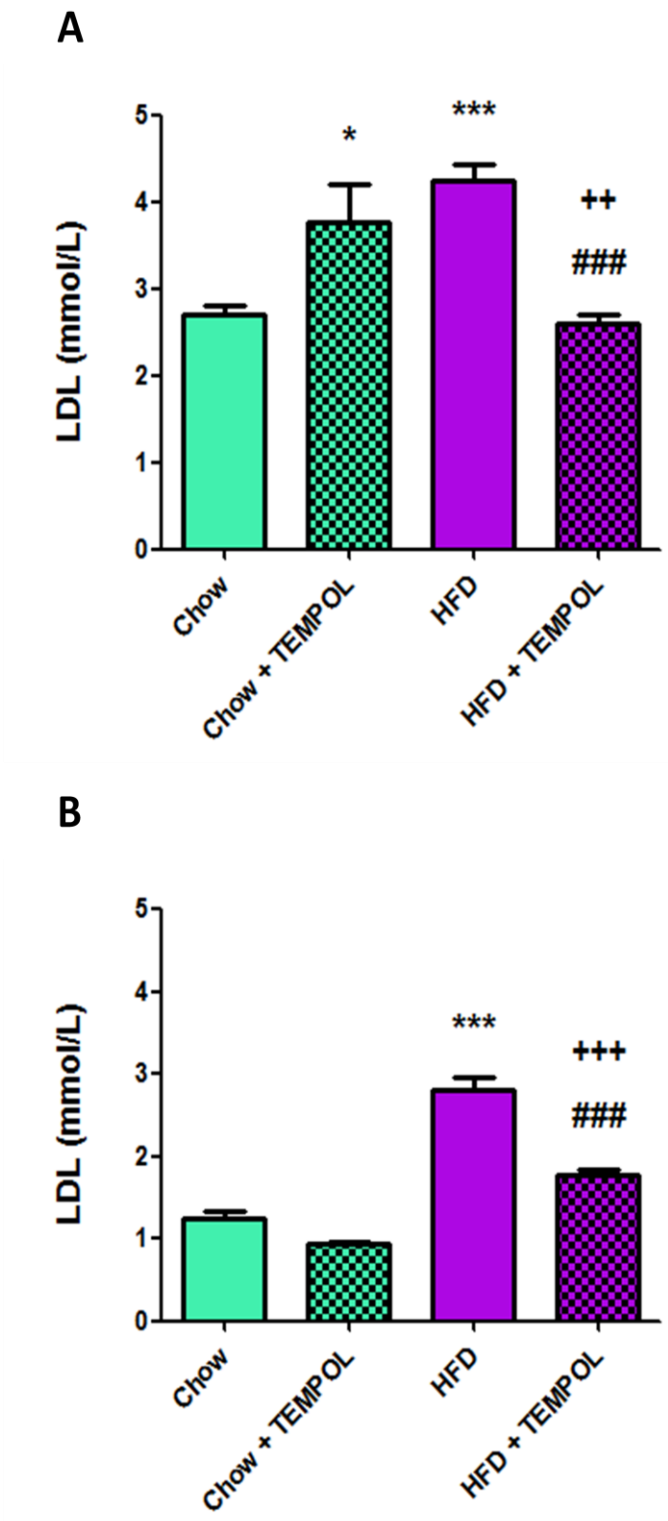

Figure 6.9: Plasma LDL levels for apo $E^{-/-}$ (Panel A) and C57BL/6 (Panel B) mice.

HDL levels (mmol/L) were measured in mice that were fed a chow or a high fat diet (HFD) with or without TEMPOL supplementation. Statistical significance was achieved at * $p < 0.05$, *** $p < 0.001$ versus chow, ++ $p < 0.01$, +++ $p < 0.001$ versus chow administered TEMPOL and ### $p < 0.001$ versus HFD fed mice using two-way ANOVA analysis followed by Bonferroni's post-hoc test. Values are expressed as mean ± SEM.

6.5 Effects of TEMPOL on cytokine levels in high fat diet (HFD) fed apo $E^{-/-}$ and wild type C57BL/6 mice

6.5.1 Effects of TEMPOL on Tumour Necrosis Factor-α (TNF-α) levels

TEMPOL had a dramatic effect in suppressing body weight gain and hyperlipidaemia in mice that consumed a HFD (see Sections 6.4.1, 6.4.3 - 6.4.6). The consequences of obesity include the development of insulin-resistance and inflammation which may play central roles in atherosclerosis. A deficiency of the proinflammatory cytokine TNF-α has been shown previously to protect against insulin resistance induced by a HFD in TNF-α knockout mice [360]. The levels of the pro-inflammatory cytokine TNF-α levels were therefore investigated to determine whether the profound effect of TEMPOL upon body mass gain suppressesed inflammation possibly induced by the HFD. TNF-α levels (pg/ mL) were measured in the mouse plasma as described in Section 2.11.3.

Although HFD had a dramatic effect on obesity and hyperlipidaemia there were no significant differences observed in TNF-α levels between the chow and HFD fed mice. There were also no statistical differences observed across all the groups for both the apo $E^{-/-}$ and C57BL/6 strains as shown in Figure 6.10. Thus neither the high fat diet nor the supplementation with TEMPOL modulated the TNF-α levels in the mouse plasma.

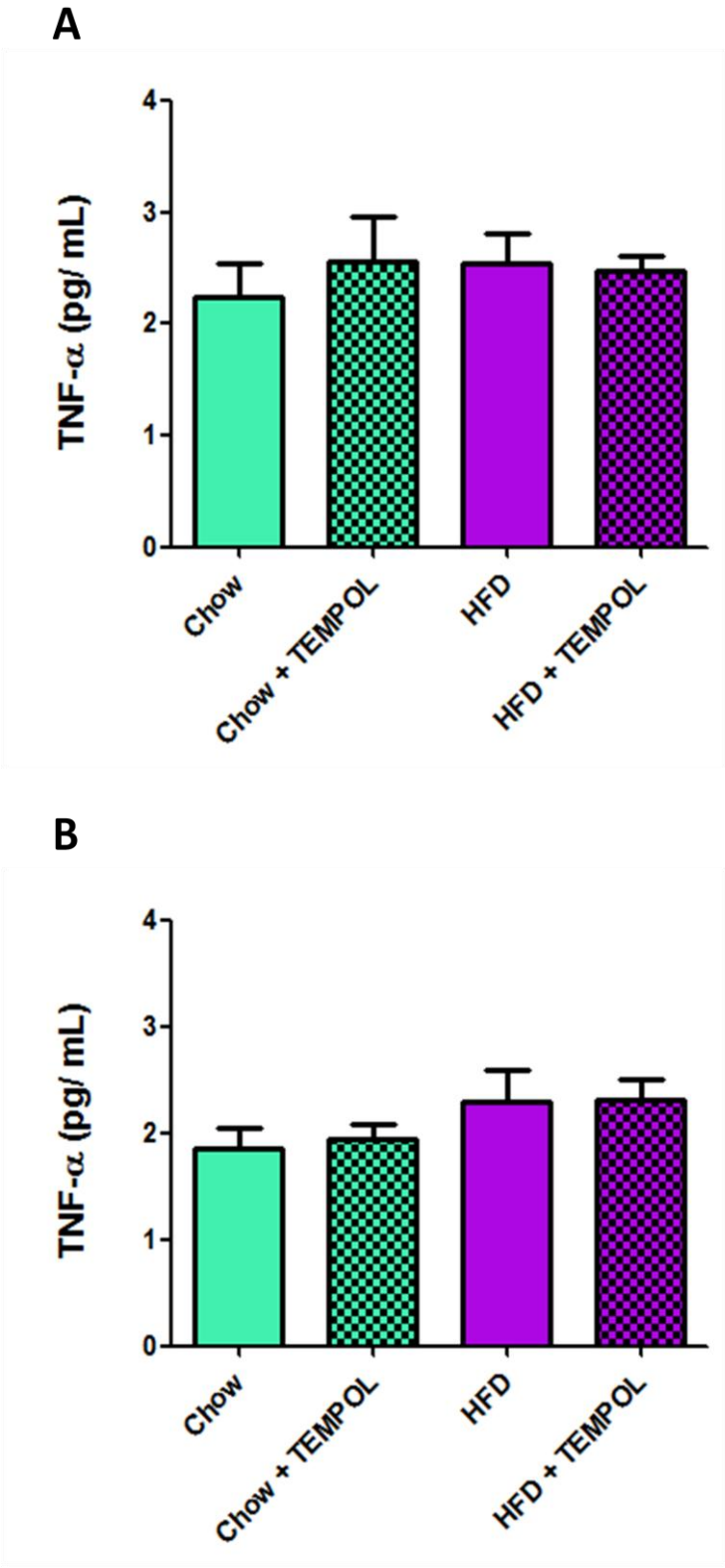

Figure 6.10: Plasma TNF-α levels for apo $E^{-/-}$ (Panel A) and C57BL/6 (Panel B) mice.

TNF-α levels (pg/mL) were measured in the plasma of mice that were fed a chow or a high fat diet (HFD) with or without TEMPOL supplementation. Values are expressed as mean ± SEM. No statistical differences were detected between the various groups using 2-way ANOVA with Bonferroni's post-hoc test.

6.5.2 Effects of TEMPOL on Monocyte Chemotactic Protein-1 (MCP-1) levels

MCP-1 is an inflammatory marker commonly associated with atherosclerosis, obesity, diabetes, insulin resistance, metabolic dysfunction, adiposity and macrophage behaviour [312,361]. MCP-1 levels (pg/mL) were measured in the mouse plasma as described in Section 2.11.3.

There were no statistical differences in MCP-1 levels detected between the apo $E^{-/-}$ chow and HFD fed groups. However significantly lower MCP-1 levels were observed in the apo $E^{-/-}$ HFD mice supplemented with TEMPOL (28.2 ± 4 pg/mL, $p < 0.01$) when compared to HFD mice (43.8 ± 3.5 pg/mL). HFD mice supplemented with TEMPOL also contained lower MCP-1 levels than the chow apo $E^{-/-}$ mice supplemented with TEMPOL (53.8 ± 4.1 mmol/L, $p < 0.01$) as shown in Figure 6.11 (Panel A).

HFD fed C57BL/6 mice contained higher MCP-1 levels (36.6 ± 2.7 pg/mL) than the chow control (18.2 ± 4 pg/mL, $p < 0.001$) as shown in Panel B of Figure 6.11. Lower levels of MCP-1 were also detected in the HFD fed TEMPOL mice (23.4 ± 2.9 pg/mL, $p < 0.01$) than the HFD fed mice.

Overall HFD fed mice had higher MCP-1 levels than the non-HFD fed mice in C57BL/6 mice, and TEMPOL significantly attenuated this elevation. The MCP-1 levels in the plasma of the HFD mice administered TEMPOL were similar to that of the non-HFD fed apo $E^{-/-}$ mice, with the mean values not statistically different.

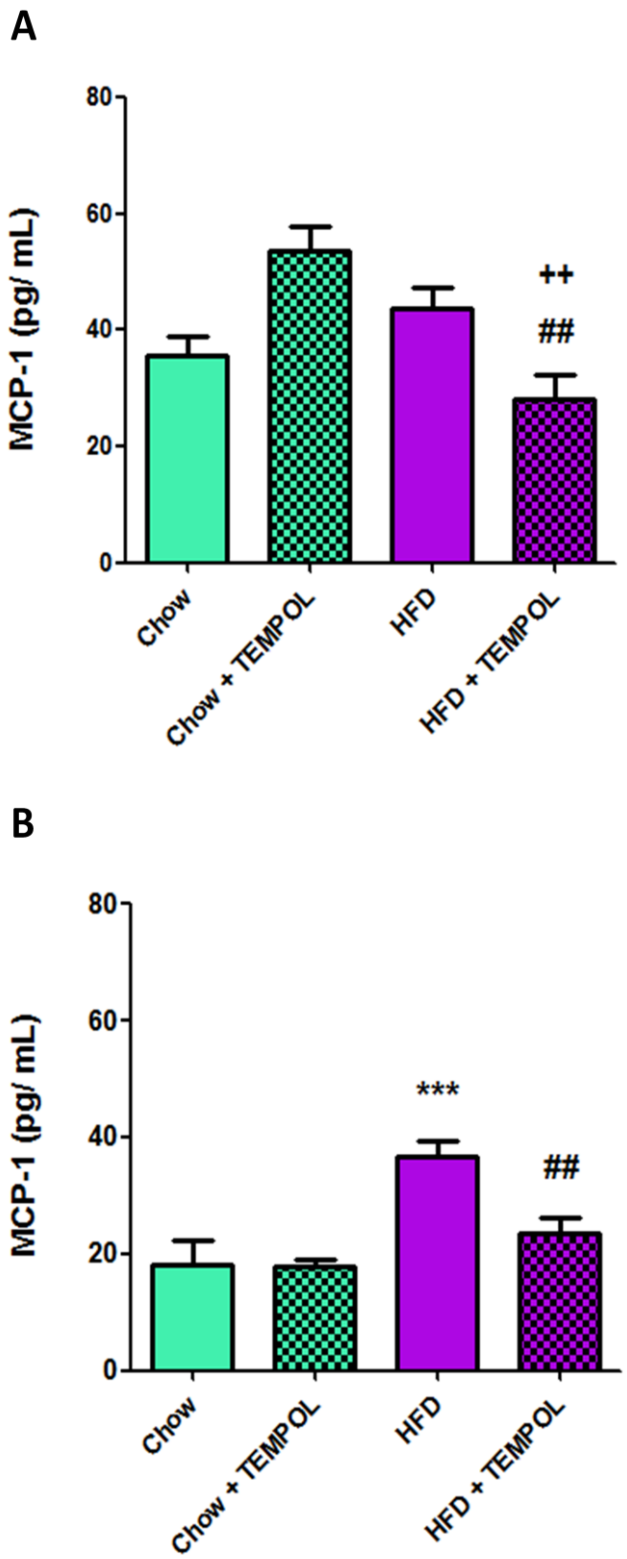

Figure 6.11: Plasma MCP-1 levels for apo $E^{-/-}$ (Panel A) and C57BL/6 (Panel B) mice.

MCP-1 levels (pg/mL) were measured in plasma of mice that were fed a chow or a high fat diet (HFD) with or without TEMPOL supplementation. Statistical significance was achieved at *** $p < 0.001$ versus chow, ++ $p < 0.01$ versus chow supplemented with TEMPOL and ## $p < 0.01$ versus HFD fed mice using two-way ANOVA analysis followed by Bonferroni's post-hoc test. Values are expressed as mean ± SEM.

6.5.3 Effects of TEMPOL on interleukin-6 (IL-6) levels

IL-6 is a biomarker of inflammation and is associated with the metabolic syndrome and obesity [313,362]. The levels of this species were therefore measured in the mouse plasma as described in Section 2.11.3.

IL-6 levels were significantly higher in the HFD fed apo $E^{-/-}$ mice (47 ± 2.7 pg/mL) than the chow (10.4 ± 1.9 pg/mL, $p < 0.001$) control as presented in Panel A of Figure 6.12. Lower levels of IL-6 were observed in the HFD mice supplemented with TEMPOL (16.8 ± 1.5 pg/mL, $p < 0.001$) than the HFD fed mice.

The IL-6 levels were greater in the HFD fed C57BL/6 mice (27.5 ± 2.2 pg/mL) than the chow control (4.9 ± 0.9 pg/mL, $p < 0.001$) as shown in Panel B of Figure 6.12. Lower IL-6 levels were detected in the HFD mice supplemented with TEMPOL (14.1 ± 1.7 pg/mL, $p < 0.001$) than the HFD fed mice. The HFD supplemented mice with TEMPOL contained higher IL-6 levels than the chow supplemented mice with TEMPOL (4.8 ± 0.9 pg/mL, $p < 0.01$).

Overall the HFD fed mice had higher levels of IL-6 than the non-HFD fed mice and TEMPOL significantly attenuated this elevation in both animal types. The IL-6 values examined in the HFD mice supplemented with TEMPOL were similar to those of the non-HFD apo $E^{-/-}$ mice with no statistical difference observed between these groups.

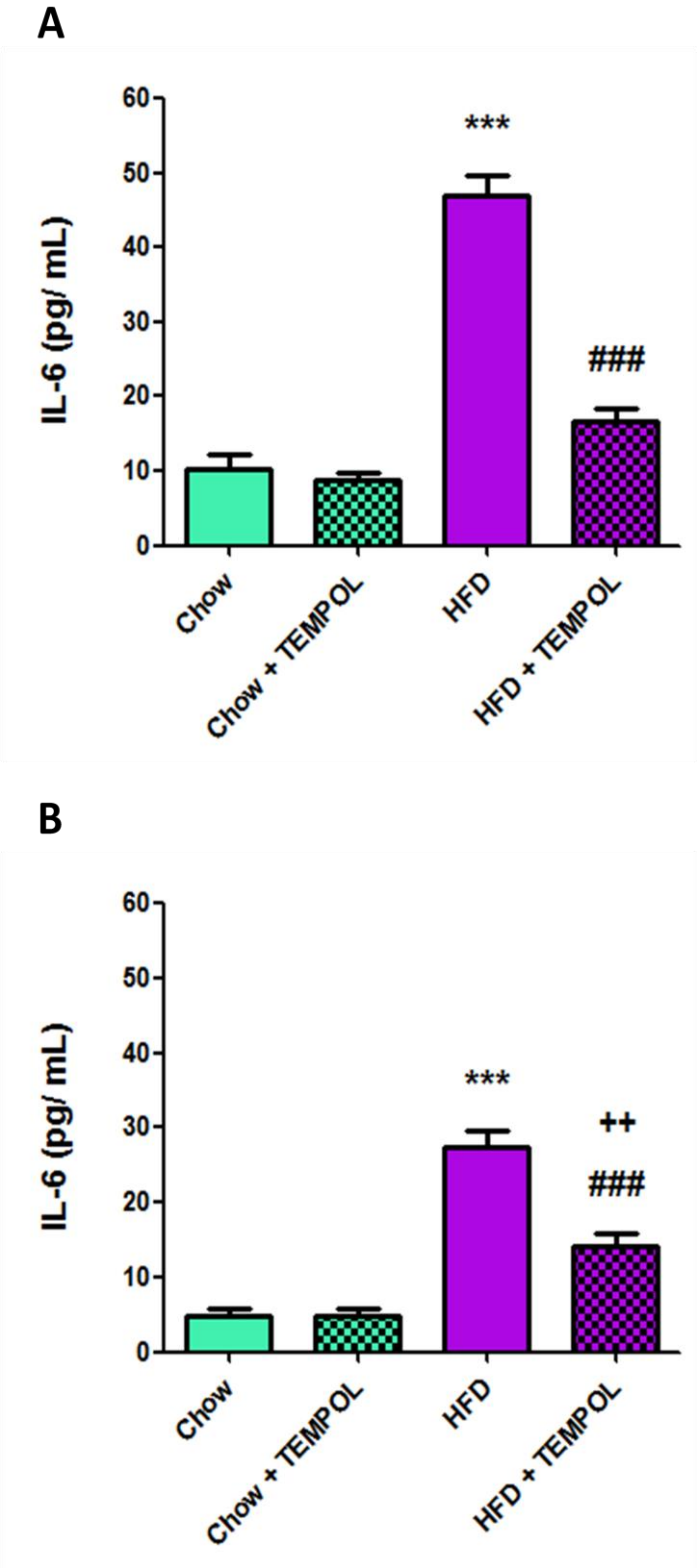

Figure 6.12: Plasma IL-6 levels for apo $E^{-/-}$ (Panel A) and C57BL/6 (Panel B) mice. IL-6 levels (pg/mL) were measured in plasma of mice that were fed a chow or a high fat diet (HFD) with or without TEMPOL supplementation. Statistical significance was achieved at *** $p < 0.001$ versus chow and ++ $p < 0.01$ versus chow with TEMPOL supplementation and ### $p < 0.001$ versus HFD fed mice using two-way ANOVA analysis followed by Bonferroni's post-hoc test. Values are expressed as mean ± SEM.

6.5.4 Effects of TEMPOL on serum amyloid-A (SAA) levels

SAA is an acute-phase apolipoprotein predominantly produced by hepatocytes, the plasma levels of which have been positively correlated with the incidence of obesity, adiposity, diabetes and insulin resistance [363,364,365]. SAA levels were therefore measured in the mouse plasma as described in Section 2.11.3.

SAA levels were significantly elevated in the HFD fed apo $E^{-/-}$ mice (312.3 ± 32.5 ng/mL) when compared to chow control mice (65.8 ± 15.4 ng/mL, $p < 0.001$) as presented in Panel A of Figure 6.13. The HFD mice supplemented with TEMPOL (127.3 ± 35.2 ng/mL, $p < 0.001$) had lower SAA levels than the HFD fed mice.

HFD fed C57BL/6 mice exhibited higher SAA levels (294.4 ± 33.6 ng/mL) than the chow control (132 ± 9.6 ng/mL, $p < 0.001$) as shown in Panel B of Figure 6.13. HFD supplemented with TEMPOL mice (130.7 ± 9.4ng/mL, $p < 0.001$) showed lower SAA levels than the HFD fed mice.

Overall the HFD mice had higher levels of SAA than the non-HFD fed mice and TEMPOL significantly attenuated this elevation in both the animal types. The SAA values examined in the HFD mice supplemented with TEMPOL were similar to that of the non-HFD fed mice in both animal types and there were no statistical differences observed between these groups.

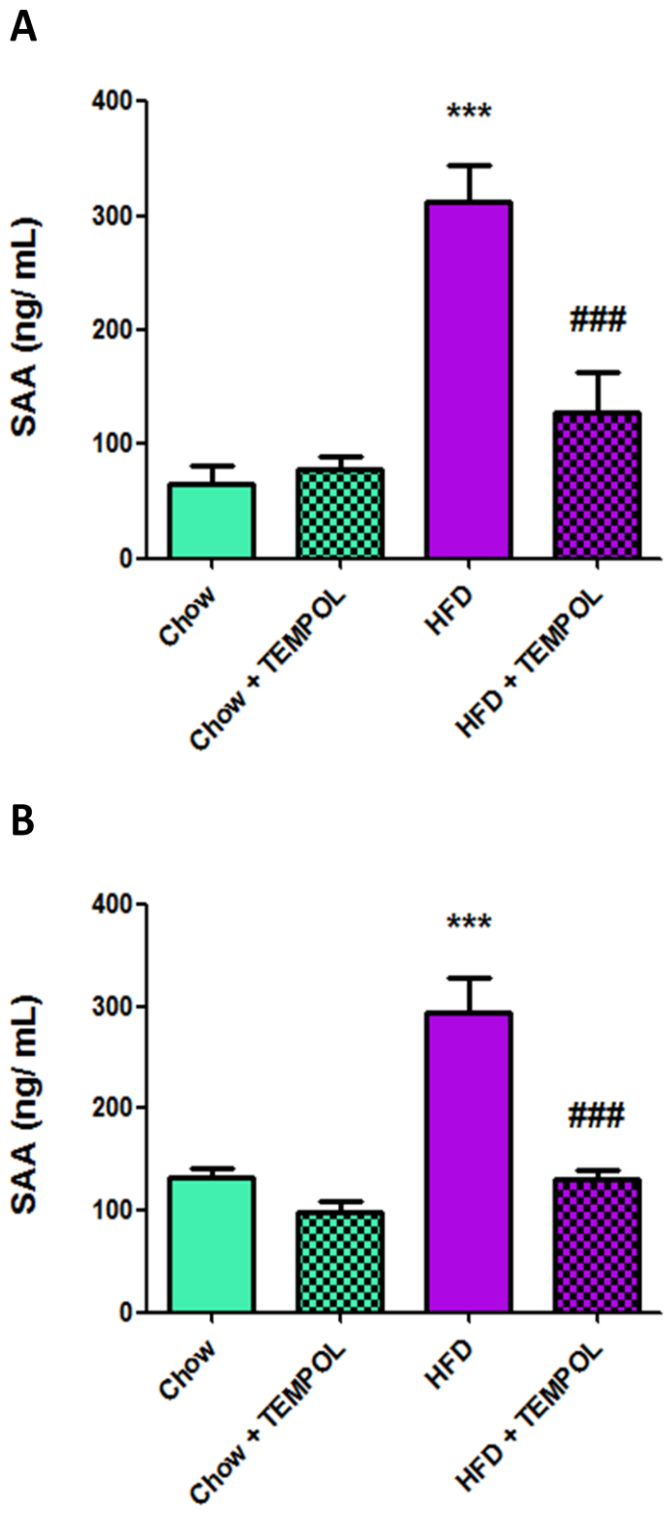

Figure 6.13: Plasma SAA levels for apo E$^{-/-}$ (Panel A) and C57BL/6 (Panel B) mice. SAA levels (ng/mL) were measured in plasma of mice that were fed a chow or a high fat diet (HFD) with or without TEMPOL supplementation. Statistical significance was achieved at *** $p < 0.001$ versus chow and ### $p < 0.001$ versus HFD fed mice using two-way ANOVA analysis followed by Bonferroni's post-hoc test. Values are expressed as mean ± SEM.

6.5.5 Effects of TEMPOL on myeloperoxidase (MPO) levels

MPO, a heme enzyme released by activated neutrophils and monocytes at sites of inflammation, catalyzes the oxidation of chloride ions to hypochlorous acid using hydrogen peroxide as a co-substrate [24]. Elevation of MPO levels have been reported to be an early biomarker of atherosclerosis and positively correlated with the incidence of obesity and cardiovascular disease in both children and adults [366,367]. MPO protein levels were therefore measured in the mouse plasma as described in Section 2.11.3.

MPO protein levels were significantly elevated in the HFD fed apo $E^{-/-}$ mice (108.2 ± 7.1 ng/mL) when compared to chow control (39.8 ± 6 ng/mL, $p < 0.001$) as presented in Panel A of Figure 6.14. HFD mice supplemented with TEMPOL (28.8 ± 2.2 ng/mL, $p < 0.001$) contained lower MPO levels than the HFD fed mice. Lower MPO levels were observed in the HFD supplemented with TEMPOL mice than the apo $E^{-/-}$ mice fed on chow supplemented with TEMPOL (57.6 ± 3.9 ng/mL, $p < 0.01$).

HFD fed C57BL/6 mice had higher MPO levels (69.8 ± 5.3 ng/mL) than the chow control (23 ± 0.7 ng/mL, $p < 0.001$) as shown in Panel B of Figure 6.14. Lower levels of MPO were detected in the HFD mice supplemented with TEMPOL (43 ± 4.1ng/mL, $p < 0.001$) than the HFD fed mice. Higher levels of MPO were present in the HFD mice supplemented with TEMPOL than the chow C57BL/6 mice supplemented with TEMPOL (22.7 ± 1.7 ng/mL, $p < 0.01$).

Overall HFD fed mice of both strains had higher levels of MPO than the non-HFD fed mice and TEMPOL significantly attenuated this elevation in both the animal types. The MPO levels detected in the HFD apo $E^{-/-}$ mice supplemented with TEMPOL were the lowest of any of the apo $E^{-/-}$ mouse groups examined.

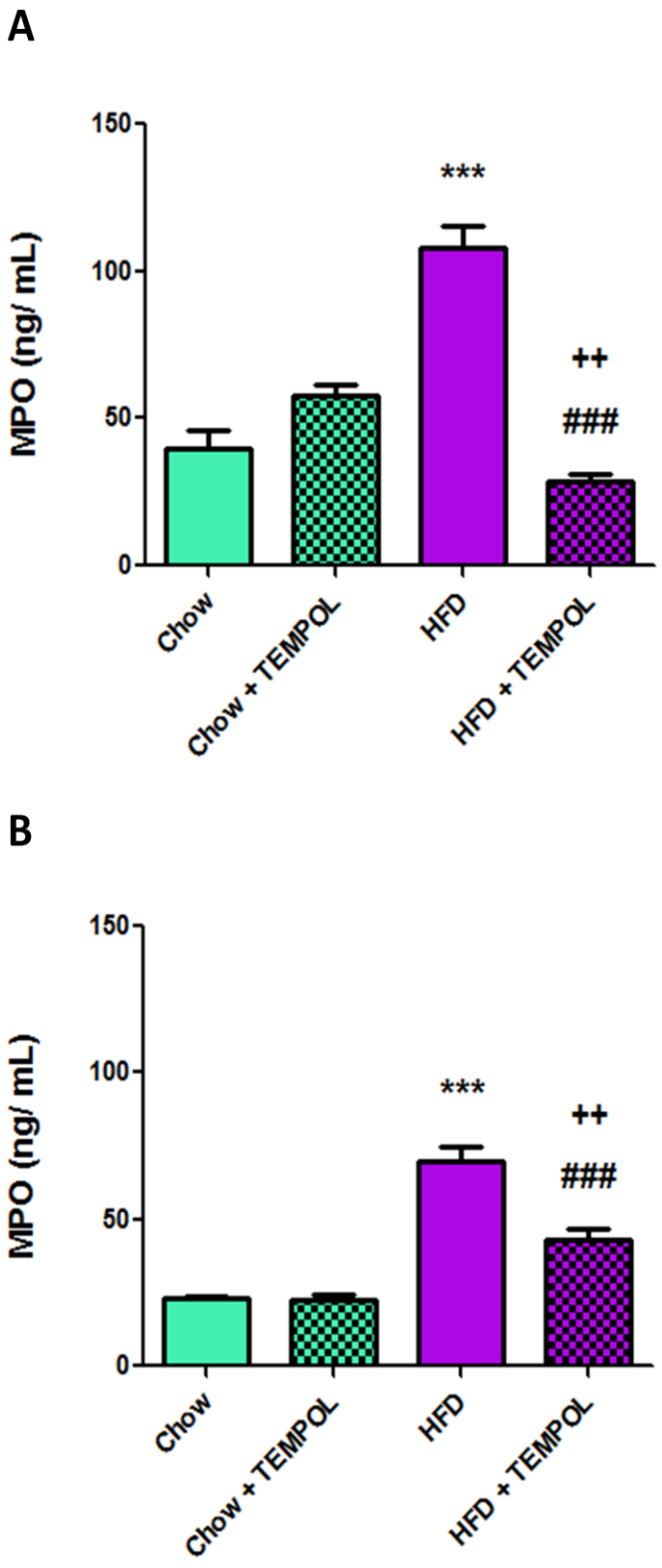

Figure 6.14: Plasma MPO levels for apo $E^{-/-}$ (Panel A) and C57BL/6 (Panel B) mice.

MPO levels (ng/mL) were measured in plasma of mice that were fed a chow or a high fat diet (HFD) with or without TEMPOL supplementation. Statistical significance was achieved at *** $p < 0.001$ versus chow, ++ $p < 0.01$ versus chow with TEMPOL supplementation and ### $p < 0.001$ versus HFD fed mice using two-way ANOVA analysis followed by Bonferroni's post-hoc test. Values are expressed as mean ± SEM.

6.5.6 Effects of TEMPOL on adiponectin levels

Adipose tissue is a major energy reservoir in the body and a primary source of adipocytokines [368]. Adiponectin is a fat-derived hormone, secreted by adipocytes which exerts cardio-protective, anti-atherogenic, anti-inflammatory and anti-diabetic effects [369,370]. A reduction in adiponectin expression has been associated with obesity-related metabolic and cardiovascular diseases [368,370]. As a number of other cytokines and inflammatory agents were observed to be suppressed by TEMPOL in the obese and hyperlipidaemic high fat-fed mice examined in this project, it was of interest to determine whether adiponectin levels were also modulated in the mouse plasma. This adipokine was quantified as described in Section 2.11.3.

Adiponectin levels were significantly decreased in the HFD fed apo $E^{-/-}$ mice (9608 ± 592 ng/mL) compared to chow control (22091 ± 1202 ng/mL, $p < 0.001$). The HFD mice supplemented with TEMPOL (19103 ± 2035 ng/mL, $p < 0.001$) contained higher levels of adiponectin than the HFD fed mice, as presented in Panel A of Figure 6.15. For the C57BL/6 mice there were no statistical differences in the levels of adiponectin amongst the groups as shown in Panel B of Figure 6.15.

The HFD fed mice had the lowest levels of adiponectin, and TEMPOL significantly attenuated this decrease in adiponectin levels. The adiponectin values detected in the HFD mice supplemented with TEMPOL were similar to those of the non-HFD fed apo $E^{-/-}$ mice and these data were not statistically different. Neither the HFD nor TEMPOL had any effect upon adiponectin levels in the C57BL/6 mice.

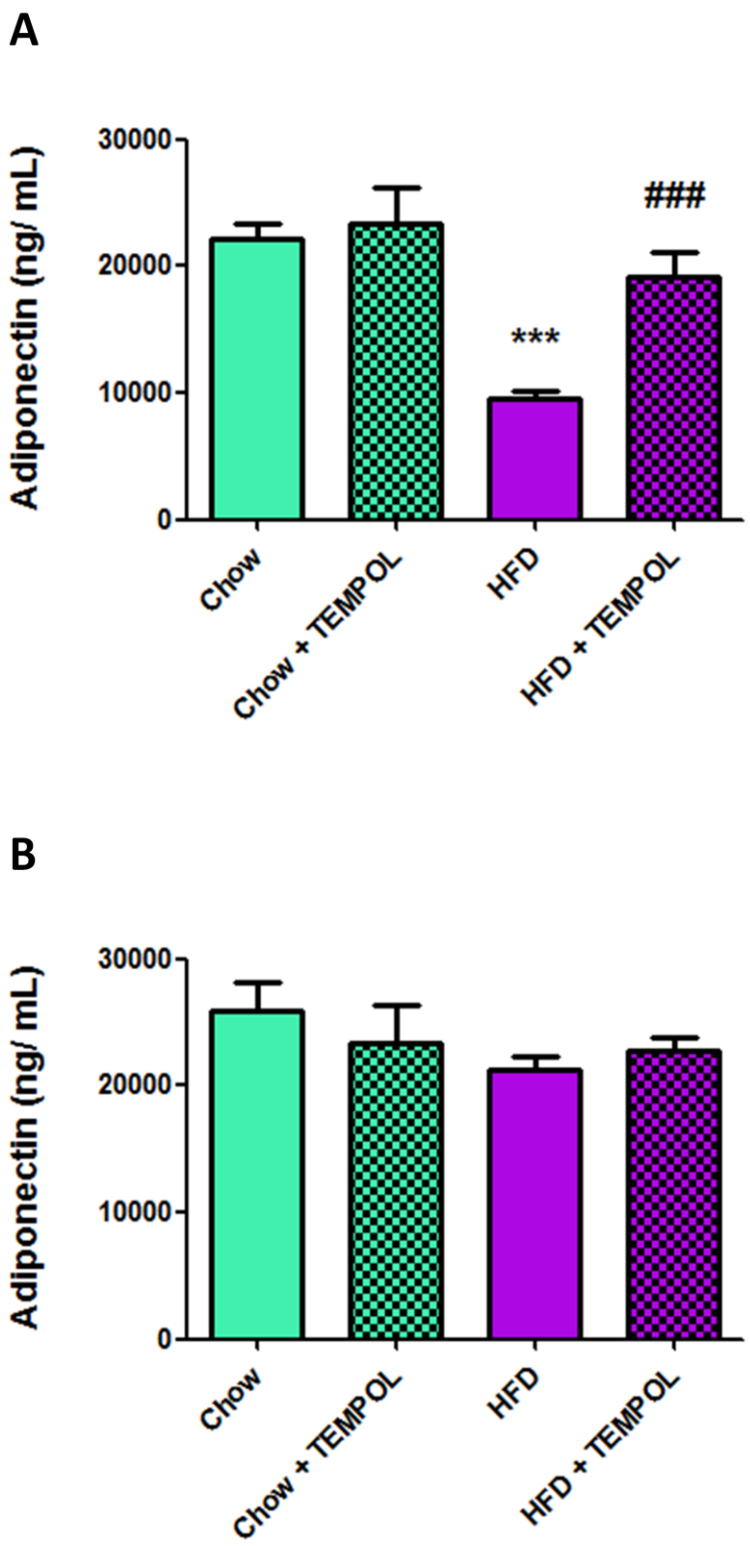

Figure 6.15: Plasma adiponectin levels for apo $E^{-/-}$ (Panel A) and C57BL/6 (Panel B) mice.

Adiponectin levels (ng/mL) were measured in plasma of mice that were fed a chow or a high fat diet (HFD) with or without TEMPOL supplementation. Statistical significance was achieved at *** $p < 0.001$ versus chow and ### $p < 0.001$ versus HFD fed mice using two-way ANOVA analysis followed by Bonferroni's post-hoc test. Values are expressed as mean ± SEM.

6.5.7 Effects of TEMPOL on leptin levels

Leptin is a hormone, secreted by adipocytes, that serves as a major negative regulator of food intake and engenders energy expenditure [368]. Dietary obesity is strongly correlated with hyperleptinaemia and hyperlipidaemia [78,312,330,371]. Leptin levels were therefore measured to confirm the inhibitory effects of TEMPOL upon inflammation, adiposity and body weight gain observed in the obese and hyperlipidaemic mice that were fed a HFD.

The leptin levels were measured in the mouse plasma as described in Section 2.11.3. The leptin levels were significantly elevated in the HFD fed apo $E^{-/-}$ mice (95.2 ± 2.5 ng/mL) when compared to the chow control (4.3 ± 0.5 ng/mL, $p < 0.001$). HFD mice supplemented with TEMPOL (6.7 ± 0.6 ng/mL, $p < 0.001$) exhibited lower leptin levels than the HFD fed mice as presented in Panel A of Figure 6.16.

HFD fed C57BL/6 mice produced higher leptin levels (112.5 ± 1.8 ng/mL) than the chow control (18.4 ± 0.4 ng/mL, $p < 0.001$) as shown in Panel B of Figure 6.16. The HFD mice supplemented with TEMPOL (15.1 ± 1.2 ng/mL, $p < 0.001$) contained lower leptin levels than the HFD fed mice. Lower leptin values were also observed in the chow fed mice supplemented with TEMPOL (6.4 ± 0.5 ng/mL, $p < 0.001$) than the chow control. Higher leptin levels were observed in the HFD supplemented with TEMPOL than the chow supplemented with TEMPOL mice ($p < 0.001$).

Overall the HFD fed mice had higher levels of leptin than the non-HFD fed mice and TEMPOL significantly attenuated this elevation in both the animal types. The leptin values examined in the HFD mice supplemented with TEMPOL were similar to those of the chow control mice and these values were not statistically different in both animal types. For the apo $E^{-/-}$ mice the leptin levels observed in the HFD supplemented with TEMPOL mice were similar to the non-HFD fed mice, and these values were not statistically different.

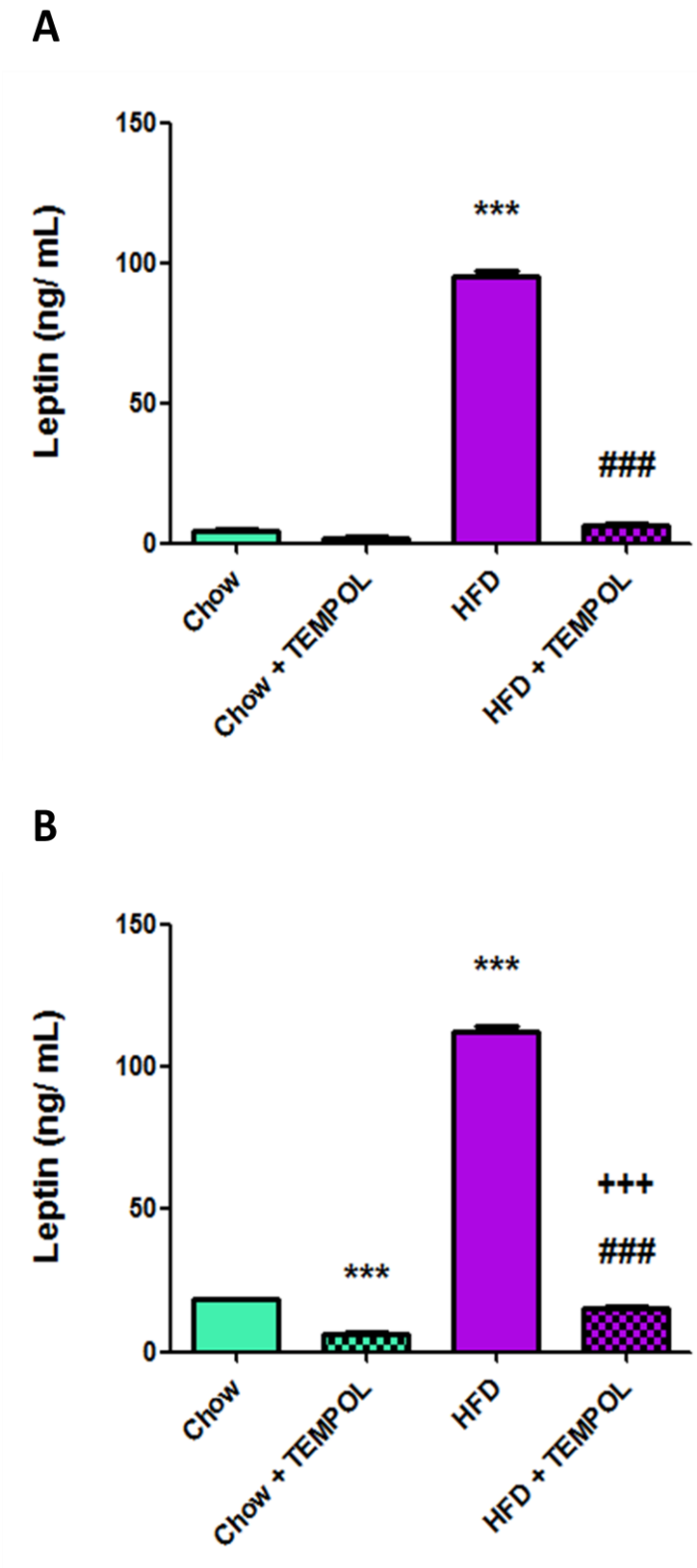

Figure 6.16: Plasma leptin levels for apo $E^{-/-}$ (Panel A) and C57BL/6 (Panel B) mice.

Leptin levels (ng/mL) were measured in plasma of mice that were fed a chow or a high fat diet (HFD) with or without TEMPOL supplementation. Statistical significance was achieved at *** $p < 0.001$ versus chow, +++ $p < 0.001$ versus chow with TEMPOL supplementation and ### $p < 0.001$ versus HFD fed mice using two-way ANOVA analysis followed by Bonferroni's post-hoc test. Values are expressed as mean ± SEM.

6.5.8 Effects of TEMPOL on resistin levels

As the data reported in the previous sections indicate that TEMPOL had an effect upon both adiponectin and leptin levels in the apo $E^{-/-}$ obese and hyperlipidaemic mice that were on a HFD, resistin, an adipocyte secreted cytokine recently proposed to be associated with obesity and diabetes [78,372] was also quantified in the mouse plasma as described in Section 2.11.3.

There were no statistical differences in resistin levels examined in the apo $E^{-/-}$ mice amongst the groups as shown in Panel A of Figure 6.17. There were also no statistical differences observed between the chow and HFD fed C57BL/6 mice as presented in Panel B of Figure 6.17. Resistin levels were however significantly higher in the HFD mice supplemented with TEMPOL C57BL/6 mice (52 ± 1.8 ng/mL) compared to chow fed mice supplemented with TEMPOL (26.2 ± 0.7 ng/mL, $p < 0.001$) and the HFD fed mice (23.7 ± 0.8 ng/mL, $p < 0.001$).

Overall, there were no changes in resistin levels observed amongst the animals on the HFD, and TEMPOL did not have an effect upon resistin levels in the apo $E^{-/-}$ mice. However resistin values were greater in the HFD C57BL/6 mice supplemented with TEMPOL than the remaining groups of C57BL/6 mice.

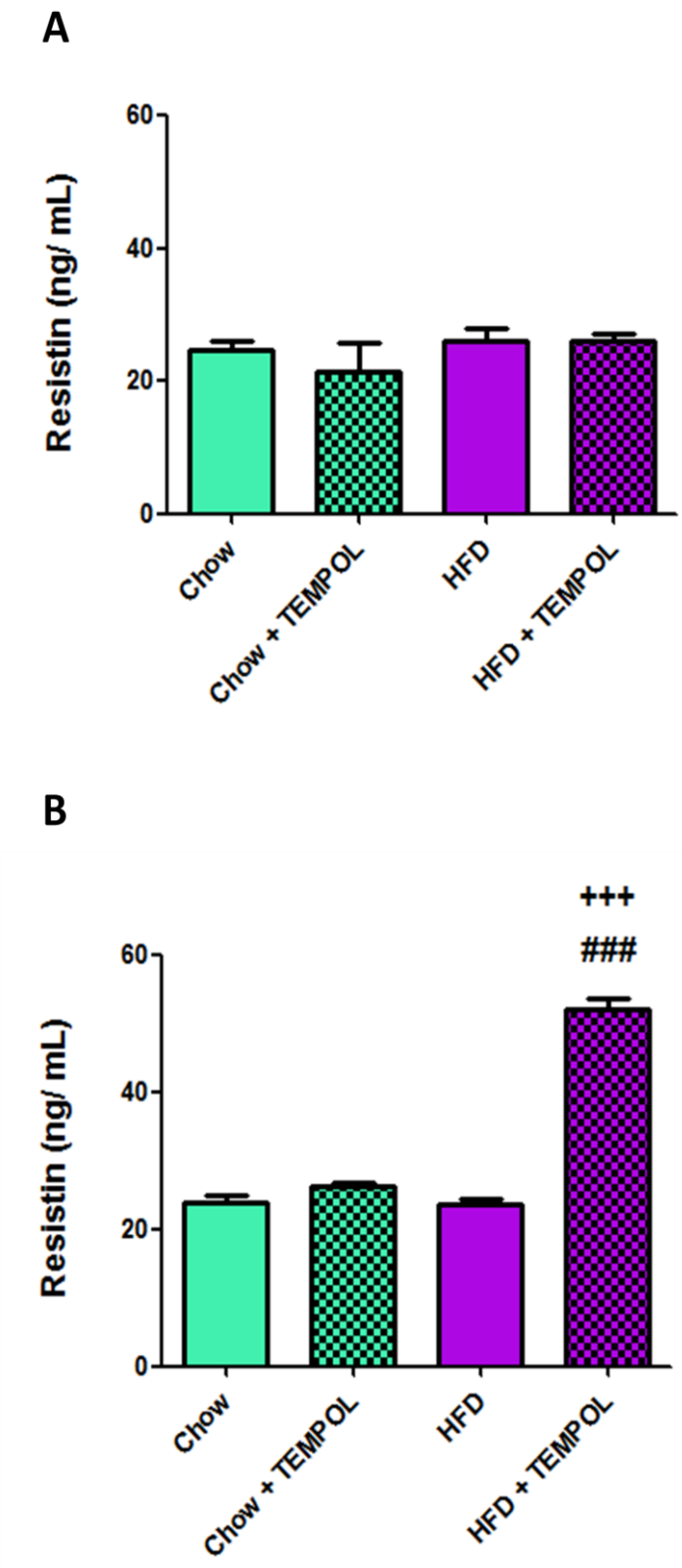

Figure 6.17: Plasma resistin levels for apo $E^{-/-}$ (Panel A) and C57BL/6 (Panel B) mice.

Resistin levels (ng/mL) were measured in plasma of mice that were fed a chow or a high fat diet (HFD) with or without TEMPOL supplementation. Statistical significance was achieved at +++ $p < 0.001$ versus chow with TEMPOL supplementation and ### $p < 0.001$ versus HFD fed mice using two-way ANOVA analysis followed by Bonferroni's post-hoc test. Values are expressed as mean ± SEM.

6.6 Discussion

The antioxidant activity and the antihypertensive effects of TEMPOL have been extensively studied with regard to inflammatory diseases including cancer [331,332,334,335], atherosclerosis [373,374,375,376], obesity [330,340,341,342] and diabetes [343,344,345] where oxidative damage is purported to contribute to pathogenesis and disease progression. In the present project, post mortem analyses was undertaken upon the aortic sinuses from atherosclerosis-prone mice (high fat-fed apo $E^{-/-}$ mice as well as the parent strain C57BL/6 strain) to elucidate the therapeutic potential of TEMPOL.

Direct administration of TEMPOL has been shown to decrease blood pressure levels in many hypertensive rodent models [337,338,339,346,347]. TEMPOL and other nitroxides are considered safe to administer as no adverse effects appeared on cell growth and viability at concentrations of up to 1 mM [377]. Notably incubation with TEMPOL as high as 50 mM was shown to not provoke damage to chromosomal structures but instead was able to protect against radiation-induced chromosomal aberrations in cultured human peripheral blood lymphocytes [378]. Low loses of TEMPOL (0.4 mM/kg) given via intravenous injections have however been reported to cause restlessness and seizures [379,380]. However, TEMPOL concentrations as high as 275 mg/kg were shown to be radioprotective in mice that were exposed to whole-body radiation [380]. TEMPO (2,2,6,6-tetramethylpiperidinoxyl radical; $(CH_2)_3(CMe_2)_2NO^{\cdot}$ as shown in Figure 6.18) administration to mice was shown to result in rapid metabolism to produce the less toxic species TEMPOL [381]. Overall these studies imply that nitroxides are generally safe to administer except at exceptionally high dosages. Therefore we predicted that the 10 mg/g (equivalent to approx. 58 mM) TEMPOL that was utilised in these studies was likely to be well tolerated. Similar levels have been used in previous studies including long term feeding trials without any problems [330,331].

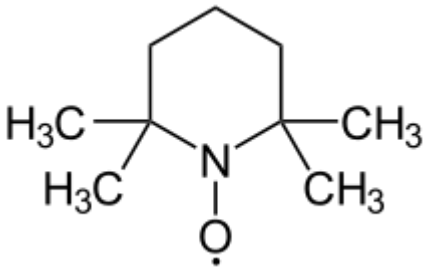

Figure 6.18: Chemical structure of TEMPO.
TEMPO is also referred to as 2,2,6,6-tetramethylpiperidinoxidanyl, and 2,2,6,6-tetramethylpiperidinoxyl radical.

In this study, TEMPOL supplementation via food had a profound inhibitory effect, in both apo $E^{-/-}$ and the parent C57BL/6 mice, upon the typical body mass gain that is the result of a high fat diet. Adult male apo $E^{-/-}$ (or the parent C57BL/6) mice were fed for 7 weeks either on a standard chow diet or a high-fat diet (HFD) with the high fat feeding resulting in a substantial increase in body mass in both strains. TEMPOL feeding resulted in marked reduction in body mass gain. These findings confirm a previous study carried out by Mitchell *et al.* where TEMPOL administration via drinking water (2.9 - 58 mM) or food (10 mg/g food: 58 mM as used here) was also reported to result in significantly reduced body mass gain in C3H mice that were fed a bacon-flavoured mouse chow [330]. There seemed to be a dose dependent response as the degree of inhibition of body weight gain increased with increasing dosages of TEMPOL, with 29 mM and above giving statistically significantly differences compared to both control groups (sucrose or ad lib). TEMPOL treated animals consumed approximately 20 to 30% less food than the non-TEMPOL administered mice.

Although TEMPOL suppressed high fat feeding-induced body mass gain in both these previous studies [330,331] and the current investigation, the effect of this treatment on atherosclerosis remains under characterised. This was therefore further examined in the two animal models. Atherosclerotic plaque was assessed at one location, the aortic sinus. Regardless of diet, no plaque was observed in the aortic sinuses collected from the C57BL/6 parent strain. In contrast to this, plaques of substantial size were detected in the apo $E^{-/-}$ mice. However, the plaque areas in the aortic sinuses from chow fed mice were significantly larger than those determined for the high fat-fed mice. This is a major limitation to the study as more plaque area should

be observed in the high fat-fed mice across all well-established atherosclerotic animal models. This may be due to fact that the animals may have been kept for too long before analysis as all animals possessed large plaques regardless of diet. Where plaque area could be determined for the purpose of comparison, TEMPOL was observed to have no impact upon plaque size. However, failure to develop a good model of atherosclerotic plaque induced by a high fat diet is a potential reason for the lack of reduction in plaque size detected with the TEMPOL treatment. An earlier time point would have been a more suitable approach to address this issue, before both the chow and high fat-fed apo $E^{-/-}$ mice produced highly advanced atherosclerotic lesions. Although, in this pilot study, TEMPOL supplementation did not significantly modulate plaque area, refined experiments with a larger cohort kept for shorter periods and an assessment of atherosclerotic plaque development at more than one site may help elucidate the effect of TEMPOL upon atherosclerosis.

The C57BL/6 wild type mice under the conditions employed do not appear to be suitable for examining atherosclerosis as no plaque was detected; this observation is in line with a study on hypercholesterolaemia induced by HFD diet in wild type and apo $E^{-/-}$ mice. Oil red O staining of the aortic arch, thoracic and abdominal aorta did not give rise to significant plaques in the wild type C57BL/6 mice despite the high cholesterol diet; in contrast visible macroscopic plaques were detected in all three regions of the aorta in the apo $E^{-/-}$ mice [382].

TEMPOL supplementation was observed to have a marked effect upon the hyperlipidaemia induced by high fat feeding in both animal types, with supplementation significantly reducing plasma triglycerides, total cholesterol, HDL-C and LDL-C levels. These results are similar to those detected in both lean Zucker rats (LZR) and obsese Zucker rats (OZR) that were fed a HFD which invoked hyperlipidaemia with significantly elevated total cholesterol, very low-density lipoprotein-cholesterol and triglyceride levels. This hyperlipidaemia was attenuated by TEMPOL (1 mM in drinking water for 10 weeks) [340]. In this previous study HDL-C levels were significantly lower in the HFD fed animals, and TEMPOL restored HDL-C to near control levels in both the OZR and LZR animal types [340].

TEMPOL supplementation (1 mM in drinking water for four weeks in old Fischer 344 rats) has been shown previously to significantly decrease plasma glucose, insulin and triglycerides compared to non-TEMPOL supplemented rats [343]. Another

study also measured plasma metabolic parameters, where TEMPOL supplementation (1 mM in drinking water for four weeks) in diabetic KK/Ta-Akita mice did not alter blood glucose, HbA1c, bodyweight or total cholesterol levels. Despite the unaltered metabolic parameters, TEMPOL treatment had an impact on renal function as it effectively decreased albuminuria and inhibited elevation of glomerular filtration rate (GFR) and renal hypertropy [344]. Furthermore although TEMPOL supplementation (29-58 mM) inhibited body weight gain in C3H mice [330], it did not affect plasma triglycerides, cholesterol and HDL levels, where all the mice, including controls were fed a high fat diet with or without various concentrations of TEMPOL. These differences compared to the current study may be due to the different mouse strains utilised. In the two animal models used in the current study, high fat feeding resulted in a substantial elevation of lipid levels, and TEMPOL treatment resulted in a marked reduction in these parameters.

The effects of TEMPOL on weight gain as well as hyperlipidaemia were associated with a decrease in several pro-inflammatory cytokines and agents including MCP-1, IL-6, SAA and MPO levels, elevations in which are commonly seen in obesity-related metabolic complications. Higher plasma levels and protein expression of TNF-α has been reported in obese patients than lean control subjects [383,384] and animal models [385,386]. The elevation of TNF-α levels and iNOS expression resulted in endothelial dysfunction in the small arteries observed from visceral fat of obese patients [348]. Vascular superoxide radical generation which was also elevated in obese patients was attenuated by TEMPOL [348]. TNF-α levels were shown to be also elevated in Zucker obese fatty (ZOF) rats, a model for prediabetic metabolic syndrome in comparison to lean control rats [340,386]. TEMPOL was shown to significantly decrease the elevation of TNF-α levels [340] in the cortical tissues of the lean Zucker rat (LZR) and ZOF animals that were fed a HFD. However in the current study there were no differences detected between plasma TNF-α levels detected between the chow (non-obese) and HFD (obese) fed mice in both animal strains; this may be due to differences in animal type as well as the use of the high fat diet in the current study.

MCP-1 levels were significantly elevated in the C57BL/6 wild type mice fed a HFD in comparison to the chow. MCP-1 expression was also found to be significantly elevated by high fat feeding in Wistar-Kyoto (WKY) rats and spontaneous hypertensive rats (SHR) [341]. TEMPOL supplementation (1 mM in the drinking water) was shown to prevent the increase in MCP-1 levels, along with an inhibition of renal oxidative stress by suppressing an elevation of 8-isoprostane levels and elevation in macrophage

infiltration in both WKY and SHR animal types [341]. TEMPOL was shown to inhibit MCP-1 and IL-6 levels in endothelial cells that were incubated with TNF-α, IL-1 and IFN-γ cytokines in order to stimulate the ROS production which resulted in an elevation of MCP-1 and IL-6 [387].

In the current study IL-6 and MPO plasma levels were showed to be suppressed by TEMPOL in the HFD fed obese mice of both animal strains. A reduction in serum IL-6 has been reported previously, together with an inhibition of colonic MPO levels, in dextran sulfate sodium (DSS) induced colitis in male BABL/cA mice that were treated with TEMPOL (5 - 15 mg/kg/day) [388]. TEMPOL has been shown previously to inhibit MPO mediated inflammation and tissue damage in multiple inflammatory pathologies such as renal disease [389], respiratory syndrome [390] and edema [391] and this was also seen in the current study, with TEMPOL shown to effectively suppress MPO levels in the hyperlipidaemic obese mice. TEMPOL has been shown previously to attenuate carrageenan-induced inflammation arising from MPO mediated damage in rat paws and also was shown to inhibit rat neutrophil migration *in vitro* [391]. Renal dysfunction and injury induced by ischaemia / reperfusion has also been shown to be reduced by TEMPOL with MPO activity significantly inhibited in the rat kidneys, along with cell infiltration and lipid peroxidation as measured by malondialdehyde (MDA) [389]. Treatment with TEMPOL has also been reported to significantly ameliorate MPO activity in LPS (1 mg/kg) induced acute lung injury where MPO, MDA and NO levels were elevated in lung tissues of male albino mice [390]. Elevation of the cytokines, TNF-α, IL-1β and IFN-γ were also significantly reduced after the administration of TEMPOL in both bronchoalveolar lavage fluid and lung tissue homogenates [390].

Plasma SAA levels have been shown to be increased in disorders linked with chronic inflammation such as rheumatic diseases, atherosclerosis, diabetes and obesity [392,393,394,395,396]. It has been reported previously that SAA is expressed at the highest concentrations by large adipocytes separated from adipose tissue from obese patients [397]. This is consistent with the data obtained from the two animal strains examined in the current study, where the obese hyperlipidaemic mice had very high levels of plasma SAA. Although there are no previous studies on the effects of TEMPOL upon SAA expression, TEMPOL was observed in the current study to have a significant effect upon plasma SAA levels in the HFD fed mice of both animal strains suggesting that TEMPOL may target adipose tissue in hyperlipidaemic obese mice.

The inhibitory effects of TEMPOL upon obesity, hyperlipidaemia and pro-inflammatory agents and markers were also associated with changes in the levels of the adipocytokines adiponectin, leptin and resistin. Adiponectin exerts strong anti-inflammatory and athero-protective effects on vascular tissue, and has an insulin-sensitising effect on tissues associated with glucose and lipid metabolism [398,399]. A significant reduction in plasma adiponectin levels was detected in the high fat fed mice that became obese and hyperlipidaemic, when compared to the lean control apo $E^{-/-}$ mice. Similar findings have been reported in other animal models [314,315,398,400,401,402] of obesity, diabetes and coronary artery disease. Lower adiponectin levels have been reported in various human cohort studies in subjects with obesity, diabetes and coronary artery disease [403,404,405,406,407,408]. In contrast, TEMPOL prevented the decrease in adiponectin levels that was induced by high fat feeding and obesity. TEMPOL has been reported to inhibit the expression of adipogenesis markers, adipose differentiation and lipid storage in mouse pre-adipocytes (3T3-L1) and human mesenchymal stem cells [342], which may be the underlying cause of the effects of TEMPOL on body weight gain, and the protective effects upon adiponectin levels seen *in vivo*.

Resistin, another adipokine associated with obesity and metabolic disorders [78,372,409] was reported to be positively correlated with serum lipid levels and negatively associated with HDL-C levels in Indian male subjects [410]. However in the current study no differences were detected in plasma resistin levels between the lean and obese mice that were fed a high fat diet in both animal strains. Although elevated plasma levels of fat-derived signalling molecules are correlated with obesity and vascular endothelial dysfunction and coronary heart disease, little is known about their specific roles, and the relationship with obesity remains controversial [411,412]. This species may therefore not be a suitable adipokine marker to elucidate the potential inhibitory mechanism of TEMPOL in obesity-related vascular and metabolic complications.

High fat feeding in mice has been shown previously to result in hyperleptinaemia, a phenomena commonly seen in obesity as higher leptin levels are indicative of greater adipose tissue reservoirs and excess secretion causing leptin resistance [78,312,316,371]. TEMPOL was shown to prevent elevation of plasma leptin levels in the current study; this is consistent with the data of Mitchell *et al.* with similar TEMPOL dosages, where the mice were also shown to consume less food [330].

TEMPOL (2 mM in drinking water) has also been shown to be effective in controlling blood pressure in leptin-induced hypertensive male Wistar rats [413].

Given the increasing incidence and economic burden of obesity, vascular and metabolic disorders, there is a pressing need to develop new therapeutic treatments to improve, delay and prevent these complications [5]. TEMPOL and its analogues have been shown to possess anti-hypertensive, anti-cancer, anti-inflammatory, anti-hyperlipidaemic, cardio and renal protective actions. This present study is the first to demonstrate that this well tolerated nitroxide administered at relatively high concentrations also may be of importance in inhibiting or decreasing several cytokines and inflammatory factors associated with obesity and hyperlipidaemia resulting from high fat feeding in two animal strains.

6.7 Conclusion

Short term TEMPOL supplementation has been shown to have a significant impact upon body mass gain and hyperlipidaemia in a well-established model of obesity induced by high fat feeding. High fat fed mice had elevated levels of plasma triglycerides, total cholesterol, LDL and HDL compared animals fed a normal chow diet. However the progression and severity of atherosclerosis did not appear to be directly correlated with obesity in the apo $E^{-/-}$ mice and there were no observable plaques in the C57BL/6 parent strain. Thus it is hard to discern whether TEMPOL had a significant effect upon atherosclerosis in this pilot study. Further studies are therefore necessary to elucidate the effect of TEMPOL on atherosclerotic lesions.

However potential anti-hyperlipidaemic and anti-atherosclerotic effects of TEMPOL were detected when various systemic inflammatory responses were quantified. High fat feeding was observed to induce profound inflammatory responses with elevated levels of MCP-1, IL-6, SAA and MPO plasma levels detected when compared to the chow fed mice, for both the apo $E^{-/-}$ and C57BL/6 strains, and these have been reported to be early biomarkers or correlate positively with atherosclerosis, obesity and cardiovascular diseases.

TEMPOL was shown to decrease plasma levels of cholesterol and triglycerides, inflammatory responses and prevent body weight gain in the HFD fed mice. This was associated with changes in adipocytokines that are secreted by adipose tissue, as high

fat feeding induced hyperleptinaemia in both animal types and hypoadiponectinaemia in the apo $E^{-/-}$ mice only. Dietary obesity is strongly correlated with hyperlipidaemia, hyperleptinaemia and hypoadiponectinaemia [78,312,330,368,370,371]. The elevated leptin levels were considerably suppressed by TEMPOL in both animal types and the lower adiponectin levels observed in the HFD fed apo $E^{-/-}$ mice was reversed with TEMPOL. Therefore TEMPOL may exert cardio-protective, anti-atherogenic, anti-inflammatory and anti-diabetic effects.

The present chapter focused on the hyperlipidaemic effect of TEMPOL upon vascular manifestations *in vivo*. TEMPOL was shown to block weight gain, and also the systemic inflammatory response, in these fat-fed animals. The next chapter describes a follow up study to examine potential effects of TEMPOL against the deleterious manifestations of high glucose levels in human monocyte-derived macrophages (HMDM) in which elevated glucose levels engendered lysosomal dysfunction (see Chapters 3 and 4). It also addresses whether TEMPOL has an effect upon inflammatory responses induced by high glucose.

CHAPTER 7:

EFFECTS OF TEMPOL UPON CYTOKINE PRODUCTION AND LYSOSOMAL FUNCTION OF HUMAN MONOCYTE-DERIVED MACROPHAGES EXPOSED TO NORMAL AND HIGH GLUCOSE CONCENTRATIONS

7.1 Introduction

Dysfunction of macrophages is a common feature of diabetic complications, manifested as inflammation, augmented susceptibility to infection, atherosclerotic progression and impaired wound healing after tissue damage [50,94,317,414,415], as such dysfunction would lead to defects or down regulation of non-specific immunity, inflammation and the adaptive immune response. Several studies have investigated defence mechanisms against infectious disease in people with diabetes [416,417,418]. Monocytes from patients with diabetes have been reported to possess impaired chemostatic responses [419], and suppressed phagocytic activity [420]. This may be due to the inhibition of chemotactic, phagocytic and bactericidal functions in people with diabetes [420]. Finally many investigations have associated the severity of diabetes with an increased risk of cardiovascular disease attributable to the chronic hyperglycaemia in addition to other well-defined cardiovascular risk factors [114,236].

Macrophages are believed to be involved in every phase of atherogenesis from early stage through to late-stage atherosclerotic lesions [266], most noted as lipid-laden foam cells which are critical to cholesterol accumulation in the vessel well and lesion development [421]. The main pathway of cholesterol accumulation in macrophage cells is via endocytic uptake of modified forms of (lipo) protein particles [422]. Macrophage lysosomal cholesterol accumulation is a major factor in the development of late-stage atherosclerotic lesions [423]. The presence of cholesterol and cholesteryl esters in foam cells is indicative of impaired cholesteryl ester hydrolysis and free cholesterol clearance [239,422]. Cholesterol accumulation in lysosomes and associated lysosomal dysfunction may therefore be critical in plaque progression.

Functional changes in lysosomes induced by high glucose levels may affect the capacity of monocytes and macrophages, to catabolise modified (lipo) proteins specifically, and more generally impact upon macrophage function and survival. Lysosomal dysfunction induced by elevated glucose levels is evident in monocytes and macrophages exposed to high glucose *in vitro* [244] as reported in Chapters 3 and 4. The impact of hyperglycaemia upon atherosclerotic development is consistent with the data presented in Chapter 5 where diabetic mice plaques were larger in size with greater amounts of extracellular lipid and lower collagen content; characteristics of plaques with a higher risk of rupture. The beneficial effects of carnosine in this model were associated with reduced blood triglyceride levels as well as a greater portion of the

plaque being occupied by collagen in place of extracellular lipid, though this was without any impact on the chronic hyperglycaemia.

For most subjects with diabetes the increased prevalence and rate of progression of atherosclerosis is likely to be the result of a combination of hyperglycaemia (and the associated oxidative and glycative stress), insulin resistance, a pro-inflammatory state and obesity. TEMPOL, a cell-permeable nitroxide is known to be capable of reacting, and detoxifying a number of free radicals and reactive oxygen species [336], and has reported impacts upon hypertension [336,337,339,346,347], diabetes [345,424,425], obesity [330,374], and cancer [331,332,426].

The studies reported in the previous chapter indicated that exposure of fat-fed mice to TEMPOL had a profound inhibitory effect upon body weight gain, prevented obesity and attenuated hyperlipidaemia. The hypolipidaemic effect of TEMPOL was also associated with an inhibition of several pro-inflammatory cytokines and inflammatory agents, where these levels increased with obesity. Notably the source of these cytokines is not fully characterised in that both local adipocytes as well as infiltrating macrophages are implicated.

This was the driver for the studies reported on this chapter whereby the effects of TEMPOL upon human monocyte-derived macrophages were examined. Further as chronic exposure of HMDM to high glucose levels has been shown to cause lysosomal dysfunction [244] and induce various innate and inflammatory responses, the impact of TEMPOL upon cytokine production as well as lysosomal function was examined for HMDM under normal and high glucose levels.

7.2 Aims

Firstly, to see if TEMPOL reverses the effect of lysosomal dysfunction seen in HMDM exposed to elevated glucose concentrations and in particular the detrimental impact upon the lysosomal enzymes studied in Chapters 3 and 4, and secondly to determine whether TEMPOL also has an effect upon cytokine production in the same macrophages in the light of the effects of TEMPOL on cytokine expression *in vivo* presented in Chapter 6.

7.3 Methods

Human monocytes isolated from buffer coats of healthy donors were matured into macrophages over 10 days as described in Section 2.2.4 in RPMI media that contained normal (5.5 mM) or high (20 mM) glucose concentration and with or without supplementation with TEMPOL (100 μM). Cell pellets were obtained as detailed in Sections 2.2.5 to determine the lysosomal activities of cathepsins B, L and LAL as outlined in Sections 2.3 to 2.3.2 and 2.3.6.

7.3.1 Secretion of cytokines by lipopolysaccharide (LPS) treatment

Human monocytes were matured over 10 days in normal (5.5 mM) or high (20 mM) glucose with or without TEMPOL added into the RPMI media. The pilot studies were conducted where the cells were initially stimulated with 0, 50 and 200 ng/mL of LPS on day 10. The cell culture supernatants were collected after 24 and 48 hrs of incubation and the levels of protein, interleukin-6 (IL-6), monocyte / macrophage chemotactic protein-1 (MCP-1), C-reactive protein (CRP), macrophage migration inhibitory factor (MIF), macrophage inflammatory protein-1α (MIP-1α) and tumour necrosis factor-α (TNF-α) were determined as previously described in Sections 2.11.3 - 2.12.2. Based on these pilot studies, the cells were stimulated with 0, 25 and 50 ng/mL of LPS for 24 hrs before collection of the supernatants for analysis of the levels of protein, CRP, MIP-1α and TNF-α.

7.4 Results

7.4.1 The effect of TEMPOL upon lysosomal activities of cathepsin B, L and LAL in HMDM

The lysosomal activities of human monocytes matured under normal (5.5 mM) and high (20 mM) glucose concentrations with and without TEMPOL supplementation (100 μM) were examined to determine whether TEMPOL counteracts the inhibition of lysosomal activity induced by high glucose.

In agreement with studies present in Chapters 3 and 4, maturation of human monocytes in high glucose concentrations for 10 days modulated the activities of the three lysosomal activities as shown in Figure 7.1. In cells incubated in the high glucose concentrations the measured cathepsin B (64.5 ± 5.1%, $p < 0.001$), L (64.5 ± 5.1, $p < 0.001$) and LAL (68.5 ± 6, $p < 0.001$) activities were significantly lower than the cells that were incubated in the normal 5.5 mM glucose (activity taken as 100%). However the presence of TEMPOL in either condition did not result in any significant differences. Thus addition of TEMPOL did not modulate the inhibition of lysosomal activities observed between the different concentrations of glucose as there were no statistical differences observed within the equivalent glucose treatment groups.

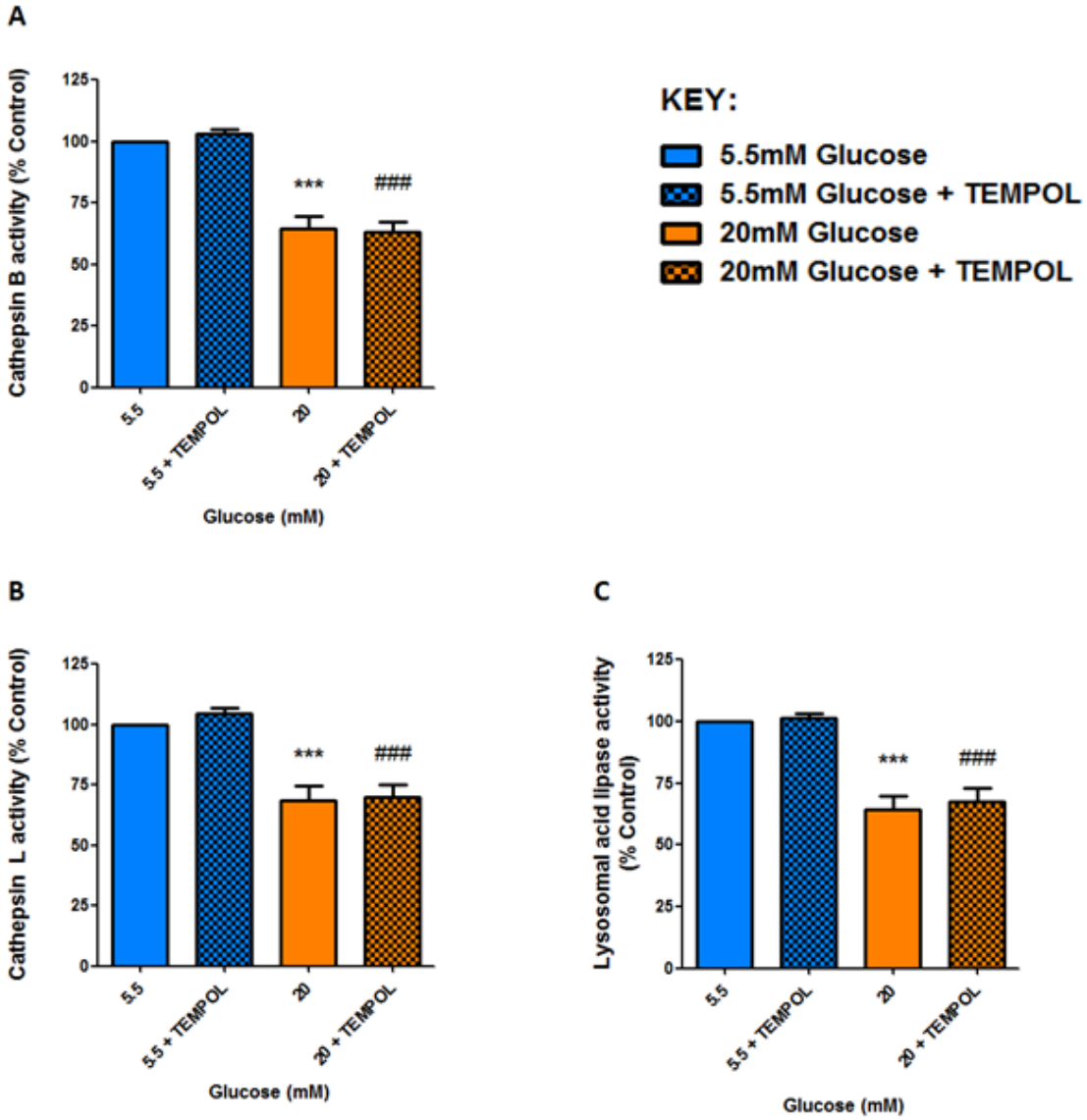

Figure 7.1: Lysosomal enzymatic activities in human monocytes matured under normal 5.5 mM or high 20 mM glucose concentrations with or without 100 µM TEMPOL supplementation for 10 days.

Lysates of human monocytes that had been exposed to the normal 5.5 mM (blue) or 20 mM (orange) glucose with or without TEMPOL (100 µM) were examined for the activities of lysosomal cathepsin B (Panel A), L (Panel B) and LAL (Panel C). Data (mean ± SEM) are the linear change in fluorescence intensity with time from 5 independent donors. Statistical significant inhibition of lysosomal activities were examined at *** $p < 0.001$ against the normal 5.5 mM glucose conditions, and ### $p < 0.001$ versus the normal glucose with TEMPOL supplementation. No statistical differences were detected between the samples with the same glucose treatment.

7.4.2 Protein content of human monocyte cells matured in varying glucose and LPS concentrations

Initially the human monocytes from a single donor were incubated with the normal 5.5 mM and high 20 mM glucose concentrations for 10 days with this followed by 24 or 48 hr treatment with LPS (0, 50 and 200 ng/mL). This was to determine whether different times or concentrations of LPS affected cell confluence and total concentration of protein in HMDM that were matured in the presence of normal or high glucose. The protein levels of the cells from various conditions were determined by the BCA protein assay by use of a standard curve generated using BSA as discussed in Section 2.4.1. The protein concentration in the zero LPS and zero time condition was 0.6 µg/µL and there were no statistical differences observed in the protein content in the normal and high glucose treated HMDM that were subsequently stimulated for 24 or 48 hr incubations with 0, 50 and 200 ng/mL of LPS as shown in Figure 7.2.

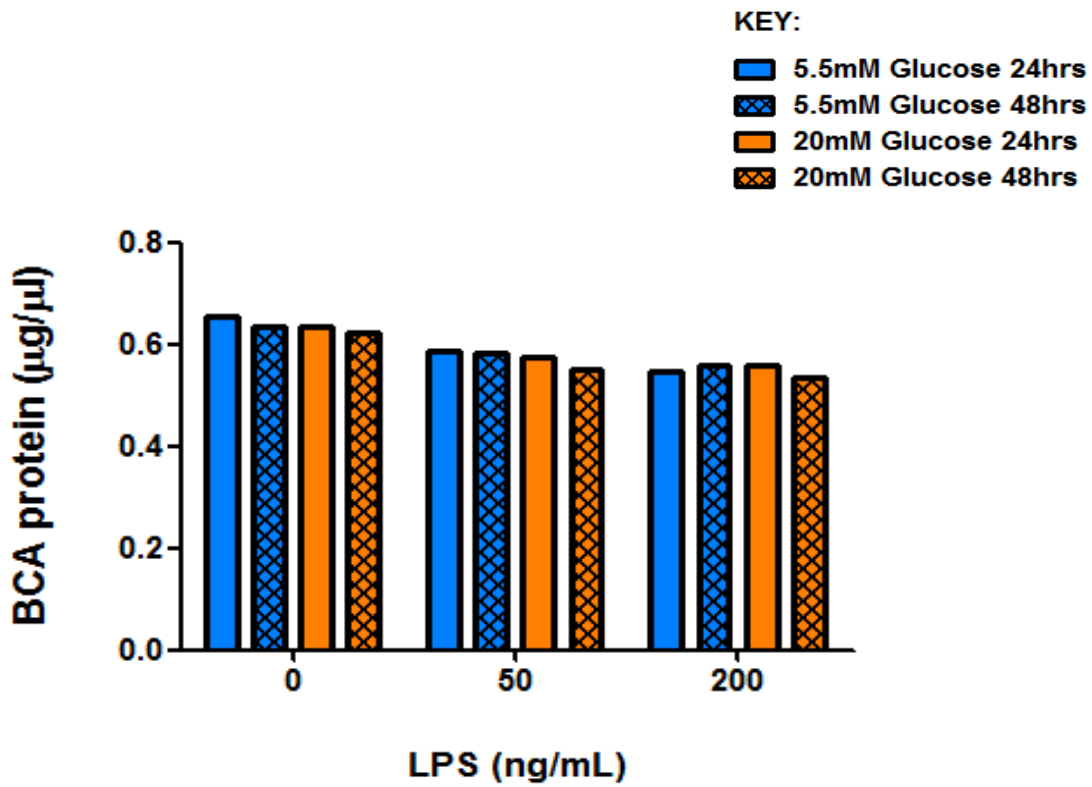

Figure 7.2: Protein levels for HMDM cells subject to LPS stimulation (0, 50 and 200 ng/mL) for 24 or 48 hrs after maturation for 10 days in normal 5.5 mM (blue) and high 20 mM (orange) glucose concentrations.
BCA protein levels were determined for HMDM that had been matured in normal 5.5 mM or high 20 mM glucose levels for 10 days followed by LPS stimulation at 0, 50 and 200 ng/mL for 24 or 48 hrs. Values (µg/µL) are expressed as a mean of triplicate experiments from one monocyte donor.

7.4.3 MCP-1, IL-6, MIF, CRP, TNF-α and MIP- 1α expression by normal and hyperglycaemic HMDM after LPS stimulation

Macrophages play a key role in the chronic inflammatory response in part by generating cytokines such as MCP-1, IL-6, MIF, CRP, TNF-α and MIP- 1α. MCP-1 is part of the chemostatic family and therefore also referred to as chemokine (C-C motif) ligand 2 (CCL2) and small inducible cytokine A2. MCP-1 is over secreted by many cell types including monocytes and macrophages at sites of inflammation triggered by either tissue injury or infection, which are commonly encountered with atherosclerosis, obesity, diabetes, insulin resistance, metabolic dysfunction and adiposity [312,361]. IL-6 is a biomarker of inflammation that is secreted by T cells and macrophages to stimulate the immune response in particularly after tissue injury leading to inflammation, and elevated levels have been associated with the metabolic syndrome and obesity [313,362]. MIF (also known as glycosylation-inhibiting factor, GIF), is an important regulatory protein of the innate immune response released by the anterior pituitary gland. Elevated levels of MIF have been associated with diabetes, atherosclerosis and obesity [427,428,429,430,431,432,433,434,435,436], and lower levels of MIF protect against pancreatic beta-cell apoptosis and dysfunction [428].

CRP is a circulating plasma protein, which is secreted by the liver in response to inflammatory processes [437] and has been associated with the metabolic syndrome, insulin resistance and hyperglycaemia [438,439,440,441,442]. CRP has been shown to be a sensitive biomarker for cardiovascular disease (CVD) and CRP-inhibitors have been investigated as a treatment for cardiovascular disease [440,443,444,445,446].

TNF-α is a cytokine produced by multiple cell types, primarily monocytes and macrophages, which are key inflammatory cells heavily involved in systemic inflammation and innate immunity [440]. Various studies have correlated elevated levels of TNF-α with diabetes [414,416,447,448,449,450], obesity [385,386,451,452,453] and cardiovascular disease [440,454,455,456,457,458,459].

MIP-1α belongs to the chemokine family, and is also known as chemokine (C-C motif) ligand 3 (CCL3). This chemokine is secreted by many cell types, but particularly monocytes, macrophages, dendritic cells and lymphocytes and it is important for immune responses in infection and inflammation [460]. Higher levels of MIP-1α have been implicated in a number of studies of hyperglycaemia, obesity and atherosclerosis [449,460,461,462,463,464,465,466,467].

These cytokines which are associated with inflammation and tissue injury have been shown to be enhanced with hyperglycaemia, accelerated atherosclerosis and altered vascular wall function [387,414,447,448,449,450,468]. Therefore the concentrations of these cytokines were determined to examine the effect of high glucose and TEMPOL upon these potential pro-inflammatory factors.

As normal and hyperglycaemic HMDM that were exposed to high concentrations of LPS for 24 or 48 hrs did not have significantly different levels of cell protein, the levels of cytokines were further examined at both time points. The levels of MCP-1, IL-6, MIF, CRP, TNF-α and MIP-1α were determined in the supernatants from cells that were stimulated with 0, 50 and 200 ng/mL of LPS as described in Sections 2.12.1 and 2.12.2.

Levels of MCP-1, IL-6, TNF-α and MIP-1α were increased with LPS stimulation, however there were no significant differences observed in MCP-1 and IL-6 levels in HMDM that were stimulated with 50 or 200 ng/mL of LPS for either 24 or 48 hr incubation periods as shown in Figure 7.4.

A dose dependent increase in TNF-α and MIP-1α expression was seen with increasing concentrations of LPS as shown in Panels E and F in Figure 7.4. There was a marked up-regulation of TNF-α and MIP-1α levels in the hyperglycaemic HMDM when compared to the normal glucose cells that were stimulated with LPS at 50 and 200 ng/mL for either 24 or 48 hrs. The differences between the two glucose treatment groups were more evident in the cells that were stimulated with 50 or 200 ng/mL LPS for 24 hrs.

MIF was detected in the supernatants however there were no differences between the two incubation periods and no differences were observed between the different glucose concentrations and LPS levels. CRP was also detected in the supernatants that were not stimulated with LPS. There was a decrease in CRP levels in hyperglycaemic HMDM when compared to the normal glucose condition, with the reduction observed with high glucose more noticeable with LPS stimulation.

Overall there was also an elevation in TNF-α and MIP-1α expression and a reduction in CRP levels in HMDM that were incubated with high glucose (20 mM). The largest differences between the normal and high glucose conditions occurred between 0 and 50 ng/mL LPS at 24 hrs. This was followed by smaller changes between 50 and 200

ng/mL LPS, with even fewer differences observed for the 48 hr incubation periods. Hence lower concentrations of LPS of 0, 25 and 50 ng/mL and a 24 hr incubation period were used for subsequent experiments, as the differences in TNF-α, MIP-1α and CRP levels between the two glucose treatments were greatest with 50 ng/mL LPS for 24 hrs. These three cytokines were therefore investigated in depth for five donors to see if the up regulation of TNF-α and MIP-1α, and down regulation of CRP levels were reproducible for the two glucose concentrations in macrophages with lower levels of LPS stimulation for 24 hrs. Simultaneously the effect of TEMPOL upon both normal and hyperglycaemic HMDM was investigated.

7.4.4 Protein content of human monocyte cells matured in varying glucose, TEMPOL and LPS concentrations

In these follow up experiments lower LPS levels of 0, 25 and 50 ng/mL were used as the optimal changes were observed to occur between 0 and 50 ng/mL of LPS at 24 hrs (refer to Figure 7.3). Differences in TNF-α, MIP-1α and CRP levels between the two (5.5 mM and 20 mM) glucose treatments were then assessed after 24 hrs in the absence and presence of (100 μM) TEMPOL. Data was obtained from cells from five different donors. BCA protein contents were determined for the cells at 0 and 24 hrs and LPS concentrations of 0, 25 and 50 ng/mL with and without TEMPOL (100 μM) for normal and high glucose treated HMDM cells. A protein concentration of 0.6 μg/μL was determined for the control cells and there were no statistical differences observed in the protein content in the HMDM that were stimulated with 0, 25 and 50 ng/mL of LPS with normal and high glucose concentrations with or without TEMPOL supplementation as shown in Figure 7.4.

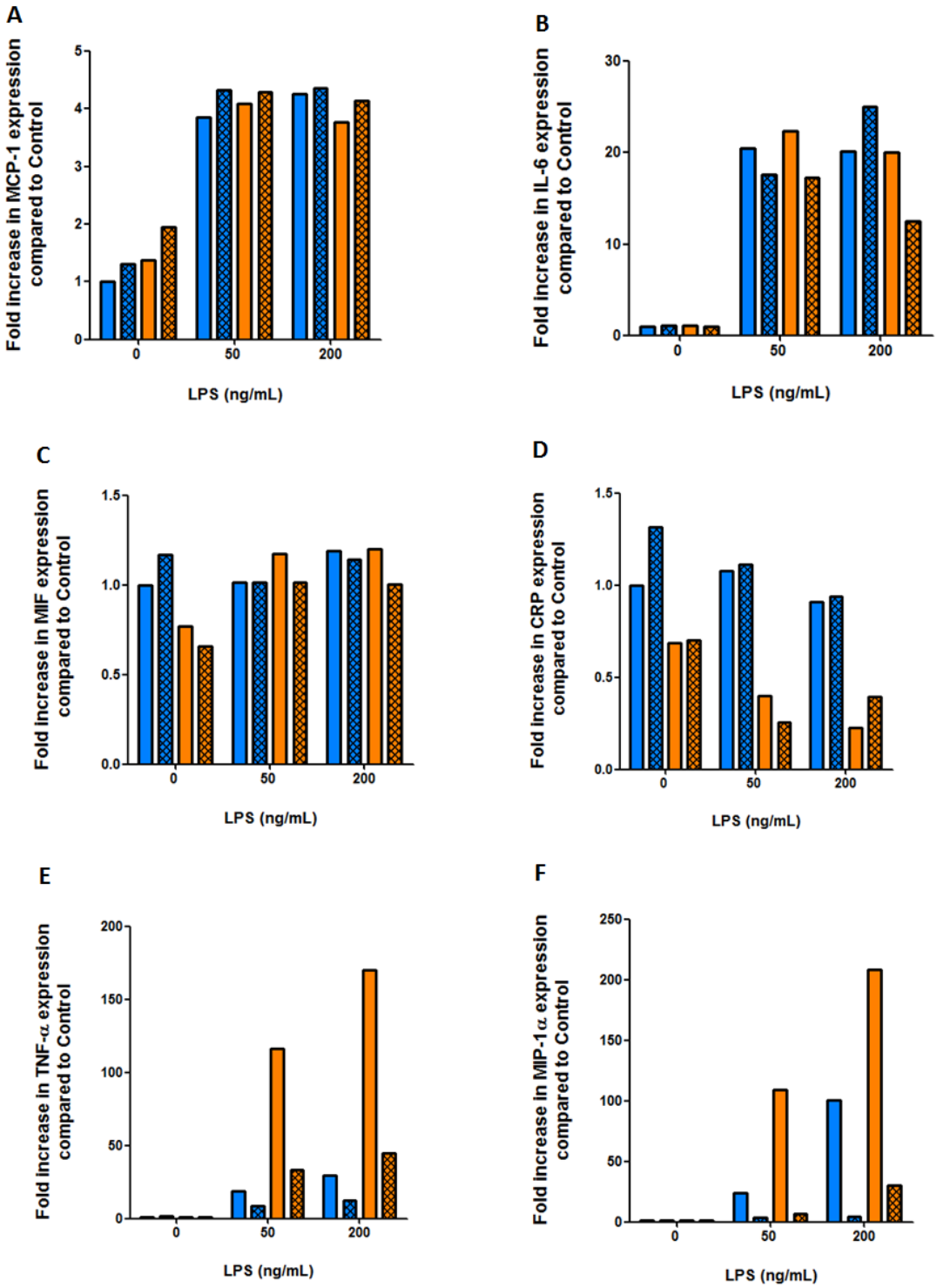

Figure 7.3: Fold increase in MCP-1 (Panel A), IL-6 (B), MIF (C), CRP (D), TNF-α (E) and MIP-1α (F) expression compared to control (5.5 mM glucose) for 24 (clear bars) and 48 hrs (hatched bars) of LPS stimulation (0, 50 and 200 ng/mL) in HMDM that were matured for 10 days in normal 5.5 mM (blue) and high 20 mM (orange) glucose concentrations.

Measurement of fold increase in MCP-1, IL-6, MIF, CRP, TNF-α and MIP- 1α expression compared to the normal 5.5 mM glucose (used as control) HMDM were incubated with normal (5.5 mM) or high (20 mM) glucose levels for 10 days followed by LPS stimulation with 0, 50 and 200 ng/mL for 24 or 48 hrs. Values in μg/μL are expressed as a mean of triplicate experiments from one monocyte donor.

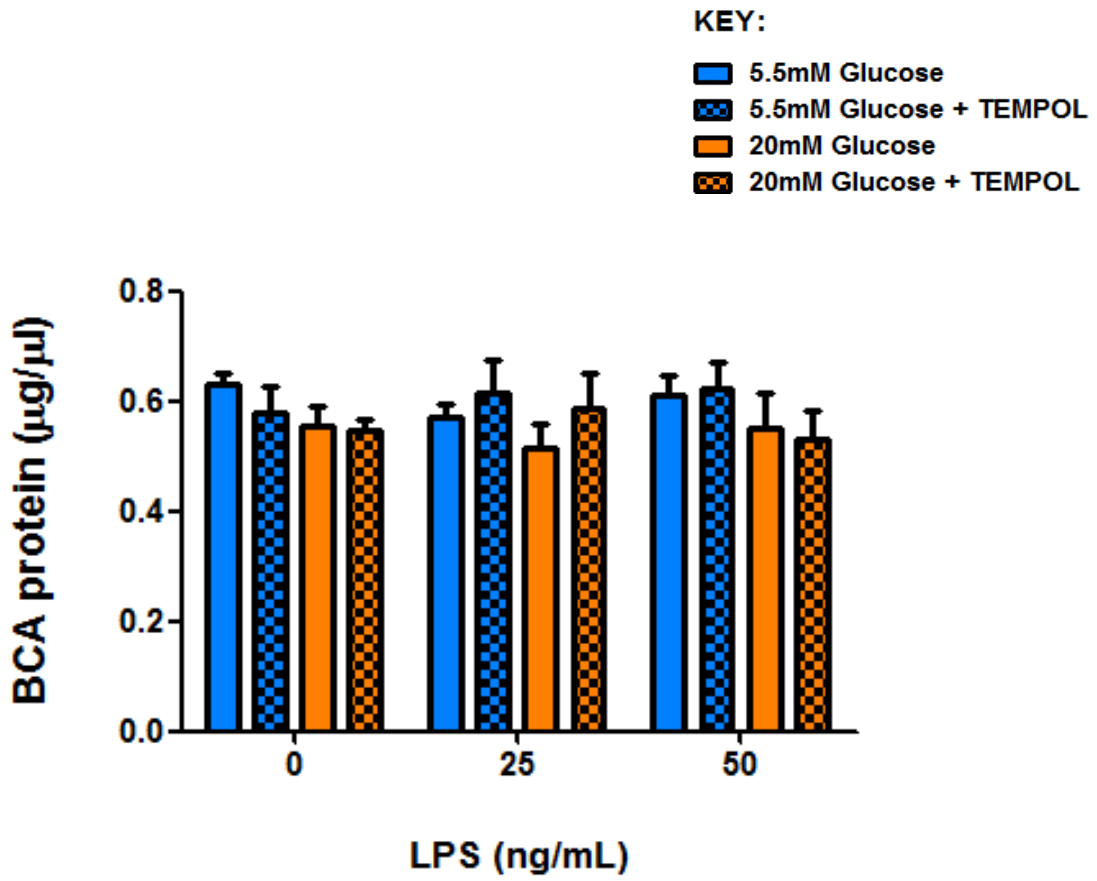

Figure 7.4: Protein levels for HMDM cells after LPS stimulation (0, 25 and 50 ng/ mL) for 24 hrs after maturation for 10 days in normal 5.5 mM (blue) and high 20 mM (orange) glucose concentrations with and without 100 µM TEMPOL supplementation.

BCA protein levels (in µg/µL) were measured for HMDM that were matured in the normal 5.5 mM and high 20 mM glucose levels supplemented with and without TEMPOL for 10 days followed by LPS stimulation at 0, 25 and 50 ng/mL for 24 hrs. Data (mean ± SEM) are from five independent donors. No statistical differences were detected between any of the conditions.

7.4.5 Effects of TEMPOL on C-Reactive Protein (CRP) levels from LPS induced normal and hyperglycaemic HMDM

CRP levels were shown to be reduced with high glucose conditions in the pilot study, as shown in Figure 7.5, and this was further examined with multiple donors. The CRP levels were also determined in HMDM to examine the potential effects of TEMPOL upon CRP levels secreted by HMDM that were matured in normal (5.5 mM) and high (20 mM) glucose concentrations supplemented with and without TEMPOL. There were no statistical differences in CRP levels in the HMDMs that were incubated

in the normal 5.5 mM and high 20 mM glucose concentrations with 0, 25 or 50 ng/mL of LPS stimulation. There were no statistical changes observed in the normal and high glucose treated HMDM with or without TEMPOL supplemented in the media.

Overall these results showed that there were no changes in CRP levels when the cells were exposed to 100 µM compared to 0 µM TEMPOL at either concentration of glucose or the different concentrations of LPS as shown in Figure 7.5.

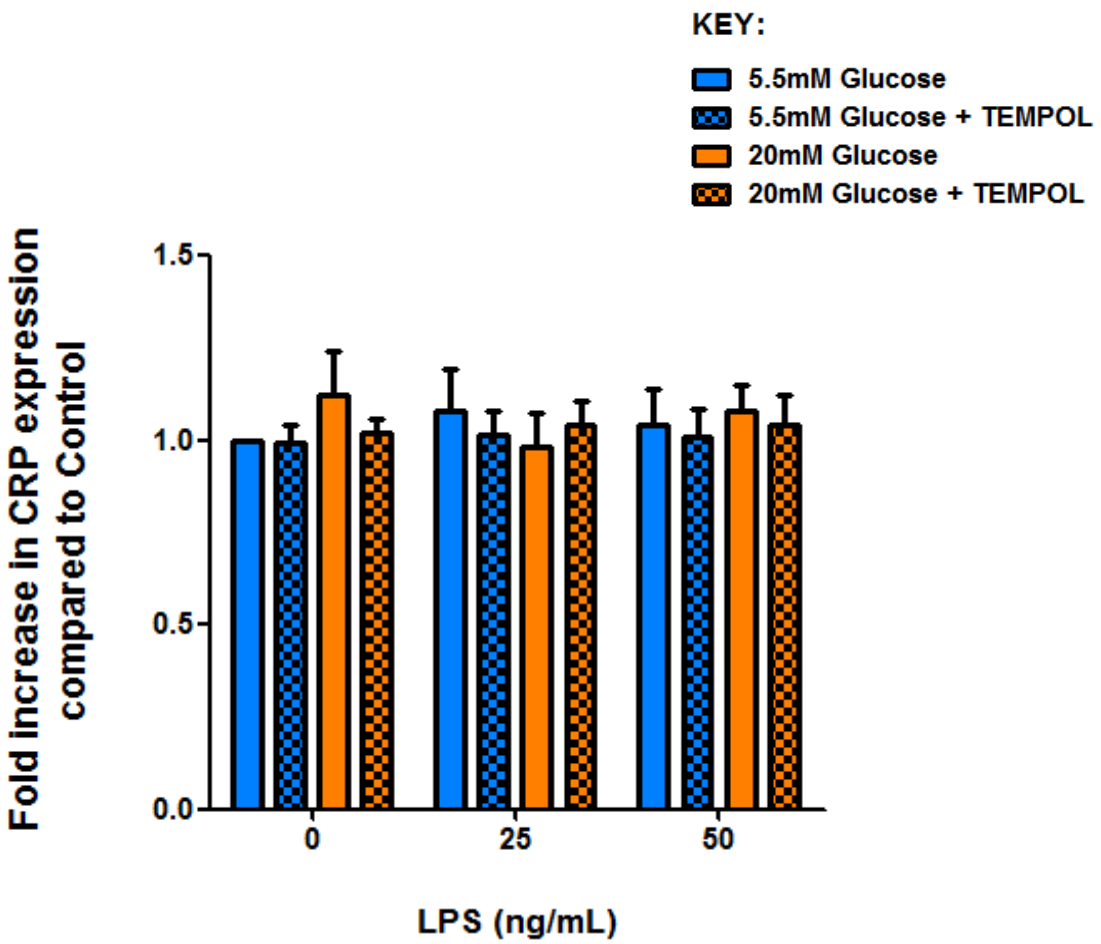

Figure 7.5: Fold increase in CRP expression compared to control (5.5 mM glucose) after 24 hrs of LPS stimulation (0, 25 and 50 ng/mL) for HMDM that had been matured for 10 days in normal 5.5 mM (blue) or high 20 mM (orange) glucose concentrations with and without 100 µM TEMPOL supplementation.
Measurement of fold increase in CRP expression compared to the normal (5.5 mM) glucose (used as control) HMDM that were incubated with normal (5.5 mM) or high (20 mM) glucose levels supplemented with and without TEMPOL for 10 days followed by LPS stimulation at 0, 25 and 50 ng/mL for 24 hrs. Data (mean ± SEM) are expressed in µg/µL from five independent donors.

7.4.6 Effects of TEMPOL on Tumour Necrosis Factor-α (TNF-α) levels from LPS induced normal and hyperglycaemic HMDM

As enhanced secretion of TNF-α was detected with high glucose compared to the normal glucose treated HMDM in the initial experiments, this was investigated further with multiple donors. TEMPOL was investigated to determine whether it counteracts the increased secretion of TNF-α induced by high glucose levels. Therefore TNF-α levels were assessed in media from HMDM to examine the effect of TEMPOL upon TNF-α levels for cells matured in normal 5.5 mM and high 20 mM glucose concentrations with and without TEMPOL supplementation.

Cells were exposed to 0, 25 and 50 ng/mL of LPS for 24 hrs after the maturation of monocytes to macrophages over 10 days. There was a dose dependent increase in TNF-α levels with increasing concentrations of LPS, as shown in Figure 7.6. There were no statistical differences in TNF-α levels across the groups when HMDM were not stimulated with LPS.

For the cells that were exposed to 25 ng/mL of LPS for 24 hrs, TNF-α levels were significantly upregulated in HMDM that were incubated with high glucose (360.3 ± 161.9 fold increase over control) when compared to the normal glucose condition (131.4 ± 55.6 fold increase over control, $p < 0.01$), normal glucose with TEMPOL (132.3 ± 64.2 fold increase over control, $p < 0.01$) and high glucose with TEMPOL (124.6 ± 58.8 fold increase over control, $p < 0.01$).

Similarly when identical groups of cells were exposed to 50 ng/mL of LPS there was a significant elevation of TNF-α levels in HMDM that were incubated with high glucose (485.6 ± 197.8 fold increase over control) when compared to normal glucose (188.5 ± 80 fold increase over control, $p < 0.001$), normal glucose with TEMPOL (202.6 ± 96.5 fold increase over control, $p < 0.001$) and high glucose with TEMPOL (157.3 ± 69.8 fold increase over control, $p < 0.001$).

HMDM incubated in high glucose levels (20 mM) had significantly elevated TNF-α levels when compared to both the HMDM groups that were incubated with normal glucose regardless of TEMPOL supplementation. TEMPOL significantly attenuated the elevation of TNF-α expression that was induced by high glucose. The TNF-α levels determined for the cells incubated in high glucose with TEMPOL were

similar to those of the normal glucose treated cells with no statistical differences observed.

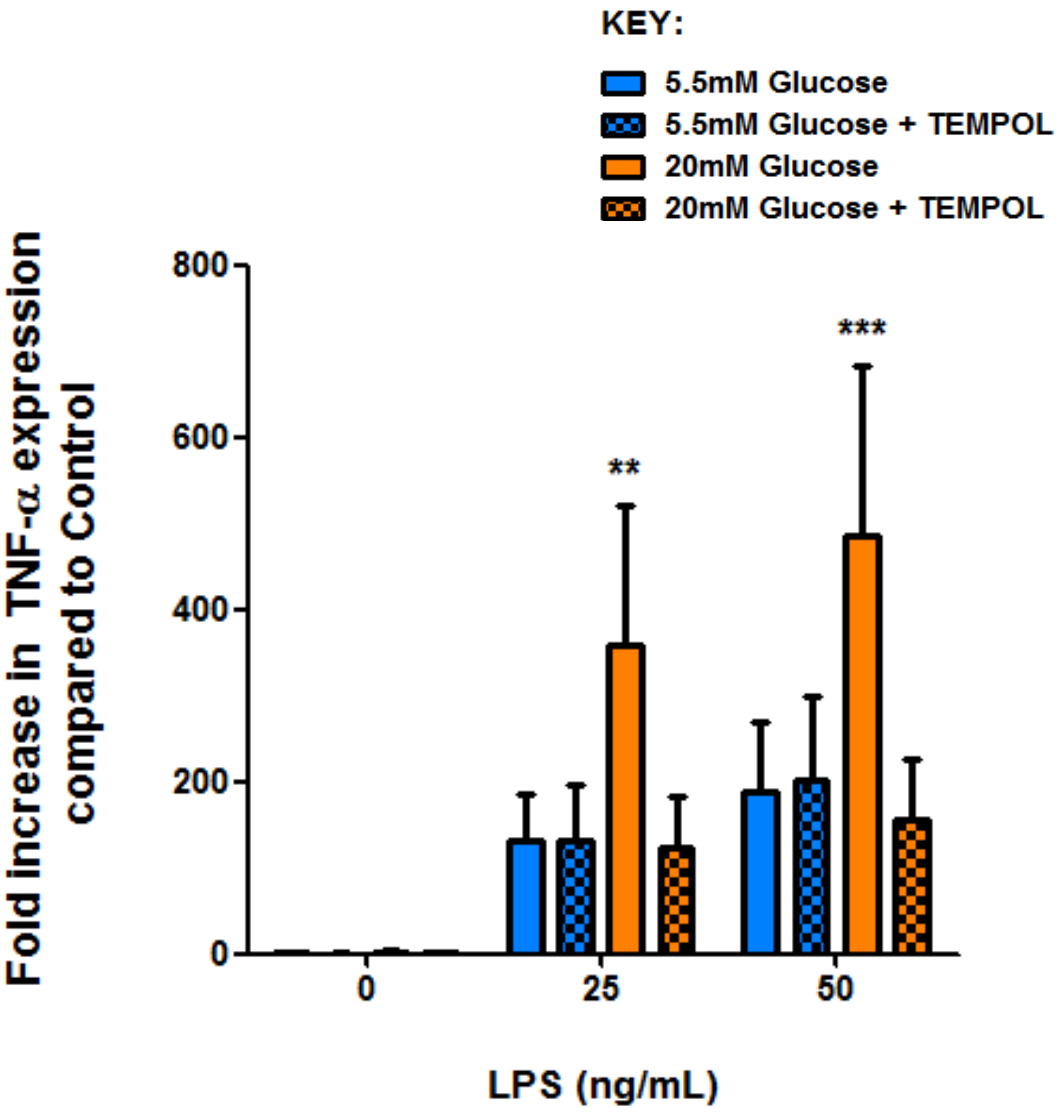

Figure 7.6: Fold increase in TNF-α expression compared to control (5.5 mM glucose) after 24 hrs of LPS stimulation (0, 25 and 50 ng/mL) for HMDM that were matured for 10 days in normal 5.5 mM (blue) and high 20 mM (orange) glucose concentrations with and without 100 µM TEMPOL supplementation.
Measurement of fold increase in TNF-α expression compared to the normal (5.5 mM) glucose (used as control) HMDM that were incubated with normal (5.5 mM) or high (20 mM) glucose levels supplemented with and without TEMPOL for 10 days followed by LPS stimulation at 0, 25 and 50 ng/mL for 24 hrs. Data (mean ± SEM) are expressed as µg/µL from five independent donors. Statistical significance is achieved at ** $p < 0.01$ and *** $p < 0.001$ versus the remaining groups; 5.5 mM glucose, 5.5 mM glucose with TEMPOL and 20 mM glucose with TEMPOL by two-way ANOVA followed by Bonferroni's post-hoc test.

7.4.7 Effects of TEMPOL on Macrophage Inhibitory Protein-1α (MIP-1α) secretion by LPS induced normal and hyperglycaemic HMDM

As elevation of MIP-1α levels was observed with high glucose compared to the normal glucose treated HMDM cells in the pilot studies, this was subsequently examined for multiple donors. TEMPOL was also investigated to observe whether it suppresses the MIP-1α levels induced by high glucose levels. MIP-1α levels were assessed in HMDM to examine the effect of TEMPOL upon MIP-1α levels secreted by HMDM that were matured in normal 5.5 mM and high 20 mM glucose concentrations supplemented with and without TEMPOL.

Cells were exposed to 0, 25 and 50 ng/mL of LPS for 24 hrs after the maturation of monocytes to macrophages. There was a dose dependent increase in MIP-1α levels when cells were exposed to 0, 25 and 50 ng/mL of LPS, as shown in Figure 7.7. There were no statistical differences in MIP-1α levels across the groups when HMDM were not stimulated with LPS.

For the cells that were exposed to 25 ng/mL of LPS for 24 hrs, MIP-1α levels were significantly increased in HMDM that were matured in high glucose (46.1 ± 7.7 fold increase over control) when compared to the normal glucose (16.9 ± 3 fold increase over control, $p < 0.001$), normal glucose with TEMPOL (18.2 ± 1.7 fold increase over control, $p < 0.001$) and high glucose with TEMPOL (17 ± 2.7 fold increase over control, $p < 0.001$).

Similarly when identical groups of cells were exposed to 50 ng/mL of LPS there was a significant elevation of MIP-1α levels in HMDM that were incubated with high glucose (49 ± 10.2 fold increase over control) when compared to normal glucose (28.4 ± 1.8 fold increase over control, $p < 0.001$), normal glucose with TEMPOL (29 ± 3.8 fold increase over control, $p < 0.001$) and high glucose with TEMPOL (28.2 ± 5.6 fold increase over control, $p < 0.001$).

HMDM matured in high glucose (20 mM) had significantly higher MIP-1α levels than both the HMDM groups that were incubated with normal glucose regardless of TEMPOL supplementation. TEMPOL significantly attenuated the elevation of MIP-1α expression that was induced by high glucose. The MIP-1α levels detected form the cells exposed to high glucose with TEMPOL were similar to those of the normal glucose treated cells, with no statistical differences detected.

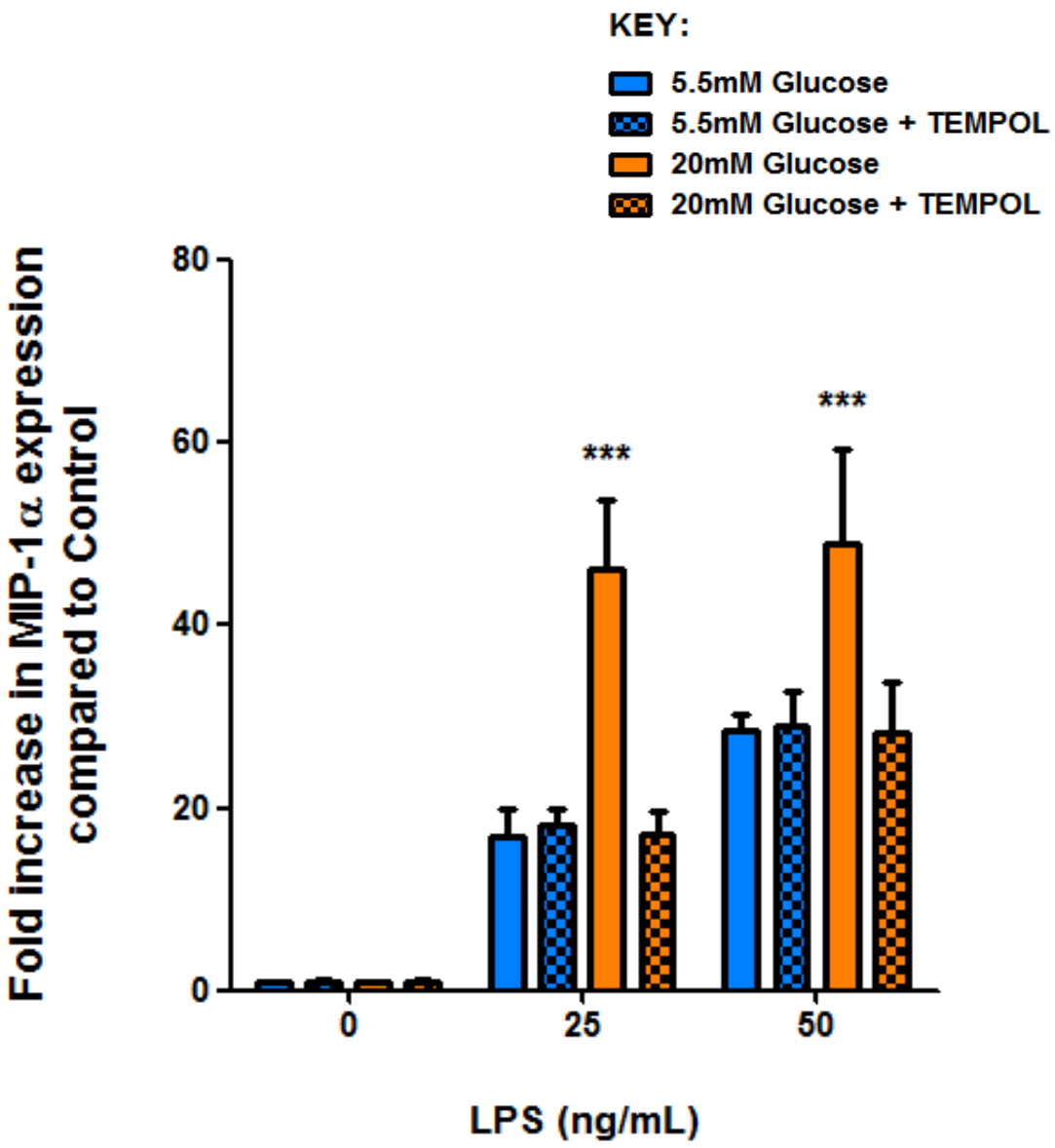

Figure 7.7: Fold increase in MIP-1α expression compared to control (5.5 mM glucose) after 24 hrs of LPS stimulation (0, 25 and 50 ng/mL) for HMDM that were matured for 10 days in normal 5.5 mM (blue) and high 20 mM (orange) glucose concentrations with and without 100 µM TEMPOL supplementation.
Measurement of fold increase in MIP-1α expression compared to the normal (5.5 mM) glucose (used as control) HMDM that were incubated with normal (5.5 mM) or high (20 mM) glucose levels supplemented with and without TEMPOL for 10 days followed by LPS stimulation at 0, 25 and 50 ng/mL for 24 hrs. Data (mean ± SEM) are expressed as µg/µL from five independent donors. Statistical significance is achieved at *** $p < 0.001$ versus the remaining groups; 5.5 mM glucose, 5.5 mM glucose with TEMPOL and 20 mM glucose with TEMPOL by two-way ANOVA followed by Bonferroni's post-hoc test.

7.5 Discussions

TEMPOL has been studied extensively as it has been reported to have potent anti-inflammatory activity which may therefore have therapeutic benefits in addition to reducing oxidative and / or glycative damage that initiates and accelerates progression of a number of inflammatory diseases [330,336,340,341,342,343,344,345,373,375,424]. Therefore compounds like TEMPOL may be valuable as novel therapies for the treatment of diabetes [343,344,345,424], obesity [330,340,341,342] and atherosclerosis [373,375]. Monocytes and macrophages are heavily involved in inflammatory diseases such as atherosclerosis, and the current studies demonstrated that their functions are influenced by hyperglycaemia [228,317]. Human monocyte-derived macrophages provide an ideal *in vitro* model to assess lysosomal function, and potential anti-inflammatory and other immune-modulatory effects [244].

Dosages of 5 mM TEMPOL have been reported as being relatively safe, as no adverse effects emerged on cell growth and viability in various *in vitro* studies [377,447,469,470]. Therefore it was assumed that TEMPOL supplementation at 100 μM was likely to be well tolerated at both test levels for glucose. Indeed a previous study has examined human monocytes that were exposed to 30 mM glucose with 100 μM TEMPOL [447]. In the present study TEMPOL at 100 μM did not affect the cellular protein levels significantly for the various glucose conditions or LPS treatments.

Glucose levels ranging from 10 to 30 mM are commonly used in *in vitro* studies of diabetes [244,471,472,473]. Potential defects in lysosomal degradation induced by exposure to high glucose have been investigated in monocytes and macrophages that were incubated with 10 to 30 mM glucose [244] and the extent of these changes have been examined in Chapters 3 and 4. For maturing monocytes and developed macrophages the inhibition of lysosomal activities, and the reductions detected in protein expression and lysosomal number were seen at 20 mM glucose and higher. Likewise, in the current study, reductions in cathepsins B, L and LAL enzymatic activities were detected in macrophages that were exposed to equivalent glucose conditions. This impairment of lysosomal activities may result in poor clearance of both native and modified proteins, including those internalised by endocytosis, or trafficked intracellularly and may help account for the lipid accumulation detected in macrophages causing foam cells.

TEMPOL (100 μM) supplementation did not arrest the inhibition of lysosomal activity induced by high glucose in HMDM cells. Therefore TEMPOL may not have an effect upon the lysosomal dysfunction induced by high glucose, or a higher dosage of TEMPOL may be required to observe any distinctive changes. Notably, TEMPOL appears to have an effect upon protein degradation system via a different mechanistic pathway, possibly via activating the protein kinase RNA-like endoplasmic reticulum kinase (PERK) [474]. Activation of the unfolding protein response (UPR) caused by endoplasmic reticulum- and oxidative-stress may stimulate c-jun N-terminal kinase (JNK). ROS generated from this activation can result in an accumulation of misfolded proteins, beta cell dysfunction, apoptosis and altered protein secretion [475,476]. Rats infused with TEMPOL (2.41 μM/kg/min) and high glucose (15 - 22 mM) were shown to have preserved endoplasmic reticulum function and reduced oxidative stress and beta cell dysfunction in isolated islets compared to the high glucose alone condition [474,477]. Butylated hydroxyanisole (BHA), a lipid-soluble antioxidant was also shown to suppress endoplasmic reticulum stress and protein secretion in $chop^{-/-}$ C57BL/6 mice [475].

Although TEMPOL (100 μM) did not arrest the decrease in lysosomal enzymatic activities induced by high glucose, further studies were carried to investigate the anti-inflammatory potential of TEMPOL. Macrophages play a critical role in innate immunity and inflammatory processes by synthesising and releasing particular cytokines, and elevated levels of MCP-1, IL-6, MIF, CRP, TNF-α, MIP-1α have been associated with hyperglycaemia, accelerated atherosclerosis and altered vascular wall function [387,414,447,448,449,450,468]. A range of pro-inflammatory cytokines and agents were significantly reduced by TEMPOL (58 mM) in hyperlipidaemic and obese mice resulting from feeding with a HFD as reported in Chapter 6. Up-regulation of inflammatory pro-cytokines has been reported in various studies of diabetes [317,414,416,418,438,439,447,448,449,450,468], atherosclerosis [50,415,440,454,462,463] and obesity-related metabolic dysfunction [94,385,386,442,451,452,453,461] and cardiovascular diseases [443,445,455,456,457,458,459]. Therefore the potential inhibitory action of TEMPOL upon inflammatory cytokine release was investigated in HMDM exposed to high glucose and LPS.

Hyperglycaemia is a well known risk factor for both micro- and macrovascular disease and a number of studies have implicated changes in the inflammatory response in the early stages of diabetes and obesity [478,479]. People with diabetes with microvascular complications have been reported to have augmented production of inflammatory biomarkers, such as pro-inflammatory cytokines, over and above the levels detected in Type 1 diabetic (T1D) patients without microvascular complications and healthy control subjects [480,481,482,483]. Higher MIF have been detected in pregnant women with gestational diabetes [427] and a deficiency in MIF was shown to be protective from palmitic acid-induced apoptosis in pancreatic islets [428]. Although up-regulation of pro-inflammatory cytokines is commonly encountered in people with hyperglycaemia, the pilot study carried out here with cells from one healthy donor showed that high glucose did not affect LPS-induced MCP-1, IL-6 and MIF levels. However TNF-α and MIP-1α levels were notably raised, and CRP levels were decreased, in macrophages that were matured in high glucose.

Subsequent studies were carried out with human monocytes from five independent healthy donors that were matured to HMDM cells to confirm the elevation of TNF-α and MIP-1α and the reduction of CRP levels detected in the pilot studies. Further studies confirmed that high glucose (20 mM) matured in HMDM cells elevated the secretion of TNF-α and MIP-1α levels in response to LPS.

High glucose did not affect CRP levels, despite the increasing levels of LPS and glucose concentrations to which the HMDM were exposed. CRP levels have been reported to be higher in Type 2 diabetes and diabetic nephropathy patients compared to healthy subjects and IL-6 levels were positively associated with severity of the disease [468]. Furthermore higher levels of CRP have been detected in the plasma of diabetic patients [438,439,440,441,442] and this has been reported to be a sensitive biomarker for CVD and atherosclerosis [440,443,444,445,446]. However this was not shown for human macrophages in *in vitro* studies. CRP is predominantly produced and released by the liver [437] which may be another reason as to why no differences were observed despite the varying levels of LPS (0 - 200 ng/mL) used to treat the human macrophages. This may suggest that only low levels of CRP are available in HMDM for secretion when induced by LPS. Testing for CRP levels in a different cell types may be worthwhile, in particularly in hepatocytes where CRP is primarily synthesised, and where the effect of TEMPOL upon CRP levels induced by high glucose may be more obvious. In contrast, the levels of TNF-α and MIP-1α were extremely responsive to

higher glucose concentrations for the same HMDM donors used to assess CRP levels suggesting that there were no problems with the cells in the experiments used.

High glucose elevated the secretion of TNF-α and MIP-1α in response to LPS. Elevation of pro-inflammatory cytokines induced by high glucose has been reported in both *in vitro* and *in vivo* studies. Thus human monocytes that were incubated with 30 mM glucose and treated with LPS (500 ng/mL; 24 hrs) increased secretion of MIP-1α levels, and higher levels of IL-6, IL-8, and MIP-1β were observed when compared to normal 5.6 mM glucose from U-937 monocytes [449]. Increases in TNF-α expression along with IL-1β, IL-6, IL-12, IL-18 were detected and found to be stimulated by hyperglycaemia *in vivo* from mouse peritoneal macrophages from STZ-induced diabetic C57BL/6 mice [414]. Macrophages from mice with diabetes (16.8 - 28 mM glucose) were also found to produce significantly more TNF-α, IL-6 and reactive oxygen intermediates than cells from normoglycaemic control CBA/J mice [450].

TEMPOL has been reported to alleviate high glucose induced oxidative stress [424,425,447,474]. In the current study, TEMPOL (100 μM) significantly attenuated the elevation of TNF-α and MIP-1α levels released from human macrophages induced by 20 mM glucose, where many studies have reported an increase in these cytokines [414,447,448,449,450,460,461,462,463,464,465,466,467]. Given that TEMPOL at the same concentration also inhibited TNF-α levels in human monocytes exposed to a glucose concentration of 30 mM, and this was associated with inhibited ROS production, the probable mechanism in the current study would be the antioxidant activity of TEMPOL [447]. Interestingly TEMPOL was shown to block MCP-1 and IL-6 release from endothelial cells that were stimulated with TNF-α, IL-1 and IFN-γ cytokines in order to engender the production of ROS [387]. TEMPOL (1 mM in drinking water) has also been shown to exert protective antioxidative effects against renal dysfunction in streptozotocin-induced diabetic rats, as malondialdehyde levels were significantly reduced, and this was coupled with a decrease in activity of superoxide dismutase and glutathione peroxidase [424]. In another animal model the same dose of TEMPOL (1 mM in drinking water) did not prevent early renal injury (proteinuria) induced by caffeine, but was found to suppress late stage renal inflammatory, proliferative and fibrotic changes that were inflicted by chronic caffeine consumption in obese ZSF1 rats [484]. Further to this, hypertension and insulin resistance were found to be associated with greater secretion of MCP-1 and TNF-α levels in the soleus rat muscle, with these changes being attenuated by TEMPOL [485].

These findings suggest that TEMPOL ameliorates inflammation and oxidative stress caused by conditions that include high blood glucose levels. However, it cannot be excluded that the inhibition by TEMPOL of TNF-α and MIP-1α secretion induced by high glucose treatment may also indicate that other pathways may contribute to the inhibition of the inflammatory responses seen in diabetes and cardiovascular disorders such as atherosclerosis. Chemokine receptors have been shown to influence lipoprotein metabolism and atherosclerosis in mice [486,487,488,489,490]. Thus MIP-1α (CCL3) levels have been found to play a crucial role in lipid metabolism in hyperlipidaemic fat-fed mice and to be positively associated with disease in various mouse models of atherosclerosis [462,491], and in human carotid endarterectomy samples [492]. Plasma lipids, leptin and insulin concentrations, atherosclerotic lesion area, the presence of lesional T lymphocytes, body adiposity, hepatic triglycerides and TNF-α levels in the adipose tissue were also significantly lower in $CCL3^{-/-}$ hyperlipidaemic mice [462].

MIP-1α levels have also been shown to be elevated on incubation of mouse peritoneal macrophages with VLDL [493], however the effect of TEMPOL upon MIP-1α secretion engendered by lipid remains unknown. The current study is the first to reveal that enhanced generation of TNF-α and MIP-1α levels by human macrophages induced by high glucose can be significantly inhibited by TEMPOL. These anti-inflammatory effects strongly suggest that TEMPOL may have a significant role to play in diabetes-associated atherosclerosis which deserves further studies. In the previous chapter, TEMPOL was shown to prevent body weight gain and decrease the levels of several cytokines and inflammatory factors in hyperlipidaemic and obese mice. In the current study, TEMPOL was found to have a profound inhibitory impact upon the secretion of some of these species by human macrophages that had been previously exposed to high glucose.

7.6 Conclusion

Lysosomal dysfunction is evident in HMDM exposed to hyperglycaemic (20 mM) conditions as shown by a decrease in lysosomal cathepsin B, L and acid lipase activities. However, TEMPOL was unable to arrest these detrimental effects on lysosomal function induced by high glucose.

High glucose induced an inflammatory response in HMDM as the levels of TNF-α and MIP-1α levels were significantly elevated. TEMPOL (100 μM) supplementation of these cells exposed to high glucose significantly attenuated the elevation of TNF-α and MIP-1α levels induced by LPS. These are early biomarkers of inflammation and are known to be positively associated with hyperglycaemia, obesity and atherosclerosis. However, the effects of high glucose did not appear to be directly correlated with CRP secretion as there were no notable differences in CRP levels between normal and high glucose concentrations. Therefore it is hard to determine whether TEMPOL had a significant effect upon CRP levels and further studies are required to elucidate the effect of TEMPOL on CRP levels which are elevated in people with diabetes, obesity and related cardiovascular diseases [440,443,444,445,446].

Overall the anti-inflammatory effects exerted by TEMPOL observed in the present and previous chapters, strongly suggest that TEMPOL may have a potential protective role to play in diabetes-associated atherosclerosis.

CHAPTER 8:

DISCUSSION AND FUTURE DIRECTIONS

8.1 Overview

The research undertaken in this project sought to provide molecular insights into the links between diabetes and atherosclerosis, as well as exploring potential anti-glycative and anti-oxidant compounds which may alleviate cardiovascular related diseases induced by hyperglycaemia and hyperlipidaemia.

Hyperglycaemia, which may lead to chronically elevated levels of AGE and glycated proteins, is an independent risk factor for the diabetic complications of atherosclerosis [317]. In atherosclerosis, modified lipoproteins and lipid-laden macrophage-derived foam cells accumulate within lesions and formation of the latter may be partially due to an increased uptake of lipoproteins, decreased or altered intracellular metabolism and / or decreased cholesterol efflux. Modified (lipo) proteins in particular appear to accumulate in cells as a result of the impairment of the endo-lysosomal system, which is responsible for the degradation or turnover of native or modified LDL particles. The potential role of hyperglycaemia in macrophage lysosomal dysfunction has not been fully elucidated, and the impact that high glucose concentrations may have on lysosomes was therefore investigated in both murine and human macrophages (Chapter 3), and monocytes during their maturation to macrophages (Chapter 4).

These studies were subsequently extended to a diabetes-associated atherosclerotic animal model, where diabetes was induced by streptozotocin. This model was then used to investigate the potential anti-glycative, anti-lipidaemic and anti-atherogenic properties of carnosine (Chapter 5).

Hyperlipidaemia, a dominant feature of the metabolic syndrome, is also commonly seen in people with diabetes and cardiovascular diseases. Potential anti-obesity, anti-lipidaemic and anti-inflammatory effects of TEMPOL (Chapter 6) were therefore examined in an animal model where mice were fed a high fat diet or normal chow with or without added TEMPOL. The potent anti-inflammatory effects of TEMPOL that were observed in these hyperlipidaemic obese mice were further investigated in human macrophages exposed to hyperglycaemia-like conditions (Chapter 7). The results obtained in each of these systems are discussed in further detail below.

8.2 Lysosomal dysfunction caused by high glucose in maturing monocytes and macrophages

Lysosomes, are major sub-cellular organelles in macrophages and play a major role in degradation and the removal of a range of biomacromolecules [494]. Dysfunction of lysosomes may be responsible for the accumulation of damaged/glycated proteins and decreased or altered turnover of native or modified low density lipoprotein particles in macrophage foam cells [240,495]. Understanding the factors that influence lipid accumulation in macrophages is therefore an important line of study in diabetes-associated atherosclerosis.

In the initial stages of atherosclerosis, excess sterol is primarily located within lipid droplets of the cell cytoplasm [496]. However, as lesions progress a significant amount of sterol is accumulated within the lysosomes of foam cells [423]. Furthermore an accumulation of oxidised lipids and proteins is known to occur in human atherosclerotic lesions [496,497,498,499], and previous studies have reported an enhanced accumulation of modified proteins and lipids during the development of diabetes-associated atherosclerosis [151,240,495,500].

A possible mechanism for this accumulation is that modified proteins (e.g. glycated, oxidised or chemically modified) LDL are endocytosed via interaction with macrophage scavenger receptors. The endocytosed LDL is transported to the lysosomes to be degraded, with the free cholesterol released into the cytosol. The free cholesterol is then available for efflux from the cell to lipid-free or lipid-poor apolipoprotein A1 and HDL [501,502,503].

Hyperglycaemia may have an impact on a number of these steps such as increased scavenger receptor expression and thus uptake of lipoprotein particles, impeded efflux of cytosolic cholesterol and impaired apolipoprotein A1 and HDL transport [272,504,505]. Macrophage scavenger receptor mRNA and protein levels have been shown to be modulated in HMDM by high glucose, with elevation of LOX1 mRNA and decreased expression of SR-A1, SRB1, LDL-R and CD36 mRNA, however this did not impact the accumulation of cholesteryl esters in the HMDM [272]. This suggests that macrophage scavenger receptor levels may not be the key or sole determining factor in lipid accumulation in human macrophages.

Exposure of macrophages, but not smooth muscle and endothelial cells to glycated LDLs in the absence of high glucose has been shown to result in cholesterol and cholesterol ester accumulation. [151,500]. Furthermore lipid and cholesterol ester accumulation was observed in HMDM that were exposed to LDL glycated with methyglyoxal and glycoaldehyde [240]. This lipid accumulation was accompanied by greater endocytosis, degradation, and intracellular accumulation of modified apo B protein from glycoaldehyde-modified LDL [240]. Inhibition of LDL glycation by hydrazine compounds has been reported to inhibit and reduce lipid loading and foam cell formation in murine macrophage cells [506]. However extensive modification of the LDL was required to see intracellular accumulation of cholesteryl esters, and this may not reflect the situation in people with diabetes. It remains to be established whether high glucose levels alone drives this lipid or protein accumulation and to what degree hyperglycaemia impairs the metabolism and turnover rate of endogenous levels of glycated and oxidised lipoproteins, as these previous studies reported used high amounts of modified and glycated proteins and / or cells with unimpaired lysosomal metabolism.

Cholesterol efflux from cells to apoA-1 and HDL metabolism may be affected by hyperglycaemia with this leading to lipid accumulation and contributing to the progression of atherosclerosis [507,508]. It has been shown that increasing glycation of apo A-1 is associated with a decreased activity of LCAT, a key enzyme in the metabolism of HDL [507]. A deficiency in LCAT activity has been reported for glycated apoA-1 isolated from people with Type 2 diabetes [429,431] and cardiovascular disease [430]. This reduction in enzyme reactivity may result in a decreased or impeded cholesterol efflux, as LCAT drives reverse cholesterol transport by esterifying cellular cholesterol and therefore allowing removal by HDL. Although glycation of apoA-1 may adversely affect reverse cholesterol and HDL function, this pathway alone may be insufficient to be the main driving factor of intracellular cholesterol accumulation in atherosclerosis.

The studies reported in this thesis initially examined the potential impact of high glucose concentrations upon lysosomal enzymatic activities and number of lysosomes in murine J774A.1 macrophage-like cells that were incubated with normal (5.5 mM) or elevated concentrations of glucose (10 - 30 mM). The activities of three lysosomal cysteine proteases (cathepsins B, L and S), the aspartic acid protease cathepsin D and lysosomal acid lipase (all of which are highly expressed in normal macrophage

lysosomes), were found to be inhibited in cells exposed to high glucose concentrations. This decrease in multiple lysosomal activities may be due to a number of factors including; direct inactivation of these enzymes by glucose or materials derived from it, altered lysosomal pH, decreased protein levels or altered lysosome numbers. An acidic lysosomal environment must be achieved in order for the lysosomal enzymes to be fully activated; a higher pH may decrease the activity of these lysosomal enzymes. Alternatively a decrease in enzyme activity may also be due to a reduction in lysosomal protein levels or number. In the current study it has been shown that lysosomal cathepsin S protein levels were reduced by high glucose (30 mM) in HMDM cells [244]. Multiple lysosomal cathepsin activities along with acid lipase enzymatic activities were also decreased with high but lower concentrations of glucose (10 and 20 mM) [244]. A deficiency in the activity of these enzymes may result in inadequate degradation of the ingested materials, further slowing down the breakdown and removal process of these particles. Lysosomal deficiency or lysosomal defects from hyperglycaemia may therefore lead to the accumulation of lipids in lysosomes.

In order to provide a more suitable model of the situation in people with diabetes, these experiments were subsequently extended to human monocyte-derived macrophages (HMDM) that were collected from healthy donors. Long term exposure of these monocyte/ macrophage cells to elevated glucose levels resulted in a depression of lysosomal proteolytic and lipase activities.

Lysosomal numbers were assessed in the murine J774A.1 and HMDM cells by LAMP-1 levels, aryl sulfatase activity and Lysotracker Red dye accumulation. There was also less aryl sulfatase activity and LysoTracker Red staining, which are indicative of decreased lysosomal populations in the HMDM and J774A.1 cells that were exposed to 30 mM glucose [244]. High glucose modulated the levels of LAMP-1 protein, which is used as a general indicator for the presence of lysosomes [269]. LAMP-1 has been shown to play a key role in the generation of lysosomes, their translocation and the subsequent fusion of phagosomes with lysosomes [432]. Hyperglycaemia was also shown to decrease aryl sulfatase activity, Lysotracker dye accumulation and cathepsin protein levels supporting the LAMP-1 results with regard to the impact upon lysosomal number [244].

As lysosomal enzymes and lipases were shown to be inhibited by hyperglycaemia, this may cause lysosomal dysfunction and a reduced capacity to

degrade and hydrolyse proteins, triglycerides and cholesterol esters, thereby contributing to lipid accumulation. LAL is the only lysosomal hydrolase, available for the cleavage of cholesteryl esters and triglycerides delivered to the lysosomes [509]. A significant decrease in atherosclerotic plaques by LAL administration was observed in mice with LDL receptor deficiency with a HFD. Repeated dosages of additional LAL have also been reported to almost completely eradicate early stage lesions, and there were considerable improvement in the quality and quantity of advanced lesions [510]. Intravenous injections of LAL into LAL-deficient mice corrected macrophage lipid storage disorders and decreased cholesterol and triglyceride content in multiple tissues [511,512].

Lysosomal impairment in the murine J774A.1 and HMDM cells were seen with elevated glucose concentrations. However, whether the lysosomal dysfunction that was detected in these cellular studies can also be seen *in vivo* remains unanswered. This could be addressed by examining a standard diabetes atherosclerosis model to examine whether high glucose alone causes an accumulation of LDL particles within the lysosomes *in vivo*. This can be determined by lysosomal cathepsin and acid lipase markers in atherosclerotic lesions via immunohistology [510,511,513]. If lower levels of lysosomal markers are detected in the diabetic mice, this may confirm that lysosomal dysfunction or reduction of lysosomes within plaque macrophages can be potentially exacerbated by hyperglycaemia leading to plaque growth and instability. This would further define the roles of lysosomes and the magnitude of lysosomal damage that is inflicted by hyperglycaemia and the effect of this on plaque composition. Such studies would therefore provide key mechanistic data linking diabetes and atherosclerosis as postulated in Figure 8.1.

Additional studies on the mechanisms of modified and oxidised lipid accumulation in cells as a result of hyperglycaemia could be carried out to examine the turnover and degradation rates of LDL in macrophages that are exposed to high glucose and which are known to be susceptible to LDL accumulation. The endocytosis, degradation rates, turnover of exogenous protein and net intracellular accumulation of native and glycated LDL could be examined by using ^{125}I- of labeling LDL particles and radioactive counting. Lipid and cholesterol ester accumulation has been previously shown to be associated with greater endocytosis, degradation and intracellular accumulation of modified apo B lipoproteins in HMDM cells that were exposed to high amounts of glycoaldehyde-modified LDLs [240]. In such studies it would be of interest

to see whether high levels of glucose alone affects endocytosis and degradation of ^{125}I-BSA and ^{125}I-LDL relative to the normal glucose conditions and whether high glucose-exposed cells accumulate native and glycated LDLs. A possible reduction in endocytic and degradative activity may explain the diminished proteolytic capacity of lysosomal cathepsins and acid lipases in cells that are exposed to high glucose.

Further mechanistic studies could be carried out to investigate possible detrimental effects of hyperglycaemia on various lysosomal gene expression pathways. The effect of high glucose concentrations on lysosomal cathepsin and lipase mRNA expression can be further examined by RT-PCR techniques. Structural changes to lysosomes can be viewed under routine electron microscopy and changes in lysosomal markers in hyperglycaemic macrophages in atherosclerotic lesions from diabetic mice or humans can be examined via immunohistochemistry [513]. This would provide a more solid understanding of the causes of lysosomal dysfunction induced by hyperglycaemia.

Early endosome antigen 1 (EEA1) is responsible for translocation and fusion of early endosomes along with Arf and Rab GTPases, which are important in the regulation of fusion of transport vesicles [514,515]. The CD63/68 antigen is a glycoprotein of the LAMP family which binds to LDL and plays an important role in phagocytotic activity and intracellular lysosomal metabolism in late endosomes [516,517,518,519] and protein p62 mRNA is responsible for delivery of ubiquitin-tagged proteins into autophagosomes [520,521,522]. Electron microscopic immunocytochemistry has revealed that fatty streaks of human aortas contained diminished amounts of EEA1 and Rab5a mRNAs, whilst the levels of CD68 and p62 mRNAS were elevated in comparison to normal intima [513]. These data indicate that both early and late endo-lysosomal systems are affected in atherogenesis. Further investigations on the impairment that may be occurring in the early or late endo-lysosomal systems, along with lysosomal structural changes arising from hyperglycaemia may determine whether alterations in lysosomal enzyme levels and activity result in a reduced capacity to clear native and modified lipoprotein particles, and hence whether this contributes to lipid accumulation within lysosomes.

The studies in Chapter 4 were carried out to determine at which time point high glucose levels begin to impede lysosomal function. High glucose concentrations were shown to have an inhibitory effect on lysosomal cathepsin activity in monocytes within

two days of exposure *in vitro.* The magnitude of the glucose-induced changes in lysosomal cathepsin activities increased as the cells matured into macrophages. A similar but less marked trend was seen in lysosomal acid lipase activity.

The reduced activities of lysosomal cysteine proteases observed in the monocytes and macrophages exposed to high glucose concentrations may be due to modification of the active site cysteine residues by reactive aldehydes and glycated proteins that may form intracellularly [243]. The loss of these active site residues in the lysosomal cysteine proteases could be quantified in further studies by use of an assay (e.g. Thio Glo) that measures thiol levels. Cathepsin D and L activity have been previously reported to reduce the toxicity of AGE [269]. Greater amounts of endosomes and lysosomes, as well as increased cathepsin D and L activity has been associated with endocytosis of AGEs and the phagocytic function of macrophages [269]. Cathepsin D activity has been shown to be essential for the degradation or modification of age-related proteins [523], and this enzyme has been demonstrated to be capable of degrading AGEs [274]. Excessive intracellular AGE accumulation within lysosomes and a reduction in AGE modified protein degradation were observed in fibroblasts isolated from cathepsin D knockout mice in comparison to the wild type animals [274].

The results obtained in the current study demonstrate that lysosomal cathepsin enzymes and numbers are affected by high glucose during monocyte maturation to macrophages. Further investigations are required to determine whether this lysosomal inhibition also occurs in other cell types that are known to be capable of accelerating the oxidation and accumulation of LDL *in vitro*, such as endothelial cells, smooth muscle cells and lymphocytes. However whether hyperglycaemia causes lysosomal damage *in vivo* and to what degree lysosomal dysfunction influences the metabolism and turnover rate of glycated and oxidised proteins in humans remains to be determined. Therefore further research is necessary to verify the extent and mechanism of lysosomal impairment *in vivo* / clinical samples and whether this occurs in the same way as seen in the current cell studies.

Examination of monocytes and macrophages from people with and without Type 1 and 2 diabetes would provide a more tangible insight into whether the roles of cathepsins and lysosomal dysfunction are associated with hyperlipidaemia, and the severity of cardiovascular diseases. However one of the major limitations of this type of

study is that human tissue macrophages are difficult to obtain. Monocytes may be obtained from elutriation of human blood and matured into macrophages. However, the key issue to overcome is incubating the monocytes with the same (fluctuating) glucose concentrations that may be present *in vivo* in the donor.

People with diabetes have varying levels of glucose throughout the day, which will produce inconsistency for sample collection and analysis. This glucose reading at the time of collection may not accurately reflect the patient's overall glucose history and hence the glucose levels to which the cells have been exposed.

Therefore further research on *in vivo* samples may be necessary to verify the extent and mechanism of lysosomal impairment before translation into clinical studies. Resident peritoneal macrophages could be obtained from normal and diabetic mice, and lysosomal enzymes, number and protein expression measured. Lysosomal number (as measured by LAMP-1 protein levels), multiple cathepsins, and acid lipase are known to be detectable in atherosclerotic lesions via immunohistochemistry techniques. The effect of high glucose concentrations on lysosomal cathepsin and lipase mRNA expression could be further assessed by RT-PCR techniques in aortic samples from healthy donors and these with established cardiovascular disease. Such studies may provide a deeper understanding of the molecular mechanisms behind lysosomal dysfunction induced by hyperglycaemia *in vivo*.

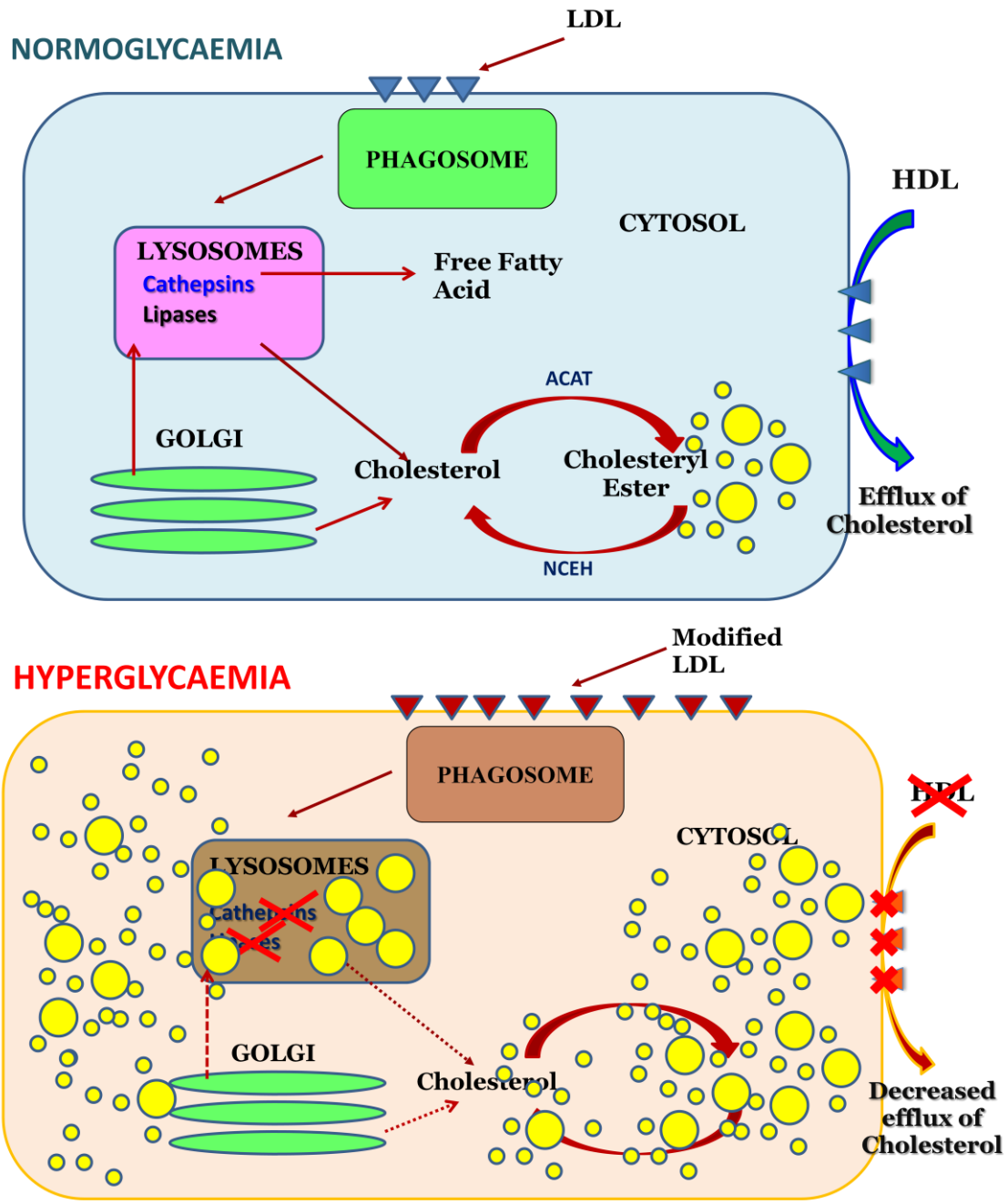

Figure 8.1: Proposed mechanisms for macrophage lysosomal dysfunction caused by high glucose in monocytes and macrophages.

In normal blood glucose conditions as shown in the top panel, modified proteins (e.g. glycated, oxidised or chemically modified) LDL are taken up by the macrophage scavenger receptors and endocytosed and transported to the lysosomes. A diversity of lysosomal enzymes such as cathepsins and lipases work actively to degrade the internalised particles. The current studies indicate that additionally hyperglycaemia may modify scavenger receptor expression such that the rate of modified protein uptake is increased to a point where it is a burden upon the lysosomal system. Hyperglycaemia may affect the activity of lysosomal enzymes such as cathepsins and lipases, and thus alter intracellular protein and lipid metabolism as shown in the bottom panel. Finally hyperglycaemia has been shown to impair reverse cholesterol transport. Together, these could lead to impaired removal of modified proteins, LDL and excess cellular cholesterol accumulation generating macrophage foam cells and thus accelerate plaque development under conditions of hyperglycaemia.

8.3 Effects of carnosine on atherosclerotic plaque development in diabetic apo $E^{-/-}$ mice

As protein glycation and glycoxidation appear to contribute to the development of diabetic complications such as atherosclerosis, agents which block or reverse protein glycation / glycoxidation may have therapeutic potential in the treatment of these complications. Carnosine is an endogenous dipeptide that has been shown to; a) block and detoxify glycated proteins; b) act as an antioxidant; c) act as a buffer; and d) act as a sensitiser for Ca^{2+} [524]. Carnosine has been shown to modulate triglycerides and glycation levels in both cell [169] and whole animal systems [282,499]. The studies reported in Chapter 5 were therefore carried out to examine whether prolonged supplementation with carnosine inhibits atherosclerosis in hyperglycaemic and hyperlipidaemic mice.

Diabetes was confirmed in the experimental system chosen (streptozotocin was used to induce Type 1 diabetes in apo $E^{-/-}$ mice) by significant increases in blood glucose, glycated haemoglobin and a significantly lower body mass. In these mice were also hyperlipidaemic as evidenced by increased plasma triglycerides and total cholesterol levels. The brachiocephalic artery and aortic sinus plaque area were significant greater in the diabetic mice. Plasma carnosine levels were elevated in mice that were supplemented with carnosine in both the non-diabetic and diabetic groups. Whilst carnosine supplementation had no effect upon the diabetes-induced hyperglycaemia or hypercholesterolaemia of the diabetic mice, supplementation significantly reduced plasma triglyceride levels by 23%. Thus, carnosine may have anti-lipogenic actions as this compound, notably it has been shown to significantly reduce triglyceride and cholesterol levels in the heart and livers of diabetic Balb/cA mice [525]. Plasma and hepatic triglycerides and cholesterol levels have also been reported to be lowered by carnosine supplementation in high fat fed non-diabetic C67BL/6 mice that were hyperlipidaemic and obese with hepatic steatosis [283].

In the diabetic mice, increases in plaque areas were observed at both aortic sites, however this was not significantly reduced by carnosine. Further histochemical studies were carried out to elucidate whether the observed hypolipidaemic action of carnosine modulated plaque composition by assessing the presence and number of smooth muscle cells and macrophages and the levels of lipid and collagen in the atherosclerotic plaques.

The major finding of this study is that carnosine can alter plaque composition potentially increasing plaque stability in diabetes-associated atherosclerosis. This was evidenced by an approximate 60% reduction in the area occupied by extracellular lipid and an increase in both the number of macrophages by 70% and collagen content by 50% within the plaques assessed. Carnosine has been previously shown to inhibit glucose-induced oxidation and glycation of human LDL [525] and effectively block pro-atherosclerotic AGE formation by preventing glycation of LDL that promotes foam cell formation in human macrophages [169]. An anti-atherosclerotic activity of this type of compound has also been demonstrated in fat-fed apo $E^{-/-}$ mice that were supplemented with D-carnosine octyl ester [282,499]. In addition significantly smaller atherosclerotic lesions has been reported in carnosine-supplemented mice compared to controls, and a lower extent of macrophage apoptosis, in animals exposed to 4-hydroxy-2-nonenal (4-HNE) [499]. A more stable plaque phenotype with less accumulation of lipid and foam cells, reduced inflammation, apoptosis and necrotic core formation has also been observed in the aortic sinus in apo E null mice that were fed a pro-atherogenic diet with D-carnosine octylester compared to the untreated controls [282].

The anti-atherogenic activities of carnosine detected in the current study (and its derivatives in other studies [169,282,499]) may be due to these agents scavenging species that modify LDL (either radicals or reactive aldehydes), thereby impeding oxidation and glycation processes. The results obtained in this study indicate that in a well-established model of diabetes-associated atherosclerosis, prolonged carnosine supplementation had a significant impact on markers of atherosclerotic plaque stability. Interestingly there was no effect of carnosine on either blood glucose or glycated haemoglobin levels, so whether the carnosine levels achieved in the plasma are sufficient to cause substantive anti-glycative / oxidative activity in these mice remain unresolved. It is however clear that significant changes are induced in the artery wall.

Further studies are required to confirm whether there was a greater accumulation of glycation and lipid peroxidation products within the plaques of the diabetic mice used in this study. Various markers of oxidative stress including protein and lipid oxidation products have been associated with the initiation and progression of atherosclerosis [526,527]. AGE products have also been shown to accumulate in the plaques of diabetic and atherogenic mice [528,529]. Reactive aldehydes / lipid peroxidation products such as malondialdehyde (MDA) [530,531], 4-hydroxy-2-nonenal (4-HNE) [282,532], *N*-epsilon-carboxymethyl-lysine (CML) [528,533], methylgloxal and AGE products

[534,535,536] can be detected in atherosclerotic lesions by immunohistochemical techniques. Quantification of some of these markers in the lesions of the carnosine-treated and control mice would therefore allow conclusions to be drawn as to whether the levels of plasma carnosine achieved by supplementation in this study were also sufficient to prevent and / or reverse glycative and glycoxidative modifications within the atherosclerotic plaques.

Further mechanistic studies on the hypolipidaemic effect of carnosine could be carried out in other organ systems such as the liver, muscles and adipose tissues of these mice. This would allow a clearer and deeper understanding of the hypolipidaemic and other potential pathways by which carnosine lowers plasma triglyceride and lipid content in this model. In this regard carnosine has been previously demonstrated to block increases in plasma and hepatic triglycerides and cholesterol in high fat diet fed C67BL/6 mice [283], and mechanistic studies showed that carnosine supplementation significantly decreased mRNA expression of lipogenic enzymes (malic enzyme, fatty acid synthase, HMG-CoA reductase) and the sterol regulatory element-binding proteins, SREBP-1c and SREBP-2, which have been shown to be elevated in high fat fed mice [283]. In the study reported in this thesis carnosine supplementation was not only shown to lower plasma triglycerides, but plaque lipid levels were also significantly reduced. This hypolipidaemic action may also have an impact upon hepatic, adipose and skeletal muscle triglyceride content, but this remains unknown. Examining liver morphology may be a good indicator of whether sterols or triglycerides have accumulated in the hepatocytes. Excessive fat accumulation in hepatocytes gives rise to non- alcoholic fatty liver disease and steatosis in its severe form, and carnosine has been previously reported to have protective effects against hepatic steatosis and to lower epidydymal fat in high fat fed mice [283]. A more quantitative approach would be directly measure the triglyceride and cholesterol levels of homogenised liver samples by, for example, HPLC / UPLC. Similarly triglyceride measurements could also be made on adipose tissue (visceral, epididymal and inguinal fat) and skeletal muscles from the leg, such as the gastrocnemius, quadriceps and soleus. Quantification of lipids from these tissues may allow conclusions to be reached as to whether the intake of carnosine ameliorates systemic, adipocytic and hepatic inflammation in diabetes-associated atherosclerosis.

The hypolipidaemic and protective effect of carnosine upon plaque composition may also provide a clearer insight into the involvement of lysosomes in the

accumulation of damaged / glycated proteins and turnover of oxidised low density lipoprotein particles. It would also be interesting to determine whether the hypolipidaemic action of carnosine has a protective effect upon macrophage lysosomes in atherosclerotic plaques. A higher content of F4/80-positive macrophages were detected in the lesions of the carnosine-treated mice regardless of their glycaemic status, and it would be of interest to determine whether lysosomal acid lipase activity (i.e. lipid hydrolysis) was enhanced by supplementation with carnosine. An enhanced rate of hydrolysis of cholesterol esters and triglycerides may explain why there was considerably less extracellular lipid accumulation observed in the diabetic mice that were supplemented with carnosine compared to the non-supplemented mice.

Further clinical trials of carnosine, a well tolerated dipeptide in diabetic and hyperlipidaemic subjects may be of significant value in the treatment of the vascular complications of diabetes. However plasma levels of carnosine levels in humans are low due to rapid hydrolysis by carnosinase in plasma and a corresponding short half life making it hard to achieve therapeutic doses of carnosine [524,537]. Synthetic derivates have been shown to be less susceptible to such hydrolysis, and may therefore have therapeutic potential [287]. The use of these novel derivatives may provide a promising preventive and therapeutic strategy for diabetic vascular complications in humans and as such would appear to warrant further investigations.

8.4 Impact of TEMPOL on lipid profiles and cytokine expression in hyperlipidaemic obese mice

TEMPOL has been shown to have hypotensive and cardio-protective actions in rodents however the potential anti-atherogenic action of TEMPOL remains inadequately characterised. Administration of TEMPOL has also been shown to effectively suppress body weight gain in obese C3H male and female mice that were fed a high fat diet. In the light of this previous data, the studies reported in Chapter 6 attempted to investigate whether TEMPOL supplementation inhibited atherosclerosis and obesity in high fat fed mice. Hyperlipidaemia was confirmed by significant increases in blood cholesterol, triglycerides, LDL-C levels and excess body mass gain; however this was not reflected in the plaque areas of the aortic sinus. Although the results of this study showed that plaque areas were not attenuated by TEMPOL, this compound effectively suppressed

hyperlipidaemia, blocked fat accumulation and inflammatory responses in both mouse strains when these were fed a high fat diet (HFD).

Although TEMPOL suppressed high fat feeding-induced body mass gain and hyperlipidaemia in both the C57BL/6 wild type and the apo $E^{-/-}$ mice the plaque areas in the aortic sinuses from chow fed mice were significantly larger than those determined for the high fat-fed apo $E^{-/-}$ mice. This may be due to the presence of highly advanced disease in the high fat feeding, leading to lesion remodelling and contraction. This suggests an earlier time point should have been chosen for examination of this parameter. In the apo $E^{-/-}$ mice, TEMPOL inhibited the elevation of MCP-1, IL-6, SAA, MPO and leptin levels that were observed in the hyperlipidaemic mice. No changes were seen in resistin levels, however a significant decrease in adiponectin levels were observed between the chow and HFD fed mice, and TEMPOL was shown to reverse these changes. A similar scenario was seen for the C57BL/6 mice, with MCP-1, IL-6, SAA, MPO and leptin levels reduced in the high fat fed mice that were supplemented with TEMPOL. No changes were however seen in the adiponectin levels in these mice; however an increase in resistin levels was observed in the HFD fed mice that were supplemented with TEMPOL. Unlike the apo $E^{-/-}$ strain, the C57BL/6 mice did not produce any observable atherosclerotic plaques and therefore this does not appear to be a sensible model to assess whether TEMPOL can inhibit atherosclerosis. However the veracity of this conclusion needs to be tempered by the fact that only one location was examined and more plaque may have existed in other regions of the vasculature, in particularly the brachiocephalic artery, as it is a key site for atherosclerotic progression. However other regions were not available for analysis. An assessment of atherosclerotic plaque development at other sites may rationalise the observed differences between atherosclerotic progression between the chow and HFD fed groups for the two mouse strains.

Examination of the plaque composition between the supplemented and control chow and HFD mice may allow differences in atherosclerotic lesion structure to be determined. TEMPOL supplementation was shown to have an impact upon obesity, preventing body weight gain, hyperlipidaemia, and decreasing a range of plasma lipids and inflammatory markers; these changes were also associated with striking differences in plaque compositional changes between the HFD, and HFD supplemented with TEMPOL, mice. This could be determined by staining the lesions for α-actin for smooth muscle cells, F4/80 for macrophages, picrosirius red for collagen content and

calculating extracellular lipid content. The results in the previous carnosine study showed significant hypolipidaemic effects on plaque composition (using these staining procedures) although there were no statistical differences in the atherosclerotic plaque size. Further experiments with a larger cohort of apo $E^{-/-}$ mice fed for shorter periods would be beneficial with regard to assessing possible changes in lesion extent induced by TEMPOL.

The results obtained in this study indicate that in a well-established model of obesity related-hyperlipidaemia, prolonged TEMPOL supplementation had a significant impact on various inflammatory and cytokine levels. Elevation of MCP-1, IL-6, SAA and MPO levels as seen in the HFD fed mice in both animal types have been reported to be early biomarkers of, or correlate positively with, atherosclerosis, obesity and cardiovascular diseases [312,313,361,362,363,364,365,366,367,538] and TEMPOL was shown to inhibit the elevation of these cytokines. Inflammatory cells that infiltrate adipose tissue are known to contribute substantially to the increased cytokine release of this tissue [539]. Obesity, with greater body mass and adipose tissue, is also known to induce changes in the secretion of adipose-specific cytokines (i.e. adipokines) [538,539]. Hence the potential inhibitory effects of TEMPOL on these adipokines were examined and significant changes in the levels of adiponectin and leptin were detected. HFD induced obesity led to hyperleptinaemia in both animal strains and decreased adiponectin secretion in the apo $E^{-/-}$ mice. The elevated leptin levels were suppressed by TEMPOL in both animal types and the lower adiponectin levels observed in the HFD fed apo $E^{-/-}$ mice were reversed with TEMPOL. Further mechanistic studies on the hypolipidaemic effect of TEMPOL could be carried out on other organ systems such as the liver, muscle and adipose tissue, as previously discussed in Section 8.3. This would provide a clearer and deeper understanding of the hypolipidaemic roles and other potential systemic inflammatory mechanisms by which TEMPOL lowers plasma lipid content in obesity related metabolic syndrome complications.

Although TEMPOL was shown to lower plasma lipid levels, and also the systemic inflammatory response, in these fat-fed animals, the mechanisms that underlie these changes remain unknown. Further work needs to be carried out in order to understand the anti-obesity and anti-inflammatory actions of TEMPOL using an *in vitro* model of adipocyte proliferation and differentiation to elucidate whether TEMPOL inhibits production of adipokines by decreasing adipocyte size and / or number. That is whether: (i) the inhibition of gain in mass represents a TEMPOL-mediated inhibition of

adipocyte proliferation or differentiation; (ii) the changes in the pattern of cytokine and adipokine secretion are a consequence of the effects of TEMPOL upon adipocyte proliferation / differentiation; and / or (iii) whether the action of TEMPOL is mediated by its antioxidant activities.

The murine preadipocyte cell line 3T3-L1 is a commonly used model for preadipocyte proliferation and adipocyte differentiation *in vitro.* Cell proliferation of pre-adipocytes in the absence or presence of TEMPOL could be determined using the 3-(4,5-dimethylthiazol-2-yl)-2,5-diphenltetrazolium bromide (MTT) assay, and the degree of adipocyte hypertrophy could be digitally imaged and quantified. Comparison of adipocyte differentiation, and lipid accumulation, between TEMPOL treated and untreated cells could be quantified by staining lipid droplets via Oil-Red staining, or by HPLC/ UPLC quantification of triglycerides and fatty acids in cell lysates.

High fat intake has been proposed to induce a degree of endotoxaemia [540] and recently Lassenius and colleagues [541] have demonstrated an elevated serum lipopolysaccharide (LPS) / HDL ratio in people with Type 1 diabetes particularly those diagnosed with features of the metabolic syndrome. Adipocytes express receptors for LPS [542] and activation of adipocytes by LPS, via Toll-like receptors, induces fatty acid release [543]. Thus the capacity of TEMPOL to inhibit fatty acid release could be compared between TEMPOL treated and untreated cultures in the presence of LPS. A number of cytokines which are secreted by adipocytes are known to be induced by LPS stimulation [342,363,364]. The secreted levels of adipokines (e.g. leptin and adiponectin) and cytokines (TNF-α, IL-6, IL-8, serum amyloid A and CCL-2 and -5) from pre and matured adipocytes could be determined using immunoassay kits to assess whether TEMPOL inhibits cytokine production and secretion from these cells.

The inhibitory effect of TEMPOL upon adipocyte proliferation, differentiation and / or pro-inflammatory responses may be influenced by its superoxide dismutase-mimetic activity [336,346,544]. Quantification of superoxide levels in TEMPOL-treated and untreated cells may therefore be worth assessing, and this could be measured by using the dihydroethidine / 2-hyxdroxy ethidium fluorimetric assay [545].

Such work on adipocytes from 3T3-L1 cells would pave the way for future projects. 3T3-L1 cells could provide a standard model system to screen novel compounds e.g. structural analogues of TEMPOL before use in expensive animal models. Investigations on primary adipocytes obtained from fat-fed obese mice and

obese subjects (e.g. those who have undergone liposuction) would also provide a more complete systematic understanding of the anti-obesity and anti-inflammatory actions of TEMPOL.

The results obtained in these studies suggest that TEMPOL supplementation may be beneficial in lowering plasma lipid levels and suppressing obesity and hyperlipidaemia. Thus TEMPOL may be of significant value in arresting body fat accumulation and promoting body fat loss where management of body mass is resistant to behavioural modifications alone. Although TEMPOL is well known for its potent hypotensive effects, the anti-atherogenic properties of TEMPOL remain unestablished, and deserve further study.

8.5 Effects of TEMPOL upon lysosomal function and cytokine expression in HMDM cells incubated with high glucose

In the light of the above data which shows that TEMPOL can down regulate inflammation and lower cytokine levels, further studies were carried out to determine whether this compound affected lysosomal function and cytokine expression in HMDM exposed to high glucose. The studies carried out to assess the potential anti-inflammatory effects of TEMPOL against the deleterious effects of high glucose levels in HMDM on lysosomal dysfunction (Chapters 3 and 4), showed that TEMPOL was not able to reverse or arrest this inhibition.

The studies reported in Chapter 7 examined the potential impact of high glucose concentrations on a range of cytokine factors produced by HMDM upon stimulation with LPS, in order to establish a suitable model to assess the potential anti-inflammatory action of TEMPOL. This was of interest because the antioxidant TEMPOL has been shown to protect against renal dysfunction and inhibit the production of hepatic reactive oxygen species induced by streptozotocin *in vivo* [345,424]. TEMPOL has also been demonstrated to inhibit AGE induced TNF-α and ROS production *in vitro* [425].

In the studies reported in Chapter 7 high glucose was found to significantly elevate secretions of TNF-α and MIP-1α and lower CRP expression in macrophages when compared to normal glucose conditions. Subsequent experiments with multiple donors confirmed the significant elevation in TNF-α and MIP-1α induced by high

glucose, and TEMPOL was shown to significantly attenuate the elevation of TNF-α and MIP-1α expression across all donors. This may be due to TEMPOL having a protective effect against the oxidative stress and damage inflicted by high glucose, and further studies would be required to determine and elucidate the potential protective effects of TEMPOL in human macrophages against oxidative and glycative damage. This could be achieved by the generation of various reactive oxygen species or the inclusion of advanced glycation end products markers by LPS stimulation in the media to examine whether TEMPOL inhibits or reverses potential elevations in ROS and AGE markers. The potential induction of inflammatory markers by high glucose and its modulation by TEMPOL could also be examined in other cell types such as monocytes, neutrophils, dendritic cells, lymphocytes and other leukocytes which act as key communicators between the innate and immune response. Studies on mouse peritoneal macrophages obtained from mice with diabetes (with and without TEMPOL supplementation) would also be potentially worthwhile to examine whether TEMPOL, which has been shown to inhibit TNF-α and MIP-1α elevations induced by high glucose at a cellular level, also has such actions in animals suffering from diabetes. Examination of the effects of TEMPOL on monocytes elutriated from the blood of people with Type 1 or 2 diabetes may further elucidate the roles of TEMPOL in humans.

CRP secretion was not found to be affected by stimulation with LPS or exposure to high glucose; therefore it is difficult to conclude whether high glucose or TEMPOL supplementation had an effect upon these levels. Plasma CRP levels have been reported to be higher in people with diabetes, cardiovascular diseases and atherosclerosis, however this was not reflected in the human monocyte-derived macrophages examined in these studies. This may be due to the absence or only levels of low concentrations of CRP generated by HMDM. Further investigations would therefore be beneficial in other cell types, such as hepatocytes where CRP is primarily synthesised [437]. CRP levels are a sensitive marker for cardiovascular diseases and particularly atherosclerosis, and therefore further investigations in diabetic and hyperlipidaemic subjects may be warranted to elucidate potential beneficial effects of TEMPOL.

8.6 Concluding remarks

The chronic elevated blood glucose levels detected in people with diabetes may have a detrimental impact upon macrophage lysosomal function that could promote atherosclerosis. The studies in this thesis attempted to demonstrate for the first time, some of the deleterious effects of high glucose upon lysosomes, and it has been shown that this includes inhibition of lysosomal enzymes and reduced lysosomal number in murine and human monocytes / macrophages. Lysosomal dysfunction may therefore be an underlying cause for the increased incidence, and rate of development of atherosclerosis in people with diabetes.

The endogenous agent carnosine was examined in a murine model of diabetes-induced atherosclerosis. Carnosine supplementation was shown to have anti-hyperlipidaemic effects and properties that may enhance plaque stability which may be of therapeutic value in the treatment of diabetes-accelerated atherosclerosis.

The nitroxide TEMPOL was investigated in two well-established murine models of obesity induced by high fat feeding. TEMPOL was shown to effectively block weight gain in mice and relieve the associated hyperlipidaemia induced by a high fat diet. Further mechanistic studies showed that TEMPOL was able to reduce systemic inflammation and reverse the changed adipokine profile of obesity. Furthermore TEMPOL was shown to have an impact upon inflammation induced by high glucose in human macrophages. The anti-hyperlipidaemic, anti-obesity and anti-diabetic actions of TEMPOL may therefore be of therapeutic value in the treatment of many complications that arise from metabolic dysfunction.

REFERENCES

1. Zimmet P, Alberti K, Shaw J (2001) Global and societal implications of the diabetes epidemic. Nature 414: 782-787.
2. Eckel RH, Grundy SM, Zimmet PZ (2005) The metabolic syndrome. Lancet 365: 1415-1428.
3. Eckel RH, Alberti K, Grundy SM, Zimmet PZ (2010) The metabolic syndrome. Lancet 375: 181-183.
4. Zimmet P, Magliano D, Matsuzawa Y, Alberti G, Shaw J (2005) The metabolic syndrome: A global public health problem and a new definition. Journal of Atherosclerosis and Thrombosis 12: 295-300.
5. Keating CL, Moodie ML, Bulfone L, Swinburn BA, Stevenson CE, et al. (2012) Healthcare utilization and costs in severely obese subjects before bariatric surgery. Obesity 20: 2412-2419.
6. Guize L, Thomas F, Pannier B, Bean K, Jego B, et al. (2007) All-cause mortality associated with specific combinations of the metabolic syndrome according to recent definitions. Diabetes Care 30: 2381-2387.
7. Thomas GN, Schooling CM, McGhee SM, Ho SY, Cheung BMY, et al. (2007) Metabolic syndrome increases all-cause and vascular mortality: The Hong Kong Cardiovascular Risk Factor Study. Clinical Endocrinology 66: 666-671.
8. Cheung BMY, Thomas GN (2007) The metabolic syndrome and vascular disease in Asia. Cardiovascular & Hematological Disorders - Drug Targets 7: 79-85.
9. John AP, Koloth R, Dragovic M, Lim SCB (2009) Prevalence of metabolic syndrome among Australians with severe mental illness. Medical Journal of Australia 190: 176-179.
10. Ford ES (2005) Risks for all-cause mortality, cardiovascular disease, and diabetes associated with the metabolic syndrome - A summary of the evidence. Diabetes Care 28: 1769-1778.
11. Ford ES, Zhao GX, Li CY (2010) Pre-diabetes and the risk for cardiovascular disease a systematic review of the evidence. Journal of the American College of Cardiology 55: 1310-1317.
12. Dunstan DW, Thorp AA, Healy GN (2011) Prolonged sitting: is it a distinct coronary heart disease risk factor? Current Opinion in Cardiology 26: 412-419.
13. Crawford AG, Cote C, Couto J, Daskiran M, Gunnarsson C, et al. (2010) Prevalence of obesity, type II diabetes mellitus, hyperlipidemia, and hypertension in the United States: Findings from the GE centricity electronic medical record database. Population Health Management 13: 151-161.
14. Park YW, Zhu SK, Heymsfield SB, Heshka S (2003) The metabolic syndrome: All criteria are equal, but some criteria are more equal than others - In reply. Archives of Internal Medicine 163: 2788-2788.
15. Enzi G, Busetto L, Inelmen EM, Coin A, Sergi G (2003) Historical perspective: visceral obesity and related comorbidity in Joannes Baptista Morgagni's 'De sedibus et Causis Morborum per Anatomen Indagata'. International Journal of Obesity 27: 534-535.
16. Alberti K, Zimmet P, Shaw J (2006) Metabolic syndrome - a new world-wide definition. A consensus statement from the International Diabetes Federation. Diabetic Medicine 23: 469-480.
17. Vague J (1956) The degree of masculine differentiation of obesities - a factor determining predisposition to diabetes, atherosclerosis, gout, and uric calculous disease. American Journal of Clinical Nutrition 4: 20-34.
18. Reaven GM, Javorski WC, Reaven EP, Olefsky J, Jen P (1975) Diabetic hypertriglyceridemia. American Journal of the Medical Sciences 269: 382-389.

19. Reaven GM, Olefsky JM (1978) Role of insulin resistance in the pathogenesis of hyper glycemia. Washington, D.C., USA: Illus Hemisphere Publishing Corporation pp. 229-266.
20. Reaven GM, Hoffman BB (1987) A role for insulin in the etiology and course of hypertension. Lancet 2: 435-437.
21. Reaven GM (1988) Role of insulin resistance in human-disease. Diabetes 37: 1595-1607.
22. Gale AE (February 12–13, 1998) Chronic Fatigue Syndrome associated with insulin resistance Chronic Fatigue Syndrome. Sydney: Current Medical Diagnosis & Treatment 38th Ed. Case Study Poster Presentation.
23. Silva V, Stanton KR, Grande AJ (2013) Harmonizing the diagnosis of metabolic syndrome-focusing on abdominal obesity. Metabolic Syndrome and Related Disorders 11: 102-108.
24. Alberti K, Zimmet PZ, Consultation WHO (1998) Definition, diagnosis and classification of diabetes mellitus and its complications Part 1: Diagnosis and classification of diabetes mellitus - Provisional report of a WHO consultation. Diabetic Medicine 15: 539-553.
25. Simmons RK, Alberti K, Gale EAM, Colagiuri S, Tuomilehto J, et al. (2010) The metabolic syndrome: useful concept or clinical tool? Report of a WHO Expert Consultation. Diabetologia 53: 600-605.
26. Cheal KL, Abbasi F, Lamendola C, McLaughlin T, Reaven GM, et al. (2004) Relationship to insulin resistance of the Adult Treatment Panel III diagnostic criteria for identification of the metabolic syndrome. Diabetes 53: 1195-1200.
27. Alberti K, Zimmet P, Shaw J (2005) The metabolic syndrome - a new worldwide definition. Lancet 366: 1059-1062.
28. WHO (2013) Cardiovascular Diseases (CVDs), Fact Sheet No. 317 World Health Organisation.
29. Bonow RO (2010) ACC/AHA 2006 Guidelines for the management of patients with valvular heart disease: A report of the American College of Cardiology/American Heart Association task force on practice guidelines (Writing committee to develop guidelines for the management of patients with valvular heart disease). Circulation 121: E443-E443.
30. AIHW (2012) Health expenditure Australia 2010–11. Australian Institute of Health and Welfare.
31. AIHW (2013) Impact of cardiovascular disease. Australian Institute of Health and Welfare (AIHW).
32. Begg S, Vos T, Goss J, Mann N (2008) An alternative approach to projecting health expenditure in Australia. Australian Health Review 32: 148-155.
33. ABS (2006) Diabetes in Australia: A Snapshot, 2004-05 Australian Bureau of Statistics.
34. Falk E (2006) Pathogenesis of atherosclerosis. Journal of the American College of Cardiology 47: C7-C12.
35. Cheung N, Sharrett AR, Klein R, Criqui MH, Islam A, et al. (2007) Aortic distensibility and retinal arteriolar narrowing - The multi-ethnic study of atherosclerosis. Hypertension 50: 617-622.
36. Jenkins AJ, Best JD, Klein RL, Lyons TJ (2004) 'Lipoproteins, glycoxidation and diabetic angiopathy'. Diabetes-Metabolism Research and Reviews 20: 349-368.
37. Faghihnia N, Tsimikas S, Miller ER, Witztum JL, Krauss RM (2010) Changes in lipoprotein(a), oxidized phospholipids, and LDL subclasses with a low-fat high-carbohydrate diet. Journal of Lipid Research 51: 3324-3330.

38. Orlova EV, Sherman MB, Chiu W, Mowri H, Smith LC, et al. (1999) Three-dimensional structure of low density lipoproteins by electron cryomicroscopy. Proceedings of the National Academy of Sciences of the United States of America 96: 8420-8425.
39. Jenkins AJ, Lyons TJ, Zheng DY, Otvos JD, Lackland DT, et al. (2003) Lipoproteins in the DCCT/EDIC cohort: Associations with diabetic nephropathy. Kidney International 64: 817-828.
40. Feng M, Morales AB, Beugeling T, Bantjes A, vander Werf K, et al. (1996) Absorption of high density lipoproteins (HDL) on solid surfaces. Journal of Colloid and Interface Science 177: 364-371.
41. Segrest JP, Jones MK, De Loof H, Dashti N (2001) Structure of apolipoprotein B-100 in low density lipoproteins. Journal of Lipid Research 42: 1346-1367.
42. Fievet C, Fruchart JC (1991) HDL heterogeneity and coronary heart-disease. Diabetes-Metabolism Reviews 7: 155-162.
43. Tabet F, Rye KA (2009) High-density lipoproteins, inflammation and oxidative stress. Clinical Science 116: 87-98.
44. Hayden MR, Tyagi SC (2004) Vasa vasorum in plaque angiogenesis, metabolic syndrome, type 2 diabetes mellitus, and atheroscleropathy: a malignant transformation. Cardiovascular Diabetology 3: 1-16.
45. Crowther MA (2005) Pathogenesis of atherosclerosis. Hematology / the Education Program of the American Society of Hematology. American Society of Hematology. Education Program: 436-441.
46. Stary HC, Chandler AB, Dinsmore RE, Fuster V, Glagov S, et al. (1995) A definition of advanced types of atherosclerotic lesions and a histological classification of atherosclerosis - a report from the committee-on-vascular-lesions of the council-on-arteriosclerosis, American-Heart-Association. Arteriosclerosis Thrombosis and Vascular Biology 15: 1512-1531.
47. Ross R, Glomset J, Harker L (1977) Response to injury and atherogenesis. American Journal of Pathology 86: 675-684.
48. D'Souza A, Hussain M, Howarth FC, Woods NM, Bidasee K, et al. (2009) Pathogenesis and pathophysiology of accelerated atherosclerosis in the diabetic heart. Molecular and Cellular Biochemistry 331: 89-116.
49. Steinberg D, Witztum JL (2010) History of discovery oxidized low-density lipoprotein and atherosclerosis. Arteriosclerosis Thrombosis and Vascular Biology 30: 2311-2316.
50. Libby P (2002) Inflammation in atherosclerosis. Nature 420: 868-874.
51. Stary HC (2000) Natural history of calcium deposits in atherosclerosis progression and regression. Zeitschrift Fur Kardiologie 89: 28-35.
52. Stary HC, Chandler AB, Glagov S, Guyton JR, Insull W, et al. (1994) A definition of initial, fatty streak, and intermediate lesions of atherosclerosis - a report from the committee on vascular-lesions of the council on arteriosclerosis, American-Heart-Association. Circulation 89: 2462-2478.
53. Anonymous (2012) Is it diabetes yet? [Cited 6th June 2013]; Available from: http://myghisite.com/is-it-diabetes-yet-part-2-of-2-article/atherosclerosis-stages/
54. Negrato CA, Tarzia O (2010) Buccal alterations in diabetes mellitus. Diabetology & Metabolic Syndrome 2: 1-11.
55. Rathmann W, Giani G (2004) Global prevalence of diabetes: Estimates for the year 2000 and projections for 2030. Diabetes Care 27: 2568-2569.
56. IDF (2012) International Diabetes Federation (IDF) Diabetes Atlas 2012 [Cited 1st April 2013]; Available from: http://www.idf.org/diabetesatlas/5e/Update2012
57. Sherwin R, Jastreboff AM (2012) Year in Diabetes 2012: The Diabetes Tsunami. Journal of Clinical Endocrinology & Metabolism 97: 4293-4301.

58. NIH (November 2008) National Diabetes Information Clearinghouse (NDIC). In: 09–3873 NPN, editor: National Institute of Diabetes and Digestive and Kidney Diseases (NIDDK), National Institutes of Health (NIH).
59. American Diabetes Association (2013) Diagnosis and Classification of Diabetes Mellitus. Diabetes Care 36: S67-S74.
60. Miller RA, Chu QW, Xie JX, Foretz M, Viollet B, et al. (2013) Biguanides suppress hepatic glucagon signalling by decreasing production of cyclic AMP. Nature 494: 256-260.
61. Dorkhan M, Frid A (2007) A review of pioglitazone HCL and glimepiride in the treatment of type 2 diabetes. Vascular health and risk management 3: 721-731.
62. Loh KC, Leow MKS (2002) Current therapeutic strategies for type 2 diabetes mellitus. Annals Academy of Medicine Singapore 31: 722-730.
63. Stumvoll M, Nurjhan N, Perriello G, Dailey G, Gerich JE (1995) Metabolic effects of metformin in non-insulin-dependent diabetes-mellitus. New England Journal of Medicine 333: 550-554.
64. Berner B, Hummel KM, Strutz F, Ritzel U, Ramadori G, et al. (2002) Metformin-induced lactic acidosis with acute renal failure in type 2 diabetes mellitus. Medizinische Klinik 97: 99-103.
65. Ahima RS (2011) Digging deeper into obesity. Journal of Clinical Investigation 121: 2076-2079.
66. Godfrey JR (2006) Toward optimal health: Robert Kushner, M.D., offers a practical approach to assessment of overweight patients. Journal of Womens Health 15: 991-995.
67. Cornier MA, Despres JP, Davis N, Grossniklaus DA, Klein S, et al. (2011) Assessing adiposity a scientific statement from the American Heart Association. Circulation 124: 1996-2019.
68. WHO (2013) Obesity and overweight Fact sheet N°311. World Health Organisation. Last update: March 2013 [Cited 1st April 2013] http://www.who.int/mediacentre/factsheets/fs311/en/
69. Wellman NS, Friedberg B (2002) Causes and consequences of adult obesity: health, social and economic impacts in the United States. Asia Pacific Journal of Clinical Nutrition 11: S705-S709.
70. Seth A, Sharma R (2013) Childhood obesity. Indian Journal of Pediatrics 80: 309-317.
71. Sharifi M, Rifas-Shiman SL, Marshall R, Simon SR, Gillman MW, et al. (2013) Evaluating the implementation of expert committee recommendations for obesity assessment. Clinical Pediatrics 52: 131-138.
72. Narang I, Mathew JL (2012) Childhood obesity and obstructive sleep apnea. Journal of Nutrition and Metabolism 2012: 1-8.
73. Wing RR (1995) Changing diet and exercise behaviors in individuals at risk for weight-gain. Obesity Research 3: S277-S282.
74. Malik VS, Popkin BM, Bray GA, Despres JP, Hu FB (2010) Sugar-sweetened beverages, obesity, type 2 diabetes mellitus, and cardiovascular disease risk. Circulation 121: 1356-1364.
75. Bray GA (2012) Fructose and risk of cardiometabolic disease. Current Atherosclerosis Reports 14: 570-578.
76. Mavoa HM, McCabe M (2008) Sociocultural factors relating to Tongans' and Indigenous Fijians' patterns of eating, physical activity and body size. Asia Pacific Journal of Clinical Nutrition 17: 375-384.
77. Sibai AM, Nasreddine L, Mokdad AH, Adra N, Tabet M, et al. (2011) Nutrition transition and cardiovascular disease risk factors in Middle East and North

Africa countries: Reviewing the evidence. Annals of Nutrition and Metabolism 57: 193-203.
78. Piya MK, McTernan PG, Kumar S (2013) Adipokine inflammation and insulin resistance: the role of glucose, lipids and endotoxin. The Journal of Endocrinology 216: T1-T15.
79. Sun K, Kusminski CM, Scherer PE (2011) Adipose tissue remodeling and obesity. Journal of Clinical Investigation 121: 2094-2101.
80. Greenberg AS, Coleman RA, Kraemer FB, McManaman JL, Obin MS, et al. (2011) The role of lipid droplets in metabolic disease in rodents and humans. Journal of Clinical Investigation 121: 2102-2110.
81. Sundell J, Laine H, Luotolahti M, Kalliokoski K, Raitakari O, et al. (2002) Obesity affects myocardial vasoreactivity and coronary flow response to insulin. Obesity Research 10: 617-624.
82. Ramachandrappa S, Farooqi IS (2011) Genetic approaches to understanding human obesity. Journal of Clinical Investigation 121: 2080-2086.
83. Farooqi IS (2011) Genetic, molecular and physiological insights into human obesity. European Journal of Clinical Investigation 41: 451-455.
84. Sierra-Johnson J, Romero-Corral A, Lopez-Jimenez F, Gami AS, Kuniyoshi FHS, et al. (2007) Relation of increased leptin concentrations to history of myocardial infarction and stroke in the United States population. American Journal of Cardiology 100: 234-239.
85. Hajer GR, van Haeften TW, Visseren FLJ (2008) Adipose tissue dysfunction in obesity, diabetes, and vascular diseases. European Heart Journal 29: 2959-2971.
86. Wang ZV, Scherer PE (2008) Adiponectin, cardiovascular function, and hypertension. Hypertension 51: 8-14.
87. Seino S, Shibasaki T, Minami K (2011) Dynamics of insulin secretion and the clinical implications for obesity and diabetes. Journal of Clinical Investigation 121: 2118-2125.
88. Prentki M, Nolan CJ (2006) Islet beta cell failure in type 2 diabetes. Journal of Clinical Investigation 116: 1802-1812.
89. Shoelson SE, Lee J, Goldfine AB (2006) Inflammation and insulin resistance Journal of Clinical Investigation 116: 1793.
90. Stienstra R, Tack CJ, Kanneganti TD, Joosten LAB, Netea MG (2012) The inflammasome puts obesity in the danger zone. Cell Metabolism 15: 10-18.
91. Nov O, Shapiro H, Ovadia H, Tarnovscki T, Dvir I, et al. (2013) Interleukin-1 beta regulates fat-liver crosstalk in obesity by auto-paracrine modulation of adipose tissue inflammation and expandability. Plos One 8: 1-12.
92. Furukawa S, Fujita T, Shimabukuro M, Iwaki M, Yamada Y, et al. (2004) Increased oxidative stress in obesity and its impact on metabolic syndrome. Journal of Clinical Investigation 114: 1752-1761.
93. Sprague AH, Khalil RA (2009) Inflammatory cytokines in vascular dysfunction and vascular disease. Biochemical Pharmacology 78: 539-552.
94. Weisberg SP, McCann D, Desai M, Rosenbaum M, Leibel RL, et al. (2003) Obesity is associated with macrophage accumulation in adipose tissue. Journal of Clinical Investigation 112: 1796-1808.
95. Vlasova M, Purhonen AK, Jarvelin MR, Rodilla E, Pascual J, et al. (2010) Role of adipokines in obesity-associated hypertension. Acta Physiologica 200: 107-127.
96. Chen CY, Jiang J, Lu JM, Chai H, Wang XW, et al. (2010) Resistin decreases expression of endothelial nitric oxide synthase through oxidative stress in human coronary artery endothelial cells. American Journal of Physiology-Heart and Circulatory Physiology 299: H193-H201.

97. Verma S, Li SH, Wang CH, Fedak PWM, Li RK, et al. (2003) Resistin promotes endothelial cell activation - Further evidence of adipokine-endothelial interaction. Circulation 108: 736-740.
98. Azuma K, Katsukawa F, Oguchi S, Murata M, Yamazaki H, et al. (2003) Correlation between serum resistin level and adiposity in obese individuals. Obesity Research 11: 997-1001.
99. Savage DB, Sewter CP, Klenk ES, Segal DG, Vidal-Puig A, et al. (2001) Resistin/Fizz3 expression in relation to obesity and peroxisome proliferator-activated receptor-gamma action in humans. Diabetes 50: 2199-2202.
100. Catenacci VA, Hill JO, Wyatt HR (2009) The obesity epidemic. Clinics in Chest Medicine 30: 415-444.
101. Lopez-Jimenez F, Cortes-Bergoderi M (2011) Obesity and the heart. Revista Espanola De Cardiologia 64: 140-149.
102. Dorresteijn JAN, Visseren FLJ, Spiering W (2012) Mechanisms linking obesity to hypertension. Obesity Reviews 13: 17-26.
103. McGill HC, McMahan CA, Herderick EE, Zieske AW, Malcom GT, et al. (2002) Obesity accelerates the progression of coronary atherosclerosis in young men. Circulation 105: 2712-2718.
104. Lopez-Jimenez F, Jacobsen SJ, Reeder GS, Weston SA, Meverden RA, et al. (2004) Prevalence and secular trends of excess body weight and impact on outcomes after myocardial infarction in the community. Chest 125: 1205-1212.
105. Poirier P, Giles TD, Bray GA, Hong YL, Stern JS, et al. (2006) Obesity and cardiovascular disease: Pathophysiology, evaluation, and effect of weight loss - An update of the 1997 American Heart Association Scientific Statement on obesity and heart disease from the Obesity Committee of the Council on Nutrition, Physical Activity, and Metabolism. Circulation 113: 898-918.
106. Licata G, Argano C, Di Chiara T, Parrinello G, Scaglione R (2006) Obesity: a main factor of metabolic syndrome? Panminerva Medica 48: 77-85.
107. Remick J, Underberg JA, Shah NR (2008) Utility of different lipid measures to predict coronary heart disease. JAMA-Journal of the American Medical Association 299: 35-36.
108. Chaowalit N, Lopez-Jimenez F (2008) Epicardial adipose tissue: friendly companion or hazardous neighbour for adjacent coronary arteries? European Heart Journal 29: 695-697.
109. Romero-Corral A, Montori VM, Somers VK, Korinek J, Thomas RJ, et al. (2006) Association of bodyweight with total mortality and with cardiovascular events in coronary artery disease: a systematic review of cohort studies. Lancet 368: 666-678.
110. Romero-Corral A, Sierra-Johnson J, Lopez-Jimenez F, Thomas RJ, Singh P, et al. (2008) Relationships between leptin and C-reactive protein with cardiovascular disease in the adult general population. Nature Clinical Practice Cardiovascular Medicine 5: 418-425.
111. Tong B, Stevenson C (2007) Comorbidity of cardiovascular disease, diabetes and chronic kidney disease in Australia. Canberra, ACT, Australia: Australian Institute of Health and Welfare.
112. Haffner SM, Lehto S, Ronnemaa T, Pyorala K, Laakso M (1998) Mortality from coronary heart disease in subjects with type 2 diabetes and in nondiabetic subjects with and without prior myocardial infarction. New England Journal of Medicine 339: 229-234.
113. Brownlee M (2013) Hyperglycemia-stimulated myelopoiesis causes impaired regression of atherosclerosis in type 1 diabetes. Cell Metabolism 17: 631-633.

114. Bianchi C, Miccoli R, Daniele G, Penno G, Del Prato S (2009) Is there evidence that oral hypoglycemic agents reduce cardiovascular morbidity/mortality? Yes. Diabetes Care 32, Suppl 2: S342-S348.
115. Brownlee M (2005) The pathobiology of diabetic complications - A unifying mechanism. Diabetes 54: 1615-1625.
116. Yabe-Nishimura C (1998) Aldose reductase in glucose toxicity: A potential target for the prevention of diabetic complications. Pharmacological Reviews 50: 21-33.
117. Brownlee M (2001) Biochemistry and molecular cell biology of diabetic complications. Nature 414: 813-820.
118. Lipinski B (2002) Evidence in support of a concept of reductive stress. British Journal of Nutrition 87: 93-94.
119. Ramasamy R, Oates PJ, Schaefer S (1997) Aldose reductase inhibition protects diabetic and nondiabetic rat hearts from ischemic injury. Diabetes 46: 292-300.
120. Gleissner CA, Galkina E, Nadler JL, Ley K (2007) Mechanisms by which diabetes increases cardiovascular disease. Drug Discovery Today: Disease Mechanisms 4: 131–140.
121. Trueblood N, Ramasamy R (1998) Aldose reductase inhibition improves altered glucose metabolism of isolated diabetic rat hearts. American Journal of Physiology-Heart and Circulatory Physiology 275: H75-H83.
122. Beckman JA, Creager MA, Libby P (2002) Diabetes and atherosclerosis - Epidemiology, pathophysiology, and management. JAMA-Journal of the American Medical Association 287: 2570-2581.
123. Du XL, Edelstein D, Dimmeler S, Ju QD, Sui C, et al. (2001) Hyperglycemia inhibits endothelial nitric oxide synthase activity by posttranslational modification at the Akt site. Journal of Clinical Investigation 108: 1341-1348.
124. Duan WL, Paka L, Pillarisetti S (2005) Distinct effects of glucose and glucosamine on vascular endothelial and smooth muscle cells: Evidence for a protective role for glucosamine in atherosclerosis. Cardiovascular Diabetology 4: 1- 10.
125. Farhangkhoee H, Khan ZA, Kaur H, Xin XP, Chen SL, et al. (2006) Vascular endothelial dysfunction in diabetic cardiomyopathy: Pathogenesis and potential treatment targets. Pharmacology & Therapeutics 111: 384-399.
126. Rask-Madsen C, King GL (2005) Proatherosclerotic mechanisms involving protein kinase C in diabetes and insulin resistance. Arteriosclerosis Thrombosis and Vascular Biology 25: 487-496.
127. Griendling KK, FitzGerald GA (2003) Oxidative stress and cardiovascular injury - Part I: Basic mechanisms and *in vivo* monitoring of ROS. Circulation 108: 1912-1916.
128. Steinberg D, Parthasarathy S, Carew TE, Khoo JC, Witztum JL (1989) Beyond cholesterol - modifications of low-density lipoprotein that increase its atherogenicity. New England Journal of Medicine 320: 915-924.
129. Steinberg D (2009) The LDL modification hypothesis of atherogenesis: an update. Journal of Lipid Research 50: S376-S381.
130. Stocker R, Keaney JF (2004) Role of oxidative modifications in atherosclerosis. Physiological Reviews 84: 1381-1478.
131. Kojda G, Harrison D (1999) Interactions between NO and reactive oxygen species: pathophysiological importance in atherosclerosis, hypertension, diabetes and heart failure. Cardiovascular Research 43: 562-571.
132. Giacco F, Brownlee M (2010) Oxidative stress and diabetic complications. Circulation Research 107: 1058-1070.

133. Marchioli R (1999) Antioxidant vitamins and prevention of cardiovascular disease: Laboratory, epidemiological and clinical trial data. Pharmacological Research 40: 227-238.
134. Maxwell SRJ (1999) Antioxidant vitamin supplements - Update of their potential benefits and possible risks. Drug Safety 21: 253-266.
135. Goldin A, Beckman JA, Schmidt AM, Creager MA (2006) Advanced glycation end products - Sparking the development of diabetic vascular injury. Circulation 114: 597-605.
136. Wolff SP, Dean RT (1987) Glucose autoxidation and protein modification - the potential role of autoxidative glycosylation in diabetes. Biochemical Journal 245: 243-250.
137. Meerwaldt R, Links T, Zeebregts C, Tio R, Hillebrands JL, et al. (2008) The clinical relevance of assessing advanced glycation endproducts accumulation in diabetes. Cardiovascular Diabetology 7: 1-8.
138. Sparvero LJ, Asafu-Adjei D, Kang R, Tang DL, Amin N, et al. (2009) RAGE (Receptor for Advanced Glycation Endproducts), RAGE Ligands, and their role in Cancer and Inflammation. Journal of Translational Medicine 7: 1-21.
139. Yan SF, Ramasamy R, Schmidt AM (2008) Mechanisms of disease: advanced glycation end-products and their receptor in inflammation and diabetes complications. Nature Clinical Practice Endocrinology & Metabolism 4: 285-293.
140. Turk B, Turk D, Turk V (2000) Lysosomal cysteine proteases: more than scavengers. Biochimica Et Biophysica Acta-Protein Structure and Molecular Enzymology 1477: 98-111.
141. Jandeleit-Dahm K, Cooper ME (2008) The role of AGEs in cardiovascular disease. Current Pharmaceutical Design 14: 979-986.
142. Fu MX, Wellsknecht KJ, Blackledge JA, Lyons TJ, Thorpe SR, et al. (1994) Glycation, glycoxidation, and cross-linking of collagen by glucose - kinetics, mechanisms, and inhibition of late stages of the maillard reaction. Diabetes 43: 676-683.
143. Baynes JW, Thorpe SR (1999) Role of oxidative stress in diabetic complications - A new perspective on an old paradigm. Diabetes 48: 1-9.
144. Stadtman ER, Levine RL (2003) Free radical-mediated oxidation of free amino acids and amino acid residues in proteins. Amino Acids 25: 207-218.
145. Lo TWC, Westwood ME, McLellan AC, Selwood T, Thornalley PJ (1994) Binding and modification of proteins by methylglyoxal under physiological conditions - a kinetic and mechanistic study with n-alpha-acetylarginine, n-alpha-acetylcysteine, and n-alpha-acetyllysine, and bovine serum-albumin. Journal of Biological Chemistry 269: 32299-32305.
146. Wellsknecht MC, Thorpe SR, Baynes JW (1995) Pathways of formation of glycoxidation products during glycation of collagen. Biochemistry 34: 15134-15141.
147. Miyata T, Kurokawa K, de Strihou CV (2000) Relevance of oxidative and carbonyl stress to long-term uremic complications. Kidney International 58: S120-S125.
148. Yin DZ, Chen KJ (2005) The essential mechanisms of aging: Irreparable damage accumulation of biochemical side-reactions. Experimental Gerontology 40: 455-465.
149. Artwohl M, Graier WF, Roden M, Bischof M, Freudenthaler A, et al. (2003) Diabetic LDL triggers apoptosis in vascular endothelial cells. Diabetes 52: 1240-1247.

150. Zimmermann R, Panzenbock U, Wintersperger A, Levak-Frank S, Graier W, et al. (2001) Lipoprotein lipase mediates the uptake of glycated LDL in fibroblasts, endothelial cells, and macrophages. Diabetes 50: 1643-1653.
151. Knott HM, Brown BE, Davies MJ, Dean RT (2003) Glycation and glycoxidation of low-density lipoproteins by glucose and low-molecular mass aldehydes - Formation of modified and oxidized particles. European Journal of Biochemistry 270: 3572-3582.
152. Dan T, de Strihou CV, Miyata T (2011) Advanced Glycation End Products Inhibitor. Studies on Renal Disorders; Miyata T, Eckardt KU, Nangaku M, editors. New York: Springer pp. 389-406.
153. Inagi R (2011) Inhibitors of advanced glycation and endoplasmic reticulum stress. Methods in Enzymology, Vol 491: Unfolded Protein Response and Cellular Stress; Conn PM, editor. San Diego, USA: Elsevier Academic Press Incorporation 361-380 p.
154. Jandeleit-Dahm KA, Lassila M, Allen TJ (2005) Advanced glycation end products in diabetes associated atherosclerosis and renal disease - Interventional studies. Maillard Reaction: Chemistry at the Interface of Nutrition, Aging, and Disease; Baynes JW, Monnier VM, Ames JM, Thorpe SR, editors. New York, USA: New York Academy Sciences pp. 759-766.
155. Rahbar S, Figarola JL (2003) Novel inhibitors of advanced glycation endproducts. Archives of Biochemistry and Biophysics 419: 63-79.
156. Reddy VP, Beyaz A (2006) Inhibitors of the Maillard reaction and AGE breakers as therapeutics for multiple diseases. Drug Discovery Today 11: 646-654.
157. Ahmed N, Thornalley PJ (2007) Advanced glycation endproducts: what is their relevance to diabetic complications? Diabetes Obesity & Metabolism 9: 233-245.
158. Smit AJ, Lutgers HL (2004) The clinical relevance of advanced glycation endproducts (AGE) and recent developments in pharmaceutics to reduce AGE accumulation. Current Medicinal Chemistry 11: 2767-2784.
159. Jerums G, Panagiotopoulos S, Forbes J, Osicka T, Cooper M (2003) Evolving concepts in advanced glycation, diabetic nephropathy, and diabetic vascular disease. Archives of Biochemistry and Biophysics 419: 55-62.
160. Forbes JM, Soldatos G, Thomas MC (2005) Below the radar: advanced glycation end products that detour "around the side". Is HbA1c not an accurate enough predictor of long term progression and glycaemic control in diabetes? The Clinical Biochemist Reviews 26: 123-134.
161. Peng X, Ma J, Chen F, Wang M (2011) Naturally occurring inhibitors against the formation of advanced glycation end-products. Food & Function 2: 289-301.
162. Booth AA, Khalifah RG, Hudson BG (1996) Thiamine pyrophosphate and pyridoxamine inhibit the formation of antigenic advanced glycation end-products: Comparison with aminoguanidine. Biochemical and Biophysical Research Communications 220: 113-119.
163. Bolton WK, Cattran DC, Williams ME, Adler SG, Appel GB, et al. (2004) Randomized trial of an inhibitor of formation of advanced glycation end products in diabetic nephropathy. American Journal of Nephrology 24: 32-40.
164. Guiotto A, Calderan A, Ruzza P, Borin G (2005) Carnosine and carnosine-related antioxidants: A review. Current Medicinal Chemistry 12: 2293-2315.
165. Baguet A, Reyngoudt H, Pottier A, Everaert I, Callens S, et al. (2009) Carnosine loading and washout in human skeletal muscles. Journal of Applied Physiology 106: 837-842.

166. Jackson MC, Lenney JF (1996) The distribution of carnosine and related dipeptides in rat and human tissues. Inflammation Research 45: 132-135.
167. Gardner MLG, Illingworth KM, Kelleher J, Wood D (1991) Intestinal-absorption of the intact peptide carnosine in man, and comparison with intestinal permeability to lactulose. Journal of Physiology-London 439: 411-422.
168. Teufel M, Saudek V, Ledig JP, Bernhardt A, Boularand S, et al. (2003) Sequence identification and characterization of human carnosinase and a closely related non-specific dipeptidase. Journal of Biological Chemistry 278: 6521-6531.
169. Rashid I, van Reyk DM, Davies MJ (2007) Carnosine and its constituents inhibit glycation of low-density lipoproteins that promotes foam cell formation *in vitro*. FEBS Letters 581: 1067-1070.
170. Yeum KJ, Orioli M, Regazzoni L, Carini M, Rasmussen H, et al. (2010) Profiling histidine dipeptides in plasma and urine after ingesting beef, chicken or chicken broth in humans. Amino Acids 38: 847-858.
171. Quinn PJ, Boldyrev AA, Formazuyk VE (1992) Carnosine - its properties, functions and potential therapeutic applications. Molecular Aspects of Medicine 13: 379-444.
172. Babizhayev MA (2004) Rejuvenation of visual functions in older adult drivers and drivers with cataract during a short-term administration of N-acetylcarnosine lubricant eye drops. Rejuvenation Research 7: 186-198.
173. Babizhayev MA (2005) Analysis of lipid peroxidation and electron microscopic survey of maturation stages during human cataractogenesis: pharmacokinetic assay of Can-C N-acetylcarnosine prodrug lubricant eye drops for cataract prevention. Drugs in R&D 6: 345-369.
174. Babizhayev MA, Micans P, Guiotto A, Kasus-Jacobi A (2009) N-Acetylcarnosine lubricant eyedrops possess all-in-one universal antioxidant protective effects of L-carnosine in aqueous and lipid membrane environments, aldehyde scavenging, and transglycation activities inherent to cataracts: A clinical study of the new vision-saving drug N-Acetylcarnosine eyedrop therapy in a database population of over 50,500 patients. American Journal of Therapeutics 16: 517-533.
175. Kaczor T (2010) L-carnosine effects of cataract development. Natural Medicine Journal 2: 13-17.
176. Meijer AJ, Codogno P (2009) Autophagy: Regulation and role in disease. Critical Reviews in Clinical Laboratory Sciences 46: 210-240.
177. Peters JM, Franke WW, Kleinschmidt JA (1994) Distinct 19-S and 20-S subcomplexes of the 26-S proteasome and their distribution in the nucleus and the cytoplasm. Journal of Biological Chemistry 269: 7709-7718.
178. Konstantinova IM, Tsimokha AS, Mittenberg AG (2008) Role of proteasomes in cellular regulation. International Review of Cell and Molecular Biology Volume 267; Jeon KW, editor., San Diego, USA: Elsevier Academic Press Incorporation pp 59-124.
179. McNaught KSP, Olanow CW, Halliwell B, Isacson O, Jenner P (2001) Failure of the ubiquitin-proteasome system in Parkinson's disease. Nature Reviews Neuroscience 2: 589-594.
180. Lutgens SPM, Cleutjens K, Daemen M, Heeneman S (2007) Cathepsin cysteine proteases in cardiovascular disease. FASEB Journal 21: 3029-3041.
181. Wolters PJ, Chapman HA (2000) Importance of lysosomal cysteine proteases in lung disease. Respiratory Research 1: 170-177.
182. Turk V, Turk B, Turk D (2001) Lysosomal cysteine proteases: facts and opportunities. EMBO Journal 20: 4629-4633.

183. Kuester D, Lippert H, Roessner A, Krueger S (2008) The cathepsin family and their role in colorectal cancer. Pathology Research and Practice 204: 491-500.
184. Colbert JD, Matthews SP, Miller G, Watts C (2009) Diverse regulatory roles for lysosomal proteases in the immune response. European Journal of Immunology 39: 2955-2965.
185. Stoka V, Turk B, Turk V (2005) Lysosomal cysteine proteases: Structural features and their role in apoptosis. IUBMB Life 57: 347-353.
186. Sasaki M, Miyakoshi M, Sato Y, Nakanuma Y (2010) Autophagy mediates the process of cellular senescence characterizing bile duct damages in primary biliary cirrhosis. Laboratory Investigation 90: 835-843.
187. Sukhova GK, Shi GP, Simon DI, Chapman HA, Libby P (1998) Expression of the elastolytic cathepsins S and K in human atheroma and regulation of their production in smooth muscle cells. Journal of Clinical Investigation 102: 576-583.
188. Mattock KL, Gough PJ, Humphries J, Burnand K, Patel L, et al. (2010) Legumain and cathepsin-L expression in human unstable carotid plaque. Atherosclerosis 208: 83-89.
189. Liu J, Sukhova GK, Yang JT, Sun JS, Ma LK, et al. (2006) Cathepsin L expression and regulation in human abdominal aortic aneurysm, atherosclerosis, and vascular cells. Atherosclerosis 184: 302-311.
190. Chen JQ, Tung CH, Mahmood U, Ntziachristos V, Gyurko R, et al. (2002) *In vivo* imaging of proteolytic activity in atherosclerosis. Circulation 105: 2766-2771.
191. Lutgens E, Lutgens SPM, Faber BCG, Heeneman S, Gijbels MMJ, et al. (2006) Disruption of the Cathepsin K gene reduces atherosclerosis progression and induces plaque fibrosis but accelerates macrophage foam cell formation. Circulation 113: 98-107.
192. Sukhova GK, Zhang Y, Pan JH, Wada Y, Yamamoto T, et al. (2003) Deficiency of cathepsin S reduces atherosclerosis in LDL receptor-deficient mice. Journal of Clinical Investigation 111: 897-906.
193. Rodgers KJ, Watkins DJ, Miller AL, Chan PY, Karanam S, et al. (2006) Destabilizing role of cathepsin S in murine atherosclerotic plaques. Arteriosclerosis Thrombosis and Vascular Biology 26: 851-856.
194. Sasaki T, Kuzuya M, Nakamura K, Cheng XW, Hayashi T, et al. (2010) AT1 blockade attenuates atherosclerotic plaque destabilization accompanied by the suppression of cathepsin S activity in apo E-deficient mice. Atherosclerosis 210: 430-437.
195. Podgorski I (2009) Future of anticathepsin K drugs: dual therapy for skeletal disease and atherosclerosis? Future Medicinal Chemistry 1: 21-34.
196. Tang J, Wong RNS (1987) Evolution in the structure and function of aspartic proteases. Journal of Cellular Biochemistry 33: 53-63.
197. Benes P, Vetvicka V, Fusek M (2008) Cathepsin D-Many functions of one aspartic protease. Critical Reviews in Oncology Hematology 68: 12-28.
198. Abd-Elgaliel WR, Tung C-H (2010) Selective detection of Cathepsin E proteolytic activity. Biochimica Et Biophysica Acta-General Subjects 1800: 1002-1008.
199. Haidar B, Kiss RS, Sarov-Blat L, Brunet R, Harder C, et al. (2006) Cathepsin D, a lysosomal protease, regulates ABCA1-mediated lipid efflux. Journal of Biological Chemistry 281: 39971-39981.
200. Jormsjo S, Wuttge DM, Sirsjo A, Whatling C, Hamsten A, et al. (2002) Differential expression of cysteine and aspartic proteases during progression of

atherosclerosis in apolipoprotein E-deficient mice. American Journal of Pathology 161: 939-945.
201. Wu KK, Huan YM (2007) Diabetic atherosclerosis mouse models. Atherosclerosis 191: 241-249.
202. Plump AS, Breslow JL (1995) Apolipoprotein-E and the apolipoprotein E-deficient mouse. Annual Review of Nutrition 15: 495-518.
203. Zhang SH, Reddick RL, Piedrahita JA, Maeda N (1992) Spontaneous hypercholesterolemia and arterial lesions in mice lacking apolipoprotein-E. Science 258: 468-471.
204. Nakashima Y, Plump AS, Raines EW, Breslow JL, Ross R (1994) Apo E-deficient mice develop lesions of all phases of atherosclerosis throughout the arterial tree. Arteriosclerosis and Thrombosis 14: 133-140.
205. Forbes JM, Yee LTL, Thallas V, Lassila M, Candido R, et al. (2004) Advanced glycation end product interventions reduce diabetes-accelerated atherosclerosis. Diabetes 53: 1813-1823.
206. Johnson J, Carson K, Williams H, Karanam S, Newby A, et al. (2005) Plaque rupture after short periods of fat feeding in the apolipoprotein E-knockout mouse - Model characterization and effects of pravastatin treatment. Circulation 111: 1422-1430.
207. Martinic G, Hazell L, Stocker R (2003) Vascular microdissection, perfusion, and excision of the murine arterial tree for use in atherogenic disease investigations. Contemporary Topics in Laboratory Animal Science 42: 47-52.
208. Zuccollo A, Shi CM, Mastroianni R, Maitland-Toolan KA, Weisbrod RM, et al. (2005) The thromboxane A(2) receptor antagonist S18886 prevents enhanced atherogenesis caused by diabetes mellitus. Circulation 112: 3001-3008.
209. Renard CB, Kramer F, Johansson F, Lamharzi N, Tannock LR, et al. (2004) Diabetes and diabetes-associated lipid abnormalities have distinct effects on initiation and progression of atherosclerotic lesions. Journal of Clinical Investigation 114: 659-668.
210. Wendt T, Harja E, Bucciarelli L, Wu Q, Lu Y, et al. (2006) RAGE modulates vascular inflammation and atherosclerosis in a murine model of type 2 diabetes. Atherosclerosis 185: 70-77.
211. Candido R, Allen TJ, Lassila M, Cao ZM, Thallas V, et al. (2004) Irbesartan but not amlodipine suppresses diabetes-associated atherosclerosis. Circulation 109: 1536-1542.
212. Tse J, Martin-McNaulty B, Halks-Miller M, Kauser K, DelVecchio V, et al. (1999) Accelerated atherosclerosis and premature calcified cartilaginous metaplasia in the aorta of diabetic male Apo E knockout mice can be prevented by chronic treatment with 17 beta-estradiol. Atherosclerosis 144: 303-313.
213. Hayek T, Hussein K, Aviram M, Coleman R, Keidar S, et al. (2005) Macrophage-foam cell formation in streptozotocin-induced diabetic mice: Stimulatory effect of glucose. Atherosclerosis 183: 25-33.
214. Kanasaki K, Koya D (2011) Biology of Obesity: Lessons from Animal Models of Obesity. Journal of Biomedicine and Biotechnology 2011:1-11.
215. Tesch GH, Lim AKH (2011) Recent insights into diabetic renal injury from the db/db mouse model of type 2 diabetic nephropathy. American Journal of Physiology-Renal Physiology 300: F301-F310.
216. Alpers CE, Hudkins KL (2011) Mouse models of diabetic nephropathy. Current Opinion in Nephrology and Hypertension 20: 278-284.
217. Violaine Rolland KC, Isabelle Dugail, Bernard Guy-Grand, Arnaud Basdevant, Philippe Fropel ML (1998) Leptin receptor gene in a large cohort of massively

obese subjects: No indication of the fa/fa rat mutation. Detection of an intronic variant with no association with obesity. Obesity Research 6: 122-127.
218. Matsuoka N, Ogawa, Y., Hosoda, K., Matsuda, H. Masuzaki, J., Miyawaki, T., Azuma, N., Natsui, K., Nishimura H, Yoshimasa, Y., Nishi, S., Thompson, D.B. , Nakao, K. (1997) Human leptin receptor gene in obese Japanese subjects: evidence against either obesity-causing mutations or association of sequence variants with obesity. Diabetologia 40: 1204–1210.
219. Vickers SP, Jackson, H. C. and Cheetham, S. C (2011) The utility of animal models to evaluate novel anti-obesity agents. British Journal of Pharmacology 164: 1248-1262.
220. West DB, Boozer, C. N., Moody, D. L.and Atkinson, R. L. (1992) Dietary obesity in nine inbred mouse strains. American Journal of Physiology-Cell Physiology 262: R1025-R1032.
221. Srinivasan KaR, P (2007) Animal models in type 2 diabetes research: An overview. Indian Journal of Medical Research 125: 451-472.
222. Speakman J, Hambly, C., Mitchell, S., Krol, E. (2007) Animal models of obesity. Obesity Reviews 8: 55-61.
223. Clee SMaA, A. D. (2007) The genetic landscape of type 2 diabetes in mice. Endocrine Reviews 28: 48-83.
224. Wang CY, Liao JK (2012) A mouse model of diet-induced obesity and insulin resistance. mTOR Methods and Protocols; Weichhart T, editor. Totowa, NJ, USA: Humana Press Incorporation pp. 421-433.
225. Guo JE, Hall KD (2011) Predicting changes of body weight, body fat, energy expenditure and metabolic fuel selection in C57BL/6 mice. Plos One 6: 1-9.
226. Williams TD, Chambers JB, Roberts LM, Henderson RP, Overton JM (2003) Diet-induced obesity and cardiovascular regulation in C57BL/6J mice. Clinical and Experimental Pharmacology and Physiology 30: 769-778.
227. Lijnen HR, Maquoi E, Holvoet P, Mertens A, Lupu F, et al. (2001) Adipose tissue expression of gelatinases in mouse models of obesity. Thrombosis and Haemostasis 85: 1111-1116.
228. Garner B, Dean RT, Jessup W (1994) Human macrophage-mediated oxidation of low-density-lipoprotein is delayed and independent of superoxide production. Biochemical Journal 301: 421-428.
229. Headlam HA, Gracanin M, Rodgers KJ, Davies MJ (2006) Inhibition of cathepsins and related proteases by amino acid, peptide, and protein hydroperoxides. Free Radical Biology and Medicine 40: 1539-1548.
230. Yan C, Lian XM, Li Y, Dai Y, White A, et al. (2006) Macrophage-specific expression of human lysosomal acid lipase corrects inflammation and pathogenic phenotypes in lal(-/-) mice. American Journal of Pathology 169: 916-926.
231. Park L, Raman KG, Lee KJ, Lu Y, Ferran LJ, et al. (1998) Suppression of accelerated diabetic atherosclerosis by the soluble receptor for advanced glycation endproducts. Nature Medicine 4: 1025-1031.
232. McRobb L, Handelsman DJ, Heather AK (2009) Androgen-induced progression of arterial calcification in apolipoprotein E-null mice is uncoupled from plaque growth and lipid levels. Endocrinology 150: 841-848.
233. Bursill CA, Choudhury RP, Ali Z, Greaves DR, Channon KM (2004) Broad-spectrum CC-chemokine blockade by gene transfer inhibits macrophage recruitment and atherosclerotic plaque formation in apolipoprotein E-knockout mice. Circulation 110: 2460-2466.

234. Reimers GJ, Jackson CL, Rickards J, Chan PY, Cohn JS, et al. (2011) Inhibition of rupture of established atherosclerotic plaques by treatment with apolipoprotein A-I. Cardiovascular Research 91: 37-44.
235. Ross R (1999) Mechanisms of disease - Atherosclerosis - An inflammatory disease. New England Journal of Medicine 340: 115-126.
236. Davidson JA, Parkin CG (2009) Is Hyperglycemia a Causal Factor in Cardiovascular Disease? Does proving this relationship really matter? Yes. Diabetes Care 32: S331-S333.
237. Yan ZQ, Hansson GK (2007) Innate immunity, macrophage activation, and atherosclerosis. Immunological Reviews 219: 187-203.
238. Weber C, Zernecke A, Libby P (2008) The multifaceted contributions of leukocyte subsets to atherosclerosis: lessons from mouse models. Nature Reviews Immunology 8: 802-815.
239. Jerome WG (2006) Advanced atherosclerotic foam cell formation has features of an acquired lysosomal storage disorder. Rejuvenation Research 9: 245-255.
240. Brown BE, Rashid I, van Reyk DM, Davies MJ (2007) Glycation of low-density lipoprotein results in the time-dependent accumulation of cholesteryl esters and apolipoprotein B-100 protein in primary human monocyte-derived macrophages. FEBS Journal 274: 1530-1541.
241. Dunlop RA, Brunk UT, Rodgers KJ (2009) Oxidized Proteins: Mechanisms of Removal and Consequences of Accumulation. IUBMB Life 61: 522-527.
242. Moheimani F, Morgan PE, van Reyk DM, Davies MJ (2010) Deleterious effects of reactive aldehydes and glycated proteins on macrophage proteasomal function: Possible links between diabetes and atherosclerosis. Biochimica Et Biophysica Acta-Molecular Basis of Disease 1802: 561-571.
243. Zeng JM, Dunlop RA, Rodgers KJ, Davies MJ (2006) Evidence for inactivation of cysteine proteases by reactive carbonyls via glycation of active site thiols. Biochemical Journal 398: 197-206.
244. Moheimani F, Kim CHJ, Rahmanto AS, van Reyk DM, Davies MJ (2012) Inhibition of lysosomal function in macrophages incubated with elevated glucose concentrations: A potential contributory factor in diabetes-associated atherosclerosis. Atherosclerosis 223: 144-151.
245. Kisugi R, Kouzuma T, Yamamoto T, Akizuki S, Miyamoto H, et al. (2007) Structural and glycation site changes of albumin in diabetic patient with very high glycated albumin. Clinica Chimica Acta 382: 59-64.
246. Urbich C, Dernbach E, Rossig L, Zeiher AM, Dimmeler S (2008) High glucose reduces cathepsin L activity and impairs invasion of circulating progenitor cells. Journal of Molecular and Cellular Cardiology 45: 429-436.
247. Thornalley PJ (1996) Pharmacology of methylglyoxal: Formation, modification of proteins and nucleic acids, and enzymatic detoxification - A role in pathogenesis and antiproliferative chemotherapy. General Pharmacology 27: 565-573.
248. Patschan S, Goligorsky MS (2008) Auotphagy: The missing link between non-enzymatically glycated proteins inducing apoptosis and premature senescence of endothelial cells. Autophagy 4: 521-523.
249. Ishibashi F (2006) Chronic high glucose inhibits albumin reabsorption by lysosomal alkalinization in cultured porcine proximal tubular epithelial cells (LLC-PK1). Diabetes Research and Clinical Practice 72: 223-230.
250. Hideshima T, Bradner JE, Chauhan D, Anderson KC (2005) Intracellular protein degradation and its therapeutic implications. Clinical Cancer Research 11: 8530-8533.

251. Finegold DN, Coates PM (1984) Effect of diabetes and insulin therapy on human mononuclear leukocyte lysosomal acid lipase activity. Metabolism-Clinical and Experimental 33: 85-89.
252. Henze K, Chait A (1981) Lysosomal enzyme-activities and low-density lipoprotein receptors in circulating mononuclear-cells - effect of insulin therapy in diabetic-patients. Diabetologia 20: 625-629.
253. Du H, Sheriff S, Bezerra J, Leonova T, Grabowski GA (1998) Molecular and enzymatic analyses of lysosomal acid lipase in cholesteryl ester storage disease. Molecular Genetics and Metabolism 64: 126-134.
254. Wolman M (1995) Wolman-disease and its treatment. Clinical Pediatrics 34: 207-212.
255. Zschenker O, Illies T, Ameis D (2006) Overexpression of lysosomal acid lipase and other proteins in atherosclerosis. Journal of Biochemistry 140: 23-38.
256. Heltianu C, Robciuc A, Botez G, Musina C, Stancu C, et al. (2011) Modified low density lipoproteins decrease the activity and expression of lysosomal acid lipase in human endothelial and smooth muscle cells. Cell Biochemistry and Biophysics 61: 209-216.
257. Liu J, Ma LK, Yang JT, Ren A, Sun ZM, et al. (2006) Increased serum cathepsin S in patients with atherosclerosis and diabetes. Atherosclerosis 186: 411-419.
258. Vivanco F, Martin-Ventura JL, Duran MC, Barderas MG, Blanco-Colio L, et al. (2005) Quest for novel cardiovascular biomarkers by proteomic analysis. Journal of Proteome Research 4: 1181-1191.
259. Oberg G, Hallgren R, Moberg L, Venge P (1986) Bactericidal proteins and neutral proteases in diabetes neutrophils. Diabetologia 29: 426-429.
260. Sodha NR, Clements RT, Boodhwani M, Xu SH, Laham RJ, et al. (2009) Endostatin and angiostatin are increased in diabetic patients with coronary artery disease and associated with impaired coronary collateral formation. American Journal of Physiology-Heart and Circulatory Physiology 296: H428-H434.
261. Miyata S, Liu BP, Shoda H, Ohara T, Yamada H, et al. (1997) Accumulation of pyrraline-modified albumin in phagocytes due to reduced degradation by lysosomal enzymes. Journal of Biological Chemistry 272: 4037-4042.
262. Lougheed M, Zhang HF, Steinbrecher UP (1991) Oxidized low-density-lipoprotein is resistant to cathepsins and accumulates within macrophages. Journal of Biological Chemistry 266: 14519-14525.
263. Brunk UT, Terman A (2002) Lipofuscin: Mechanisms of age-related accumulation and influence on cell function. Free Radical Biology and Medicine 33: 611-619.
264. Ylaherttuala S, Palinski W, Rosenfeld ME, Parthasarathy S, Carew TE, et al. (1989) Evidence for the presence of oxidatively modified low-density lipoprotein in atherosclerotic lesions of rabbit and man. Journal of Clinical Investigation 84: 1086-1095.
265. Palinski W, Rosenfeld ME, Ylaherttuala S, Gurtner GC, Socher SS, et al. (1989) Low-density lipoprotein undergoes oxidative modification *in vivo*. Proceedings of the National Academy of Sciences of the United States of America 86: 1372-1376.
266. Ylaherttuala S, Palinski W, Rosenfeld ME, Steinberg D, Witztum JL (1990) Lipoproteins in normal and atherosclerotic aorta. European Heart Journal 11: 88-99.
267. Morgan PE, Dean RT, Davies MJ (2002) Inactivation of cellular enzymes by carbonyls and protein-bound glycation/glycoxidation products. Archives of Biochemistry and Biophysics 403: 259-269.

268. Stolzing A, Widmer R, Jung T, Voss P, Grune T (2006) Degradation of glycated bovine serum albumin in microglial cells. Free Radical Biology and Medicine 40: 1017-1027.
269. Grimm S, Horlacher M, Catalgol B, Hoehn A, Reinheckel T, et al. (2012) Cathepsins D and L reduce the toxicity of advanced glycation end products. Free Radical Biology and Medicine 52: 1011-1023.
270. Xiang G, Schinzel R, Simm A, Sebekova K, Heidland A (2001) Advanced glycation end products impair protein turnover in LLC-PK1: amelioration by trypsin. Kidney International. Supplement 78: S53-57.
271. Sebekova K, Schinzel R, Ling H, Simm A, Xiang GS, et al. (1998) Advanced glycated albumin impairs protein degradation in the kidney proximal tubules cell line LLC-PK1. Cellular and Molecular Biology 44: 1051-1060.
272. Moheimani F, Tan JTM, Brown BE, Heather AK, van Reyk DM, et al. (2011) Effect of exposure of human monocyte-derived macrophages to high, versus normal, glucose on subsequent lipid accumulation from glycated and acetylated low-density lipoproteins. Experimental Diabetes Research 2011 : 1-10.
273. Grune T, Merker K, Sandig G, Davies KJA (2003) Selective degradation of oxidatively modified protein substrates by the proteasome. Biochemical and Biophysical Research Communications 305: 709-718.
274. Grimm S, Ernst L, Grotzinger N, Hohn A, Breusing N, et al. (2010) Cathepsin D is one of the major enzymes involved in intracellular degradation of AGE-modified proteins. Free Radical Research 44: 1013-1026.
275. Davidson JA, Parkin CG (2009) Is hyperglycemia a causal factor in cardiovascular disease? Does proving this relationship really matter? Yes. Diabetes Care 32 Suppl 2: S331-S333.
276. Park L, Raman KG, Lee KJ, Lu Y, Ferran LJ, et al. (1998) Suppression of accelerated diabetic atherosclerosis by the soluble receptor for advanced glycation endproducts. Nature Medicine 4: 1025-1031.
277. Hsueh WA, Abel ED, Breslow JL, Maeda N, Davis RC, et al. (2007) Recipes for creating animal models of diabetic cardiovascular disease. Circulation Research 100: 1415-1427.
278. Jandeleit-Dahm K, Cooper ME (2008) The role of AGEs in cardiovascular disease. Current Pharmaceutical Design 14: 979-986.
279. Harris RC, Tallon MJ, Dunnett M, Boobis L, Coakley J, et al. (2006) The absorption of orally supplied β-alanine and its effect on muscle carnosine synthesis in human vastus lateralis. Amino Acids 30: 279-289.
280. Hipkiss AR (2009) Carnosine and its possible roles in nutrition and health. Advances in Food & Nutrition Research 57: 87-154.
281. Rashid I, van Reyk DM, Davies MJ (2007) Carnosine and its constituents inhibit glycation of low-density lipoproteins that promote foam cell formation *in vitro*. FEBS Letters 581: 1067-1070.
282. Menini S, Iacobini C, Ricci C, Scipioni A, Fantauzzi CB, et al. (2012) D-carnosine octylester attenuates atherosclerosis and renal disease in ApoE null mice fed a Western diet through reduction of carbonyl stress and inflammation. British Journal of Pharmacology 166: 1344-1356.
283. Mong M, Chao C, Yin M (2011) Histidine and carnosine alleviated hepatic steatosis in mice consumed high saturated fat diet. European Journal of Pharmacology 653: 82-88.
284. Asatoor AM, Bandoh JK, Lant AF, Milne MD, Navab F (1970) Intestinal absorption of carnosine and its constituent amino acids in man. Gut 11: 250-254.

285. Fontana M, Pinnen F, Lucente G, Pecci L (2002) Prevention of peroxynitrite-dependent damage by carnosine and related sulphonamido pseudodipeptides. Cellular and Molecular Life Sciences 59: 546-551.
286. Cacciatore I, Cocco A, Costa M, Fontana M, Lucente G, et al. (2005) Biochemical properties of new synthetic carnosine analogues containing the resdiue of 2,3-diaminopropionic acid: the effect of N-acetylation. Amino Acids 28: 77-83.
287. Stvolinsky SL, Bulygina ER, Fedorova TN, Meguro K, Sato T, et al. (2010) Biological Activity of Novel Synthetic Derivatives of Carnosine. Cellular and Molecular Neurobiology 30: 395-404.
288. Lee Y-T, Hsi C-C, Lin M-H, Liu K-S, Yimn M-C (2005) Histidine and carnosine delay diabetic deterioration in mice and protect human low density lipoprotein against oxidation and glycation. European Journal of Pharmacology 513: 145-150.
289. Aldini G, Orioli M, Rossoni G, Savi F, Braidotti P, et al. (2011) The carbonyl scavenger carnosine ameliorates dyslipidemia and renal function in Zucker obese rats. Journal of Cellular Molecular Medicine 15: 1339-1356.
290. Park YJ, Volpe SL, Decker EA (2005) Quantitation of carnosine in humans plasma after dietary consumption of beef. Journal of Agriculture Food Chemistry 53: 4736-4739.
291. Nestel P, Fujii A, Allen T (2006) The cis-9,trans-11 isomer of conjugated linoleic acid (CLA) lowers plasma triglyceride and raises HDL cholesterol concentrations but does not suppress aortic atherosclerosis in diabetic apo E-deficient mice. Atherosclerosis 189: 282-287.
292. Yamano T, Niijima A, Iimori S, Tsuruoka N, Kiso Y, et al. (2001) Effect of L-carnosine on the hyperglycemia caused by intracranial injection of 2-deoxy-D-glucose in rats. Neuroscience Letters 313: 78-82.
293. McClellan AC, Phillips SA, Thornalley PJ (1992) The assay of methylglyoxal in biological systems by derivatization with 1,2-diamino-4,5-dimethoxybenzene. Analytical Biochemistry 206: 17-23.
294. Odani H, Shinzato T, Matsumoto Y, Usami J, Maeda K (1999) Increase in three a,b-dicarbonyl compound levels in human uremic plasma: specific *in vivo* determination of intermediates in advanced Maillard reaction. Biochemical and Biophysical Ressearch Communications 256: 89-93.
295. Lapolla A, Flamini R, dalla Vedova A, Senesi A, Reitano R, et al. (2003) Glyoxal and methylglyoxal levels in diabetic patients: quantitative determination by a new GC/MS method. Clinical Chemistry and Laboratory Medicine 41: 1166-1173.
296. Mukhopadhyay S, Sen S, Majhi B, Das KP, Kar M (2007) Methyl glyoxal elevation is associated with oxidative stress in rheumatoid arthritis. Free Radical Research 41: 507 - 514.
297. Lo TWC, Westwood ME, McLellan AC, Selwood T, Thornalley PJ (1994) Binding and modification of proteins by methylglyoxal under physiological conditions. A kinetic and mechanistic study with Na-acetylarginine, Na-acetylcysteine, and Na-acetyllysine, and bovine serum albumin. Journal of Biolological Chemistry 269: 32299-32305.
298. Small DM, Shipley GG (1974) Physical-chemical basis of lipid deposition in atherosclerosis. Science 185: 222-229.
299. Levi Z, Shaish A, Yacov N, Levkovitz H, Trestman S, et al. (2003) Rosiglitazone (PPAR-g-agonist) attenuates atherogenesis with no effect on hyperglycaemia in a combined diabetes-atherosclerosis mouse model. Diabetes, Obesity and Metabolism 5: 45-50.

300. Finn AV, Nakano M, Narula J, Kolodgie FD, Virmani R (2010) Concept of vulnerable/unstable plaque. Arteriosclerosis Thrombosis and Vascular Biology 30: 1282-1292.
301. van der Wal AC, Becker AE (1999) Atherosclerotic plaque rupture - pathologic basis of plaque stability and instability. Cardiovascular Research 41: 334-344.
302. Koskinas KC SG, Baker AB, Papafaklis MI, Chatzizisis YS, Coskun AU, Quillard T, Jonas M, Maynard C, Antoniadis AP, Shi GP, Libby P, Edelman ER, Feldman CL, Stone PH. (2013) Thin-capped atheromata with reduced collagen content in pigs develop in coronary arterial regions exposed to persistently low endothelial shear stress. Arteriosclerosis Thrombosis and Vascular Biology 33: 1494-1504.
303. Toutouzas K, Synetos A, Nikolaou C, Tsiamis E, Tousoulis D, et al. (2012) Matrix metalloproteinases and vulnerable atheromatous plaque. Current Topics in Medicinal Chemistry 12: 1166-1180.
304. Graham I, Cooney M-T, Bradley D, Dudina A, Reiner Z (2012) Dyslipidemias in the prevention of cardiovascular disease: risks and causality. Current Cardiology Reports 14: 709-720.
305. Singhal A (2013) Early growth and later atherosclerosis. World Review of Nutrition and Dietetics 106: 162-167.
306. Manduteanu I, Simionescu M (2012) Inflammation in atherosclerosis: a cause or a result of vascular disorders? Journal of Cellular and Molecular Medicine 16: 1978-1990.
307. Shanker J, Rao VS, Ravindran V, Dhanalakshmi B, Hebbagodi S, et al. (2012) Relationship of adiponectin and leptin to coronary artery disease, classical cardiovascular risk factors and atherothrombotic biomarkers in the IARS cohort. Thrombosis and Haemostasis 108: 769-780.
308. Rudkowska I, Dewailly E, Hegele RA, Boiteau V, Dube-Linteau A, et al. (2013) Gene-diet interactions on plasma lipid levels in the Inuit population. British Journal of Nutrition 109: 953-961.
309. Alciati A, Gesuele F, Casazza G, Foschi D (2013) The Relationship between Childhood Parental Loss and Metabolic Syndrome in Obese Subjects. Stress and Health 29: 5-13.
310. Carroll MD, Lacher DA, Sorlie PD, Cleeman JI, Gordon DJ, et al. (2005) Trends in serum lipids and lipoproteins of adults, 1960-2002. JAMA-Journal of the American Medical Association 294: 1773-1781.
311. Kanthe PS, Patil BS, Shrilaxmi B, Anita D, Shaikh GB, et al. (2012) Atherogenic index as a predictor of cardiovascular risk among women with different grades of obesity. International Journal of Collaborative Research on Internal Medicine and Public Health (IJCRIMPH) 4: 1767-1774.
312. Enos RT, Davis JM, Velazquez KT, McClellan JL, Day SD, et al. (2013) Influence of dietary saturated fat content on adiposity, macrophage behavior, inflammation, and metabolism: composition matters. Journal of Lipid Research 54: 152-163.
313. Choi Y, Kim Y, Park S, Lee KW, Park T (2012) Indole-3-carbinol prevents diet-induced obesity through modulation of multiple genes related to adipogenesis, thermogenesis or inflammation in the visceral adipose tissue of mice. Journal of Nutritional Biochemistry 23: 1732-1739.
314. Lee YS, Cha BY, Choi SS, Choi BK, Yonezawa T, et al. (2013) Nobiletin improves obesity and insulin resistance in high-fat diet-induced obese mice. Journal of Nutritional Biochemistry 24: 156-162.
315. Scott NJA, Cameron VA, Raudsepp S, Lewis LK, Simpson ER, et al. (2012) Generation and characterization of a mouse model of the metabolic syndrome:

apolipoprotein E and aromatase double knockout mice. American Journal of Physiology-Endocrinology and Metabolism 302: E576-E584.
316. Park Y, Booth FW, Lee S, Laye MJ, Zhang CH (2012) Physical activity opposes coronary vascular dysfunction induced during high fat feeding in mice. Journal of Physiology-London 590: 4255-4268.
317. Forbes JM, Cooper ME (2013) Mechanisms of diabetic complications. Physiological Reviews 93: 137-188.
318. Wattanakit K, Lutsey PL, Bell EJ, Gornik H, Cushman M, et al. (2012) Association between cardiovascular disease risk factors and occurrence of venous thromboembolism A time-dependent analysis. Thrombosis and Haemostasis 108: 508-515.
319. Jeppesen J, Hein HO, Suadicani P, Gyntelberg F (1998) Triglyceride concentration and ischemic heart disease - An eight-year follow-up in the Copenhagen Male Study. Circulation 97: 1995-1995.
320. Di Angelantonio E, Sarwar N, Perry P, Kaptoge S, Ray KK, et al. (2009) Major lipids, apolipoproteins, and risk of vascular disease. JAMA-Journal of the American Medical Association 302: 1993-2000.
321. Gluba A, Mikhailidis DP, Lip GYH, Hannam S, Rysz J, et al. (2013) Metabolic syndrome and renal disease. International Journal of Cardiology 164: 141-150.
322. Li Z, Deng ML, Tseng C-H, Heber D (2013) Hypertriglyceridemia is a practical biomarker of metabolic syndrome in individuals with abdominal obesity. Metabolic Syndrome and Related Disorders 11: 87-91.
323. Garcia C, Feve B, Ferre P, Halimi S, Baizri H, et al. (2010) Diabetes and inflammation: Fundamental aspects and clinical implications. Diabetes & Metabolism 36: 327-338.
324. Altay U, Gurgan CA, Agbaht K (2013) Changes in inflammatory and metabolic parameters after periodontal treatment in patients with and without obesity. Journal of Periodontology 84: 13-23.
325. Dallal RM, Hatalski A, Trang A, Chernoff A (2012) Longitudinal analysis of cardiovascular parameters after gastric bypass surgery. Surgery for Obesity and Related Diseases 8: 703-709.
326. Giannetti M, Piaggi P, Ceccarini G, Mazzeo S, Querci G, et al. (2012) Hepatic left lobe volume is a sensitive index of metabolic improvement in obese women after gastric banding. International Journal of Obesity 36: 336-341.
327. Algahim MF, Sen S, Taegtmeyer H (2012) Bariatric surgery to unload the stressed heart: a metabolic hypothesis. American Journal of Physiology-Heart and Circulatory Physiology 302: H1539-H1545.
328. Moustarah F, Gilbert A, Despres JP, Tchernof A (2012) Impact of gastrointestinal surgery on cardiometabolic risk. Current Atherosclerosis Reports 14: 588-596.
329. Kenary AY, Notash AY, Nazari M, Borjian A, Afshin N, et al. (2012) Measuring the rate of weight gain and the influential role of diet in patients undergoing elective laparoscopic cholecystectomy: a 6-month follow-up study. International Journal of Food Sciences and Nutrition 63: 645-648.
330. Mitchell JB, Xavier S, DeLuca AM, Sowers AL, Cook JA, et al. (2003) A low molecular weight antioxidant decreases weight and lowers tumor incidence. Free Radical Biology and Medicine 34: 93-102.
331. Mitchell JB, Anver MR, Sowers AL, Rosenberg PS, Figueroa M, et al. (2012) The antioxidant TEMPOL reduces carcinogenesis and enhances survival in mice when administered after nonlethal total body radiation. Cancer Research 72: 4846-4855.

332. Cotrim AP, Sowers AL, Lodde BM, Vitolo JM, Kingman A, et al. (2005) Kinetics of TEMPOL for prevention of xerostomia following head and neck irradiation in a mouse model. Clinical Cancer Research 11: 7564-7568.
333. Vissink A, Mitchell JB, Baum BJ, Limesand KH, Jensen SB, et al. (2010) Clinical management of salivary gland hypofunction and xerostomia in head-and-neck cancer patients: successes and barriers. International Journal of Radiation Oncology Biology Physics 78: 983-991.
334. Metz JM, Smith D, Mick R, Lustig R, Mitchell J, et al. (2004) A phase I study of topical TEMPOL for the prevention of alopecia induced by whole brain radiotherapy. Clinical Cancer Research 10: 6411-6417.
335. Metz JM, Smith D, Mick R, Lustig R, Steal B, et al. (2006) A phase I/II study of the safety, pharmacokinetics, and preliminary efficacy of MTS-01 for the prevention of alopecia induced by whole brain radiotherapy (WBRT). International Journal of Radiation Oncology Biology Physics 66: S537-S538.
336. Wilcox CS, Pearlman A (2008) Chemistry and antihypertensive effects of TEMPOL and other nitroxides. Pharmacological Reviews 60: 418-469.
337. Schnackenberg CG, Welch WJ, Wilcox CS (1998) Normalization of blood pressure and renal vascular resistance in SHR with a membrane-permeable superoxide dismutase mimetic - Role of nitric oxide. Hypertension 32: 59-64.
338. Zicha J, Dobesova Z, Kunes J (2001) Relative deficiency of nitric oxide-dependent vasodilation in salt-hypertensive Dahl rats: the possible role of superoxide anions. Journal of Hypertension 19: 247-254.
339. Park JB, Touyz RM, Chen X, Schiffrin EL (2002) Chronic treatment with a superoxide dismutase mimetic prevents vascular remodeling and progression of hypertension in salt-loaded stroke-prone spontaneously hypertensive rats. American Journal of Hypertension 15: 78-84.
340. Ebenezer PJ, Mariappan N, Elks CM, Haque M, Francis J (2009) Diet-induced renal changes in Zucker rats are ameliorated by the superoxide dismutase mimetic TEMPOL. Obesity 17: 1994-2002.
341. Knight SF, Yuan JH, Roy S, Imig JD (2010) Simvastatin and TEMPOL protect against endothelial dysfunction and renal injury in a model of obesity and hypertension. American Journal of Physiology-Renal Physiology 298: F86-F94.
342. Samuni Y, Cook JA, Choudhuri R, DeGraff W, Sowers AL, et al. (2010) Inhibition of adipogenesis by TEMPOL in 3T3-L1 cells. Free Radical Biology and Medicine 49: 667-673.
343. Asghar M, Lokhandwala MF (2006) Antioxidant TEMPOL lowers age-related increases in insulin resistance in Fischer 344 rats. Clinical and Experimental Hypertension 28: 533-541.
344. Fujita H, Fujishima H, Chida S, Takahashi K, Qi ZH, et al. (2009) Reduction of renal superoxide dismutase in progressive diabetic nephropathy. Journal of the American Society of Nephrology 20: 1303-1313.
345. Frances DE, Ronco MT, Ingaramo PI, Monti JA, Pisani GB, et al. (2011) Role of reactive oxygen species in the early stages of liver regeneration in streptozotocin-induced diabetic rats. Free Radical Research 45: 1143-1153.
346. Patel K, Chen YF, Dennehy K, Blau J, Connors S, et al. (2006) Acute antihypertensive action of nitroxides in the spontaneously hypertensive rat. American Journal of Physiology-Regulatory Integrative and Comparative Physiology 290: R37-R43.
347. Welch WJ, Mendonca M, Blau J, Karber A, Dennehy K, et al. (2005) Antihypertensive response to prolonged TEMPOL in the spontaneously hypertensive rat. Kidney International 68: 179-187.

348. Virdis A, Santini F, Colucci R, Duranti E, Salvetti G, et al. (2011) Vascular generation of tumor necrosis factor-alpha reduces nitric oxide availability in small arteries from visceral fat of obese patients. Journal of the American College of Cardiology 58: 238-247.
349. Thomas SR, Witting PK, Drummond GR (2008) Redox control of endothelial function and dysfunction: Molecular mechanisms and therapeutic opportunities. Antioxidants & Redox Signaling 10: 1713-1765.
350. Haghjooyejavanmard S, Nematbakhsh M (2008) Endothelial function and dysfunction: clinical significance and assessment. Journal of Research in Medical Sciences 13: 207-221.
351. Panza JA, Cannon RO, III (1999) Endothelium, nitric oxide, and atherosclerosis: From basic mechanisms to clinical implications; Panza JA, Cannon RO, III, editors. New York, USA: Futura Publishing Company, Incorporation pp. 320.
352. Deanfield J, Donald A, Ferri C, Giannattasio C, Halcox J, et al. (2005) Endothelial function and dysfunction. Part I: Methodological issues for assessment in the different vascular beds: A statement by the working group on endothelin and endothelial factors of the European Society of Hypertension. Journal of Hypertension 23: 7-17.
353. Brunner H, Cockcroft JR, Deanfield J, Donald A, Ferrannini E, et al. (2005) Endothelial function and dysfunction. Part II: Association with cardiovascular risk factors and diseases. A statement by the working group on endothelins and endothelial factors of the European Society of Hypertension. Journal of Hypertension 23: 233-246.
354. Subramanian S, Chait A (2012) Hypertriglyceridemia secondary to obesity and diabetes. Biochimica Et Biophysica Acta-Molecular and Cell Biology of Lipids 1821: 819-825.
355. Rodriguez A, Doshi RR (2003) Potential therapeutic agents that raise high-density lipoprotein cholesterol levels. Expert Opinion on Therapeutic Patents 13: 167-175.
356. Tian L, Fu MD (2010) The relationship between high density lipoprotein subclass profile and plasma lipids concentrations. Lipids in Health and Disease 9.
357. Subramanian S, Turner M, Ding Y, Kim J, Buckner J, et al. (2013) An increased complement of natural killer t cells contributes to metabolic dysfunction and atherosclerosis in obese mice. Journal of Investigative Medicine 61: 113-114.
358. Norata GD, Raselli S, Grigore L, Garlaschelli K, Vianello D, et al. (2009) Small dense LDL and VLDL predict common carotid artery IMT and elicit an inflammatory response in peripheral blood mononuclear and endothelial cells. Atherosclerosis 206: 556-562.
359. Rizzo M, Berneis K (2006) Low-density lipoprotein size and cardiovascular prevention. European Journal of Internal Medicine 17: 77-80.
360. Salles J, Tardif N, Landrier JF, Mothe-Satney I, Guillet C, et al. (2012) TNF alpha gene knockout differentially affects lipid deposition in liver and skeletal muscle of high-fat-diet mice. Journal of Nutritional Biochemistry 23: 1685-1693.
361. Arya AK, Pokharia D, Bhan S, Tripathi R, Tripathi K (2012) Correlation between IL-7 and MCP-1 in diabetic chronic non healing ulcer patients at higher risk of coronary artery disease. Cytokine 60: 767-771.
362. Gobel RJ, Larsen N, Jakobsen M, Molgaard C, Michaelsen KF (2012) Probiotics to Adolescents With Obesity: Effects on Inflammation and Metabolic Syndrome. Journal of Pediatric Gastroenterology and Nutrition 55: 673-678.

363. Filippin-Monteiro FB, de Oliveira EM, Sandri S, Knebel FH, Albuquerque RC, et al. (2012) Serum amyloid A is a growth factor for 3T3-L1 adipocytes, inhibits differentiation and promotes insulin resistance. International Journal of Obesity 36: 1032-1039.
364. Nakarai H, Yamashita A, Nagayasu S, Iwashita M, Kumamoto S, et al. (2012) Adipocyte-macrophage interaction may mediate LPS-induced low-grade inflammation: Potential link with metabolic complications. Innate Immunity 18: 164-170.
365. Faty A, Ferre P, Commans S (2012) The acute phase protein serum amyloid A induces lipolysis and inflammation in human adipocytes through distinct pathways. Plos One 7: 1-10.
366. Olza J, Aguilera CM, Gil-Campos M, Leis R, Bueno G, et al. (2012) Myeloperoxidase is an early biomarker of inflammation and cardiovascular risk in prepubertal obese children. Diabetes Care 35: 2373-2376.
367. Zur B, Look M, Holdenrieder S, Stoffel-Wagner B (2011) Elevated plasma myeloperoxidase concentration in adults with obesity. Clinica Chimica Acta 412: 1891-1892.
368. Yadav A, Kataria MA, Saini V, Yadav A (2013) Role of leptin and adiponectin in insulin resistance. Clinica Chimica Acta; International Journal of Clinical Chemistry 417: 80-84.
369. Yamauchi T, Kadowaki T (2013) Adiponectin receptor as a key player in healthy longevity and obesity-related diseases. Cell Metabolism 17: 185-196.
370. Wang Y, Lam KSL, Xu AM (2006) Adiponectin as a therapeutic target for obesity-related metabolic and cardiovascular disorders. Drug Development Research 67: 677-686.
371. Xie X, Yang S, Zou Y, Cheng S, Wang Y, et al. (2013) Influence of the core circadian gene "Clock" on obesity and leptin resistance in mice. Brain Research 1491: 147-155.
372. Boumaiza I, Omezzine A, Rejeb J, Rebhi L, Ben Rejeb N, et al. (2012) Association between four resistin polymorphisms, obesity, and metabolic syndrome parameters in tunisian volunteers. Genetic Testing and Molecular Biomarkers 16: 1356-1362.
373. Judkins CP, Dusting GJ, Drummond GR (2006) The effects of chronic TEMPOL treatment on athersclerosis vary from attenuation to exacerbation depending on treatment duration. Journal of Hypertension 24: 326-326.
374. Wang H, Luo W, Wang JT, Guo C, Wang XH, et al. (2012) Obesity-induced endothelial dysfunction is prevented by deficiency of P-selectin glycoprotein ligand-1. Diabetes 61: 3219-3227.
375. Cannizzo B, Lujan A, Estrella N, Lembo C, Cruzado M, et al. (2012) Insulin resistance promotes early atherosclerosis via increased proinflammatory proteins and oxidative stress in fructose-Fed ApoE-KO mice. Experimental Diabetes Research 2012: 1-8.
376. Dong YZ, Zhang M, Liang B, Xie ZL, Zhao ZX, et al. (2010) Reduction of AMP-activated protein kinase alpha 2 increases endoplasmic reticulum stress and atherosclerosis *in vivo*. Circulation 121: 792-803.
377. Ankel EG, Lai CS, Hopwood LE, Zivkovic Z (1987) Cytotoxicity of commonly used nitroxide radical spin probes. Life Sciences 40: 495-498.
378. Johnstone PAS, Degraff WG, Mitchell JB (1995) Protection from radiation-induced chromosomal-aberrations by the nitroxide TEMPOL. Cancer 75: 2323-2327.

379. Gallez B, Demeure R, Debuyst R, Leonard D, Dejehet F, et al. (1992) Evaluation of nonionic nitroxyl lipids as potential organ-specific contrast agents for magnetic-resonance-imaging. Magnetic Resonance Imaging 10: 445-455.
380. Hahn SM, Tochner Z, Krishna CM, Glass J, Wilson L, et al. (1992) TEMPOL, a stable free-radical, is a novel murine radiation protector. Cancer Research 52: 1750-1753.
381. Kroll C, Borchert HH (1999) Metabolism of the stable nitroxyl radical 4-oxo-2,2,6,6-tetramethylpiperidine-N-oxyl (TEMPONE). European Journal of Pharmaceutical Sciences 8: 5-9.
382. Miller AA, De Silva M, Judkins CP, Diep H, Drummond GR, et al. (2010) Augmented superoxide production by Nox2-Containing NADPH oxidase causes cerebral artery dysfunction during hypercholesterolemia. Stroke 41: 784-789.
383. Dandona P, Weinstock R, Thusu K, Abdel-Rahman E, Aljada A, et al. (1998) Tumor necrosis factor-alpha in sera of obese patients: Fall with weight loss. Journal of Clinical Endocrinology & Metabolism 83: 2907-2910.
384. Dandona P, Aljada A, Chaudhuri A, Mohanty P, Garg R (2005) Metabolic syndrome - A comprehensive perspective based on interactions between obesity, diabetes, and inflammation. Circulation 111: 1448-1454.
385. Hotamisligil GS, Shargill NS, Spiegelman BM (1993) Adipose expression of tumor-necrosis-factor-alpha - direct role in obesity-linked insulin resistance. Science 259: 87-91.
386. Picchi A, Gao X, Belmadani S, Potter BJ, Focardi M, et al. (2006) Tumor necrosis factor-alpha induces endothelial dysfunction in the prediabetic metabolic syndrome. Circulation Research 99: 69-77.
387. Volk T, Hensel M, Schuster H, Kox WJ (2000) Secretion of MCP-1 and IL-6 by cytokine stimulated production of reactive oxygen species in endothelial cells. Molecular and Cellular Biochemistry 206: 105-112.
388. Araki Y, Sugihara H, Hattori T (2006) The free radical scavengers edaravone and TEMPOL suppress experimental dextran sulfate sodium-induced colitis in mice. International Journal of Molecular Medicine 17: 331-334.
389. Chatterjee PK, Cuzzocrea S, Brown PAJ, Zacharowski K, Stewart KN, et al. (2000) TEMPOL, a membrane-permeable radical scavenger, reduces oxidant stress-mediated renal dysfunction and injury in the rat. Kidney International 58: 658-673.
390. El-Sayed NS, Mahran LG, Khattab MM (2011) TEMPOL, a membrane-permeable radical scavenger, ameliorates lipopolysaccharide-induced acute lung injury in mice: A key role for superoxide anion. European Journal of Pharmacology 663: 68-73.
391. Queiroz RF, Jordao AK, Cunha AC, Ferreira VF, Brigagao M, et al. (2012) Nitroxides attenuate carrageenan-induced inflammation in rat paws by reducing neutrophil infiltration and the resulting myeloperoxidase-mediated damage. Free Radical Biology and Medicine 53: 1942-1953.
392. Kumon Y, Suehiro T, Hashimoto K, Nakatani K, Sipe JD (1999) Local expression of acute phase serum amyloid A mRNA in rheumatoid arthritis synovial tissue and cells. Journal of Rheumatology 26: 785-790.
393. O'Hara R, Murphy EP, Whitehead AS, FitzGerald O, Bresnihan B (2004) Local expression of the serum amyloid a and formyl peptide receptor-like 1 genes in synovial tissue is associated with matrix metalloproteinase production in patients with inflammatory arthritis. Arthritis and Rheumatism 50: 1788-1799.
394. Poitou C, Viguerie N, Cancello R, De Matteis R, Cinti S, et al. (2005) Serum amyloid A: production by human white adipocyte and regulation by obesity and nutrition. Diabetologia 48: 519-528.

395. Meek RL, Urielishoval S, Benditt EP (1994) Expression of apolipoprotein serum amyloid-A messenger-RNA in human atherosclerotic lesions and cultured vascular cells - implications for serum amyloid-A function. Proceedings of the National Academy of Sciences of the United States of America 91: 3186-3190.
396. Eren MA, Vural M, Cece H, Camuzcuoglu H, Yildiz S, et al. (2012) Association of serum amyloid A with subclinical atherosclerosis in women with gestational diabetes. Gynecological Endocrinology 28: 1010-1013.
397. Jernas M, Palming J, Sjoholm K, Jennische E, Svensson PA, et al. (2006) Separation of human adipocytes by size: hypertrophic fat cells display distinct gene expression. FASEB Journal 20: 1540-1542.
398. Hattori Y, Akimoto K, Gross SS, Hattori S, Kasai K (2005) Angiotensin-II-induced oxidative stress elicits hypoadiponectinaemia in rats. Diabetologia 48: 1066-1074.
399. Villarreal-Molina MT, Antuna-Puente B (2012) Adiponectin: Anti-inflammatory and cardioprotective effects. Biochimie 94: 2143-2149.
400. Qin FZ, Siwik DA, Luptak I, Hou XY, Wang L, et al. (2012) The polyphenols resveratrol and S17834 prevent the structural and functional sequelae of diet-induced metabolic heart disease in mice. Circulation 125: 1757-U1127.
401. Vecoli C, Cao J, Neglia D, Inoue K, Sodhi K, et al. (2011) Apolipoprotein A-I mimetic peptide L-4F prevents myocardial and coronary dysfunction in diabetic mice. Journal of Cellular Biochemistry 112: 2616-2626.
402. Lee S, Park Y, Dellsperger KC, Zhang CH (2011) Exercise training improves endothelial function via adiponectin-dependent and independent pathways in type 2 diabetic mice. American Journal of Physiology-Heart and Circulatory Physiology 301: H306-H314.
403. Arita Y, Kihara S, Ouchi N, Takahashi M, Maeda K, et al. (2012) Paradoxical decrease of an adipose-specific protein, adiponectin, in obesity. Biochemical and Biophysical Research Communications 425: 560-564.
404. Kumada M, Kihara S, Sumitsuji S, Kawamoto T, Matsumoto S, et al. (2003) Association of hypoadiponectinemia with coronary artery disease in men. Arteriosclerosis Thrombosis and Vascular Biology 23: 85-89.
405. Rubio-Martin E, Soriguer F, Gutierrez-Repiso C, Garrido-Sanchez L, de Adana MSR, et al. (2013) C-reactive protein and incidence of type 2 diabetes in the Pizarra study. European Journal of Clinical Investigation 43: 159-167.
406. Al-Daghri NM, Al-Attas OS, Alokail MS, Alkharfy KM, Charalampidis P, et al. (2013) Visceral adiposity index is highly associated with adiponectin values and glycaemic disturbances. European Journal of Clinical Investigation 43: 183-189.
407. Sans S, Padro T, Tuomilehto J, Badimon L (2013) Incidence of diabetes and serum adipokines in Catalonian men. The ADIPOCAT study. Annals of Medicine 45: 97-102.
408. Chen CY, Asakura M, Asanuma H, Hasegawa T, Tanaka J, et al. (2012) Plasma adiponectin levels predict cardiovascular events in the observational Arita Cohort Study in Japan: the importance of the plasma adiponectin levels. Hypertension Research 35: 843-848.
409. Gerrits AJ, Gitz E, Koekman CA, Visseren FL, van Haeften TW, et al. (2012) Induction of insulin resistance by the adipokines resistin, leptin, plasminogen activator inhibitor-1 and retinol binding protein 4 in human megakaryocytes. Haematologica-the Hematology Journal 97: 1149-1157.
410. Singh AK, Tiwari S, Gupta A, Natu SM, Mittal B, et al. (2012) Association of resistin with metabolic syndrome in Indian subjects. Metabolic syndrome and Related Disorders 10: 286-291.

411. Dick GM, Katz PS, Farias M, Morris M, James J, et al. (2006) Resistin impairs endothelium-dependent dilation to bradykinin, but not acetylcholine, in the coronary circulation. American Journal of Physiology-Heart and Circulatory Physiology 291: H2997-H3002.
412. Kwakernaak AJ, Lambert G, Dullaart RPF (2012) Relationship of proprotein convertase subtilisin-kexin type 9 levels with resistin in lean and obese subjects. Clinical Biochemistry 45: 1522-1524.
413. Beltowski J, Jamroz-Wisniewska A, Borkowska E, Nazar J, Marciniak A (2005) Antioxidant treatment normalizes renal Na+, K+-ATPase activity in leptin-treated rats. Pharmacological Reports 57: 219-228.
414. Wen YS, Gu JL, Li SL, Reddy MA, Natarajan R, et al. (2006) Elevated glucose and diabetes promote interleukin-12 cytokine gene expression in mouse macrophages. Endocrinology 147: 2518-2525.
415. Wan WZ, Murphy PM (2013) Regulation of atherogenesis by chemokines and chemokine receptors. Archivum Immunologiae Et Therapiae Experimentalis 61: 1-14.
416. Zykova SN, Jenssen TG, Berdal M, Olsen R, Myklebust R, et al. (2000) Altered cytokine and nitric oxide secretion *in vitro* by macrophages from diabetic type II-like db/db mice. Diabetes 49: 1451-1458.
417. Josefsen K, Nielsen H, Lorentzen S, Damsbo P, Buschard K (1994) Circulating monocytes are activated in newly-diagnosed type-1 diabetes-mellitus patients. Clinical and Experimental Immunology 98: 489-493.
418. Desfaits AC, Serri O, Renier G (1998) Normalization of plasma lipid peroxides, monocyte adhesion, and tumor necrosis factor-alpha production in NIDDM patients after gliclazide treatment. Diabetes Care 21: 487-493.
419. Hill HR, Augustine NH, Rallison ML, Santos JI (1983) Defective monocyte chemotactic responses in diabetes-mellitus. Journal of Clinical Immunology 3: 70-77.
420. Geisler C, Almdal T, Bennedsen J, Rhodes JM, Kolendorf K (1982) Monocyte functions in diabetes-mellitus. Acta Pathologica Microbiologica Et Immunologica Scandinavica Section C-Immunology 90: 33-37.
421. Tegos TJ, Kalodiki E, Sabetai MM, Nicolaides AN (2001) The genesis of atherosclerosis and risk factors: A review. Angiology 52: 89-98.
422. Brown MS, Basu SK, Falck JR, Ho YK, Goldstein JL (1980) The scavenger cell pathway for lipoprotein degradation - specificity of the binding-site that mediates the uptake of negatively-charged LDL by macrophages. Journal of Supramolecular Structure 13: 67-81.
423. Jerome WG (2010) Lysosomes, cholesterol and atherosclerosis. Clinical Lipidology 5: 853-865.
424. Luan JJ, Li WP, Han J, Zhang W, Gong HL, et al. (2012) Renal protection of *in vivo* administration of TEMPOL in streptozotocin-induced diabetic rats. Journal of Pharmacological Sciences 119: 167-176.
425. Morita M, Yano S, Yamaguchi T, Sugimoto T (2013) Advanced glycation end products-induced reactive oxygen species generation is partly through NF-kappa B activation in human aortic endothelial cells. Journal of Diabetes and its Complications 27: 11-15.
426. Han YH, Park WH (2012) TEMPOL inhibits growth of As4.1 juxtaglomerular cells via cell cycle arrest and apoptosis. Oncology Reports 27: 842-848.
427. Yilmaz O, Kucuk M, Kebapcilar L, Altindag T, Yuksel A, et al. (2012) Macrophage migration-inhibitory factor is elevated in pregnant women with gestational diabetes mellitus. Gynecological Endocrinology 28: 76-79.

428. Saksida T, Stosic-Grujicic S, Timotijevic G, Sandler S, Stojanovic I (2012) Macrophage migration inhibitory factor deficiency protects pancreatic islets from palmitic acid-induced apoptosis. Immunology and Cell Biology 90: 688-698.
429. Muller, II, Muller KAL, Schonleber H, Karathanos A, Schneider M, et al. (2012) Macrophage migration inhibitory factor is enhanced in acute coronary syndromes and is associated with the inflammatory response. Plos One 7: 1-7.
430. Kong YZ, Huang XR, Ouyang X, Tan JJ, Fingerle-Rowson G, et al. (2005) Evidence for vascular macrophage migration inhibitory factor in destabilization of human atherosclerotic plaques. Cardiovascular Research 65: 272-282.
431. Pan JH, Sukhova GK, Yang JT, Wang B, Xie T, et al. (2004) Macrophage migration inhibitory factor deficiency impairs atherosclerosis in low-density lipoprotein receptor-deficient mice. Circulation 109: 3149-3153.
432. Verschuren L, Kooistra T, Bernhagen J, Voshol PJ, Ouwens DM, et al. (2009) MIF deficiency reduces chronic inflammation in white adipose tissue and impairs the development of insulin resistance, glucose intolerance, and associated atherosclerotic disease. Circulation Research 105: 99-U275.
433. Kamchybekov U, Figulla HR, Gerdes N, Jung C (2012) Macrophage migration inhibitory factor is elevated in obese adolescents. Archives of Physiology and Biochemistry 118: 204-209.
434. Zernecke A, Bernhagen J, Weber C (2008) Macrophage migration inhibitory factor in cardiovascular disease. Circulation 117: 1594-1602.
435. Herder C, Illig T, Baumert J, Muller M, Klopp N, et al. (2008) Macrophage migration inhibitory factor (MIF) and risk for coronary heart disease: Results from the MONICA/KORA Augsburg case-cohort study, 1984-2002. Atherosclerosis 200: 380-388.
436. Toso C, Emamaullee JA, Merani S, Shapiro AMJ (2008) The role of macrophage migration inhibitory factor on glucose metabolism and diabetes. Diabetologia 51: 1937-1946.
437. Thompson D, Pepys MB, Wood SP (1999) The physiological structure of human C-reactive protein and its complex with phosphocholine. Structure with Folding & Design 7: 169-177.
438. Rivero A, Mora C, Muros M, Garcia J, Herrera H, et al. (2009) Pathogenic perspectives for the role of inflammation in diabetic nephropathy. Clinical Science 116: 479-492.
439. Navarro JF, Mora C (2006) Diabetes, inflammation, proinflammatory cytokines, and diabetic nephropathy. The Scientific World Journal 6: 908-917.
440. Blake GJ, Ridker PM (2002) Tumour necrosis factor-alpha, inflammatory biomarkers, and atherogenesis. European Heart Journal 23: 345-347.
441. Greenfield JR, Campbell LV (2006) Relationship between inflammation, insulin resistance and type 2 diabetes: 'cause or effect'? Current Diabetes Reviews 2: 195-211.
442. Pickup JC, Mattock MB, Chusney GD, Burt D (1997) NIDDM as a disease of the innate immune system: association of acute-phase reactants and interleukin-6 with metabolic syndrome X. Diabetologia 40: 1286-1292.
443. Kaptoge S, Di Angelantonio E, Pennells L, Wood AM, White IR, et al. (2012) C-reactive protein, fibrinogen, and cardiovascular disease prediction. New England Journal of Medicine 367: 1310-1320.
444. Pepys MB, Hirschfield GM, Tennent GA, Gallimore JR, Kahan MC, et al. (2006) Targeting C-reactive protein for the treatment of cardiovascular disease. Nature 440: 1217-1221.

445. Pepys MB, Hirschfield GM (2001) C-reactive protein and its role in the pathogenesis of myocardial infarction. Italian Heart Journal : Official Journal of the Italian Federation of Cardiology 2: 804-806.
446. Ballou SP, Lozanski G (1992) Induction of inflammatory cytokine release from cultured human monocytes by C-reactive protein. Cytokine 4: 361-368.
447. Wuensch T, Thilo F, Krueger K, Scholze A, Ristow M, et al. (2010) High glucose-induced oxidative stress increases transient receptor potential channel expression in human monocytes. Diabetes 59: 844-849.
448. Shanmugam N, Reddy MA, Guha M, Natarajan R (2003) High glucose-induced expression of proinflammatory cytokine and chemokine genes in monocytic cells. Diabetes 52: 1256-1264.
449. Haidet J, Cifarelli V, Trucco M, Luppi P (2012) C-peptide reduces pro-inflammatory cytokine secretion in LPS-stimulated U937 monocytes in condition of hyperglycemia. Inflammation Research 61: 27-35.
450. Ptak W, Klimek M, Bryniarski K, Ptak M, Majcher P (1998) Macrophage function in alloxan diabetic mice: expression of adhesion molecules, generation of monokines and oxygen and NO radicals. Clinical and Experimental Immunology 114: 13-18.
451. Gao X, Belmadani S, Picchi A, Xu XB, Potter BJ, et al. (2007) Tumor necrosis factor-alpha induces endothelial dysfunction in Lepr(db) mice. Circulation 115: 245-254.
452. Xie XY, Kong PR, Wu JF, Li Y, Li YX (2013) Curcumin attenuates lipolysis stimulated by tumor necrosis factor-et or isoproterenol in 3T3-L1 adipocytes. Phytomedicine 20: 3-8.
453. El-Wakkad A, Hassan NE, Sibaii H, El-Zayat SR (2013) Proinflammatory, anti-inflammatory cytokines and adipokines in students with central obesity. Cytokine 61: 682-687.
454. Skoog T, Dichtl W, Boquist S, Skoglund-Andersson C, Karpe F, et al. (2002) Plasma tumour necrosis factor-alpha and early carotid atherosclerosis in healthy middle-aged men. European Heart Journal 23: 376-383.
455. Ridker PM, Rifai N, Pfeffer M, Sacks F, Lepage S, et al. (2000) Elevation of tumor necrosis factor-alpha and increased risk of recurrent coronary events after myocardial infarction. Circulation 101: 2149-2153.
456. Ansari N, Hasan A, Owais M (2012) A study of inflammatory markers and their correlation with severity, in patients with chronic heart failure. Biomedical Research-India 23: 408-415.
457. Kosar F, Aksoy Y, Ozguntekin G, Ozerol I, Varol E (2006) Relationship between cytokines and tumour markers in patients with chronic heart failure. European Journal of Heart Failure 8: 270-274.
458. Levine B, Kalman J, Mayer L, Fillit HM, Packer M (1990) Elevated circulating levels of tumor-necrosis-factor in severe chronic heart-failure. New England Journal of Medicine 323: 236-241.
459. Talvani A, Rocha MOC, Barcelos LS, Gomes YM, Ribeiro AL, et al. (2004) Elevated concentrations of CCL2 and tumor necrosis factor-alpha in chagasic cardiomyopathy. Clinical Infectious Diseases 38: 943-950.
460. Kherbeck N, Tamby MC, Bussone G, Dib H, Perros F, et al. (2013) The role of inflammation and autoimmunity in the pathophysiology of pulmonary arterial hypertension. Clinical Reviews in Allergy & Immunology 44: 31-38.
461. Samaras K, Botelho NK, Chisholm DJ, Lord RV (2010) Subcutaneous and visceral adipose tissue gene expression of serum adipokines that predict type 2 diabetes. Obesity 18: 884-889.

462. Kennedy A, Gruen ML, Gutierrez DA, Surmi BK, Orr JS, et al. (2012) Impact of macrophage inflammatory protein-1 alpha deficiency on atherosclerotic lesion formation, hepatic steatosis, and adipose tissue expansion. Plos One 7: 1-12.
463. Vistnes M (2012) Macrophage inflammatory protein-1 beta: a novel prognostic biomarker in atherosclerosis? Cardiology 121: 149-151.
464. Schulte BM, Lanke KHW, Piganelli JD, Kers-Rebel ED, Bottino R, et al. (2012) Cytokine and chemokine production by human pancreatic islets upon enterovirus infection. Diabetes 61: 2030-2036.
465. Tang SCW, Leung JCK, Lai KN (2011) Diabetic tubulopathy: An emerging entity. Diabetes and the kidney; Lai KN, Tang SCW, editors. Basel, Switzerland: Karger pp. 124-134.
466. Cherney DZI, Scholey JW, Sochett E, Bradley TJ, Reich HN (2011) The acute effect of clamped hyperglycemia on the urinary excretion of inflammatory cytokines/chemokines in uncomplicated type 1 diabetes a pilot study. Diabetes Care 34: 177-180.
467. Rosa JS, Oliver SR, Mitsuhashi M, Flores RL, Pontello AM, et al. (2008) Altered kinetics of interleukin-6 and other inflammatory mediators during exercise in children with type 1 diabetes. Journal of Investigative Medicine 56: 701-713.
468. Yang MX, Gan H, Shen Q, Tang WX, Du XG, et al. (2012) Proinflammatory CD14(+)CD16(+) monocytes are associated with microinflammation in patients with type 2 diabetes mellitus and diabetic nephropathy uremia. Inflammation 35: 388-396.
469. Alpert E, Altman H, Totary H, Gruman A, Barnea D, et al. (2004) 4-hydroxy TEMPOL-induced impairment of mitochondrial function and augmentation of glucose transport in vascular endothelial and smooth muscle cells. Biochemical Pharmacology 67: 1985-1995.
470. May JM, Qu ZC, Juliao S, Cobb CE (2005) Ascorbic acid decreases oxidant stress in endothelial cells caused by the nitroxide TEMPOL. Free Radical Research 39: 195-202.
471. Muniyappa R, Srinivas PR, Ram JL, Walsh MF, Sowers JR (1998) Calcium and protein kinase C mediate high-glucose-induced inhibition of inducible nitric oxide synthase in vascular smooth muscle cells. Hypertension 31: 289-295.
472. Dasu MR, Jialal I (2011) Free fatty acids in the presence of high glucose amplify monocyte inflammation via Toll-like receptors. American Journal of Physiology-Endocrinology and Metabolism 300: E145-E154.
473. Williams CR, Lu XH, Sutliff RL, Hart CM (2012) Rosiglitazone attenuates NF-kappa B-mediated Nox4 upregulation in hyperglycemia-activated endothelial cells. American Journal of Physiology-Cell Physiology 303: C213-C223.
474. Tang C, Koulajian K, Schuiki I, Zhang L, Desai T, et al. (2012) Glucose-induced beta cell dysfunction *in vivo* in rats: link between oxidative stress and endoplasmic reticulum stress. Diabetologia 55: 1366-1379.
475. Malhotra JD, Miao H, Zhang K, Wolfson A, Pennathur S, et al. (2008) Antioxidants reduce endoplasmic reticulum stress and improve protein secretion. Proceedings of the National Academy of Sciences of the United States of America 105: 18525-18530.
476. Urano F, Wang XZ, Bertolotti A, Zhang YH, Chung P, et al. (2000) Coupling of stress in the ER to activation of JNK protein kinases by transmembrane protein kinase IRE1. Science 287: 664-666.
477. Tang C, Han P, Oprescu AI, Lee SC, Gyulkhandanyan AV, et al. (2007) Evidence for a role of superoxide generation in glucose-induced beta-cell dysfunction *in vivo*. Diabetes 56: 2722-2731.

478. Erbagci AB, Tarakcioglu M, Coskun Y, Sivasli E, Namiduru ES (2001) Mediators of inflammation in children with type I diabetes mellitus: cytokines in type I diabetic children. Clinical Biochemistry 34: 645-650.
479. Cifarelli V, Libman IM, Deluca A, Becker D, Trucco M, et al. (2007) Increased expression of monocyte CD11b (Mac-1) in overweight recent-onset type 1 diabetic children. The Review of Diabetic Studies 4: 112-117.
480. Devaraj S, Cheung AT, Jialal I, Griffen SC, Nguyen D, et al. (2007) Evidence of increased inflammation and microcirculatory abnormalities in patients with type 1 diabetes and their role in microvascular complications. Diabetes 56: 2790-2796.
481. Saraheimo M, Teppo AM, Forsblom C, Fagerudd J, Groop PH, et al. (2003) Diabetic nephropathy is associated with low-grade inflammation in Type 1 diabetic patients. Diabetologia 46: 1402-1407.
482. Schalkwijk CG, Ter Wee PM, Stehouwer CDA (2005) Plasma levels of AGE peptides in type 1 diabetic patients are associated with serum creatinine and not with albumin excretion rate: Possible role of AGE peptide-associated endothelial dysfunction. Maillard Reaction: Chemistry at the Interface of Nutrition, Aging, and Disease; Baynes JW, Monnier VM, Ames JM, Thorpe SR, editors. New York, USA: Annals of New York Academy of Sciences pp. 662-670.
483. Schram MT, Chaturvedi N, Schalkwijk C, Giorgino F, Ebeling P, et al. (2003) Vascular risk factors and markers of endothelial function as determinants of inflammatory markers in type 1 diabetes - The EURODIAB prospective complications study. Diabetes Care 26: 2165-2173.
484. Tofovic SP, Salah EM, Jackson EK, Melhem M (2007) Early renal injury induced by caffeine consumption in obese, diabetic ZSF(1) rats. Renal Failure 29: 891-902.
485. Togashi N, Maeda T, Yoshida H, Koyama M, Tanaka M, et al. (2012) Angiotensin II receptor activation in youth triggers persistent insulin resistance and hypertension-a legacy effect? Hypertension Research 35: 334-340.
486. Combadiere C, Potteaux S, Rodero M, Simon T, Pezard A, et al. (2008) Combined inhibition of CCL2, CX3CR1, and CCR5 abrogates Ly6C(hi) and Ly6C(lo) monocytosis and almost abolishes atherosclerosis in hypercholesterolemic mice. Circulation 117: 1649-1657.
487. Potteaux S, Combadiere C, Esposito B, Lecureuil C, Ait-Oufella H, et al. (2006) Role of bone marrow-derived CC-chemokine receptor 5 in the development of atherosclerosis of low-density lipoprotein receptor knockout mice. Arteriosclerosis Thrombosis and Vascular Biology 26: 1858-1863.
488. Potteaux S, Combadiere C, Esposito B, Casanova S, Merval R, et al. (2005) Chemokine receptor CCRI disruption in bone marrow cells enhances atherosclerotic lesion development and inflammation in mice. Molecular Medicine 11: 16-20.
489. Zernecke A, Shagdarsuren E, Weber C (2008) Chemokines in atherosclerosis: an update. Arteriosclerosis Thrombosis and Vascular Biology 28: 1897-1908.
490. Braunersreuther V, Zernecke A, Arnaud C, Liehn EA, Steffens S, et al. (2007) Ccr5 but not Ccr1 deficiency reduces development of diet-induced atherosclerosis in mice. Arteriosclerosis Thrombosis and Vascular Biology 27: 373-379.
491. Moos MPW, John N, Grabner R, Nossmann S, Gunther B, et al. (2005) The lamina adventitia is the major site of immune cell accumulation in standard chow-fed apolipoprotein E-deficient mice. Arteriosclerosis Thrombosis and Vascular Biology 25: 2386-2391.

492. Wilcox JN, Nelken NA, Coughlin SR, Gordon D, Schall TJ (1994) Local expression of inflammatory cytokines in human atherosclerotic plaques. Journal of Atherosclerosis and Thrombosis 1 Suppl 1: S10-13.
493. Saraswathi V, Hasty AH (2006) The role of lipolysis in mediating the proinflammatory effects of very low density lipoproteins in mouse peritoneal macrophages. Journal of Lipid Research 47: 1406-1415.
494. Yang Y-P, Hu L-F, Zheng H-F, Mao C-J, Hu W-D, et al. (2013) Application and interpretation of current autophagy inhibitors and activators. Acta pharmacologica Sinica 34: 625-635.
495. Rashid I, Brown BE, Van Reyk DM, Davies MJ (2006) The roles of protein glycation, glycoxidation, and advanced glycation end-product formation in diabetes-induced atherosclerosis. Biochemistry of Atherosclerosis Volume 1. Advances in Biochemistry in Health and Diseaes; Cheema, SK editor. New York, USA: Springer pp. 247-283.
496. Steinberg D (2004) An interpretive history of the cholesterol controversy: Part I. Journal of Lipid Research 45: 1583-1593.
497. Allen D, Hasanally D, Ravandi A (2013) Role of oxidized phospholipids in cardiovascular pathology. Clinical Lipidology 8: 205-215.
498. Bernal-Lopez MR, Garrido-Sanchez L, Gomez-Carrillo V, Gallego-Perales JL, Llorente-Cortes V, et al. (2013) Antioxidized LDL antibodies are associated with different metabolic pathways in patients with atherosclerotic plaque and type 2 diabetes. Diabetes Care 36: 1006-1011.
499. Barski OA, Xie Z, Baba SP, Sithu SD, Agarwal A, et al. (2013) Dietary carnosine prevents early atherosclerotic lesion formation in apolipoprotein e-null mice. Arteriosclerosis, Thrombosis, and Vascular Biology 33: 1162-1170.
500. Brown BE, Dean RT, Davies MJ (2005) Glycation of low-density lipoproteins by methylglyoxal and glycolaldehyde gives rise to the *in vitro* formation of lipid-laden cells. Diabetologia 48: 361-369.
501. Calabresi L, Canavesi M, Bernini F, Franceschini G (1999) Cell cholesterol efflux to reconstituted high-density lipoproteins containing the apolipoprotein A-I-Milano dimer. Biochemistry 38: 16307-16314.
502. Hajj Hassan H, Blain S, Boucher B, Denis M, Krimbou L, et al. (2005) Structural modification of plasma HDL by phospholipids promotes efficient ABCA1-mediated cholesterol release. Journal of Lipid Research 46: 1457-1465.
503. Ohashi R, Mu H, Wang X, Yao Q, Chen C (2005) Reverse cholesterol transport and cholesterol efflux in atherosclerosis. QJM- An International Journal of Medicine 98: 845-856.
504. Patel DC, Albrecht C, Pavitt D, Paul V, Pourreyron C, et al. (2011) Type 2 Diabetes Is Associated with Reduced ATP-Binding Cassette Transporter A1 Gene Expression, Protein and Function. Plos One 6: 1-8.
505. Hayashi T, Juliet PAR, Miyazaki A, Ignarro LJ, Iguchi A (2007) High glucose downregulates the number of caveolae in monocytes through oxidative stress from NADPH oxidase: Implications for atherosclerosis. Biochimica Et Biophysica Acta-Molecular Basis of Disease 1772: 364-372.
506. Brown BE, Mahroof FM, Cook NL, van Reyk DM, Davies MJ (2006) Hydrazine compounds inhibit glycation of low-density lipoproteins and prevent the *in vitro* formation of model foam cells from glycolaldehyde-modified low-density lipoproteins. Diabetologia 49: 775-783.
507. Nobecourt E, Davies MJ, Brown BE, Curtiss LK, Bonnet DJ, et al. (2007) The impact of glycation on apolipoprotein A-I structure and its ability to activate lecithin : cholesterol acyltransferase. Diabetologia 50: 643-653.

508. Hadfield KA, Pattison DI, Brown BE, Hou LM, Rye KA, et al. (2013) Myeloperoxidase-derived oxidants modify apolipoprotein A-I and generate dysfunctional high-density lipoproteins: comparison of hypothiocyanous acid (HOSCN) with hypochlorous acid (HOCI). Biochemical Journal 449: 531-542.
509. Du H, Duanmu M, Witte D, Grabowski GA (1998) Targeted disruption of the mouse lysosomal acid lipase gene: long-term survival with massive cholesteryl ester and triglyceride storage. Human Molecular Genetics 7: 1347-1354.
510. Du H, Schiavi S, Wan N, Levine M, Witte DP, et al. (2004) Reduction of atherosclerotic plaques by lysosomal acid lipase supplementation. Arteriosclerosis Thrombosis and Vascular Biology 24: 147-154.
511. Du H, Schiavi S, Levine M, Mishra J, Heur M, et al. (2001) Enzyme therapy for lysosomal acid lipase deficiency in the mouse. Human Molecular Genetics 10: 1639-1648.
512. Du H, Heur M, Duanmu M, Grabowski GA, Hui DY, et al. (2001) Lysosomal acid lipase-deficient mice: depletion of white and brown fat, severe hepatosplenomegaly, and shortened life span. Journal of Lipid Research 42: 489-500.
513. Bobryshev YV, Shchelkunova, T.A.,Morozov, I. A., Rubtsov, P.M., Sobenin IA, Orekhov, A. N., Smirnov, A. N. (2013) Changes of lysosomes in the earliest stages of the development of atherosclerosis. Journal of Cellular and Molecular Medicine: 1-10.
514. Kawasaki M, Nakayama K, Wakatsuki S (2005) Membrane recruitment of effector proteins by Arf and Rab GTPases. Current Opinion in Structural Biology 15: 681-689.
515. Yoshida S, Hoppe AD, Araki N, Swanson JA (2009) Sequential signaling in plasma-membrane domains during macropinosome formation in macrophages. Journal of Cell Science 122: 3250-3261.
516. Pols MS, Lumperman J (2009) Trafficking and function of the tetraspanin CD63. Experimental Cell Research 315: 1584-1592.
517. Saito N, Pulford KAF, Bretongorius J, Masse JM, Mason DY, et al. (1991) Ultrastructural-localization of the CD68 macrophage-associated antigen in human blood neutrophils and monocytes. American Journal of Pathology 139: 1053-1059.
518. Gough PJ, Gordon S, Greaves DR (2001) The use of human CD68 transcriptional regulatory sequences to direct high-level expression of class A scavenger receptor in macrophages *in vitro* and *in vivo*. Immunology 103: 351-361.
519. Kunisch E, Fuhrmann R, Roth A, Winter R, Lungershausen W, et al. (2004) Macrophage specificity of three anti-CD68 monoclonal antibodies (KP1, EBM11, and PGM1) widely used for immunohistochemistry and flow cytometry. Annals of the Rheumatic Diseases 63: 774-784.
520. Ichimura Y, Komatsu M (2010) Selective degradation of p62 by autophagy. Seminars in Immunopathology 32: 431-436.
521. Komatsu M, Ichimura Y (2010) Selective autophagy regulates various cellular functions. Genes to Cells 15: 923-933.
522. Komatsu M, Ichimura Y (2010) Physiological significance of selective degradation of p62 by autophagy. FEBS Letters 584: 1374-1378.
523. Nakanishi H, Amano T, Sastradipura DF, Yoshimine Y, Tsukuba T, et al. (1997) Increased expression of cathepsins E and D in neurons of the aged rat brain and their colocalization with lipofuscin and carboxy-terminal fragments of Alzheimer amyloid precursor protein. Journal of Neurochemistry 68: 739-749.

524. Hipkiss AR (2009) Carnosine and its possible roles in nutrition and health. Advances in food and nutrition research; Taylor SL, editor. San Diego, USA: Elsevier Academic Press Incorporation pp. 87-154.
525. Lee YT, Hsu CC, Lin MH, Liu KS, Yin MC (2005) Histidine and carnosine delay diabetic, deterioration in mice and protect human low density lipoprotein against oxidation and glycation. European Journal of Pharmacology 513: 145-150.
526. Makia NL, Bojang P, Falkner KC, Conklin DJ, Prough RA (2011) Murine hepatic aldehyde dehydrogenase 1a1 is a major contributor to oxidation of aldehydes formed by lipid peroxidation. Chemico-Biological Interactions 191: 278-287.
527. Ishii T, Itoh K, Ruiz E, Leake DS, Unoki H, et al. (2004) Role of Nrf2 in the regulation of CD36 and stress protein expression in murine macrophages - Activation by oxidatively modified LDL and 4-hydroxynonenal. Circulation Research 94: 609-616.
528. Wang ZQ, Jiang YC, Liu NF, Ren LQ, Zhu YH, et al. (2012) Advanced glycation end-product N-epsilon-carboxymethyl-Lysine accelerates progression of atherosclerotic calcification in diabetes. Atherosclerosis 221: 387-396.
529. Li YH, Liu SY, Zhang ZY, Xu QB, Xie FK, et al. (2012) RAGE mediates accelerated diabetic vein graft atherosclerosis induced by combined mechanical stress and AGEs via synergistic ERK Activation. Plos One 7: 1-11.
530. Garcia-Heredia A, Kensicki E, Mohney RP, Rull A, Triguero I, et al. (2013) Paraoxonase-1 deficiency is associated with severe liver steatosis in mice fed a high-fat high-cholesterol diet: a metabolomic approach. Journal of Proteome Research 12: 1946-1955.
531. Ruotsalainen AK, Inkala M, Partanen ME, Lappalainen JP, Kansanen E, et al. (2013) The absence of macrophage Nrf2 promotes early atherogenesis. Cardiovascular Research 98: 107-115.
532. Motoyama K, Koyama H, Moriwaki M, Emura K, Okuyama S, et al. (2009) Atheroprotective and plaque-stabilizing effects of enzymatically modified isoquercitrin in atherogenic apoE-deficient mice. Nutrition 25: 421-427.
533. Kato M, Sada T, Mizuno M, Kitayama K, Inaba T, et al. (2005) Effect of combined treatment with an angiotensin II receptor antagonist and an HMG-CoA reductase inhibitor on atherosclerosis in genetically hyperlipidemic rabbits. Journal of Cardiovascular Pharmacology 46: 556-562.
534. Cantero AV, Portero-Otin M, Ayala V, Auge N, Sanson M, et al. (2007) Methylglyoxal induces advanced glycation end product (AGEs) formation and dysfunction of PDGF receptor-beta: implications for diabetic atherosclerosis. FASEB Journal 21: 3096-3106.
535. Kislinger T, Tanji N, Wendt T, Qu W, Lu Y, et al. (2001) Receptor for advanced glycation end products mediates inflammation and enhanced expression of tissue factor in vasculature of diabetic apolipoprotein E-null mice. Arteriosclerosis Thrombosis and Vascular Biology 21: 905-910.
536. Yu PH, Wang M, Deng YL, Fan H, Shira-Bock L (2002) Involvement of semicarbazide-sensitive amine oxidase-mediated deamination in atherogenesis in KKAy diabetic mice fed with high cholesterol diet. Diabetologia 45: 1255-1262.
537. Xie ZZ, Baba SP, Sweeney BR, Barski OA (2013) Detoxification of aldehydes by histidine-containing dipeptides: From chemistry to clinical implications. Chemico-Biological Interactions 202: 288-297.
538. Gustafson B, Gogg S, Hedjazifar S, Jenndahl L, Hammarstedt A, et al. (2009) Inflammation and impaired adipogenesis in hypertrophic obesity in man.

American Journal of Physiology-Endocrinology and Metabolism 297: E999-E1003.
539. Maury E, Ehala-Aleksejev K, Guiot Y, Detry R, Vandenhooft A, et al. (2007) Adipokines oversecreted by omental adipose tissue in human obesity. The American Journal of Physiology- Endocrinology and Metabolism 293: E656-E665.
540. Garcia C, Feve B, Ferre P, Halimi S, Baizri H, et al. (2010) Diabetes and inflammation: Fundamental aspects and clinical implications. Diabetes & Metabolism 36: 327-338.
541. Lassenius MI, Pietiläinen KH, Kaartinen K, Pussinen PJ, Syrjänen J, et al. (2011) Bacterial endotoxin activity in human serum is associated with dyslipidemia, insulin resistance, obesity, and chronic inflammation. Diabetes Care 34: 1809-1815.
542. Kopp A, Buechler C, Neumeier M, Weigert J, Aslanidis C, et al. (2009) Innate immunity and adipocyte function: ligand-specific activation of multiple toll-like receptors modulates cytokine, adipokine, and chemokine secretion in adipocytes. Obesity (Silver Spring, Md.) 17: 648-656.
543. Zu L, He J, Jiang H, Xu C, Pu S, et al. (2009) Bacterial Endotoxin Stimulates adipose lipolysis via toll-like receptor 4 and extracellular signal-regulated kinase Pathway. Journal of Biological Chemistry 284: 5915-5926.
544. Takenouchi Y, Kobayashi T, Matsumoto T, Kamata K (2009) Gender differences in age-related endothelial function in the murine aorta. Atherosclerosis 206: 397-404.
545. Sarre A, Gabrielli J, Vial G, Leverve XM, Assimacopoulos-Jeannet F (2012) Reactive oxygen species are produced at low glucose and contribute to the activation of AMPK in insulin-secreting cells. Free Radical Biology and Medicine 52: 142-150.